

# Size Reduction and Size Enlargement

**Richard H. Snow, Ph.D.,** *Engineering Advisor, IIT Research Institute; Member, American Chemical Society, Sigma Xi; Fellow, American Institute of Chemical Engineers. (Section Editor)*

**Terry Allen, Ph.D.,** *Senior Research Associate (retired), DuPont Central Research and Development. (Particle Size Analysis)*

**Bryan J. Ennis, Ph.D.,** *President, E&G Associates, and Adjunct Professor of Chemical Engineering, Vanderbilt University; Member and Chair of Powder Technology Programming Group of the Particle Technology Forum, American Institute of Chemical Engineers. (Size Enlargement)*

**James D. Litster, Ph.D.,** *Associate Professor, Department of Chemical Engineering, University of Queensland; Member, Institution of Chemical Engineers-Australia. (Size Enlargement)*

## PARTICLE-SIZE ANALYSIS

Particle-Size Distribution . . . . .	20-5
Specification for Particulates . . . . .	20-5
Particle-Size Equations . . . . .	20-5
Sampling of Powders . . . . .	20-6
Particle-Size Measurement . . . . .	20-7
Gravitational Sedimentation Methods . . . . .	20-7
Sedimentation Balance Methods . . . . .	20-8
Centrifugal Sedimentation Methods . . . . .	20-8
Microscope Methods . . . . .	20-8
Stream Scanning Methods . . . . .	20-8
Field Scanning Methods . . . . .	20-9
Light Diffraction Methods . . . . .	20-9
Photon Correlation Spectroscopy (PCS) . . . . .	20-9
Sieving Methods and Classification . . . . .	20-9
Elutriation Methods and Classification . . . . .	20-9
Surface Area Determination . . . . .	20-9
Permeametry . . . . .	20-10
On-line Procedures . . . . .	20-10

## PRINCIPLES OF SIZE REDUCTION

Properties of Solids . . . . .	20-10
Single-Particle Fracture . . . . .	20-10
Grindability . . . . .	20-11
Grindability Methods . . . . .	20-11
Operations . . . . .	20-11
Mill Wear . . . . .	20-11
Safety . . . . .	20-12
Attainable Product Size and Energy Required . . . . .	20-13
Energy Laws . . . . .	20-13

Grinding Efficiency . . . . .	20-14
Dispersing Agents and Grinding Aids . . . . .	20-15
Size Reduction Combined with Other Operations . . . . .	20-15
Systems Involving Size Reduction . . . . .	20-15
Milling Problems . . . . .	20-16
Continuous Operation . . . . .	20-16
Beneficiation . . . . .	20-16
Liberation . . . . .	20-16
Size Reduction Combined with Size Classification . . . . .	20-16
Characteristics of Size Classifiers . . . . .	20-17
Simulation of Milling Circuits . . . . .	20-18
Batch Grinding . . . . .	20-18
Solution of Batch-Mill Equations . . . . .	20-18
Continuous-Mill Simulation . . . . .	20-19
Solution for Continuous Mill . . . . .	20-19
Closed-Circuit Milling . . . . .	20-19
Data on Behavior of Grinding Functions . . . . .	20-20
Grinding-Rate Functions . . . . .	20-20
Scale-Up Based on Energy . . . . .	20-21
Parameters for Scale-Up . . . . .	20-21
Control of Grinding Circuits . . . . .	20-21

## CRUSHING AND GRINDING EQUIPMENT

Classification and Selection of Equipment . . . . .	20-22
Jaw Crushers . . . . .	20-23
Design and Operation . . . . .	20-23
Comparison of Crushers . . . . .	20-23
Performance . . . . .	20-24
Gyratory Crushers . . . . .	20-24
Design and Operation . . . . .	20-24

## 20-2 SIZE REDUCTION AND SIZE ENLARGEMENT

Performance	20-25
Crusher Product Sizes	20-25
Control of Crushers	20-27
Roll Crushers	20-27
Roll Press	20-28
Impact Breakers	20-28
Hammer Crusher	20-28
Rotor Impactors	20-29
Cage Mills	20-29
Prebreakers	20-30
Precision Cutters and Slitters	20-30
Pan Crushers	20-30
Design and Operation	20-30
Performance	20-30
Tumbling Mills	20-31
Design	20-32
Operation	20-32
Tumbling-Mill Circuits	20-33
Material and Ball Charges	20-33
Dry versus Wet Grinding	20-33
Feed and Discharge	20-34
Mill Efficiencies	20-34
Selection of Mill	20-34
Capacity and Power Consumption	20-34
Motor and Drive	20-35
Performance of Proprietary Equipment	20-35
Stirred Media Mills	20-35
Design	20-35
Performance of Bead Mills	20-36
Residence Time Distribution	20-37
Vibratory Mills	20-37
Performance	20-38
Residence Time Distribution	20-39
Novel Media Mills	20-39
Planetary Ball Milling	20-39
Particle-Size Classifiers Used with Grinding Mills	20-39
Dry Classifiers	20-39
Performance	20-39
Wet Classifiers	20-40
Hammer Mills	20-41
Hammer Mills without Internal Air Classifiers	20-41
Disintegrator	20-42
Pin Mills	20-42
Hammer Mills with Internal Air Classifiers	20-42
Ring-Roller Mills	20-43
Ring-Roller Mills without Internal Classification	20-44
Ring Mills with Internal Screen Classification	20-44
Bowl Mills	20-45
Disk Attrition Mills	20-45
Dispersion and Colloid Mills	20-45
Fluid-Energy or Jet Mills	20-47
Novel Methods	20-48
Avoiding Size Reduction	20-48

### CRUSHING AND GRINDING PRACTICE

Cereals and Other Vegetable Products	20-48
Flour and Feed Meal	20-48
Soybeans, Soybean Cake, and Other Pressed Cakes	20-48
Starch and Other Flours	20-48
Ores and Minerals	20-49
Metalliferous Ores	20-49
Nonmetallic Minerals	20-50
Clays and Kaolins	20-50
Talc and Soapstone	20-51
Carbonates and Sulfates	20-51
Silica and Feldspar	20-51
Asbestos and Mica	20-51
Refractories	20-51
Crushed Stone and Aggregate	20-52
Fertilizers and Phosphates	20-52
Oyster Shells and Lime Rock	20-52
Phosphates	20-52
Cement, Lime, and Gypsum	20-53
Dry-Process Cement	20-53
Wet-Process Cement	20-53
Finish-Grinding of Cement Clinker	20-53
Particle-Size Control	20-54
Lime	20-54
Gypsum	20-54
Coal, Coke, and Other Carbon Products	20-54
Bituminous Coal	20-54

Anthracite	20-54
Coke	20-54
Other Carbon Products	20-54
Chemicals, Pigments, and Soaps	20-54
Colors and Pigments	20-54
Lead Oxides	20-55
Chemicals	20-55
Sulfur	20-55
Soaps	20-55
Organic Polymers	20-55
Processing Waste	20-55
Cryogenic Grinding	20-56
Cell Disruption	20-56

### PRINCIPLES OF SIZE ENLARGEMENT

Scope and Applications	20-56
Approaching the Design of Size-Enlargement Processes	20-57
Agglomeration Kinetics	20-57
Granulation Rate Processes	20-57
Compaction Rate Processes	20-58
Process versus Formulation Design	20-58
Product Characterization	20-59
Size	20-59
Porosity and Density	20-59
Strength of Agglomerates	20-59
Strength Testing Methods	20-60
Flow Property Tests	20-60
Redispersion Tests	20-60
Permeability	20-60

### AGGLOMERATION RATE PROCESSES

Wetting	20-61
Methods of Measurement	20-61
Examples of the Impact of Wetting	20-62
Controlling Wetting	20-62
Growth and Consolidation	20-64
Growth Physics and Contact Mechanics	20-64
Effect of Equipment Mechanical Variables	20-64
Low-Agitation Intensity Growth	20-65
High-Agitation Intensity Growth	20-66
Extent of Noninertial Growth	20-66
Determination of $St^*$	20-66
Consolidation	20-67
Controlling Growth and Consolidation	20-67
Breakage	20-68
Fracture Properties	20-68
Fracture Measurements	20-69
Mechanisms of Breakage	20-69
Controlling Breakage	20-69
Powder Mechanics & Powder Compaction	20-70
Powder Mechanics Measurements	20-70
Compact Density	20-71
Transmission of Forces	20-71
Compact Strength	20-71
Hiestand Tableting Indices	20-72
Compaction Cycles	20-72
Powder Feeding	20-73
Controlling Powder Compaction	20-73

### SIZE ENLARGEMENT EQUIPMENT AND PRACTICE

Tumbling Granulators	20-73
Disc Granulators	20-73
Drum Granulators	20-74
Granulation Rate Processes and Effect of Operating Variables	20-75
Granulator-Dryers for Layering and Coating	20-76
Relative Merits of Disc versus Drum Granulators	20-76
Mixer Granulators	20-76
Low-Speed Mixers	20-76
High-Speed Mixers	20-76
Granulation-Rate Processes and Effect of Operating Variables	20-77
Scale-Up and Operation	20-77
Fluidized-Bed and Related Granulators	20-77
Hydrodynamics	20-78
Mass and Energy Balances	20-78
Granulation Rate Processes and Effect of Operating Variables	20-79
Equipment Operation	20-79
Draft Tube Designs and Spouted Beds	20-79
Centrifugal Granulators	20-79
Centrifugal Designs	20-80
Particle Motion and Scale-Up	20-80
Granulation Rate Processes	20-80

Spray Processes . . . . . 20-80  
 Spray Drying . . . . . 20-81  
 Prilling . . . . . 20-81  
 Flash Drying . . . . . 20-81  
 Pressure Compaction Processes . . . . . 20-81  
 Piston and Molding Presses . . . . . 20-81  
 Tableting Presses . . . . . 20-81  
 Roll Presses . . . . . 20-82  
 Pellet Mills . . . . . 20-83  
 Screw Extruders . . . . . 20-84  
 Thermal Processes . . . . . 20-84  
 Sintering and Heat Hardening . . . . . 20-84  
 Drying and Solidification . . . . . 20-85

**MODELING AND SIMULATION OF GRANULATION PROCESSES**  
 The Population Balance . . . . . 20-85  
 Modeling Individual Growth Mechanisms . . . . . 20-85  
     Nucleation . . . . . 20-85  
     Layering . . . . . 20-86  
     Coalescence . . . . . 20-86  
     Attrition . . . . . 20-87  
 Solution of the Population Balance . . . . . 20-87  
     Effects of Mixing . . . . . 20-87  
     Analytical Solutions . . . . . 20-88  
     Numerical Solutions . . . . . 20-88  
 Simulation of Granulation Circuits with Recycle . . . . . 20-89

**Nomenclature and Units for Size Enlargement and Practice**

Symbol	Definition	SI units	U.S. customary units	Symbol	Definition	SI units	U.S. customary units
<i>A</i>	Parameter in Eq. (20-47)			<i>k</i>	Coalescence rate constant	1/s	1/s
<i>A</i>	Apparent area of indenter contact	cm <sup>2</sup>	in <sup>2</sup>	<i>K</i>	Agglomerate deformability		
<i>A</i>	Attrition rate	cm <sup>3</sup> /s	in <sup>3</sup> /s	<i>K<sub>c</sub></i>	Fracture toughness	MPa·m <sup>1/2</sup>	MPa·m <sup>1/2</sup>
<i>A<sub>i</sub></i>	Spouted-bed inlet orifice area	cm <sup>2</sup>	in <sup>2</sup>	<i>l</i>	Wear displacement of indenter	cm	in
<i>B</i>	Nucleation rate	cm <sup>3</sup> /s	in <sup>3</sup> /s	<i>L</i>	Roll loading	dyn	lbf
<i>B<sub>f</sub></i>	Fragmentation rate	g/s	lb/s	$(\Delta L/L)_c$	Critical agglomerate deformation strain		
<i>B<sub>f</sub></i>	Wear rate	g/s	lb/s	<i>N<sub>i</sub></i>	Granules per unit volume	1/cm <sup>3</sup>	1/ft <sup>3</sup>
<i>c</i>	Crack length	cm	in	<i>n</i>	Feed droplet size	cm	in
$\delta_c$	Effective increase in crack length due to process zone	cm	in	<i>n(v,t)</i>	Number frequency size distribution by size volume	1/cm <sup>6</sup>	1/ft <sup>6</sup>
<i>c</i>	Unloaded shear strength of powder	kg/cm <sup>2</sup>	psf	<i>N<sub>c</sub></i>	Critical drum or disc speed	rev/s	rev/s
<i>d</i>	Harmonic average granule diameter	cm	in	<i>P</i>	Applied load	dyn	lbf
<i>d</i>	Primary particle diameter	cm	in	<i>P</i>	Pressure in powder	kg/cm <sup>2</sup>	psf
<i>d</i>	Impeller diameter	cm	in	<i>Q</i>	Maximum compressive force	kg/cm <sup>2</sup>	psf
<i>d</i>	Roll press pocket depth	cm	in	<i>Q</i>	Granulator flow rate	cm <sup>3</sup> /s	ft <sup>3</sup> /s
<i>d<sub>i</sub></i>	Indenter diameter	cm	in	<i>r<sub>p</sub></i>	Process zone radius	cm	in
<i>d<sub>a</sub></i>	Average feed particle size	cm	in	<i>R</i>	Capillary radius	cm	in
<i>D</i>	Die diameter	cm	in	<i>S</i>	Volumetric spray rate	cm <sup>3</sup> /s	ft <sup>3</sup> /s
<i>D</i>	Disc or drum diameter	cm	in	<i>St</i>	Stokes number, Eq. (20-48)		
<i>D</i>	Roll diameter	cm	in	<i>St<sup>o</sup></i>	Critical Stokes number representing energy required for rebound		
<i>D<sub>c</sub></i>	Critical limit of granule size	cm	in	<i>St<sub>0</sub></i>	Stokes number based on initial nuclei diameter		
<i>e<sub>r</sub></i>	Coefficient of restitution			<i>t</i>	Time	s	s
<i>E</i>	Strain energy stored in particle	J	J	<i>u, v</i>	Granule volumes	cm <sup>3</sup>	in <sup>3</sup>
<i>E<sup>o</sup></i>	Reduced elastic modulus	kg/cm <sup>2</sup>	psf	<i>u<sub>0</sub></i>	Relative granule collisional velocity	cm/s	in/s
<i>f<sub>c</sub></i>	Unconfined yield stress of powder	kg/cm <sup>2</sup>	psf	<i>U</i>	Fluidization gas velocity	cm/s	ft/s
<i>g</i>	Acceleration due to gravity	cm/s <sup>2</sup>	ft/s <sup>2</sup>	<i>U<sub>inf</sub></i>	Minimum fluidization gas velocity	cm/s	ft/s
<i>G<sub>c</sub></i>	Critical strain energy release rate	J/m <sup>2</sup>	J/m <sup>2</sup>	<i>U<sub>i</sub></i>	Spouted-bed inlet gas velocity	cm/s	ft/s
<i>F</i>	Indentation force	dyn	lbf	<i>V</i>	Volumetric wear rate	cm <sup>3</sup> /s	in <sup>3</sup> /s
<i>F</i>	Roll separating force	dyn	lbf	<i>V<sub>R</sub></i>	Mixer swept volume ratio of impeller	cm <sup>3</sup> /s	ft <sup>3</sup> /s
<i>G</i>	Layering rate	cm <sup>3</sup> /s	in <sup>3</sup> /s	<i>V</i>	Volume of granulator	cm <sup>3</sup>	ft <sup>3</sup>
<i>h</i>	Height of liquid capillary rise	cm	in	<i>w</i>	Weight fraction liquid		
<i>h</i>	Roll press gap distance	cm	in	<i>w</i>	Granule volume	cm <sup>3</sup>	in <sup>3</sup>
<i>h</i>	Binder liquid layer thickness	cm	in	<i>w<sup>o</sup></i>	Critical average granule volume	cm <sup>3</sup>	in <sup>3</sup>
<i>h<sub>b</sub></i>	Fluid-bed height	cm	in	<i>W</i>	Roll width	cm	in
<i>h<sub>a</sub></i>	Height of surface asperities	cm	in	<i>x</i>	Granule or particle size	cm	in
<i>h<sub>a</sub></i>	Maximum height of liquid capillary rise	cm	in	<i>y</i>	Liquid loading		
<i>H</i>	Individual bond strength	dyn	lbf	$\gamma$	Calibration factor		
<i>H</i>	Hardness of agglomerate or compact	kg/cm <sup>2</sup>	psf				

Greek symbols

Symbol	Definition	SI units	U.S. customary units	Symbol	Definition	SI units	U.S. customary units
$\beta(u, v)$	Coalescence rate constant for collisions between granules of volumes <i>u</i> and <i>v</i>	1/sec	1/sec	$\Delta\rho$	Relative fluid density with respect to displaced gas or liquid	gm/cm <sup>3</sup>	
$\epsilon$	Porosity of packed powder			$\rho$	Apparent agglomerate or granule density	gm/cm <sup>3</sup>	lb/ft <sup>3</sup>
$\epsilon_b$	Interagglomerate bed voidage			$\rho_a$	Apparent agglomerate or granule density	gm/cm <sup>3</sup>	lb/ft <sup>3</sup>
$\epsilon_g$	Intraagglomerate granule porosity			$\rho_b$	Bulk density	gm/cm <sup>3</sup>	lb/ft <sup>3</sup>
$\kappa$	Compressibility of powder			$\rho_g$	Apparent agglomerate or granule density	gm/cm <sup>3</sup>	lb/ft <sup>3</sup>
$\phi$	Disc angle to horizontal	deg	deg	$\rho_l$	Liquid density	gm/cm <sup>3</sup>	lb/ft <sup>3</sup>
$\phi$	Internal angle of friction	deg	deg	$\rho_s$	True skeletal solids density	gm/cm <sup>3</sup>	lb/ft <sup>3</sup>
$\phi_c$	Effective angle of friction	deg	deg	$\sigma_0$	Applied axial stress	kg/cm <sup>2</sup>	psf
$\phi_w$	Wall angle of friction	deg	deg	$\sigma_z$	Resulting axial stress in powder	kg/cm <sup>2</sup>	psf
$\phi_w$	Roll friction angle	deg	deg	$\sigma$	Powder normal stress during shear	kg/cm <sup>2</sup>	psf
$\phi(\eta)$	Relative size distribution			$\sigma_c$	Powder compaction normal stress	kg/cm <sup>2</sup>	psf
$\gamma^{lv}$	Liquid-vapor interfacial energy	dyn/cm	dyn/cm	$\sigma_f$	Fracture stress under three-point bend loading	kg/cm <sup>2</sup>	psf
$\gamma^{sl}$	Solid-liquid interfacial energy	dyn/cm	dyn/cm	$\sigma_T$	Granule tensile strength	kg/cm <sup>2</sup>	psf
$\gamma^{sv}$	Solid-vapor interfacial energy	dyn/cm	dyn/cm	$\sigma_y$	Granule yield strength	kg/cm <sup>2</sup>	psf
$\mu$	Binder or fluid viscosity	poise		$\tau$	Powder shear stress	kg/cm <sup>2</sup>	psf
$\mu$	Coefficient of internal friction			$\theta$	Contact angle	°	°
$\omega$	Impeller rotational speed	rad/s	rad/s	$\zeta$	Parameter in Eq. (20-47)		
				$\eta$	Parameter in Eq. (20-47)		

## 20-4 SIZE REDUCTION AND SIZE ENLARGEMENT

### Nomenclature and Units

Symbol	Definition	SI units	U.S. customary units	Symbol	Definition	SI units	U.S. customary units
<i>A</i>	Coefficient in double Schumann equation			<i>q<sub>f</sub></i>	Fine-fraction mass flow rate	g/s	lb/s
<i>a</i>	Constant			<i>q<sub>o</sub></i>	Feed mass flow rate	g/s	lb/s
<i>a<sub>k,k</sub></i>	Coefficient in mill equations			<i>q<sub>p</sub></i>	Mass flow rate of classifier product	g/s	lb/s
<i>a<sub>k,n</sub></i>	Coefficient in mill equations			<i>q<sub>R</sub></i>	Mass flow rate of classifier tailings	g/s	lb/s
<b>B</b>	Matrix of breakage function			<i>q<sub>R</sub></i>	Recycle mass flow rate to a mill	g/s	lb/s
$\Delta B_{k,u}$	Breakage function			<i>R</i>	Recycle		
<i>b</i>	Constant			<i>R</i>	Reid solution		
<i>C</i>	Constant			<i>r</i>	Dimensionless parameter in size-distribution equations		
<i>C<sub>i</sub></i>	Impact-crushing resistance	kWh/cm	(ft·lb)/in	$\underline{S}$	Rate function	S <sup>-1</sup>	S <sup>-1</sup>
<i>D</i>	Diffusivity	m <sup>2</sup> /s	ft <sup>2</sup> /s	$\bar{S}$	Corrected rate function	S <sup>-1</sup>	S <sup>-1</sup>
<i>D</i>	Mill diameter	m	ft	<b>S'</b>	Matrix of rate function	Mg/kWh	ton/(hp·h)
<i>D<sub>b</sub></i>	Ball or rod diameter	cm	in	<i>S<sub>C</sub>(X)</i>	Grindability function	S <sup>-1</sup>	S <sup>-1</sup>
<i>D<sub>mill</sub></i>	Diameter of mill	m	ft	<i>S<sub>u</sub></i>	Grinding-rate function		
<i>d</i>	Differential			<i>s</i>	Parameter in size-distribution equations		
<i>d</i>	Distance between rolls of crusher	cm	in	<i>s</i>	Peripheral speed of rolls	cm/min	in/min
<i>E</i>	Work done in size reduction	kWh	hp·h	<i>t</i>	Time	s	s
<i>E</i>	Energy input to mill	kW	hp	<i>u</i>	Settling velocity of particles	cm/s	ft/s
<i>E<sub>i</sub></i>	Bond work index	kWh/Mg	(hp·h)/ton	<b>W</b>	Vector of differential size distribution of a stream		
<i>E<sub>i</sub></i>	Work index of mill feed			<i>w<sub>k</sub></i>	Weight fraction retained on each screen		
<i>E<sub>2</sub></i>	Net power input to laboratory mill	kW	hp	<i>w<sub>u</sub></i>	Weight fraction of upper-size particles		
erf	Normal probability function			<i>w<sub>v</sub></i>	Material holdup in mill	g	lb
<i>F</i>	As subscript, referring to feed stream			<i>X</i>	Particle size or sieve size	cm	in
<i>F</i>	Bonding force	kg/kg	lb/lb	<i>X'</i>	Parameter in size-distribution equations	cm	in
<i>g</i>	Acceleration due to gravity	cm/s <sup>2</sup>	ft/s <sup>2</sup>	$\Delta X_i$	Particle-size interval	cm	in
<b>I</b>	Unit matrix in mill equations			<i>X<sub>i</sub></i>	Midpoint of particle-size interval, $\Delta X_i$	cm	in
<i>i</i>	Tensile strength of agglomerates	kg/cm <sup>2</sup>	lb/in <sup>2</sup>	<i>X<sub>0</sub></i>	Constant, for classifier design		
<i>K</i>	Constant			<i>X<sub>f</sub></i>	Feed-particle size	cm	in
<i>k</i>	Parameter in size-distribution equations	cm	in	<i>X<sub>m</sub></i>	Mean size of increment in size-distribution equations	cm	in
<i>k</i>	As subscript, referring to size of particles in mill and classifier parameters			<i>X<sub>p</sub></i>	Product-particle size	cm	in
<i>L</i>	As subscript, referring to discharge from a mill or classifier			<i>X<sub>p</sub></i>	Size of coarser feed to mill	cm	in
<i>L</i>	Length of rolls	cm	in	<i>X<sub>25</sub></i>	Particle size corresponding to 25 percent classifier-selectivity value	cm	in
<i>L</i>	Inside length of tumbling mill	m	ft	<i>X<sub>50</sub></i>	Particle size corresponding to 50 percent classifier-selectivity value	cm	in
<b>M</b>	Mill matrix in mill equations			<i>X<sub>75</sub></i>	Particle size corresponding to 75 percent classifier-selectivity value	cm	in
<i>m</i>	Dimensionless parameter in size-distribution equations			$\Delta X_k$	Difference between opening of successive screens	cm	in
<i>N</i>	Mean-coordination number			<i>x</i>	Weight fraction of liquid		
<i>N<sub>c</sub></i>	Critical speed of mill	r/min	r/min	<i>Y</i>	Cumulative fraction by weight undersize in size-distribution equations		
$\Delta N$	Incremental number of particles in size-distribution equation			<i>Y</i>	Cumulative fraction by weight undersize or oversize in classifier equations		
<i>n</i>	Dimensionless parameter in size-distribution equations			$\Delta Y$	Fraction of particles between two sieve sizes		
<i>n</i>	Constant, general			$\Delta Y$	Incremental weight of particles in size-distribution equations	g	lb
<i>n<sub>r</sub></i>	Percent critical speed of mill			$\Delta Y_{ci}$	Cumulative size-distribution intervals of coarse fractions	cm	in
<i>O</i>	As subscript, referring to inlet stream			$\Delta Y_{fi}$	Cumulative size-distribution intervals of fine fractions	cm	in
<i>P</i>	As subscript, referring to product stream			<b>Z</b>	Matrix of exponentials		
<i>P<sub>k</sub></i>	Fraction of particles coarser than a given sieve opening						
<i>p</i>	Number of short-time intervals in mill equations						
<i>Q</i>	Capacity of roll crusher	cm <sup>3</sup> /min	ft <sup>3</sup> /min				
<i>q</i>	Total mass throughput of a mill	g/s	lb/s				
<i>q<sub>c</sub></i>	Coarse-fraction mass flow rate	g/s	lb/s				
<i>q<sub>F</sub></i>	Mass flow rate of fresh material to mill	g/s	lb/s				

### Greek symbols

$\beta$	Sharpness index of a classifier			$\rho_l$	Density of liquid	g/cm <sup>3</sup>	lb/in <sup>3</sup>
$\delta$	Angle of contact	rad	0	$\rho_s$	Density of solid	g/cm <sup>3</sup>	lb/in <sup>3</sup>
$\varepsilon$	Volume fraction of void space			$\Sigma$	Summation		
<i>Z</i>	Residence time in the mill	s	s	$\sigma$	Standard deviation		
$\eta_v$	Size-selectivity parameter			$\sigma$	Surface tension	N/cm	dyn/cm
$\mu$	Viscosity of fluid	(N·S)/m <sup>2</sup>	P	$\upsilon$	Volumetric abundance ratio of gangue to mineral		
$\rho_f$	Density of fluid	g/cm <sup>3</sup>	lb/in <sup>3</sup>				

## PARTICLE-SIZE ANALYSIS

**GENERAL REFERENCES:** Allen, *Particle Size Measurement*, Chapman and Hall, 4th ed. 1990. Barth and Sun, *Particle Size Analysis Review*, Anal. Chem., 57, 151R, 1985. Miller and Lines, *Critical Reviews in Analytical Chemistry*, 20(2), 75–116, 1988. Herdan, *Small Particle Statistics*, Butterworths, London. Orr and DalleValle, *Fine Particle Measurement*, Macmillan, New York, 2d ed., 1960. Kaye, *Direct Characterization of Fine Particles*, Wiley, New York, 1981. Van de Hulst, *Light Scattering by Small Particles*, Wiley, New York, 1957.

### PARTICLE-SIZE DISTRIBUTION

**Specification for Particulates** Feed, recycle, and product from size reduction operations are defined in terms of the sizes involved. It is also important to have an understanding of the degree of aggregation or agglomeration that exists in the measured distribution.

The fullest description of a powder is given by its **particle-size distribution**. This can be presented in tabular or graphical form. The simplest presentation is in linear form with equal size intervals (Table 20-1). The significance of the distribution is more easily grasped when the data are presented pictorially, the simplest form of which is the histogram. More usually the plot is of cumulative percentage oversize or undersize against particle diameters, or percentage frequency against particle diameters. It is common to use a weight basis for percentage but surface or number may, in some cases, be more relevant. The basis of percentage; weight, surface, or volume should be specified, together with the basis of diameter; sieve, Stokes, or otherwise. The measuring procedure should also be noted.

Figure 20-1 presents the data from Table 20-1 in both cumulative and frequency format. In order to smooth out experimental errors it is best to generate the frequency curve from the slope of the cumulative curve, to use wide-size intervals or a data-smoothing computer program. The advantage of this method of presenting frequency data is that the area under the frequency curve equals 100 percent, hence, it is easy to visually compare similar data. A typical title for such a presentation would be: *Relative and cumulative mass distributions of quartz powder by pipet sedimentation*.

An alternative presentation of the same data is given in Fig. 20-2. In this case the sizes on the abscissa are in a logarithmic progression [ $\log(x)$ ] and the frequency is  $[dP/d \ln(x)]$  so that the area under the frequency curve is, again, 100. This form of presentation is useful for wide-size distributions: Many instrument software programs generate data in a logarithmic-size interval and information is compressed in the finer-size intervals if an arithmetic-size progression is used.

It is always preferable to plot data so that the area under the frequency curve is normalized to 100 percent since this facilitates data comparison.

**Particle-Size Equations** It is common practice to plot size-distribution data in such a way that a straight line results, with all the advantages that follow from such a reduction. This can be done if the curve fits a standard law such as the normal probability law. According to the normal law, differences of equal amounts in excess or deficit from a mean value are equally likely. In order to maintain a symmetrical bell-shaped curve for the frequency distribution it is necessary to plot the population density (e.g., percentage per micron) against size.

With the **log-normal probability law**, it is ratios of equal amounts which are equally likely. In order to obtain a symmetrical bell-shaped frequency curve it is therefore necessary to plot the population density per log (micron) against log (size) [Hatch and Choate, *J. Franklin Inst.*, 207, 369 (1929)]:

$$Y = \text{erf} \left( \frac{\ln(X/X')}{\sigma} \right) \quad (20-1)$$

Other equations in general use include the Gates-Gaudin-Schumann [Schumann, *Am. Inst. Min. Metall. Pet. Eng.*, Tech. Paper 1189, Min. Tech. (1940)]:

$$Y = (X/k)^m \quad (20-2)$$

The Rosin-Rammler-Bennett [Rosin and Rammler, *J. Inst. Fuel*, 7, 29–36 (1933); Bennett, *ibid.*, 10, 22–29 (1936)]:

$$Y = 1 - [\exp\{-X/X'\}^n] \quad (20-3)$$

The Gaudin-Meloy [Gaudin and Meloy, *Trans. Am. Inst. Min. Metall. Pet. Eng.*, 223, 40–50 (1962)]:

$$Y = 1 - \left[ 1 - \left( \frac{X}{X'} \right)^r \right] \quad (20-4)$$

where  $Y$  = cumulative fraction by weight undersize;  $x$  = size;  $k$ ,  $X'$  = parameters with dimensions of size,  $m$ ,  $n$ ,  $r$  = dimensionless exponents; erf = normal probability function; and  $\sigma$  = standard deviation parameter.

The Rosin-Rammler is useful for monitoring grinding operations for highly skewed distributions, but should be used with caution since the device of taking logs always reduces scatter, hence taking logs twice is not to be recommended. The Gates-Gaudin-Schumann has the advantage of simplicity and the Gaudin-Meloy can be fitted to a variety of distributions found in practice. The log-normal distribution

**TABLE 20-1 Tabular Presentation of Particle Size Data**

Particle size in microns (x)	Percentage undersize (P)	Percentage per micron $\left(\frac{dP}{dx}\right)$	Percentage per log (micron) $\frac{dP}{d \log(x)}$	Particle size in microns (x)	Percentage undersize (P)	Percentage per micron $\left(\frac{dP}{dx}\right)$	Percentage per log (micron) $\frac{dP}{d \log(x)}$
2.5	0.00	0.000	0.00	52.5	97.41	0.425	13.21
7.5	0.29	0.058	0.12	57.5	98.59	0.236	8.16
12.5	5.06	0.953	3.21	62.5	99.24	0.130	4.92
17.5	19.44	2.875	15.54	67.5	99.59	0.071	2.92
22.5	39.93	4.098	34.68	72.5	99.79	0.039	1.71
27.5	59.68	3.951	47.97	77.5	99.89	0.021	1.00
32.5	74.91	3.047	48.92	82.5	99.95	0.012	0.58
37.5	85.18	2.054	41.04	87.5	99.98	0.006	0.34
42.5	91.55	1.273	30.31	92.5	100.00	0.004	0.20
47.5	95.28	0.748	20.58			0.000	0.12

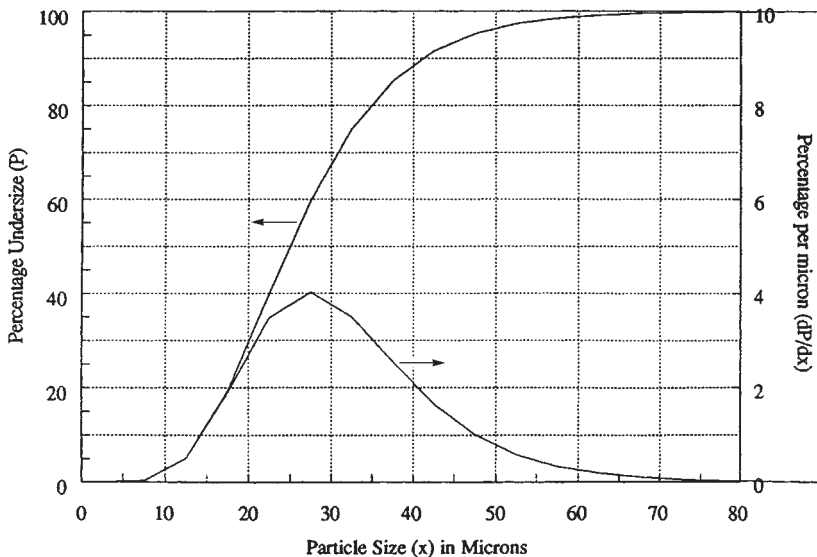


FIG. 20-1 Particle-size distribution curve plotted on linear axes.

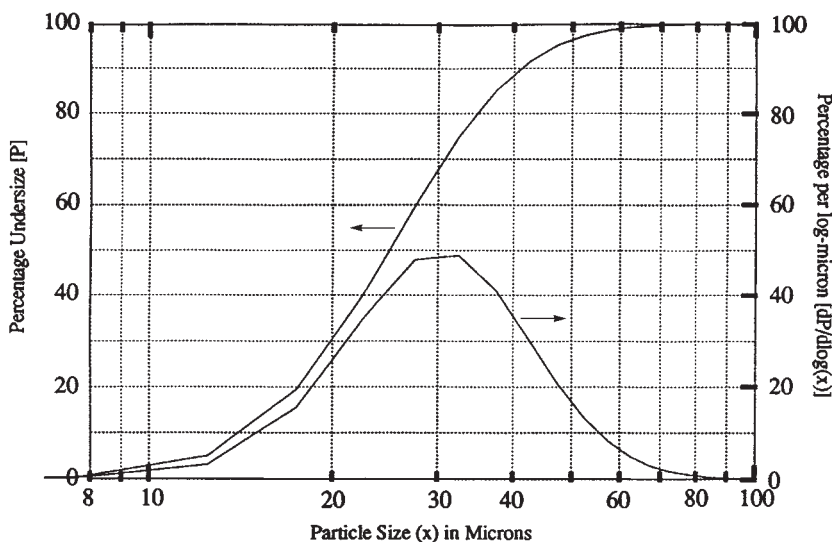


FIG. 20-2 Particle-size distribution curve plotted using a logarithmic scale for the abscissa.

has an advantage in that transformations between distributions is simple; that is, if the number distribution is log-normal, the surface and volume distributions are also log-normal with the same slope ( $\sigma$ ).

**Average Particle Size** A powder has many average sizes; hence it is essential that they be well specified. The median is the 50 percent size; half the distribution is coarser and half finer. The mode is a high-density region; if there is more than one peak in the frequency curve, the distribution is said to be multimodal. The mean is the center of gravity of the distribution. The center of gravity of a mass (volume) distribution is defined by:  $X_{VM} = \frac{\sum X dV}{\sum dV}$  where  $dV = X^3 dN$ ;  $dV$  is the volume of  $dN$  particles of size  $X$ . This is defined as the *volume-moment mean diameter* and differs from the mean for a number or surface distribution.

**Specific Surface** This can be calculated from size distribution data. For example, the Gates diagram employs a plot of cumulative

percent by weight undersize versus reciprocal diameter; the area beneath the curve represents surface. Likewise the area under the Roller diagram of weight percent per micron against log of diameter represents surface (Work and Whitby, op.cit., p 477).

**Sampling of Powders** An important prerequisite to accurate particle size analysis is proper powder sampling. Powders may be classified as nonsegregating (cohesive) or segregating (free-flowing). Representative samples are more easily taken from cohesive powders *provided* they have previously been mixed. It is difficult to mix free-flowing powders; hence it is advisable to sample them in motion. (1) A powder should always be sampled when in motion. (2) The whole of the stream of powder should be taken for many short increments of time in preference to part of the stream being taken for the whole of the time. The estimated maximum sample errors on a 60:40 blend of free-flowing sand using different sampling techniques are given in Table 20-2.

TABLE 20-2 Reliability of Selected Sampling Methods

Method	Estimated maximum sample error
Cone and quartering	22.7%
Scoop sampling	17.1%
Table sampling	7.0%
Chute splitting	3.4%
Spinning riffling	0.42%

The spinning riffler obeys the “Golden Rules of Sampling” given above and, therefore, generates the most representative samples [Allen and Khan, *The Chemical Engineer*, 103–112 (May 1970)]. In this device (Fig. 20-3) a ring of containers rotates under the powder feed. If the powder flows for a long time compared with the period of rotation (a ratio of at least 30:1), the sample in each container will be made up of many small portions drawn from all parts of the bulk. Several different configurations of this device are available for both cohesive and free-flowing powders. In the one illustrated, a single pass divides the bulk into 16 parts, two passes increases this subdivision to 256:1, and so on.

### PARTICLE-SIZE MEASUREMENT

There are many techniques available for measuring the particle-size distribution of powders. The wide size range covered, from nanometers to millimeters, cannot be analyzed using a single measurement principle. Added to this are the usual constraints of capital costs versus running costs, speed of operation, degree of skill required, and, most important, the end-use requirement.

If the particle-size distribution of a powder composed of hard, smooth spheres is measured by any of the techniques, the measured values should be identical. However, there are many different size distributions that can be defined for any powder made up of nonspherical particles. For example, if a rod-shaped particle is placed on a sieve, its diameter, not its length, determines the size of aperture through which it will pass. If, however, the particle is allowed to settle in a viscous fluid, the calculated diameter of a sphere of the same substance that would have the same falling speed in the same fluid (i.e., the Stokes diameter) is taken as the appropriate size parameter of the particle.

Since the Stokes diameter for the rod-shaped particle will obviously differ from the rod diameter, this difference represents added information concerning particle shape. The ratio of the diameters measured by two different techniques is called a **shape factor**.

Heywood [Heywood, *Symposium on Particle Size Analysis*, Inst. Chem. Engrs. (1947), Suppl. 25, 14] recognized that the word “shape” refers to two distinct characteristics of a particle—form and proportion. The first defines the degree to which the particle approaches a definite form such as cube, tetrahedron, or sphere, and the second by the relative proportions of the particle which distinguish one cuboid, tetrahedron, or spheroid from another in the same class. He replaced historical qualitative definitions of shape by numerical shape coefficients.

**Gravitational Sedimentation Methods** In gravitational sedimentation methods, particle size is determined from settling velocity

and undersize fraction by changes of concentration in a settling suspension. The equation relating particle size to settling velocity is known as Stokes law:

$$d_{st} = \sqrt{\frac{18\eta u}{(\rho_s - \rho_f)g}} \quad (20-5)$$

where  $d_{st}$  is the Stokes diameter,  $\eta$  is viscosity,  $u$  is particle settling velocity under gravity,  $\rho_s$  is the particle density,  $\rho_f$  is the fluid density, and  $g$  is the acceleration due to gravity.

Stokes diameter is defined as the diameter of a sphere having the same density and the same velocity as the particle in a fluid of the same density and viscosity settling under laminar flow conditions. Correction for deviation from Stokes law may be necessary at the large end of the size range. Sedimentation methods are limited to sizes above a  $\mu\text{m}$  due to the onset of thermal diffusion (Brownian motion) at smaller sizes.

An experimental problem is to obtain adequate dispersion of the particles before sedimentation analysis. For powders that are difficult to disperse the addition of dispersing agents is necessary, together with ultrasonic probing. It is essential to examine a sample of the dispersion under a microscope to ensure that the sample is fully dispersed.

Equations to calculate size distributions from sedimentation data are based on the assumption that the particles fall freely in the suspension. In order to ensure that particle-particle interaction does not prevent free fall, an upper-volume concentration limit of around 0.2 percent is recommended.

There are various procedures available for determining the changing solids concentration of a sedimenting suspension:

In the *pipet method*, concentration changes are monitored by extracting samples from a sedimenting suspension at known depths of fall and predetermined times. The method is best known as the *Andreasen modification* [Andreasen, *Kolloid-Z.*, **49**, 253 (1929)] shown in Fig. 20-4. Two 10-mL samples are withdrawn from a fully dispersed, agitated suspension at zero time to corroborate the 100 percent concentration given by the known weight of powder and volume of liquid making up the suspension. The suspension is then allowed to settle, and 10-mL samples are taken at time intervals in a geometric 2:1 time progression starting at 1 minute (i.e., 1, 2, 4, 8, 16, 32, 64 minutes); if longer time intervals than this are used it is necessary to enclose the pipet in a temperature-controlled environment. The amounts of powder in the extracted samples are determined by

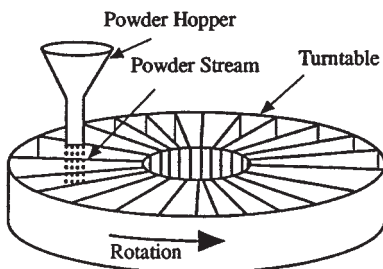


FIG. 20-3 Spinning riffler sampling device.

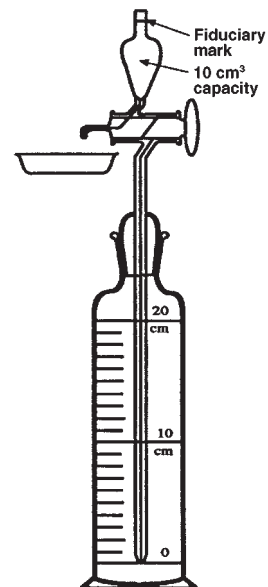


FIG. 20-4 Equipment used in the pipet method of size analysis.

drying, cooling in a dessicator, and weighing. Stokes diameters are determined from the predetermined times and the depths, with correction for the changes in depth due to the extractions. The cumulative, mass, undersize distribution comprises a plot of the normalized concentration against the Stokes diameter. A reproducibility of  $\pm 2$  percent is possible using this apparatus. The technique is versatile in that it is possible to analyze most powders which are dispersible in liquids; its disadvantages are that it is a labor-intensive procedure and a high level of skill is needed.

The *hydrometer method* is simpler in that the density of the suspension, which is related to the concentration, is read directly from the stem of the hydrometer while the depth is determined by the distance of the hydrometer bulb from the surface (ASTM Spec. Pub. 234, 1959). The method has low resolution but is widely used in soil science studies.

In *gravitational photosedimentation methods* the changing concentration with time and depth of fall is monitored using a light beam. These methods give a continuous record of changing optical density with time and depth and have the added advantage that the beam can be scanned to the surface to reduce the measurement time. A correction needs to be applied to compensate for the breakdown in the laws of geometric optics (due to diffraction effects the particles cut off more light than geometric optics predicts). The normalized measurement is a cumulative surface undersize.

In *gravitational X-ray sedimentation methods* the changing concentration with time and depth of fall is monitored using an X-ray beam. These methods give a continuous record of changing X-ray density with time and depth and have the added advantage that the beam can be scanned to the surface to reduce the measurement time. The method is limited to materials having a high atomic mass (i.e., X-ray opaque material) and gives a mass undersize distribution directly.

**Sedimentation Balance Methods** In sedimentation balances the weight of sediment is measured as it accumulates on a balance pan suspended in an initially homogeneous suspension. The technique is slow because of the time required for the smallest fine particle to settle out over a given column height. The relationship between settled weight ( $P$ ), weight undersize ( $W$ ) and time ( $t$ ) is given by the following equation.

$$P = W - \frac{dP}{d \ln(t)} \quad (20-6)$$

**Centrifugal Sedimentation Methods** These methods extend sedimentation methods into the submicron size range. Sizes are calculated from a modified version of Stokes equation:

$$d_{st} = \sqrt{\frac{18\eta u}{(\rho_s - \rho_f)\omega^2 r}} \quad (20-7)$$

where  $r$  is the measurement radius and  $\omega$  is the radial velocity of the centrifuge. The concentration calculations are complicated due to radial dilution effects (i.e., particles do not travel in parallel paths as in gravitational sedimentation but move away from each other as they settle radially outwards).

Particle velocities are given by:

$$u = \frac{\ln\left(\frac{r}{s}\right)}{t} \quad (20-8)$$

where both  $r$ , the measurement radius, and  $s$ , the surface radius can be varying; the former varies if the system is a scanning system, and the latter if the surface falls due to the extraction of samples.

Concentration undersize  $D_m$  is determined using Kamack's equation [Kamack, *Br. J. Appl. Phys.*, **5**, 1962-68 (1972)]:

$$Q(D_m) = \int_0^{D_m} \left(\frac{r_i}{s_i}\right)^2 f(D) dD \quad (20-9)$$

where  $r_i$  is the measurement radius and  $s_i$  is the surface radius, either or both of which may vary during the analysis.  $f(D)dD = F(D)$  is the fraction of particles in the narrow-size range  $dD$ .  $(r_i/s_i)^2$  is the radial dilution correction factor.

The disc centrifuge, developed by Slater and Cohen and modified by Allen and Svarovsky [Allen and Svarovsky, *Dechema Monogram*,

Nuremberg, Numbers 1589-1615, 279-292 (1975)], is essentially a centrifugal pipet device. Size distributions are calculated from the measured solids concentrations of a series of samples withdrawn through a central drainage pillar at various time intervals.

In the centrifugal disc photosedimentometer concentration changes are monitored by a light beam. In one high-resolution mode of operation, the suspension under test is injected into clear fluid in the spinning disc through an entry port, and a layer of suspension is formed over the free surface of the liquid (the line-start technique). The analysis can also be carried out using a homogeneous suspension. Very low concentrations are used, but the light-scattering properties of small particles make it difficult to interpret the measured data.

Several centrifugal cuvet photocentrifuges are commercially available. These instruments use the same theory as the disc photocentrifuges but are limited in operation to the homogeneous mode of operation.

The X-ray disc centrifuge is a centrifugal version of the gravitational instruments and extends the measuring technique well into the sub- $\mu$ m-size range.

**Microscope Methods** In microscope methods of size analysis, direct measurements are made on enlarged images of the particles. In the simplest technique, linear measurements of particles are made by using a calibrated scale on top of the particle image. Alternatively, the projected areas of the particles can be compared to areas of circles.

**Feret's diameter** (Fig. 20-5) is the perpendicular projection, in a fixed direction, of the tangents to the extremities of the particle profile. **Martin's diameter** is a line, parallel to a fixed direction, which divides the particle profile into two equal areas. Since the magnitude of these statistical diameters varies with particle orientation, these diameters have meaning only when a sufficient number of measurements are averaged.

Quantitative image microscopy has revolutionized microscopic methods of size and shape analysis. The sizes of large numbers of particles can be rapidly determined and the data manipulated. The speed and sophistication of such devices make it possible to devise new methods for characterizing the shape of fine particles. In **Fourier techniques** the shape characteristic is transformed into a signature waveform. Beddow and coworkers (Beddow, *Particulate Science and Technology*, Chemical Publishing, New York, 1980) take the particle centroid as a reference point. A vector is then rotated about this centroid with the tip of the vector touching the periphery. A plot of the magnitude of the vector against its angular position is a wave-type function. This wave form is then subjected to Fourier analysis. The lower frequency harmonics constituting the complex wave correspond to the gross external morphology, whereas the higher frequencies correspond to the texture of the fine particle. **Fractal logic** was introduced into fine-particle science by Kaye and coworkers [Kaye, op. cit. (1981)], who show that the non-Euclidean logic of Mandelbrot can be applied to describe the ruggedness of a particle profile. A combination of fractal dimension, and geometric-shape factors such as aspect ratio, can be used to describe a population of fine particles of various shapes, and these can be related to the functional properties of the particle.

**Stream Scanning Methods** In these techniques, the particles to be measured are examined individually in a stream of fluid. As the particles pass through a sensing zone they are counted and measured through their interaction with the sensor. It is essential to use very low particle concentrations since the signals received from two particles is indistinguishable from the signal received from a single larger particle.



FIG. 20-5 Statistical (Martin's and Feret's) and projected area diameters for an irregular particle.



In the **electrical sensing zone method** a dilute well-dispersed suspension in an electrolyte is caused to flow through a small aperture [Kubitschek, *Research*, **13**, 129 (1960)]. The changes in the resistivity between two electrodes on either side of the aperture, as the particles pass through, are directly related to the volumes of the particles. The pulses are fed to a pulse-height analyzer where they are counted and scaled. The method is limited by the pulse-height analyzer which can resolve pulses in the range 16,000:1 (i.e., a volume diameter range of about 25:1) and the need to suspend the particles in an electrolyte.

In **light blockage methods** the size of the particle is determined from the amount of light blocked off by the particle as it passes through a sensing zone. In **light scattering methods** the particle size is determined either from the light scattered in the forward direction or at some angle, usually  $90^\circ$  from the direction of the incident beam. The light source can be incandescent or laser and the detecting mechanism ranges from simple photodetectors to parabolic mirrors. The particles can be suspended in a liquid or gas.

In the Lasentec instruments a chord-length distribution is generated, from a rotating infrared beam, and this is converted to a size distribution. Since highly concentrated systems can be interrogated this system can be used for on-line size analysis.

**Field Scanning Methods** In these techniques, the particles to be measured are examined collectively, and the signal from the assembly of particles is deconvoluted to generate a size distribution.

**Light Diffraction Methods** These comprise one of several field scanning procedures in which an assembly of particles is irradiated with a laser beam. The forward light-scattered flux contains information on the size distribution of the particles. Several assumptions are made in the transformation of the diffraction pattern into particle-size data, and the various companies manufacturing these instruments offer different interpretive programs. The dozen or so instruments currently marketed tend to disagree with each other and also generate a wider distribution than other methods. Their advantages are ease of use and high reproducibility. Although low-angle laser light scattering is only applicable down to around  $0.7 \mu\text{m}$ , the lower limit can be extended using secondary measurements of  $90^\circ$  degree scattering of white light, polarization ratio, and so on.

The principle of ultrasonic attenuation is that plane sound waves moving through a slurry are attenuated according to the size and concentration of the particles in the slurry. Two instruments have been described, one for sizing in the plus-one  $\mu\text{m}$  up to mm sizes (Reibel and Löffler, *European Symposium on Particle Characterization*, Nuremberg, Germany, publ. Nuremberg Messe, 1989) and the other for sub- $\mu\text{m}$  sizing (Alba, US Patent 5121629, June 16, 1992). Although in its infancy, the technique shows high promise for on-line size analysis at high-volume (+50%) concentrations.

**Photon Correlation Spectroscopy (PCS)** The size distribution of particles ranging in size from a few nanometers to a few  $\mu\text{m}$  can be determined from their random motion due to molecular bombardment. This technique involves passing a laser beam into a suspension and measuring the Doppler shift of the frequency of light scattered at an angle (usually  $90^\circ$  degrees) with respect to the incident beam. The Doppler shift is related to particle velocity which, in turn, is inversely related to their size. Multiangle instruments are also available to generate the angular variation of scattered light intensity for derivation of molecular weight, radius of gyration, translational and rotational diffusion coefficients, and other molecular properties.

Through dynamic light scattering in the controlled reference method, a laser beam is fed into an agitated measuring cell or flowing suspension using an optical-wave guide. Particles within 50 microns of the tip of the wave guide (a fiber-optic probe) scatter light some of which is reflected back into the fiber and transmitted back through the guide. The reflected light from the interface between the guide tip and the suspension is also transmitted back. If these two components are coherent they will interfere with each other and result in a component of signal which has the difference or "beat" frequency between the reflected and scattered components. The difference frequencies are the same as the desired Doppler shifts. The received signal resembles random noise at the output of the silicon photodiode as a result of the mixing of the Doppler shifts from all the particles scattering the laser light. The photodiode output is digitized and the

power spectrum of the signal is determined using Fast Fourier Transform techniques. The spectrum is then analyzed to determine the particle-size distribution. Two instruments based on this phenomenon are available, the Microtrac UPA (Fig. 20-6) [Trainer, Freud, and Weiss, *Pittsburgh Conference, Analytical and Applied Spectroscopy Symp. Particle Size Analysis* (March 1990)] and the Malvern Hi-C which operates in a similar manner to cover the size range  $0.015 \mu\text{m}$  to  $1 \mu\text{m}$  at concentrations from 0.01 to 50 percent solids.

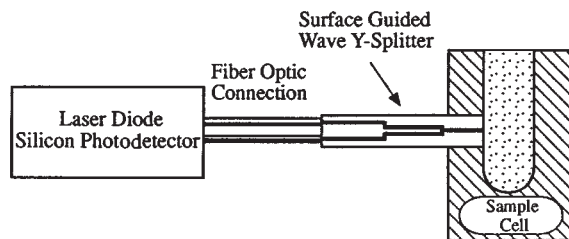
**Sieving Methods and Classification** Sieving is probably the most frequently used and abused method of analysis because the equipment, analytical procedure, and basic concepts are deceptively simple. In sieving, the particles are presented to equal-size apertures that constitute a series of go-no-go gauges. Sieve analysis presents three major difficulties: (1) with woven-wire sieves, the weaving process produces three-dimensional apertures with considerable tolerances, particularly for fine-woven mesh; (2) the mesh is easily damaged in use; (3) the particles must be efficiently presented to the sieve apertures.

Sieves are often referred to by their mesh size, which is the number of wires per linear unit. The U.S. Standard Sieve Series as described by the American Society of Testing and Materials (ASTM) document E-11-87 *Standard Specification for Wire-cloth Sieves for Testing Purposes* addresses sieve opening sizes from  $20 \mu\text{m}$  (635 mesh) to  $125 \text{mm}$  (5.00 in). Electroformed sieves with square or round apertures and tolerances of  $\pm 2 \mu\text{m}$ , are also available.

For coarse separation **dry sieving** is used, but other procedures are necessary as the powder becomes finer and more cohesive. Machine sieving is performed by stacking sieves in ascending order of aperture size and placing the powder on the top sieve. The most aggressive action is performed with Pascal Inclyno and Tyler Ro-tap sieves which combine a gyratory and jolting movement, although a simple vibratory action may be suitable in many cases. With the Air-Jet sieve a rotating jet below the sieving surface cleans the apertures and helps the passage of fines through the apertures. The sonic sifter combines two actions, a vertically oscillating column of air, and a repetitive mechanical pulse. Wet sieving is frequently used with cohesive powders.

**Elutriation Methods and Classification** In gravity elutriation the particles are classified, in a column, by a rising fluid current. In centrifugal elutriation the fluid moves inward against the centrifugal force. A *cyclone* is a centrifugal elutriator, though not usually so regarded (see Sec. 17: "Dust Collection Equipment"). The cyclosizer is a series of inverted cyclones with added apex chambers through which water flows. Suspension is fed into the largest cyclone and particles are separated into different size ranges.

**Surface Area Determination** The surface-to-volume ratio is an important powder property since it governs the rate at which a powder interacts with its surroundings. Surface area may be determined from size-distribution data or measured directly by flow through a powder bed or the adsorption of gas molecules on the powder surface. Other methods such as gas diffusion, dye adsorption from solution, and heats of adsorption have also been used. It is emphasized that a powder does not have a unique surface, unless the surface is considered to be absolutely smooth, and the magnitude of the measured surface depends upon the level of scrutiny (e.g., the smaller the gas molecules used for gas adsorption measurement the larger the measured surface).



**FIG. 20-6** Diagram of the Leeds and Northrup Ultrafine Particle Analyzer (UPA).

Gas adsorption is the preferred method of surface-area determination. An isotherm is generated of the amount of gas adsorbed against gas pressure, and the amount of gas required to form a monolayer is determined. The surface area can then be calculated using the cross-sectional area of the gas molecule. Outgassing of the powder before analysis should be conducted very carefully to ensure reproducibility. Commonly, nitrogen at liquid nitrogen vapor pressure is used but, for low surface-area powders, the adsorbed amounts of krypton or xenon are more accurately found. Many theories of gas adsorption have been advanced, but measurements are usually interpreted by using the BET theory [Brunauer, Emmett, and Teller, *J. Am. Chem. Soc.*, **60**, 309 (1938)].

In the **static method** the powder is isolated under high vacuum and surface gases driven off by heating the container. The container is next immersed in liquid nitrogen and known amounts of nitrogen vapor are admitted into the container at measured increasing pressures in the relative pressure range 0.05 to 0.35.

In the **dynamic method** the powder is flushed with an inert gas during degassing, nitrogen is then adsorbed on the powder in a carrier of helium gas at known relative pressure while the powder is in a container surrounded by liquid nitrogen. The changing concentration of nitrogen is measured by a calibrated conductivity cell so that the amount adsorbed can be determined.

**Permeametry** The flow of fluid through a packed bed of powder can be related to the surface area of the powder using the Carman-Arnell Equation [Carman and Arnell, *Can. J. Res.*, **26**, 128 (1948)]. Flow takes place through two mechanisms, viscous and diffusional flow. The latter term is often neglected leading to erroneous results [British Standard BS 4359: Part 2: (1982) *Determination of specific surface of powders. Recommended air permeability methods*]. Essentially, the pressure drop across the bed is directly related to the flow rate through it, and the constant of proportionality includes surface area. The assumptions made in deriving the equation are so sweeping that the derived value is better considered as a surface-related parameter.

**On-line Procedures** The growing trend toward automation in industry has resulted in many studies of rapid procedures for generating size information so that feedback loops can be instituted as an integral part of a process. Many of these techniques are modifications of more traditional methods. The problems associated with on-line methods include: allocation and preparation of a representative sample; analysis of the sample; evaluation of the results. The interface between the measuring apparatus and the process has the potential of high complexity, and consequently, high costs [Leschonski, *Particle Characterization*, **1**, 1 (July 1984)].

## PRINCIPLES OF SIZE REDUCTION

**GENERAL REFERENCES:** Annual reviews of size reduction, *Ind. Eng. Chem.*, October or November issues, by Work from 1934 to 1965, by Work and Snow in 1966 and 1967, and by Snow in 1968, 1969, and 1970; and in *Powder Technol.*, **5**, 351 (1972), and **7** (1973); Snow and Luckie, **10**, 129 (1973), **13**, 33 (1976), **23**(1), 31 (1979). *Chemical Engineering Catalog*, Reinhold, New York, annually. Cremer-Davies, *Chemical Engineering Practice*, vol. 3: *Solid Systems*, Butterworth, London, and Academic, New York, 1957. *Crushing and Grinding: A Bibliography*, Chemical Publishing, New York, 1960. *European Symposia on Size Reduction*: 1st, Frankfurt, 1962, publ. 1962, Rumpf (ed.), Verlag Chemie, Düsseldorf; 2d, Amsterdam, 1966, publ. 1967, Rumpf and Pietsch (eds.), *DECHEMA-Monogr.*, **57**; 3d, Cannes, 1971, publ. 1972, Rumpf and Schönert (eds.), *DECHEMA-Monogr.*, **69**. Gaudin, *Principles of Mineral Dressing*, McGraw-Hill, New York, 1939. International Mineral Processing Congresses: *Recent Developments in Mineral Dressing*, London, 1952, publ. 1953, Institution of Mining and Metallurgy; *Progress in Mineral Dressing*, Stockholm, 1957, publ. London, 1960, Institution of Mining and Metallurgy; 6th, Cannes, 1962, publ. 1965, Roberts (ed.), Pergamon, New York; 7th, New York, 1964, publ. 1965, Arbitrator (ed.), vol. 1: *Technical Papers*, vol. 2: *Milling Methods in the Americas*, Gordon and Breach, New York; 8th, Leningrad, 1968; 9th, Prague, 1970; 10th, London, 1973; 11th, Cagliari, 1975; 12th, São Paulo, 1977. Lowrison, *Crushing and Grinding*, CRC Press, Cleveland, 1974. *Pit and Quarry Handbook*, Pit & Quarry Publishing, Chicago, 1968. Richards and Locke, *Text Book of Ore Dressing*, 3d ed., McGraw-Hill, New York, 1940. Rose and Sullivan, *Ball, Tube and Rod Mills*, Chemical Publishing, New York, 1958. Snow, *Bibliography of Size Reduction*, vols. 1 to 9 (an update of the previous bibliography to 1973, including abstracts and index), U.S. Bur. Mines Rep. SO122069, available IIT Research Institute, Chicago, Ill. 60616. Stern, "Guide to Crushing and Grinding Practice," *Chem. Eng.*, **69**(25), 129 (1962). Taggart, *Elements of Ore Dressing*, McGraw-Hill, New York, 1951.

Since a large part of the literature is in the German language, availability of English translations is important. Translation numbers cited in this section refer to translations available through the National Translation Center, Library of Congress, Washington, DC. Also, volumes of selected papers in English translation are available from the Institute for Mechanical Processing Technology, Karlsruhe Technical University, Karlsruhe, Germany.

## PROPERTIES OF SOLIDS

**Grindability** is a measure of the rate of grinding of material in a particular mill (discussed later).

**Single-Particle Fracture** More fundamental knowledge of the breaking action occurring within mills depends on developing knowledge of the mechanism of single-particle fracture. The early workers [Smekal, *Z. Ver. Dtsch. Ing. Beh. Verfahrenstech.*, no. 6, 159–165 (1938), NTC translation 70-14798; and Smekal *Z. Ver. Dtsch. Ing.*, **81**(46), 1321–1326 (1937), NTC translation 70-14799] investigated

the breakage of cubes. This gives misleading results when cubes are crushed between platens because surface irregularities concentrate the load and give nonuniform load distribution. More meaningful measurements can be made with spheres, which approximate the shapes of particles broken in mills.

The force required to crush a single particle that is spherical near the contact regions is given by the equation of Hertz (Timoschenko and Goodier, *Theory of Elasticity*, 2d ed., McGraw-Hill, New York, 1951).

In an experimental and theoretical study on glass spheres Frank and Lawn [*Proc. R. Soc. (London)*, **A299**(1458), 291 (1967)] observed the repeated formation of ring cracks as increasing load was applied, causing the circle of contact to widen. Eventually a load is reached at which the crack deepens to form a cone crack, and at a sufficient load this propagates across the sphere to cause breakage into fragments. The authors' photographs show how the size of flaws that happen to be encountered at the edge of the circle of contact can result in a distribution of breakage strengths. Thus the mean value of breakage strength depends partly on intrinsic strength and partly on the extent of flaws present. From the measured breaking load and the Hertz theory one can calculate the apparent tensile strength  $\sigma_0$ , which is the maximum stress under the circle of contact normal to the direction of crack propagation. This tensile strength is the most appropriate one to use for breakage in mills, although the crushing strength of cubes still is often used as a rule of thumb. The propagation of cracks across spheres and disks has been recorded by high-speed spark cinematographs by Rumpf et al. (*Second European Symposium on Size Reduction*, op. cit., 1966, p. 57). They attempt to extend the Hertz theory deeper into the sphere although it is not valid far from the point of load application. The stress at points within the sphere far from the point of load application is given by the Boussinesque theory [Sternberg and Rosenthal, *J. Appl. Mech.*, **12**, 413 (1952); and Hiramatsu and Oka, *Int. J. Rock Mech. Min. Sci.*, **3**, 89 (1966)].

Snow and Paulding (Heywood Memorial Conference, Loughborough University, England, September 1973) observed that when breakage occurs, the finest fragments arise near the circle of contact where the stored internal stress is highest. They postulated that the fragment-size distribution could be calculated by assuming that the local fragment size is correlated with the locally stored stress energy just before fracture occurs. Calculated fragment-size distributions are roughly similar to those that they measured for glass spheres and various hard minerals as well as to distributions measured by Bergstrom and Sollenberger [*Trans. Am. Inst. Min. Metall. Pet. Eng.*, **220**, 373–

379 (1961)]. From this it can be concluded that the wide distribution of fragment sizes from milling is inherent in the breakage process itself and that attempts to improve grinding efficiency by weakening the particles will result in coarser fragments which may require a further break to reach the desired size.

Different mills are designed to apply the force in different ways [Rumpf, *Chem. Ing. Tech.*, **31**, 323–327 (1959), NTC translation 61-12395]. The detailed prediction of grinding rates and product-size distribution from mills awaits the development of a simulation model based on the physics of fracture. An initial attempt is that of Buss and Schubert (*Third European Symposium on Size Reduction*, op. cit., 1972, p. 233), who assume that mill performance is given by the sum of breakage events which are similar to *single-particle breakage experiments* in the laboratory. A paper by Schönert [*Trans. Am. Inst. Min. Metall. Pet. Eng.*, **252**(1), 21 (1972)] summarizes single-particle-breakage data from numerous publications from the Technical University of Karlsruhe, Germany. Hilding [Freiberg, *Forschungsh.*, **A480**, 19 (1970)] and Steier and Schönert (*Third European Symposium on Size Reduction*, op. cit., 1972, p. 135) report more experimental results on the probability of breakage of single particles by drop-weight experiments.

**Grindability** Grindability is the amount of product from a particular mill meeting a particular specification in a unit of grinding time e.g., tons per hour passing 200 mesh. The chief purpose of a study of grindability is to evaluate the size and type of mill needed to produce a specified tonnage and the power requirement for grinding. So many variables affect grindability that this concept can be used only as a rough guide to mill sizing; it says nothing about product-size distribution or type or size of mill. If a particular energy law is assumed, then the grinding behavior in various mills can be expressed as an energy coefficient or **work index** (discussed later). This more precise concept is limited by the inadequacies of these laws but often provides the only available information.

The technology based on grindability and energy considerations is being supplanted by computer simulation of milling circuits (see subsection "Simulation of Milling Circuits"), in which the gross concept of grindability is replaced by the **rate of breakage function** (sometimes called the selection function), which is the grindability of each particle size referred to the fraction of that size present.

Factors of hardness, elasticity, toughness, and cleavage are important in determining grindability. Grindability is related to modulus of elasticity and speed of sound in the material [Dahlhoff, *Chem. Ing. Tech.*, **39**(19), 1112–1116 (1967)].

The **hardness** of a mineral as measured by the **Mohs scale** is a criterion of its resistance to crushing [Fahrenwald, *Trans. Am. Inst. Min. Metall. Pet. Eng.*, **112**, 88 (1934)]. It is a fairly good indication of the abrasive character of the mineral, a factor that determines the wear on the grinding media. Arranged in increasing order of hardness, the Mohs scale is as follows: 1, talc; 2, gypsum; 3, calcite; 4, fluoride; 5, apatite; 6, feldspar; 7, quartz; 8, topaz; 9, corundum; and 10, diamond.

Materials of hardness 1 to 3 inclusive may be classed as soft; 4 to 7, as intermediate; and the others, as hard. Examples are:

**Soft Materials** (1) Talc, dried filter-press cakes, soapstone, waxes, aggregated salt crystals; (2) gypsum, rock salt, crystalline salts in general, soft coal; (3) calcite, marble, soft limestone, barites, chalk, brimstone.

**Intermediate Hardness** (4) Fluorite, soft phosphate, magnesite, limestone; (5) apatite, hard phosphate, hard limestone, chromite, bauxite; (6) feldspar, ilmenite, orthoclase, hornblendes.

**Hard Materials** (7) Quartz, granite; (8) topaz; (9) corundum, sapphire, emery; (10) diamond.

A hardness classification of stone based on the **compressive strength** of 1-in cubes is as follows, for loadings in pounds-force per square inch: very soft, 10,000; soft, 15,000; medium, 20,000; hard, 25,000; very hard, 30,000.

**Grindability Methods** Laboratory experiments on single particles have been used to correlate grindability. In the past it has usually been assumed that the total energy applied could be related to the grindability whether the energy is applied in a single blow or by repeated dropping of a weight on the sample [Gross and Zimmerly, *Trans. Am. Inst. Min. Metall. Pet. Eng.*, **87**, 27, 35 (1930)]. In fact, the

results depend on the way in which the force is applied (Axelson, Ph.D. thesis, University of Minnesota, 1949). In spite of this, the results of large mill tests can often be correlated within 25 to 50 percent by a simple test, such as the number of drops of a particular weight needed to reduce a given amount of feed to below a certain mesh size.

Two methods having particular application for coal are known as the ball-mill and Hardgrove methods. In the ball-mill method, the relative amounts of energy necessary to pulverize different coals are determined by placing a weighed sample of coal in a ball mill of a specified size and counting the number of revolutions required to grind the sample so that 80 percent of it will pass through a No. 200 sieve. The grindability index in percent is equal to the quotient of 50,000 divided by the average of the number of revolutions required by two tests (ASTM designation D-408).

In the **Hardgrove method** a prepared sample receives a definite amount of grinding energy in a miniature ball-ring pulverizer. The unknown sample is compared with a coal chosen as having 100 grindability. The Hardgrove grindability index =  $13 + 6.93W$ , where  $W$  is the weight of material passing the No. 200 sieve (see ASTM designation D-409).

Chandler [*Bull. Br. Coal Util. Res. Assoc.*, **29**(10), 333; (11), 371 (1965)] finds no good correlation of grindability measured on 11 coals with roll crushing and attrition, and so these methods should be used with caution. The Bond grindability method is described in the subsection "Capacity and Power Consumption."

Manufacturers of various types of mills maintain laboratories in which grindability tests are made to determine the suitability of their machines. When grindability comparisons are made on small equipment of the manufacturers' own class, there is a basis for scale-up to commercial equipment. This is better than relying on a grindability index obtained in a ball mill to estimate the size and capacity of different types such as hammer or jet mills.

## OPERATIONS

**Mill Wear** Wear of mill components costs nearly as much as the energy required for comminution, hundreds of millions of dollars a year. The finer stages of comminution result in the most wear, because the grinding effort is greatest, as measured by the energy input per unit of feed. Parameters that affect wear fall under three categories: (1) the ore, including hardness, presence of corrosive minerals, and particle size; (2) the mill, including composition, microstructure and mechanical properties of the material of construction, size of mill, and mill speed; and (3) the environment, including water chemistry and pH, oxygen potential, slurry solids content, and temperature [Moore et al., *International J. Mineral Processing*, **22**, 313–343 (1988)].

An abrasion index in terms of kilowatt-hour input per pound of metal lost furnishes a useful indication. Rough values are quoted in Table 20-3.

The use of hard-surfacing techniques by welding and by inserts has contributed greatly to better maintenance and lower downtime [Lutes and Reid, *Chem. Eng.*, **63**(6), 243 (1956)].

In *wet grinding* a synergy between mechanical wear and corrosion results in higher metal loss than with either mechanism alone [Iwasaki, *International J. Mineral Processing*, **22**, 345–360 (1988)]. This is due to removal of protective oxide films by abrasion, and by increased corrosion of stressed metal around gouge marks (Moore, loc. cit.). Wear rate is higher at lower solids content, since ball coating at high solids protects the balls from wear. This indicates that the mechanism is different from dry grinding. The rate without corrosion can be measured with an inert atmosphere such as nitrogen in the mill. Insertion of marked balls into a ball mill best measures the wear rate at conditions in industrial mills, so long as there is not a galvanic effect due to a different composition of the balls. The mill must be cleared of dissimilar balls before a new composition is tested. Sulfide ores promote corrosion due to galvanic coupling by a chemical reaction with oxygen present. Increasing the pH generally reduces corrosion.

The use of harder materials enhances wear resistance, but this conflicts with achieving adequate ductility to avoid catastrophic brittle failure, so these two effects must be balanced. Wear-resistant materials can be divided into three groups: (1) abrasion-resistant steels, (2)

TABLE 20-3 Abrasion Index Test Results\*

Material	Number tested	Product diameter, $\mu\text{m}$	Work index $E_i$	Average abrasion index† $A_i$
Alnico	1			0.3850
Alumina	6	15,500		0.6447
Asbestos cement pipe	1	13,330		0.0073
Cement clinker	2	12,100	10.9	0.0409
Cement raw material	4		10.5	0.0372
Chrome ore	1	10,200	9.6	0.1200
Coke	1		20.7	0.3095
Copper ore	12	12,900	11.2	0.0950
Coral rock	1			0.0061
Diorite	1		19.4	0.2303
Dolomite	5		11.3	0.0160
Gneiss	1		20.1	0.5360
Gold ore	2		14.8	0.2000
Granite	11	15,200	14.4	0.3937
Gravel	2		19.0	0.3051
Hematite	3		8.6	0.0952
Iron ore (misc.)	4		5.4	0.0770
Lead zinc ore	3		8.3	0.1520
Limestone	19	13,000	12.1	0.0256
Magnetite	3	14,400	16.8	0.0750
Magnetite	2		10.2	0.2517
Manganese ore	1		17.2	0.1133
Nickel ore	2		11.9	0.0215
Perlite	2			0.0452
Pumice	1		11.9	0.1187
Quartz	7		12.8	0.1831
Quartzite	3		12.2	0.6905
Rare earths	1			0.0288
Rhyolite	2	13,200		0.4993
Schist-biotite	1		23.5	0.1116
Shale	2	11,200	11.2	0.0060
Slag	1		15.8	0.0179
Slate	1		13.8	0.1423
Sulfur	1		11.5	0.0001
Taconite	7		16.2	0.6837
Trap rock	11	14,900	19.9	0.3860
Average		13,250	13.8	0.228

\*Alison-Chalmers Corporation.

†Abrasion index is the fraction of a gram weight lost by the standard steel paddle in 1 h of beating 1600 g of  $\frac{3}{4}$ - by  $\frac{1}{2}$ -in particles. The product averages 80 percent passing 13,250  $\mu\text{m}$ .

alloyed cast irons, and (3) nonmetallics [Durman, *International J. Mineral Processing*, **22**, 381–399 (1988)].

Manganese steel, containing 12 to 14 percent manganese and 1 to 1.5 percent carbon, is characterized by its exceptional toughness combined with adequate wear resistance, and enhanced by the austenitic microstructure having the ability to work harden. Although the relatively low yield strength can lead to problems of spreading in service, this can be compensated for by the addition of chromium or molybdenum; or by the use of a lower manganese grade (6–7 percent) also alloyed with up to 1 percent molybdenum. Applications are generally those involving the highest levels of stress, particularly by high-impact loading, such as jaw-crusher elements, gyratory cone-crusher mantles, and primary hammer-mill parts.

For medium- to high-impact applications a wide range of low-alloy steels are produced containing some chromium, molybdenum, phosphorus, and silicon. Economy of manufacture is a benefit for selection of these steels.

Low-alloy steel production falls into two metallurgical types. The traditional approach is heat treatment to produce a pearlitic microstructure. The other is to add sufficient alloying constituents to permit thermal processing to produce a martensitic structure. Typical applications are ball mill liners and grinding balls. Many of these components are consumed in high tonnages, and this combines with metallurgical characteristics to favor production by forging. Low-alloy steel liners, grates, and balls are also produced as castings.

Alloyed white cast irons fall into the second category. This group includes the nickel-chromium grades known as Ni-hards (Durman,

loc. cit.). These contain sufficient chromium to ensure solidification as a white cast iron (at least 2 percent), and sufficient nickel (normally at least 4 percent) to induce hardenability and prevent transformation to soft pearlitic iron. Grade 2 Ni-hard contains massive areas of ledeburite carbide within a matrix of austenite and martensite. Ni-hard 2 is a good general-purpose wear-resistant alloy, but is limited due to an inherent low level of toughness attributed to the presence of the carbide phase. It is suited to small-section components involving low-stress abrasion, such as secondary mill liners. Grade 4 Ni-hard typically contains 5 percent nickel and 8 percent chromium. This alloy is heat-treated to a martensitic matrix and has a modified carbide structure which improves toughness. It is more suited to thicker section castings where heat treatment can consistently control structure.

High-chromium cast irons contain between 12 and 30 percent chromium, 1.5 to 3.5 percent carbon, and frequently contain molybdenum and nickel as secondary constituents. They have become standard in most secondary and tertiary dry-grinding applications (Durman, loc. cit.). These alloys form a metastable austenite structure on casting. Subsequent thermal processing forms secondary chromium-carbide particles dispersed through the matrix. This depletes the austenite of alloy content and facilitates transformation to martensite on quenching. The chromium carbide results in a slightly higher level of toughness than Ni-hard, and higher wear resistance because of greater hardness of chromium carbide. Molybdenum may be added to increase hardenability in heavy sections. Elimination of austenite in the structure can improve resistance to spalling, although spalling limits the range of uses. Hardness can range from 52 to 65 Rockwell. For ball mill balls the dry wear rate is often  $\frac{1}{10}$  that of cast or forged steel. The cost is 2–3 times as great, so there is an economic advantage. In wet grinding, however, the wear rate of chrome alloys is greater, so the cost may not be competitive. For ring-roll mills, high-chromium molybdenum parts have improved wear costs over use of Ni-hard, and also reduced labor costs for maintenance.

Recent nonmetallic developments include natural rubber, polyurethane, and ceramics. Rubber, due to its high resilience, is extremely wear-resistant in low-impact abrasion. It is inert to corrosive wear in mill liners, pipe linings, and screens. It is susceptible to cutting abrasion, so that wear increases in the presence of heavy particles which penetrate, rather than rebound from the wear surface. Rubber can also swell and soften in solvents. Advantages are its low density leading to energy savings, ease of installation, and sound-proofing qualities. Polyurethane has similar resilient characteristics. Its fluidity at the formation stage makes it suitable for the production of the wearing surface of screens, diaphragms, grates, classifiers, and pump and flotation impellers. The low heat tolerance of elastomers limits their use in dry processing where heat may build up.

Ceramics fill a specialized niche in comminution where metallic contamination cannot be tolerated. Therefore ceramics are used for milling cements and pigments. Ceramic tiles have been used for lining roller mills and chutes and cyclones, where there is a minimum of impact.

**Safety** The explosion hazard of such nonmetallic materials as sulfur, starch, wood flour, cereal dust, dextrin, coal, pitch, hard rubber, and plastics is often not appreciated (Hartmann and Nagy, U.S. Bur. Mines Rep. Invest. 3751, 1944). Explosions and fires may be initiated by discharges of static electricity, sparks from flames, hot surfaces, and spontaneous combustion. Metal powders present a hazard because of their **flammability**. Their combustion is favored during grinding operations in which ball, hammer, or ring-roller mills are employed and during which a high grinding temperature may be reached.

Many finely divided metal powders in suspension in air are potential **explosion hazards**, and causes for ignition of such dust clouds are numerous [Hartmann and Greenwald, *Min. Metall.*, **26**, 331 (1945)]. Concentration of the dust in air and its particle size are important factors that determine explosibility. Below a lower limit of concentration, no explosion can result because the heat of combustion is insufficient to propagate it. Above a maximum limiting concentration, an explosion cannot be produced because insufficient oxygen is available. The finer the particles, the more easily is ignition accomplished and the more rapid is the rate of combustion. This is illustrated in Fig. 20-7.

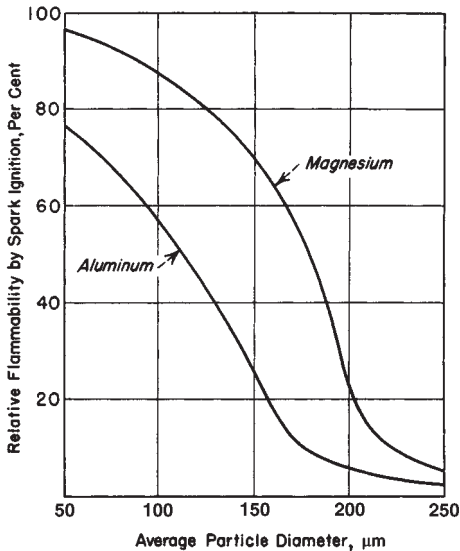


FIG. 20-7 Effect of fineness on the flammability of metal powders. (Hartmann, Nagy, and Brown, U.S. Bur. Mines Rep. Invest. 3722, 1943.)

Isolation of the mills, use of nonsparking materials of construction, and magnetic separators to remove foreign magnetic material from the feed are useful precautions (Hartman, Nagy, and Brown, U.S. Bur. Mines Rep. Invest. 3722, 1943). Stainless steel has less sparking tendency than ordinary steel or forgings.

Reduction of the oxygen content of air present in grinding systems is a means for preventing dust explosions in equipment (Brown, U.S. Dep. Agri. Tech. Bull. 74, 1928). Maintenance of oxygen content below 12 percent should be safe for most materials, but 8 percent is recommended for sulfur grinding. The use of inert gas has particular adaptation to pulverizers equipped with air classification; flue gas can be used for this purpose, and it is mixed with the air normally present in a system (see subsection "Chemicals and Soaps" for sulfur grinding). Despite the protection afforded by the use of inert gas, equipment should be provided with explosion vents, and structures should be designed with venting in mind [Brown and Hanson, *Chem. Metall. Eng.*, 40, 116 (1933)].

Hard rubber presents a fire hazard when reduced on steam-heated rolls (see subsection "Organic Polymers"). Its dust is explosive [Twiss and McGowan, *India Rubber J.*, 107, 292 (1944)].

An annual publication, *National Fire Codes for the Prevention of Dust Explosions*, is available from the National Fire Protection Association, Quincy, Massachusetts, and should be of interest to those handling hazardous powders.

### ATTAINABLE PRODUCT SIZE AND ENERGY REQUIRED

The fineness to which a material is ground has a marked effect on its production rate. Figure 20-8 is an example showing how the capacity decreases and the specific energy and cost increase as the product is ground finer.

Concern about the rising cost of energy has led to publication of a report (National Materials Advisory Board, *Comminution and Energy Consumption*, Publ. NMAB-364, National Academy Press, Washington, 1981; available National Technical Information Service, Springfield, Va. 22151). This has shown that United States industries use approximately 32 billion kWh of electrical energy per annum in size-reduction operations. More than half of this energy is consumed in the crushing and grinding of minerals, one-quarter in the production of cement, one-eighth in coal, and one-eighth in agricultural products. The report recommends that five areas be considered to save energy: classification-device design, mill design, control, addi-

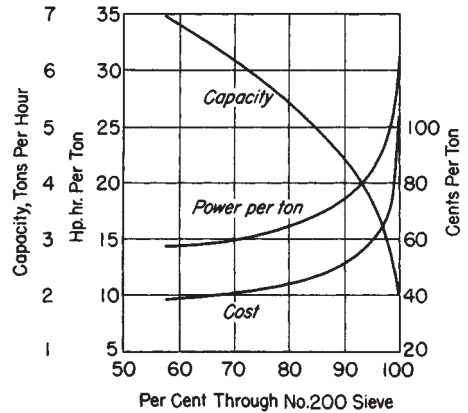


FIG. 20-8 Variation in capacity, power, and cost of grinding relative to fineness of product.

tives, and materials to resist wear. It reviews these areas with an extensive bibliography.

**Energy Laws** Several laws have been proposed to relate size reduction to a single variable, the energy input to the mill. These laws are encompassed in a general differential equation (Walker, Lewis, McAdams, and Gilliland, *Principles of Chemical Engineering*, 3d ed., McGraw-Hill, New York, 1937):

$$dE = -C dX/X^n \tag{20-10}$$

where  $E$  is the work done,  $X$  is the particle size, and  $C$  and  $n$  are constants. For  $n = 1$  the solution is *Kick's law* (Kick, *Das Gesetz der proportionalen Widerstande und seine Anwendung*, Leipzig, 1885). The law can be written

$$E = C \log (X_f/X_p) \tag{20-11}$$

where  $X_f$  is the feed-particle size,  $X_p$  is the product size, and  $X_f/X_p$  is the reduction ratio. For  $n > 1$  the solution is

$$E = \left(\frac{C}{n-1}\right) \left(\frac{1}{X_p^{n-1}} - \frac{1}{X_f^{n-1}}\right) \tag{20-12}$$

For  $n = 2$  this becomes *Rittinger's law*, which states that the energy is proportional to the new surface produced (Rittinger, *Lehrbuch der Aufbereitungskunde*, Ernst und Korn, Berlin, 1867).

The *Bond law* corresponds to the case in which  $n = 1.5$  [Bond, *Trans. Am. Inst. Min. Metall. Pet. Eng.*, 193, 484 (1952)]:

$$E = 100E_i \left(\frac{1}{\sqrt{X_p}} - \frac{1}{\sqrt{X_f}}\right) \tag{20-13}$$

where  $E_i$  is the **Bond work index**, or work required to reduce a unit weight from a theoretical infinite size to 80 percent passing 100 μm. Extensive data on the work index have made this law useful for rough mill sizing. Summary data are given in Table 20-4.

The work index may be found experimentally from laboratory crushing and grinding tests or from commercial mill operations. Some rules of thumb for extrapolating the work index to conditions different from those measured are that for dry grinding the index must be increased by a factor of 1.34 over that measured in wet grinding; for open-circuit operations another factor of 1.34 is required over that measured in closed circuit; if the product size  $X_p$  is extrapolated below 70 μm, an additional correction factor is  $(10.3 + X_p)/1.145X_p$ . Also for a jaw or gyratory crusher the work index may be estimated from

$$E_i = 2.59C_s/\rho_s \tag{20-14}$$

where  $C_s$  = impact crushing resistance, (ft · lb)/in of thickness required to break;  $\rho_s$  = specific gravity; and  $E_i$  is expressed in kWh/ton.

None of the energy laws apply well in practice, and they have failed to yield a starting point for further development of understanding of milling. They are mainly of historical interest. Most of the early papers

TABLE 20-4 Average Work Indices for Various Materials\*

Material	No. of tests	Specific gravity	Work index†	Material	No. of tests	Specific gravity	Work index†
All materials tested	2088	—	13.81	Taconite	66	3.52	14.87
Andesite	6	2.84	22.13	Kyanite	4	3.23	18.87
Barite	11	4.28	6.24	Lead ore	22	3.44	11.40
Basalt	10	2.89	20.41	Lead-zinc ore	27	3.37	11.35
Bauxite	11	2.38	9.45	Limestone	119	2.69	11.61
Cement clinker	60	3.09	13.49	Limestone for cement	62	2.68	10.18
Cement raw material	87	2.67	10.57	Manganese ore	15	3.74	12.46
Chrome ore	4	4.06	9.60	Magnesite, dead burned	1	5.22	16.80
Clay	9	2.23	7.10	Mica	2	2.89	134.50
Clay, calcined	7	2.32	1.43	Molybdenum	6	2.70	12.97
Coal	10	1.63	11.37	Nickel ore	11	3.32	11.88
Coke	12	1.51	20.70	Oil shale	9	1.76	18.10
Coke, fluid petroleum	2	1.63	38.60	Phosphate fertilizer	3	2.65	13.03
Coke, petroleum	2	1.78	73.80	Phosphate rock	27	2.66	10.13
Copper ore	308	3.02	13.13	Potash ore	8	2.37	8.88
Coral	5	2.70	10.16	Potash salt	3	2.18	8.23
Diorite	6	2.78	19.40	Pumice	4	1.96	11.93
Dolomite	18	2.82	11.31	Pyrite ore	4	3.48	8.90
Emery	4	3.48	58.18	Pyrrhotite ore	3	4.04	9.57
Feldspar	8	2.59	11.67	Quartzite	16	2.71	12.18
Ferrochrome	18	6.75	8.87	Quartz	17	2.64	12.77
Ferromanganese	10	5.91	7.77	Rutile ore	5	2.84	12.12
Ferrosilicon	15	4.91	12.83	Sandstone	8	2.68	11.53
Flint	5	2.65	26.16	Shale	13	2.58	16.40
Fluorspar	8	2.98	9.76	Silica	7	2.71	13.53
Gabbro	4	2.83	18.45	Silica sand	17	2.65	16.46
Galena	7	5.39	10.19	Silicon carbide	7	2.73	26.17
Garnet	3	3.30	12.37	Silver ore	6	2.72	17.30
Glass	5	2.58	3.08	Sinter	9	3.00	8.77
Gneiss	3	2.71	20.13	Slag	12	2.93	15.76
Gold ore	209	2.86	14.83	Slag, iron blast furnace	6	2.39	12.16
Granite	74	2.68	14.39	Slate	5	2.48	13.83
Graphite	6	1.75	45.03	Sodium silicate	3	2.10	13.00
Gravel	42	2.70	25.17	Spodumene ore	7	2.75	13.70
Gypsum rock	5	2.69	8.16	Syenite	3	2.73	14.90
Ilmenite	7	4.27	13.11	Tile	3	2.59	15.53
Iron ore	8	3.96	15.44	Tin ore	9	3.94	10.81
Hematite	79	3.76	12.68	Titanium ore	16	4.23	11.88
Hematite—specular	74	3.29	15.40	Trap rock	49	2.86	21.10
Oolitic	6	3.32	11.33	Uranium ore	20	2.70	17.93
Limanite	2	2.53	8.45	Zinc ore	10	3.68	12.42
Magnetite	83	3.88	10.21				

\* Allis-Chalmers Corporation.

† Caution should be used in applying the average work index values listed here to specific installations, since individual variations between materials in any classification may be quite large.

supporting one law or another were based on extrapolations of size distributions to finer sizes on the assumption of one or another size-distribution law. With present particle-size-analysis techniques applicable to the finest sizes, such confusion is no longer necessary. The relation of energy expenditure to the size distribution produced has been thoroughly examined [Arbiter and Bhrany, *Trans. Am. Inst. Min. Metall. Pet. Eng.*, **217**, 245–252 (1960); Harris, *Inst. Min. Metall. Trans.*, **75**(3), C37 (1966); Holmes, *Trans. Inst. Chem. Eng. (London)*, **35**, 125–141 (1957); and Kelleher, *Br. Chem. Eng.*, **4**, 467–477 (1959); **5**, 773–783 (1960)].

**Grinding Efficiency** The energy efficiency of a grinding operation is defined as the energy consumed compared with some ideal energy requirement.

The theoretical energy efficiency of grinding operations is 0.06 to 1 percent, based on values of the surface energy of quartz [Martin, *Trans. Inst. Chem. Eng. (London)*, **4**, 42 (1926); Gaudin, *Trans. Am. Inst. Min. Metall. Pet. Eng.*, **73**, 253 (1926)]. Uncertainty in these results is due to uncertainty in the theoretical surface energy.

A definitive monograph (Kuznetsov, *Surface Energy of Solids*, English translation, H. M. Stationery Office, London, 1957) established that most laboratory methods of measuring surface energy introduce large errors, but the cleavage method of Obreimov [Gilman, *J. Appl. Phys.*, **31**, 2208 (1960)] gave results for sodium chloride that agree with theoretical lattice calculations. Later studies by Raasch [*Int. J. Frac. Mech.*, **7**(9), 289 (1971)] and by Burns [*Philos.*

*Mag.*, **25**(1), 131 (1972)] conclude that these measurements are valid when 50 percent corrections are added for the bending energy of the crystal. Kuznetsov ranks other materials by a relative wear test. His results substantiate the efficiencies given earlier. Attempts to measure efficiency of the grinding process by calorimetry involve errors that exceed the theoretical surface energy of the material being ground.

**Practical energy efficiency** is defined as the efficiency of technical grinding compared with that of laboratory crushing experiments. Practical efficiencies of 25 to 60 percent have been shown [Wilson, *Min. Technol.*, Tech. Publ. 810, 1937; and Bond and Maxson, *Trans. Am. Inst. Min. Metall. Pet. Eng.*, **134**, 296 (1939)].

An **energy coefficient** is sometimes based on Rittinger's law, i.e., new surface produced per unit of energy input. Usually time of grinding is the experimental variable, which is expressed indirectly as energy. The energy coefficient may also be expressed as tons per horsepower-hour passing a certain size. The value of this coefficient is between about 0.02 and 0.1 for wet ball-mill pulverizing hard to medium-hard minerals to No. 200 sieve size (74  $\mu$ m).

The curves in Fig. 20-9 show decreasing production rate with increasing **moisture content**. (Occasionally, a small amount of water may be beneficial over complete dryness.) All three materials were being ground to 99.9 percent through a No. 200 sieve.

**Fine Size Limit** (See also Single-Particle Fracture above.)

It has long been thought that a **limiting size** is attainable. New technologies such as pressed ceramics and Xerox toners require finer sizes,

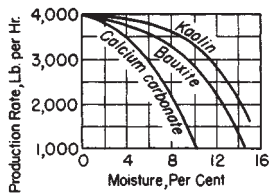


FIG. 20-9 Effect of moisture on the production rate of a pulverizer. [Work, Chem. Metall. Eng., **40**, 306 (1933).]

and this again questions the existence of a limit. There are three theories for such a limit. Bradshaw [*J. Chem. Phys.*, **19**, 1057-1059 (1951)] thought that *reagglomeration* is responsible, especially in ball mills. Schönert and Steier [*Chem. Ing. Tech.*, **43**(13), 773 (1971)] suggest two other causes: *plastic deformation* and the difficulty of *stressing* fine particles to their breaking point. The latter stems from the Griffith crack theory, which requires that the particle have enough stored stress energy to allow a crack to propagate. A 10- $\mu\text{m}$  glass particle requires 140 kPa/mm<sup>2</sup> tensile stress. Although both of these mechanisms can be limiting, recent experimental evidence indicates that plastic deformation can increase the resistance of even the most brittle materials on a fine scale. Rumpf and Schönert (*Third European Symposium on Size Reduction*, op. cit., 1972, p. 27) observed plastic deformation in crushing fine glass spheres. Schönert and Steier (loc. cit.) in electron-microscope photographs observed plastic deformation in crushing limestone particles as large as 3 to 4  $\mu\text{m}$  and quartz particles of 2 to 3  $\mu\text{m}$ . This deformation spreads a stress that would otherwise produce brittle fracture. Gane [*Philos. Mag.*, **25**(1), 25 (1972)] observed plastic deformation in magnesium oxide crystals 0.2 to 0.4  $\mu\text{m}$  in size. The strengths average 180 kg/mm<sup>2</sup>, which is 15 times the strength of large MgO crystals but one-tenth of the theoretical strength. Further proof is given by Weichert and Schönert [*J. Mech. Phys. Solids*, **22**, 127 (1974)], who analyze and measure the temperature rise at a propagating crack tip. They estimate that irreversible deformation occurs in a zone of radius about 30 A running along at the tip. The energy release causes temperatures as high as 1500 K above ambient temperature at the tip. This temperature explains plastic flow and even emitted light in some cases. Therefore, it is proved that plastic deformation can limit the grinding size attainable. Other means than size reduction must be found if particles much finer than 0.5  $\mu\text{m}$  are wanted.

**Dry versus Wet Grinding** (See under Ball Mills, and Wear.) In practice it is found that finer size can be achieved by **wet grinding** than by **dry grinding**. In wet grinding by ball mills or vibratory mills with suitable surfactants, product sizes of 0.5  $\mu\text{m}$  are attainable. In dry grinding the size is generally limited by ball coating (Bond and Agthe, *Min. Technol.*, AIME Tech. Publ. 1160, 1940) to about 15  $\mu\text{m}$ . In dry grinding with hammer mills or ring-roller mills the limiting size is about 10 to 20  $\mu\text{m}$ . Jet mills are generally limited to a product mean size of 15  $\mu\text{m}$ , although dense particles can be ground to 5  $\mu\text{m}$  because of the greater ratio of inertia to aerodynamic drag.

**Dispersing Agents and Grinding Aids** There is no doubt that grinding aids are helpful under some conditions. For example, surfactants make it possible to ball-mill magnesium in kerosene to 0.5- $\mu\text{m}$  size [Fochtman, Bitten, and Katz, *Ind. Eng. Chem. Prod. Res. Dev.*, **2**, 212-216 (1963)]. Without surfactants the size attainable was 3  $\mu\text{m}$ , and of course the rate of grinding was very slow at sizes below this. Also, the water in wet grinding may be considered to act as an additive.

Chemical agents that increase the rate of grinding are an attractive prospect since their cost is low. However, despite a voluminous literature on the subject, there is no accepted scientific method to choose such aids; there is not even agreement on the mechanisms by which they work. The subject has been recently reviewed [Fuerstenau, *KONA Powder and Particle*, **13**, 5-17 (1995)].

In wet grinding there are several theories, which have been reviewed [Somasundaran and Lin, *Ind. Eng. Chem. Process Des. Dev.*, **11**(3), 321 (1972); Snow, annual reviews, op. cit., 1970-1974. See also Rose, *Ball and Tube Milling*, Constable, London, 1958, pp. 245-249]. The *Rehbinder theory* (Rehbinder, Schreiner, and Zhi-

gach, *Hardness Reducers in Rock Drilling*, Moscow Academy of Science, 1944, transl. Council for Scientific and Industrial Research, Melbourne, Australia, 1948).

Additives can alter the rate of wet ball milling by changing the slurry viscosity or by altering the location of particles with respect to the balls. These effects are discussed under "Tumbling Mills." In conclusion, there is still no theoretical way to select the most effective additive. Empirical investigation, guided by the principles discussed earlier, is the only recourse. There are a number of commercially available grinding aids that may be tried. Also, a kit of 450 surfactants that can be used for systematic trials (Model SU-450, Chem Service Inc., West Chester, PA 19380) is available.

Numerous experimental studies lead to the conclusion that dry grinding is limited by ball coating and that additives function by reducing the tendency to coat (Bond and Agthe, op. cit.). Most materials coat if they are ground fine enough, and softer materials coat at larger sizes than hard materials. The presence of more than a few percent of soft gypsum promotes ball coating in cement-clinker grinding. The presence of a considerable amount of coarse particles above 35 mesh inhibits coating. Balls coat more readily as they become scratched. Small amounts of moisture may increase or decrease ball coating, and dry materials also coat.

Materials used as grinding aids include solids such as graphite, oleoresinous liquid materials, volatile solids, and vapors. The complex effects of vapors have been extensively studied [Goette and Ziegler, *Z. Ver. Dtsch. Ing.*, **98**, 373-376 (1956); and Locher and von Seebach, *Ind. Eng. Chem. Process Des. Dev.*, **11**(2), 190 (1972)], but water is the only vapor used in practice.

The most effective additive for dry grinding is fumed silica that has been treated with methyl silazane [Tulis, *J. Hazard. Mater.*, **4**, 3 (1980)].

## SIZE REDUCTION COMBINED WITH OTHER OPERATIONS

Practically every solid material undergoes size reduction at some point in its processing cycle. Some of the reasons for size reduction are: (1) to liberate a desired component for subsequent separation, as in separating ores from gangue; (2) to prepare the material for subsequent chemical reaction, i.e., by enlarging the specific surface as in cement manufacture; (3) to subdivide the material so that it can be intimately blended with other components; (4) to meet a size requirement for the quality of the end product, as in fillers or pigments for paints, plastics, agricultural chemicals etc.; (5) to prepare wastes for recycling.

**Systems Involving Size Reduction** Industrial applications usually involve a number of processing steps combined with size reduction [Hixon, *Chemical Engineering Progress*, **87**, 36-44 (May 1991)]. The most common of these is **size classification**. Often only a particular range of product sizes is wanted for a given application. Since the particle breakage process always yields a spectrum of sizes, the product size can not be directly controlled; however, mill operation can sometimes be varied to produce less fines at the expense of producing more coarse particles. By recycling the classified coarse fraction and regrinding it, production of the wanted size range is optimized. Such an arrangement of classifier and mill is called a **mill circuit**, and is dealt with further below.

More complex systems may include several unit operations such as mixing (Sec. 18), drying (Sec. 12), and agglomerating (see Size Enlargement, this section). Inlet and outlet silencers are helpful to reduce noise from high-speed mills. Chillers, air coolers, and explosion proofing may be added to meet requirements. Weighing and packaging facilities complete the system.

Batch ball mills with low ball charges can be used in dry mixing or standardizing of dyes, pigments, colors, and insecticides to incorporate wetting agents and inert extenders (see also Sec. 21). Disk mills, hammer mills, and other high-speed disintegration equipment are useful for final intensive blending of insecticide compositions, earth colors, cosmetic powders, and a variety of other finely divided materials that tend to agglomerate in ribbon and conical blenders. Liquid sprays or gases may be injected into the mill or air stream, for mixing with the material being pulverized to effect chemical reaction or surface treatment.

The **drying** of materials while they are being pulverized or disintegrated is known variously as “flash” or “dispersion” drying; a generic term is “pneumatic conveying” drying. Data for the grinding and drying of bauxite in a ring-roller mill are given in Table 20-5. A drying system is shown under “Clays and Kaolins,” Fig. 20-58.

**Milling Problems** Materials with low-softening temperatures, such as chocolate, are amenable to pulverizing if proper temperature control is exercised. Compositions containing fats and waxes are pulverized and blended readily if refrigerated air is introduced into their grinding systems (U.S. Patents 1,739,761 and 2,098,798; see also subsection “Organic Polymers” and Hixon loc. cit. for flow sheets). Some materials, such as salt, are very hygroscopic; they pick up water from air and deposit on mill surfaces, forming a hard cake. Mills with air-classification units may be equipped so that the circulating air can be conditioned by mixing with hot or cold air or gases introduced into the mill or by dehumidification to prepare the air for the grinding of hygroscopic materials. Flow sheets including air dryers are also described by Hixon. All organic materials and most metals can form **flammable** or **explosive** mixtures with air (see Safety above). The feed material may be toxic, bioreactive or radioactive, requiring isolation. This may best be accomplished by batch operation. Or the material may be corrosive to mill components. Iron contamination from wear or corrosion of the mill is often a problem. Jet milling is used to produce ultrapure materials for semiconductor manufacture.

**Continuous Operation** Advantages, which can be very important (Hixon, loc. cit.), are: (1) There is increased economical operation. Less time is needed for start-up and shutdown, and often less maintenance is needed. Because the operating conditions are constant, less operator attention may be needed, and automatic control is more readily applied. (2) It may be more feasible to increase the scale of a continuous system, thus improving unit economy. (3) There is better quality control. This may be the major benefit. Once the operating parameters are properly set, the continuous system will provide a more consistent product. (4) The improvement of the competitive position. A clever arrangement of a system may give an advantage either in product quality or cost. The disadvantages of a continuous system are (1) increased complexity of equipment over batch processing, and (2) the need for more thorough planning, usually requiring pilot-scale testing.

Some special requirements of continuous systems are: (1) Metering the feed. A continuous system must be fed at a precise, uniform rate. (See Sec. 21.) (2) Dust collection. This is a necessary part of most dry-processing systems. Filters are available that can effectively remove dust down to 10 mg/m<sup>3</sup> or less, and operate automatically. (Dust collection is covered in Sec. 17.) (3) On-line analysis. For more precise operation, on-line analysis of product particle size and composition may be desirable. (4) Computer control. Simulation can aid in optimizing system design and computer control.

**Beneficiation** Ball and pebble mills, batch or continuous, offer considerable opportunity for combining a number of **processing steps** that include grinding [Underwood, *Ind. Eng. Chem.*, **30**, 905 (1938)]. Mills followed by air classifiers can serve to **separate components of mixtures** because of differences in specific gravity and

**TABLE 20-5 Operating Data for Grinding and Drying of Bauxite in a Ring-Roller Mill**

Initial moisture, %	9.75
Final moisture, %	0.75
Feed, lb./hr	12,560
Product, lb./hr	11,420
Moisture evaporated, lb	1,140
Temperature of gases entering mill, °F	700
Temperature of gases leaving mill, °F	170
Temperature of feed, °F	70
Temperature of material leaving mill, °F	150
Oil consumed, gal	14.3
Heating value of oil, B.t.u./gal	142,000
Thermal efficiency, %	68.5
Total power for drying and pulverizing, hp	105
Power for drying, hp	10
Final product, % through No. 100 sieve	90

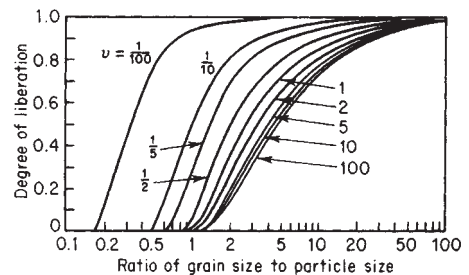
particle size. The removal of impurities by this means is known as **cleaning**, **concentrating**, or **beneficiating**. Screens are used to separate coarse particles, not easily pulverized, from fine particles of the component that are pulverized readily. Grinding followed by *froth flotation* has become the beneficiation method most widely used for metallic ores and also for nonmetallic minerals such as feldspar. Magnetic separation is the chief means used for upgrading taconite iron ore (see subsection “Ores and Minerals”). Magnetic separators frequently are employed to remove tramp magnetic solids from the feed to high-speed hammer and disk mills.

**Liberation** Most ores are heterogeneous, and the objective of grinding is to release the valuable mineral component so that it can be separated. Calculations based on a random-breakage model assuming no preferential breakage [Wiegel and Li, *Trans. Am. Inst. Min. Metall. Pet. Eng.*, **238**, 179–191 (1967)] agreed at least in general trends with plant data on the efficiency of release of mineral grains. Figure 20-10 shows that the desired mineral *B* can be liberated by coarse grinding when the grade is high so that mineral *A* becomes a small fraction and mineral *B* a large fraction of the total volume; mineral *B* can be liberated only by fine grinding below the grain size, when the grade is low so that there is a small proportion of grains of *B*. Similar curves, somewhat displaced in size, resulted from a more detailed integral geometry analysis by Barbery [*Minerals Engineering*, **5**(2), 123–141 (1992)]. There is at present no way to measure grain size on-line, and thus to control liberation. The current status of liberation modeling is given by Mehta et al. [*Powder Technology*, **58**(3), 195–209 (1989)].

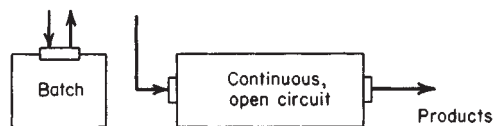
Many authors have assumed that breakage occurs preferentially along grain boundaries, but there is scant evidence for this. On the contrary, Gorski [*Bull. Acad. Pol. Sci. Ser. Sci. Tech.*, **20**(12), 929 (1972); CA 79, 20828sk], from analysis of microscope sections, finds an intercrystalline character of comminution of dolomite regardless of the type of crusher used.

The liberation of a valuable constituent does not necessarily translate directly into recovery in downstream processes. For example, flotation tends to be more efficient in intermediate sizes than at coarse or fine sizes [McIvor and Finch, *Minerals Engineering*, **4**(1), 9–23 (1991)]. For coarser sizes, failure to liberate may be the limitation; finer sizes that are liberated may still be carried through by the water flow. A conclusion is that overgrinding should be avoided by judicious use of size classifiers with recycle grinding.

**Size Reduction Combined with Size Classification** Grinding systems are batch or continuous in operation (Fig. 20-11). Most large-scale operations are continuous; batch ball or pebble mills are used



**FIG. 20-10** Fraction of mineral *B* that is liberated as a function of volumetric abundance ratio  $v$  of gangue to mineral *B* ( $1/\text{grade}$ ), and ratio of grain size to particle size of broken fragments ( $1/\text{fineness}$ ). [Wiegel and Li, *Trans. Soc. Min. Eng.-Am. Inst. Min. Metall. Pet. Eng.*, **238**, 179 (1967).]



**FIG. 20-11** Batch and continuous grinding systems.



only when small quantities are to be processed. Batch operation involves a high labor cost for charging and discharging the mill.

Continuous operation is accomplished in open or closed circuit, as illustrated in Figs. 20-11 and 20-12. **Operating economy** is the object of closed-circuit grinding with size classifiers. The idea is to remove the material from the mill before all of it is ground, separate the fine product in a classifier, and return the coarse for regrinding with the new feed to the mill. A mill with the fines removed in this way performs much more efficiently. Coarse material returned to a mill by a classifier is known as the **circulating load**; its rate may be from 1 to 10 times the production rate. The ability of the mill to transport material may limit the recycle rate; tube mills for use in such circuits may be designed with a smaller length-to-diameter ratio and hence a larger hydraulic gradient for more flow or with compartments separated by diaphragms with lifters.

**Internal size classification** plays an essential role in the functioning of machines for dry grinding in the fine-size range; particles are retained in the grinding zone until they are as small as required in the finished product; then they are allowed to discharge.

By closed-circuit operation the product size distribution is narrower and will have a larger proportion of particles of the desired size. On the other hand, making a *product size within narrow limits* (such as between 20 and 40  $\mu\text{m}$ ) is often requested but usually is not possible regardless of the grinding circuit used. The reason is that particle breakage is a random process, both as to the probability of breakage of particles and as to the sizes of fragments produced from each breakage event. The narrowest size distribution ideally attainable is one that has a slope of 1.0 when plotted on Gates-Gaudin-Schumann coordinates [Eq. (20-2) and Fig. 20-13]. This can be demonstrated by examining the Gaudin-Meloy size distribution [Eq. (20-4)]. This is the distribution produced in a mill when particles are cut into pieces of random size, with  $r$  cuts per event. The case in which  $r$  is large corresponds to a breakage event producing many fines. The case in which  $r$  is 1 corresponds to an ideal case such as a knife cutter, in which each particle is cut once per event and the fragments are removed immediately by the classifier. The Meloy distribution with  $r = 1$  reduces to the Schumann distribution with a slope of 1.0. Therefore, no practical grinding operation can have a slope greater than 1.0. Slopes typically range from 0.5 to 0.7. The specified product may still be made, but the finer fraction may have to be disposed of in some way. Within these limits, the size distribution of the classifier product depends both on the recycle ratio and on the sharpness of cut of the classifier used.

**Characteristics of Size Classifiers** (See Sec. 19: "Screening" on screening equipment and "Wet Classification" on wet classifiers.) Types of classifiers and commercially available equipment are de-

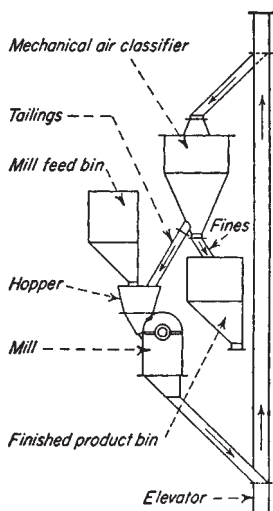


FIG. 20-12 Hammer mill in closed circuit with an air classifier.

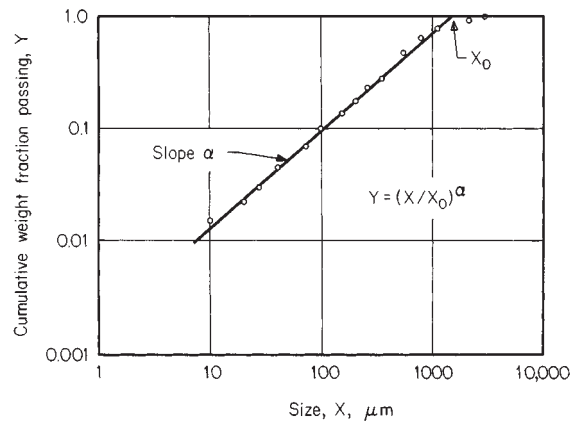


FIG. 20-13 Example of a Gates-Gaudin-Schumann plot of mill-product-size distribution.

scribed in the subsection "Particle-Size Classifiers Used with Grinding Mills." The American Institute of Chemical Engineers Equipment Testing Procedures Committee has published a procedure for particle-size classifiers (*Particle-Size Classifiers—A Guide to Performance Evaluation*, 2d ed. American Institute of Chemical Engineers, New York, 1994), including definitions which are followed here.

Three parameters define the performance of a classifier. These are *cut size*, *sharpness of cut*, and *capacity*. Cut size,  $X_{50}$ , is the size at which 50 percent of the material goes into the coarse product and 50 percent into the fine. (This should not be confused with the "cutoff size," a name sometimes given to the top size of the fine product.)

**Size selectivity** is the most thorough method of expressing classifier performance under a given set of operating conditions. Cut size and sharpness can be calculated from size-selectivity data. Size selectivity is defined by

$$\eta_x = \frac{\text{quantity of size } X \text{ entering coarse fraction}}{\text{quantity of size } X \text{ in feed}} \quad (20-15)$$

An equivalent mathematical expression is, on a mass basis,

$$\eta_x = \frac{q_c dY_c}{q_0 dY_0} = \frac{q_c dY_c}{q_c dY_c + q_f dY_f} \quad (20-16)$$

where  $Y_c$  is the cumulative percent by mass of coarse fraction less than particle size  $X$ ,  $Y_f$  is the cumulative percent by mass of fine fraction less than particle size  $X$ ,  $Y_0$  is the cumulative percent by mass of feed less than particle size  $X$ ,  $q_c$  is the coarse-fraction mass flow rate,  $q_f$  is the fine-fraction mass flow rate, and  $q_0$  is the feed mass flow rate.

For purposes of calculating size selectivity from cumulative particle size distribution data, Eq. (20-16) can be expressed in incremental form as follows:

$$\eta_{x_i} = \frac{q_c \Delta Y_{ci}}{q_c \Delta Y_{ci} + q_f \Delta Y_{fi}} \quad (20-17)$$

where  $\Delta Y_{ci}$  and  $\Delta Y_{fi}$  are the cumulative size-distribution intervals of coarse and fine fractions associated with the size interval  $\Delta X_i$ , respectively. An interval representative size  $X_i$  is arbitrarily taken as the midpoint of  $\Delta X_i$ .

See the American Institute of Chemical Engineers classifier test procedure for a sample calculation of classifier selectivity. This example is plotted in Fig. 20-14.

There are many ways in which sharpness can be expressed. One index that has been widely used is the ratio

$$\beta = X_{75}/X_{25} \quad (20-18)$$

where  $\beta$  is the sharpness index,  $X_{75}$  is the particle size corresponding to the 75 percent classifier selectivity value, and  $X_{25}$  is the particle size corresponding to the 25 percent value. For perfect classification,  $\beta$  has a value of unity; the smaller  $\beta$ , the poorer the sharpness of classification.

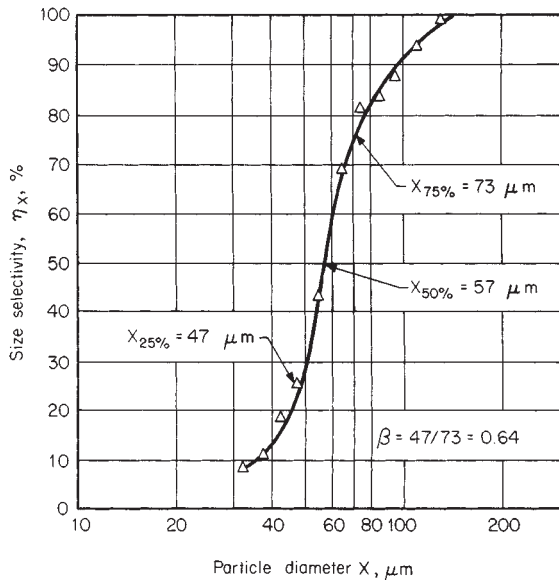


FIG. 20-14 Size-selectivity example.

Several empirical formulas for classifier selectivity have been proposed. Such a formula is needed for computer simulation of mill circuits. The following formula has been found to fit data from several field installations for classifiers of many types, including vibrating screens (Vaillant, AIME Tech. Pap. 67B26, 1967).

$$C_x = 1 - (1 - a) \exp b \left(1 - \frac{X}{X_0}\right) \quad \text{for } X > X_0$$

$$= a \quad \text{for } X \leq X_0 \quad (20-19)$$

where  $a$ ,  $b$ , and  $X_0$  are constants and  $X$  is the particle size. The agreement is especially good for wet classifying systems. For wet cyclones the factor  $a$  and  $Y_{50}$  are related to the ratio of overflow to underflow rates [Draper and Lynch, *Proc. Australas. Inst. Min. Metall.*, **209**, 109 (1964); Mizrahi and Cohen, *Trans. Inst. Min. Metall.*, C318-329 (December 1966); and Lynch and Rao, *Indian J. Tech.*, **6**, 106-114 (April 1968)]. An equation developed by stochastic reasoning for cyclones involves a similar exponential form [Molerus, *Chem. Ing. Tech.*, **39**(13), 792-796 (1967)].

It has been suggested that the circulating load can be calculated by a material balance from size analyses of the feed, fine product, and coarse product of the classifier in a closed-circuit grinding system [Bond, *Rock Prod.*, **41**, 64 (January 1938)]. However, since size analyses are subject to error, it is better to use this information to check the size analyses (Vaillant, op. cit.). The appropriate equation is (Dahl, *Classifier Test Manual*, Portland Cem. Assoc. Bull. MRB-53, 1954)

$$\frac{q_R}{q_R + q_P} = R = \frac{Y_L(X) - Y_P(X)}{Y_R(X) - Y_P(X)} = \text{a constant for all } X \quad (20-20)$$

where  $q_R$  is tailings,  $q_P$  is classifier product,  $L$  is mill discharge,  $R$  is recycle, and  $Y$  is either the fraction of particles in a stream between two sieve sizes or the cumulative fraction retained or passing a sieve of size  $X$ .

### SIMULATION OF MILLING CIRCUITS

The energy laws of Bond, Kick, and Rittinger relate to grinding from some average feed size to some product size but do not take into account the behavior of different sizes of particles in the mill. Computer simulation, based on population-balance models [Bass, *Z. Angew. Math. Phys.*, **5**(4), 283 (1954)], traces the breakage of each size of particle as a function of grinding time. Furthermore, the simu-

lation models separate the breakage process into two aspects: a breakage rate and a mean fragment-size distribution. These are both functions of the size of particle being broken. They usually are not derived from knowledge of the physics of fracture but are empirical functions fitted to milling data. The following formulation is given in terms of a discrete representation of size distribution; there are comparable equations in integrodifferential form.

**Batch Grinding** Let  $w_k$  be the weight fraction of material retained on each screen of a nest of  $n$  screens;  $w_k$  is related to  $P_k$ , the fraction coarser than size  $X_k$ , by

$$w_k = (\partial P_k / \partial X_k) \Delta X_k \quad (20-21)$$

where  $\Delta X_k$  is the difference between the openings of screens  $k$  and  $k + 1$ . The **grinding-rate function**  $S_u$  is the rate at which the material of upper size  $u$  is selected for breakage in an increment of time, relative to the amount of that size present:

$$dw_u/dt = -S_u w_u \quad (20-22)$$

The **breakage function**  $\Delta B_{k,u}$  gives the size distribution of product breakage of size  $u$  into all smaller sizes  $k$ . Since some fragments from size  $u$  are large enough to remain in the range of size  $u$ , the term  $\Delta B_{u,u}$  is not zero, and

$$\sum_{k=n}^u \Delta B_{k,u} = 1 \quad (20-23)$$

The differential equation of batch grinding is deduced from a balance on the material in the size range  $k$ . The rate of accumulation of material of size  $k$  equals the rate of production from all larger sizes minus the rate of breakage of material of size  $k$ :

$$\frac{dw_k}{dt} = \sum_{u=1}^k [w_u S_u(t) \Delta B_{k,u}] - S_k(t) w_k \quad (20-24)$$

In general,  $S_u$  is a function of all the milling variables.  $\Delta B_{k,u}$  is also a function of breakage conditions. If it is assumed that these functions are constant, then relatively simple solutions of the grinding equation are possible, including an analytical solution [Reid, *Chem. Eng. Sci.*, **20**(11), 953-963 (1965)] and matrix solutions [Broadbent and Calcott, *J. Inst. Fuel*, **29**, 524-539 (1956); **30**, 18-25 (1967); and Meloy and Bergstrom, *7th Int. Min. Proc. Congr. Tech. Pap.*, 1964, pp. 19-31].

**Solution of Batch-Mill Equations** In general, the grinding equation can be solved by numerical methods—for example, the Euler technique (Austin and Gardner, *1st European Symposium on Size Reduction*, 1962) or the Runge-Kutta technique. The matrix method is a particularly convenient formulation of the Euler technique.

Reid's **analytical solution** is useful for calculating the product as a function of time  $t$  for a constant feed composition. It is

$$w_{L,k} = \sum_{n=1}^k a_{k,n} \exp(-\bar{S}_n \Delta t) \quad (20-25)$$

where the subscript  $L$  refers to the discharge of the mill, zero to the entrance, and  $\bar{S}_n = 1$  "corrected" rate function defined by  $\bar{S}_n = (1 - \Delta B_{n,n})$  and  $B$  is then normalized with  $\Delta B_{n,n} = 0$ . The coefficients are

$$a_{k,k} = w_{0k} - \sum_{n=1}^{k-1} a_{k,n} \quad (20-26)$$

and

$$a_{k,n} = \sum_{u=n}^{k-1} \frac{S_u \Delta B_{k,u} a_{u,n}}{\bar{S}_k - \bar{S}_n} \quad (20-27)$$

The coefficients are evaluated in order since they depend on the coefficients already obtained for larger sizes.

The basic idea behind the **Euler method** is to set the change in  $w$  per increment of time as

$$\Delta w_k = (dw_k/dt) \Delta t \quad (20-28)$$

where the derivative is evaluated from Eq. (20-24). Equation (20-28) is applied repeatedly for a succession of small time intervals until the desired duration of milling is reached.

In the matrix method a modified rate function is defined,  $S'_k = S_k \Delta t$  as the amount of grinding that occurs in some small time  $\Delta t$ . The result is

$$w_L = (I + S'B - S')w_F = Mw_F \quad (20-29)$$

where the quantities  $\mathbf{w}$  are vectors,  $\mathbf{S}'$  and  $\mathbf{B}$  are the matrices of rate and breakage functions, and  $\mathbf{I}$  is the unit matrix. This follows because the result obtained by multiplying these matrices is just the sum of products obtained from the Euler method. Equation (20-29) has a physical meaning. The unit matrix times  $\mathbf{w}_F$  is simply the amount of feed that is not broken.  $\mathbf{S}'\mathbf{B}\mathbf{w}_F$  is the amount of feed that is selected and broken into the vector of products.  $\mathbf{S}'\mathbf{w}_F$  is the amount of material that is broken out of its size range and hence must be subtracted from this element of the product. The entire term in parentheses can be considered as a mill matrix  $\mathbf{M}$ . Thus the milling operation transforms the feed vector into the product vector. Meloy and Bergstrom (op. cit.) pointed out that when Eq. (20-29) is applied over a series of  $p$  short-time intervals, the result is

$$\mathbf{w}_L = \mathbf{M}^p \mathbf{w}_F \quad (20-30)$$

Matrix multiplication happens to be commutative in this special case. It is easy to raise a matrix to a power on a computer since three multiplications give the eighth power, etc. Therefore the matrix formulation is well adapted to computer use.

**Continuous-Mill Simulation** Batch-grinding experiments are the simplest type of experiments to produce data on grinding coefficients. But scale-up from batch to continuous mills must take into account the **residence-time distribution** in a continuous mill. This distribution is apparent if a tracer experiment is carried out. For this purpose background ore is fed continuously, and a pulse of tagged feed is introduced at time  $t_0$ . This tagged material appears in the effluent distributed over a period of time, as shown by a typical curve in Fig. 20-15. Because of this distribution some portions are exposed to grinding for longer times than others. Levenspiel (*Chemical Reaction Engineering*, Wiley, New York, 1962) shows several types of residence-time distribution that can be observed. Data on large mills indicate that a curve like that of Fig. 20-15 is typical (Keienberg et al., *3d European Symposium on Size Reduction*, op. cit., 1972, p. 629). This curve can be accurately expressed as a series of arbitrary functions (Merz and Molerus, *3d European Symposium on Size Reduction*, op. cit., 1972, p. 607). A good fit is more easily obtained if we choose a function that has the right shape since then only the first two moments are needed. The log-normal probability curve fits most available mill data, as was demonstrated by Mori [*Chem. Eng. (Japan)*, 2(2), 173 (1964)]. Two examples are shown in Fig. 20-16. The log-normal plot fails only when the mill acts nearly as a perfect mixer.

To measure a residence-time distribution, a pulse of tagged feed is inserted into a continuous mill and the effluent is sampled on a schedule. If it is a dry mill, a soluble tracer such as salt or dye may be used and the samples analyzed conductimetrically or colorimetrically. If it is a wet mill, the tracer must be a solid of similar density to the ore. Materials like copper concentrate, chrome brick, or barites have been used as tracers and analyzed by X-ray fluorescence. To plot results in log-normal coordinates, the concentration data must first be normalized from the form of Fig. 20-15 to the form of cumulative percent discharged, as in Fig. 20-16. For this, one must either know the total amount of pulse fed or determine it by a simple numerical integration

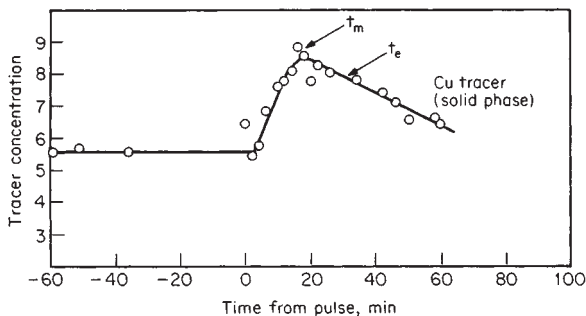
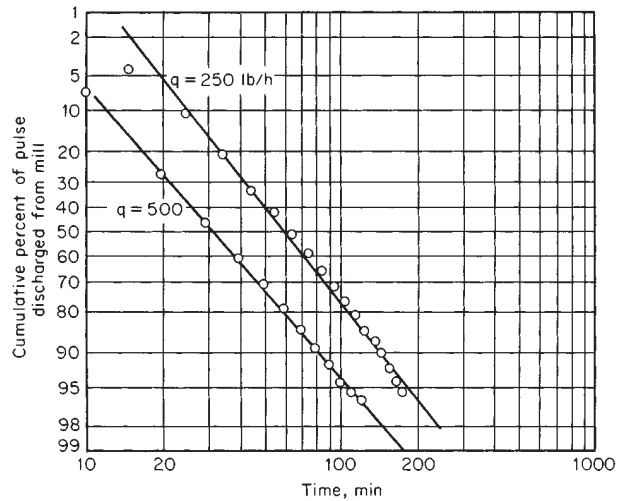


FIG. 20-15 Ore transit through a ball mill. Feed rate is 500 lb/h. (Courtesy Phelps Dodge Corporation.)



$q$ , lb/h	$\sigma$	$t_e$ , min	$Dt_e/L^2$
250	0.29	39	0.23
500	0.32	18	0.28

FIG. 20-16 Log-normal plot of residence-time distribution in Phelps Dodge mill.

by using a computer. The data are then plotted as in Fig. 20-16, and the coefficients in the log-normal formula of Mori can be read directly from the graph. Here  $t_e = t_{50}$  is the time when 50 percent of the pulse has emerged. The standard deviation  $\sigma$  is the time between  $t_{16}$  and  $t_{50}$  or between  $t_{50}$  and  $t_{84}$ . Knowing  $t_e$  and  $\sigma$ , one can reconstruct the straight line in log-normal coordinates. One can also calculate the vessel dispersion number,  $Dt_e/L^2$ , which is a measure of the sharpness of the pulse (Levenspiel, *Chemical Reactor Omnibook*, p. 100.6, Oregon State University Bookstores Inc., 1979. This number has erroneously been called by some the Peclet number). Here  $D$  is the particle diffusivity. A few available data are summarized [Snow, *International Conference on Particle Technology*, IIT Research Institute, Chicago, Ill. 60616, 1973, p. 28] for wet mills. Other experiments are presented for dry mills [Hogg et al., *Trans. Am. Inst. Min. Metall. Pet. Eng.*, 258, 194 (1975)]. The most important variables affecting the vessel dispersion number are  $L$ /diameter of the mill, ball size, mill speed, scale expressed either as diameter or as throughput, degree of ball filling, and degree of material filling.

**Solution for Continuous Mill** In the method of Mori (op. cit.) the residence-time distribution is broken up into a number of segments, and the batch-grinding equation is applied to each of them. The resulting size distribution at the mill discharge is

$$\mathbf{w}(L) = \mathbf{w}(t) \Delta\phi \quad (20-31)$$

where  $\mathbf{w}(t)$  is a matrix of solutions of the batch equation for the series of times  $t$ , with corresponding segments of the cumulative residence-time curve.

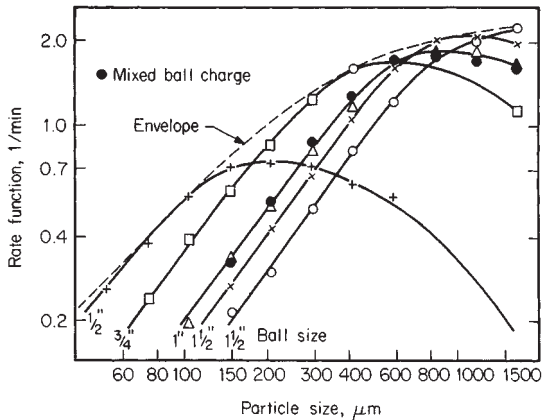
Using the Reid solution, Eq. (20-25), this becomes

$$\mathbf{w}(L) = \mathbf{RZ} \Delta\phi \quad (20-32)$$

since the Reid solution [Eq. (20-25)] can be separated into a matrix  $\mathbf{Z}$  of exponentials  $\exp(-St)$  and another factor  $\mathbf{R}$  involving only particle sizes. Austin, Klimpel, and Luckie [*Process Engineering of Size Reduction: Ball Milling*, Society of Mining Engineers of AIME, (1984)] incorporated into this form a tanks-in-series model for the residence-time distribution.

**Closed-Circuit Milling** In closed-circuit milling the tailings from a classifier are mixed with fresh feed and recycled to the mill. Calculations can be based on a material balance and an explicit solu-





**FIG. 20-19** Variation of rate function with size of feed particles and size of balls in a ball mill. [Kelsall, Reid, and Restarick, *Powder Technol.*, **1**(5), 291 (1968).]

shows that the position of this maximum depends on the ball size. In fact, the feed size for which  $S$  is a maximum can be estimated by inverting the formula for optimum ball size given by Coghill and Devaney under "Tumbling Mills."

**Scale-Up Based on Energy** Since large mills are usually sized on the basis of power draft (see subsection "Energy Laws"), it is appropriate to scale up or convert from batch to continuous data by

$$S(X)_{\text{cont}} = S(X)_{\text{batch}} \frac{(W_T/KW)_{\text{batch}}}{(W_T/KW)_{\text{cont}}} \quad (20-37)$$

$W_T$  is usually not known for continuous mills, but it can be determined from  $W_T = t_e Q$ , where  $t_e$  is determined by a tracer measurement. Eq. (20-37) will be valid if the holdup  $W_T$  is geometrically similar in the two mills or if operating conditions are in the range in which total production is independent of holdup. From studies of the kinetics of milling [Patat and Mempel, *Chem. Ing. Tech.*, **37**(9), 933; (11), 1146; (12), 1259 (1965)] there is a range of holdup in which this is true. More generally, Austin, Luckie, and Klimpel (loc. cit.) developed empirical relations to predict  $S$  as holdup varies. In particular, they observe a slowing of grinding rate when mill filling exceeds ball void volume due to cushioning.

**Parameters for Scale-Up** Before simulation equations can be used, the parameter matrices **S** and **B** must be back-calculated from experimental data, which turns out to be difficult. One reason is that **S** and **B** occur as a product, so they are to some extent indeterminate; errors in one tend to be compensated by the other. Also, the number of parameters is larger than the number of data values from a single size-distribution measurement; but this is overcome by using data from grinding tests at a series of grinding times. This should be done anyway, since the empirical parameters should be determined to be valid over the experimental range of grinding times.

It may be easier to fit the parameters by forcing them to follow specified functional forms. In earliest attempts it was assumed that the forms should be normalizable (have the same shape whatever the size being broken). With complex ores containing minerals of different friability, the grinding functions **S** and **B** exhibit complex behavior near the grain size (Choi et al., *Particulate and Multiphase Processes Conference Proceedings*, **1**, 903-916.) **B** is not normalizable with respect to feed size and **S** does not follow a simple power law.

There are also experimental problems: When a feed size distribution is ground for a short time, there is not enough change in the size distribution in the mill to distinguish between particles being broken into and out of intermediate sizes, unless individual feed-size ranges are tagged. Feeding narrow-size fractions alone solves the problem, but changes the milling environment; the presence of fines affects the grinding of coarser sizes. Gupta et al. [*Powder Technology*, **28**(1), 97-106 (1981)] ground narrow fractions separately, but subtracted out the effect of the first 3 min of grinding, after which the behavior had

become steady. Another experimental difficulty arises from the recycle of fines in a closed circuit, which soon "contaminates" the size distribution in the mill; it is better to conduct experiments in open circuit, or in batch mills on a laboratory scale.

There are few data demonstrating scale-up of the grinding-rate functions **S** and **B** from pilot- to industrial-scale mills. Weller et al. [*International J. Mineral Processing*, **22**, 119-147 (1988)] ground chalcocopyrite ore in pilot and plant mills and compared predicted parameters with laboratory data of Kelsall [*Electrical Engineering Transactions*, Institution of Engineers Australia, **EE5**(1), 155-169 (1969)] and Austin Klimpel & Luckie (*Process Engineering of Size Reduction, Ball Milling*, Society of Mining Engineers, NY, 1984) for quartz. **S** has a maximum for a particle size that depends on ball size according to Fig. 20-19, which can be expressed as

$$X_s/X_t = (d_s/d_t)^{2.4}$$

where  $s$  = scaled-up mill,  $t$  = test mill,  $d$  = ball size,  $X$  = particle size of maximum rate. Changing ball size also changes the rates according to  $S_s/S_t = (d_s/d_t)^{0.55}$ . These relations shift one rate curve onto another and allow scale-up to a different ball size. Mill diameter also affects rate by a factor  $(D_s/D_t)^{0.5}$ . Lynch [*Mineral crushing and grinding circuits, their simulation optimization design and control*, Elsevier Scientific Publishing Co., Amsterdam, New York (1977)], and Austin, Klimpel, and Luckie (loc. cit.) developed scale-up factors for ball load, mill filling, and mill speed. In addition, slurry solids content is known to affect the rate, through its effect on slurry rheology. Austin, Klimpel, and Luckie (loc. cit.) present more complete simulation examples and compare them with experimental data to study scale-up and optimization of open and closed circuits, including classifiers such as hydrocyclones and screen bends. Differences in the classifier will affect the rates in a closed circuit. For these reasons scale-up is likely to be uncertain unless conditions in the large mill are as close as possible to those in the test mill.

**Control of Grinding Circuits** Mineral processing plants require constant supervision and intervention by operators or controllers. Conditions such as feed hardness, grade, grain size, etc., change substantially as ore is delivered from different locations in the mine. Typically the objective of control is to maximize the production of the valuable component per unit time, or to maximize throughput while maintaining a constant grind size. Also, it is necessary to control individual process units so that they run smoothly and in harmony.

Measuring process parameters on full-scale plants is notoriously difficult, but is needed for control. Usually few of the important variables are accessible to measurement. Recycle of material makes it difficult to isolate the effects of changes to individual process units in the circuit. Newer plants have more instrumentation, including on-line viscosimeters [Kawatra and Eisele, *International J. Mineral Processing*, **22**, 251-259 (1988)], mineral composition by on-line X-ray fluorescence, belt feeder weighers, etc., but the information is always incomplete. Therefore it is helpful to have models to predict quantities that cannot be measured while measuring those that can.

Some plants have been using computer control for 20 years. Control systems in industrial use typically consist of individual feedback and feedforward loops. Horst and Enochs [*Engineering & Mining J.*, **181**(6), 69-171 (1980)] reported that installation of single-variable automatic controls improved performance of 20 mineral processing plants by 2 to 10 percent. But interactions among the processes make it difficult for independent controllers to control the circuit optimally.

*Optimal control* refers first to controlling the circuit dynamically so that it operates close to its optimum state. The *state* is the combination of variables that define the operation of the circuit. The optimum state varies as conditions change. Second, optimal control refers to a mathematical process to find an optimum path to move from a given state to the optimum state, based on minimizing an objective function [as used in control theory [Herbst et al., *International J. Mineral Processing*, **22**, 275-296 (1988)]. Other mathematical approaches have been published as well [Hulbert et al., *Automation in Mining, Mineral and Metal Processing: Proceedings of 3rd IFAC Symposium*, 311-322, 1980; Romberg, *First IFAC Symposium on Automation for Mineral Resource Development*, 289, 1985].

The difficulty with individual PID (proportional-integral-differential) controllers is that each controller only manipulates one variable to achieve a desired effect, whereas the grinding circuit is *multivariate*. For example [Rajamani and Herbst, *Chem. Engr. Science*, **46**(3), 861–879 (1991)], to control the fineness of a ball-mill circuit one can vary either the ore-feed rate to the circuit or the water addition to the sump. Adding water dilutes the slurry going to the hydrocyclone, causing it to separate at a finer size. But then the cyclone sends more recycle back to the mill, loading it more and resulting in a coarser grind. If instead one controls the feed rate, the mill grinds finer, and indirectly the cyclone separates out more fines. Thus, both ore-feed rate and water addition influence more than one variable. As a result PID controllers cause the output to oscillate, as Rajamani and Herbst showed experimentally. The circuit tends to be unstable, and long time delays exist (Metzner and MacLeod, 7th IFAC Symposium on Intelligent Tuning and Adaptive Control, 163–169, 1991). Another difficulty with PID controllers is that their tuning changes depending on the operating conditions. They can be tuned for a rapid response when the ore is soft, but when it is harder the response is more sensitive and the gains have to be reduced to prevent overshoot.

Developing a multivariate control model is difficult because the process is complex. One approach is simplification; meaningful control results can be obtained with as few as two particle sizes in the model (Rajamani and Herbst, loc. cit.). Another approach is to use more powerful inexpensive computers. Complex calculations that previously seemed only of academic interest are now or will soon become practical to perform on-line. The mathematical complexity is also an impediment to understanding, but the commercial availability of packaged software for on-line control will overcome this problem. Software packages that enable grinding-circuit analysis, scale-up design, and flow-sheet optimization have been developed and are widely applied (Herbst et al., *MODSIM User's Manual*, Univ of Utah, Salt Lake City, 1986; Herbst et al., *ESTIMILL User's Manual*, Univ

of Utah, Salt Lake City, 1977; King, *MODSIM, Report No. 9*, Dept. of Metallurgy, Univ. Witwatersrand, Johannesburg, 1983; Jamsa, Acta Polytechnica Scandinavica, *Mathematics and Computer Science Series No. 57*, 32 pp., 1990).

Herbst et al. [*International J. Mineral Processing*, **22**, 273–296 (1988)] describe the software modules in an optimum controller for a grinding circuit. The *process model* can be an empirical model as some authors have used. A phenomenological model can give more accurate predictions, and can be extrapolated, for example from pilot-to full-scale application, if scale-up rules are known. Normally the model is a variant of the population balance equations given in the previous section.

Rajamani and Herbst (loc. cit.) compared control of an experimental pilot-mill circuit using feedback and optimal control. Feedback control resulted in oscillatory behavior. Optimal control settled rapidly to the final value, although there was more noise in the results. A more complete model should give even better results.

If individual controllers are used instead of optimal computer control, several strategies are possible. In one strategy (Lynch and Elber, 3rd IFAC Symposium on Automation of Mining, Mineral and Metal Processing, 25–32, 1980) the slurry-pump rate is controlled to maintain sump-level constant, which results in smooth cyclone operation. The water-feed rate is ratioed to the ore-feed rate, which keeps the circulating load from oscillating. The ore-feed rate is then controlled to maintain product-particle size.

Improved instrumentation can improve control by measuring more directly the variables governing the internal behavior of the mill. By installing an electrical conductivity probe in the wall of the mill, Moys and Montini [*CIM Bulletin*, **80**(907), 52–6 (1987)] were able to detect the position of the ball mass during dynamic operation. This together with on-line measurement of slurry viscosity (see rheological properties, p. 20–32d) made it possible to control the mill at the desired operating point.

## CRUSHING AND GRINDING EQUIPMENT

### CLASSIFICATION AND SELECTION OF EQUIPMENT

A wide variety of size-reduction equipment is available. The chief reasons for lack of standardization are the variety of products to be ground and product qualities demanded, the limited amount of useful grinding theory, and the requirements by different industries in the economic balance between investment cost and operating cost. Some differences exist for the sake of difference; sometimes similarities are advertised as differences [Rumpf, *Chem. Ing. Tech.*, **37**(3), 187–202 (1965)].

Equipment may be classified according to the way in which forces are applied, as follows (Rumpf, loc. cit.):

1. Between two solid surfaces (Fig. 20-20a, crushing or attrition; Fig. 20-20b, shearing; Fig. 20-20c, crushing in a particle bed)
2. Impact at one solid surface (Fig. 20-20d), or between particles (Fig. 20-20e)
3. By shear action of the surrounding medium (Fig. 20-20f, colloid mill)
4. Nonmechanical introduction of energy (Thermal shock, explosive shattering, electrohydraulic)

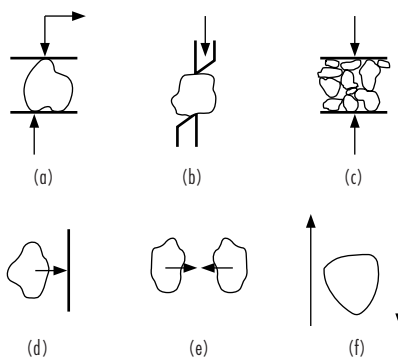
A practical **classification of crushing and grinding equipment** is given in Table 20-6.

A guide to the **selection of equipment** may be based on feed *size* and *hardness* (see subsection "Grindability") as shown in Table 20-7. It should be emphasized that Table 20-7 is merely a guide and that exceptions can be found in practice.

A number of general principles govern the **selection of crushers** [Riley, *Chem. Process Eng.* (January 1953)]. When the rock contains a predominant amount of material that has a tendency to be cohesive when moist, such as clay, any form of repeated pressure crusher will show a tendency for the fines to pack in the outlet of the crushing zone and prevent free discharge at fine settings. Impact breakers are then

suitable, provided that the rock is not harder and more abrasive than limestone with 5 percent silica.

When the rock is not hard but cohesive, toothed rolls give satisfactory performance. With harder rocks, jaw and gyratory crushers are required, and the jaw crusher is less prone to clogging than the gyratory. In crushing throughputs of a few hundred tons per hour, a jaw or impact crusher may be satisfactory, but for the largest capacities the gyratory is unsurpassed. For secondary crushing the high-speed conical-head gyratory is unsurpassed except when sticky material precludes its use. For very hard ores a rod mill may compete effectively. If a wide size distribution is to be avoided, a compression-type crusher is best; if the product requires fragments of compact shape,



**FIG. 20-20** Stressing mechanisms to cause size reduction. [Rumpf, *Chem. Eng. Tech.*, **37**(3), 187–202 (1965).]

**TABLE 20-6 Types of Size-Reduction Equipment**

A. Jaw crushers:	1. Blake 2. Overhead eccentric
B. Gyratory crushers:	1. Primary 2. Secondary 3. Cone
C. Heavy-duty impact mills:	1. Rotor breakers 2. Hammer mills 3. Cage impactors
D. Roll crushers:	1. Smooth rolls (double) 2. Toothed rolls (single and double) 3. Roll press
E. Dry pans and chaser mills	
F. Shredders:	1. Toothed shredders 2. Cage disintegrators 3. Disk mills
G. Rotary cutters and dicers	
H. Media mills:	1. Ball, pebble, rod, and compartment mills: a. Batch b. Continuous 2. Autogenous tumbling mills 3. Stirred ball and bead mills 4. Vibratory mills
I. Medium peripheral-speed mills:	1. Ring-roll and bowl mills 2. Roll mills, cereal type 3. Roll mills, paint and rubber types 4. Buhrstones
J. High-peripheral-speed mills:	1. Fine-grinding hammer mills 2. Pin mills 3. Colloid mills 4. Wood-pulp beaters
K. Fluid-energy superfine mills:	1. Centrifugal jet 2. Opposed jet 3. Jet with anvil 4. Fluidized-bed jet

**TABLE 20-7 Guide to Selection of Crushing and Grinding Equipment**

Size-reduction operation	Hardness of material	Size°				Reduction ratio‡	Types of equipment
		Range of feeds, in. †		Range of products, in. †			
		Max.	Min.	Max.	Min.		
Crushing: Primary	Hard	60	12	20	4	3 to 1 4 to 1	A to B
		20	4	5	1		
Secondary	Hard	5	1	1	0.2	5 to 1 7 to 1	A to E
		1.5	0.25	0.185 (4)	0.033 (20)		
	Soft	60	4	2	0.4	10 to 1	C to G
Grinding: Pulverizing: Coarse	Hard	0.185 (4)	0.033 (20)	0.023 (28)	0.003 (200)	10 to 1	D to I
		0.046 (14)	0.0058 (100)	0.003 (200)	0.00039 (1250)		
Fine	Hard	0.046 (14)	0.0058 (100)	0.003 (200)	0.00039 (1250)	15 to 1	H to K
Disintegration: Coarse	Soft	0.5	0.065	0.023	0.003	20 to 1 50 to 1	E, I I to K
	Soft	0.156 (5)	0.0195 (32)	0.003 (200)	0.00039 (1250)		

°85% by weight smaller than the size given.  
 †Sieve number in parentheses, mesh per inch  
 ‡Higher reduction ratios for closed-circuit operations.  
 NOTE: To convert inches to millimeters, multiply by 25.4.

an impact crusher or a gyratory is best. Further information is given under each type of mill, and also in the subsection on crushed stone and aggregate.

**JAW CRUSHERS**

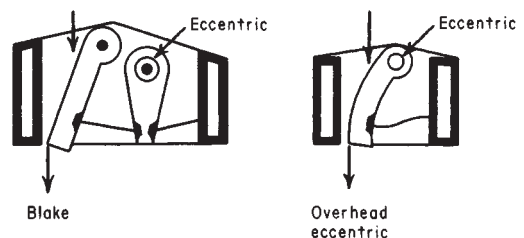
**Design and Operation** These crushers may be divided into two main groups (Fig. 20-21), the *Blake*, with a movable jaw pivoted at the top, giving greatest movement to the smallest lumps; and the *overhead eccentric*, which is also hinged at the top, but through an *eccentric-driven* shaft which imparts an elliptical motion to the jaw. Both types have a removable crushing plate, usually corrugated, fixed in a vertical position at the front end of a hollow rectangular frame. A similar plate is attached to the swinging movable jaw. The Blake jaw (Fig. 20-22) is moved through a knuckle action by the rising and falling of a second lever (pitman) carried by an eccentric shaft. The vertical movement is communicated horizontally to the jaw by double toggle plates. Because the jaw is pivoted at the top, the throw is greatest at the discharge, preventing choking.

Crushing angles in standard Allis-Chalmers-Svedala Blake-type machines generally are near 0.47 rad (27°) (see Fig. 20-21). The reduction ratios at minimum recommended settings and with straight jaw plates average about 8:1. Curved (or concave) jaw plates are designed to minimize choking.

The **overhead eccentric jaw crusher** (Nordberg, *Telsmith Inc.*, and *Cedarapids*) falls into the second type. These are single-toggle machines. The lower end of the jaw is pulled back against the toggle by a tension rod and spring.

The choice between the two types of jaw crushers is generally dictated by the feed characteristics, tonnage, and product requirements (Pryon, *Mineral Processing*, Mining Publications, London, 1960; Wills, *Mineral Processing Technology*, Pergamon, Oxford, 1979.) Greater wear caused by the elliptical motion of the overhead eccentric and direct transmittal of shocks to the bearing limit use of this type to readily breakable material, although Cedarapids has reduced the elliptical wear effect by moving the bearing over the crushing chamber. Overhead eccentric crushers are generally preferred for crushing rocks with a hardness equal to or lower than that of limestone. Operating costs of the overhead eccentric are higher for the crushing of hard rocks, but its large reduction ratio is useful for simplified low-tonnage circuits with fewer grinding steps. Double-toggle type crushers cost about 50 percent more than similar overhead-eccentric-type crushers.

**Comparison of Crushers** The jaw crusher can accommodate the same size rocks as a gyratory, with lower capacity and also lower capital and maintenance costs, but similar installation costs. Therefore they are preferred when the crusher gape is more important than the throughput. If required throughput in tons/h is less than the square of the gape in inches, a jaw crusher is more economical (Taggart, *Handbook of Mineral Dressing*, Wiley, New York, 1945). Relining the gyratory requires more effort than for the jaw, and also more space above and below the crusher. Improved alloys have reduced the need for relining, however. Gyratories are preferred for larger throughputs. In metal mines continuity of operation favors gyratories over jaws because of their low maintenance. Quarries on the other hand can use hammer or other impact crushers, while maintenance is done on second shift.



**FIG. 20-21** Jaw-crusher designs.

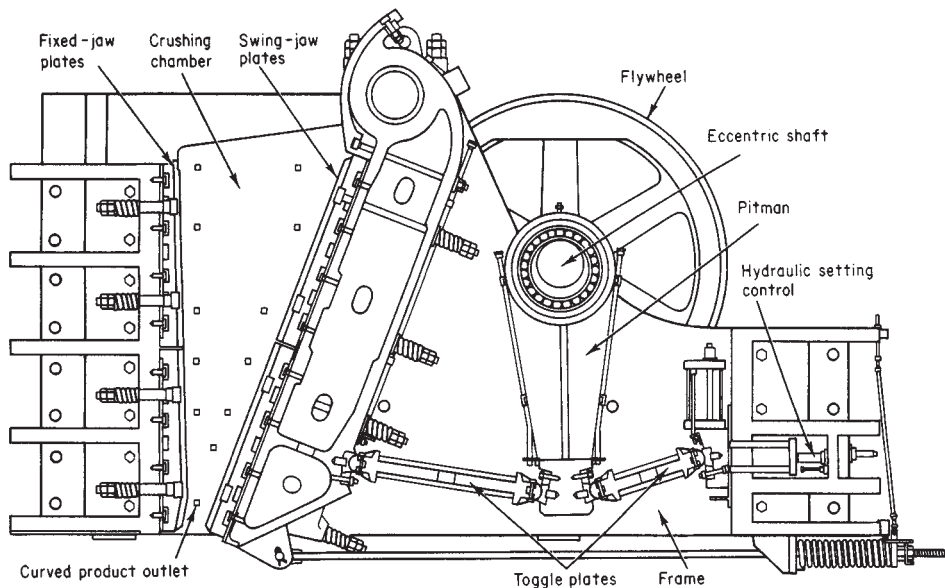


FIG. 20-22 Blake jaw crusher. (Allis Mineral Systems Grinding Div., Svedala Industries, Inc.)

**Performance** Jaw crushers are applied to the primary crushing of hard materials and are usually followed by other types of crushers. In smaller sizes they are used as single-stage machines. Jaw crushers are usually rated by the dimensions of their feed area. This depends on the width of the crushing jaws and the *gape*, which is the maximum distance between the fixed and movable jaws at the feed opening. The *setting* of a jaw crusher is the *closed* (or close) or the *wide opening* between the moving jaws at the outlet end, usually measured between tips of the corrugations. The reciprocating motion of the jaws causes the opening to vary between closed and wide, and the difference is the *throw*. Specifications are usually based on the closed settings. The setting is adjustable.

The throw of Blake jaw crushers is determined by the hardness of the ore as well as the size of the machine [Mollick et al., *Engineering & Mining J.*, **181**(6), 69–171 (1980)]. It may vary from  $\frac{1}{4}$  in for hard but friable ores to 3 in for resilient material. The Big Bite jaw crusher (Kue-Ken Div., Process Technology Inc.) is a Blake double-toggle type in which the fulcrum pinion is positioned well over the center of the grinding chamber [Anon., *Quarry Management*, **18**(1), 25–7 (1991)]. This increases the throw at the top of the jaw opening, allowing it to better crush large rocks. It can be shipped in sections. Capacities of Kue-Ken jaw crushers (Blake type) are given in Table 20-8, including both standard and Big Bite types. Performance data of overhead eccentric crushers with straight jaw plates are given in Table 20-9.

*Dragon* single-toggle primary jaw crushers are supplied (by *Fives-Cail Babcock*) in eight sizes. The smallest is the MR53 with feed opening  $550 \times 350$  mm and the largest is the MR200 with feed opening  $2000 \times 1600$  mm, the corresponding capacities being from 15 to 800 ton/h. These units can be supplied fully mobile or on skid frames. The BCS series are extra heavy-duty crushers. High flywheel inertia enables them to accept large lumps of limestone and achieve throughputs up to 6000 ton/h. Pegson Telsmith in UK has a new single-toggle primary jaw crusher with roller bearings sized at  $1000 \times 800$  mm. It is expected to be the first of a new line that incorporates the latest manufacturing techniques. Universal Engineering Corp. offers 27 sizes of overhead eccentric crusher, with long jaws and small nip angle to reduce rebound.

Smaller jaw crushers are available from Sturtevant Inc, with capacities of 1 to 10 hp (0.7 to 7 kW). Jaw settings range from  $\frac{1}{8}$  to 2.5 in (3 to 65 mm).

## GYRATORY CRUSHERS

The development of improved supports and drive mechanisms has allowed gyratory crushers to take over most large hard-ore and mineral-crushing applications. The largest expense of these units is in relining them. Operation is intermittent; so power demand is high, but the total power cost is not great.

**Design and Operation** The gyratory crusher (see Fig. 20-23) consists of a cone-shaped pestle oscillating within a larger cone-shaped mortar or bowl. The angles of the cones are such that the width of the passage decreases toward the bottom of the working faces. The pestle consists of a mantle which is free to turn on its spindle. The spindle is oscillated from an eccentric bearing below. Differential motion causing attrition can occur only when pieces are caught simultaneously at the top and bottom of the passage owing to different radii at these points.

The circular geometry of the crusher gives a favorably small **nip angle** in the horizontal direction. The nip angle in the vertical direction is less favorable and limits feed acceptance. The vertical nip angle

TABLE 20-8 Performance Data for Blake Jaw Crushers

Model	Feed opening, in.	hp	Closed setting, in.	Capacity, ton/h	Weight, 1000 lb.	Max. r/min.
Standard 22	3 × 12	10	$\frac{1}{4}$	2–5	3	400
			2	19–32		
			3	59–88		
81	12 × 36	25–40	1	32–50	17	390
			3	95–135		
95	24 × 36	30–50	2	64–95	27	390
			6	195–270		
			10	85–120		
Big Bite 110	25 × 42	50–60	2	205–275	40	390
			5	215–290		
160	42 × 48	125–150	4	520–770	117	290
			10	835–1310		
440	66 × 84	350–400	7	2625–4120	455	210
			22			

To convert inches to millimeters, multiply by 2.54; to convert pounds to kilograms, multiply by 0.4535; to convert horsepower to kilowatts, multiply by 0.746; and to convert tons per hour to kilograms per hour, multiply by 907.



TABLE 20-9 Performance Data for Overhead Eccentric Jaw Crushers\*

Crusher Size, in.	r/min.	hp	Capacity, tons/h									
			Setting, in.									
			¾	1	1½	2	3	4	6	8	12	
10 × 16	300	20-30	15	20	30	40	60					
12 × 36	275	60-75			65	85	130	175				
24 × 36	250	125-150					130	175	265			
30 × 42	250	125-175						200	300	400	610	
54 × 60	200	350-450						290	440	580	880	

\*Cedar Rapids, CO. Div. of Raytheon Co., Pocket Reference Book, 13 ed., pp. 8-12, 1993.

Capacity can vary depending on breaking characteristics and compression strength of each; installed horsepower, size of feed, rate of feed, type of fall, and proper operating conditions.

is determined by the shape of the mantle and bowl liner; it is similar to that of a jaw crusher.

**Primary** crushers have a steep cone angle and a small reduction ratio. **Secondary** crushers have a wider cone angle; this allows the finer product to be spread over a larger passage area and also spreads the wear over a wider area. Wear occurs to the greatest extent in the lower, fine-crushing zone. These features are further extended in cone crushers; therefore secondary gyratories are much less popular than secondary cone crushers, but they can be used as primaries when quarrying produces suitable feed sizes.

The three general types of gyratory crusher are the **suspended-spindle**, the **supported-spindle**, and the **fixed-spindle** types. Primary gyratories are designated by the size of feed opening, and

secondary or reduction crushers by the diameter of the head in feet and inches. There is a close opening and a wide opening as the mantle gyrates with respect to the concave ring at the outlet end. The close opening is known as the close setting or the close-side setting or the closed-side setting, while the wide opening is known as the wide-side or open-side setting. Specifications usually are based on closed settings. The setting is adjustable by raising or lowering the mantle.

The length of the crushing stroke greatly affects the capacity and the screen analysis of the crushed product. A very short stroke will give a very evenly crushed product but will not give the greatest capacity. A very long stroke will give the greatest capacity, but the product will contain a wider product-size distribution.

**Performance** Crushing occurs through the full cycle in a gyratory crusher, and this produces a higher crushing capacity than a similar-sized jaw crusher, which crushes only in the shutting half of the cycle. Gyratory crushers also tend to be easier to operate. They operate most efficiently when they are fully charged, with the main shaft fully buried in charge. Power consumption for gyratory crushers is also lower than that of jaw crushers. These are preferred over jaw crushers when capacities of 800 Mg/h (900 tons/h) or higher are required.

Gyratories make a product with open-side settings of 5 to 10 in at discharge rates from 600 to 6000 ton/h, depending on size. Most manufacturers offer a throw from ¼ to 2 in. The throughput and power draw depend on the throw and the hardness of the ore, and on the amount of undersize material in the feed. Removal of undersize (which can amount to ⅓ of the feed) by a stationary grizzly can reduce power draw.

**Crusher Product Sizes** Table 20-10 relates product size to the discharge setting of the crusher in terms of the percent smaller than that size in the product. Size-distribution curves differ for various types of materials crushed, and a general set of curves is not valid.

**Primary gyratories** will accept feed directly from truck or railcar. Most manufacturers make both mechanical and hydraulically supported types. Figure 20-23 shows a Nordberg primary gyratory crusher with spider suspension. It is available in 1- to 1.5-m (42-, 48-, 54-, and 60-in) feed sizes. Table 20-11 gives capacity data for the Superior gyratory crusher (*Allis-Chalmers*).

Gyratory crushers that feature wide-cone angles are called **cone crushers**. These are suitable for secondary crushing, because crushing of fines requires more work and causes more wear; the cone shape provides more working area than primary or jaw crushers for grinding of the finer product. Crusher performance is harmed by sticky material in the feed, more than 10 percent fines in the feed smaller than the crusher setting, excessive feed moisture, feed-size segregation, uneven distribution of feed around the circumference, uneven feed control, insufficient capacity of conveyors and closed-circuit screens, extremely hard or tough feed material, and operation at less than recommended speed. Rod mills are sometimes substituted for crushing of tough ore, since they provide more easily replaceable metal for wear.

HP Series Cone Crushers (*Nordberg Inc.*) (Fig. 20-24) are available in four sizes. The previous standard- and short-head versions have been combined into one machine, with replaceable liner shapes corresponding to either version, adapted respectively to relatively coarse and fine grinding. In addition, the throw has been increased so as to

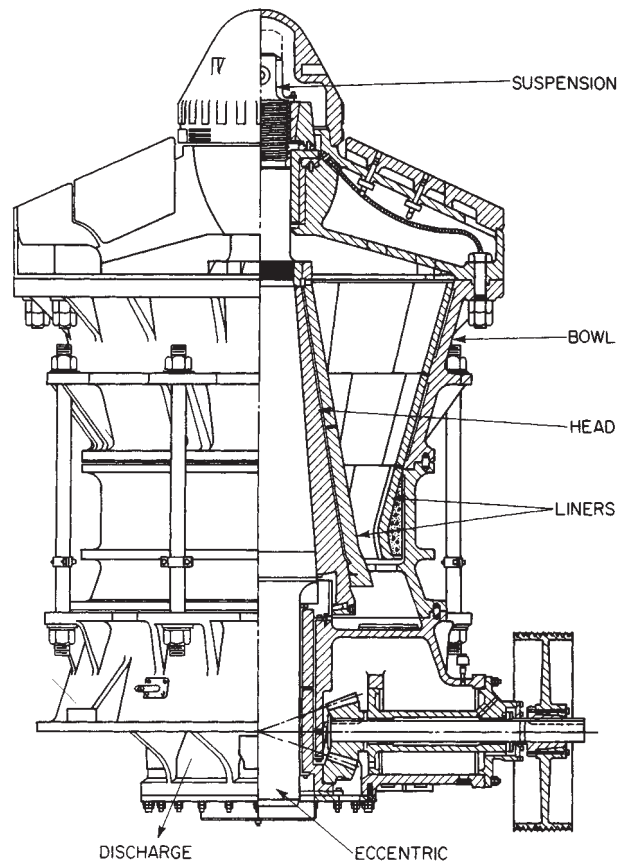


FIG. 20-23 Primary gyratory crusher with spider suspension. (Nordberg, Inc.)



10 percent fines less than the discharge setting, else scalping screens should be used. A series of Waterflush Crushers is also available from Nordberg, which flush out fines and increase capacity with some feeds, and allow its use in closed circuit with wet ball and autogenous mills (qv). It can give products with 80 percent passing as small as 0.15 in.

The Eljay Rollercone crusher (*Cedarapids Eljay Div.*) uses a different drive principle: a wedge-shaped plate rotates on a ring of roller bearings under the crushing cone, causing it to oscillate. Low wear of these bearings maintains close tolerance of settings and hence of product size, and their overdesign results in long bearing life. A hydraulic-relief system passes larger pieces of tramp iron than spring-relief systems, while a hydraulic hold-down system allows quick changing of crusher-setting shims. The massive base frame directs compression forces to the product, reducing energy losses due to structural deflection of the members. The crusher is available in sizes from 36- to 66-in diameter. With standard head the capacity ranges from 36 to 580 ton/h at closed-side settings of 3/8 to 2 in; with a fine-crushing head the capacity ranges from 37 to 368 ton/h with closed-side setting of 1.4 to 1 in and recirculating rates from 18 to 30 percent.

**Control of Crushers** Lower-grade raw materials, higher energy costs, larger-scale operations, and more complex, capital-intensive plants make automatic control of size-reduction equipment more important (Suominen, 21st International Symposium—Applications of Computers and Operations Research in the Mineral Industry, 1011–1018). Benefits are: increased productivity, process stability and safety, improved recovery of mineral values, and reduced costs [Horst and Enoch, *Engineering & Mining J.*, 181(6), 69–171 (1980)].

Improved sensors allow computer monitoring of the system for safety and protection of the equipment from damage. Sensors include lubrication-flow monitors and alarms, bearing-temperature sensors, belt scales, rotation sensors, and proximity sensors to detect ore level under the crusher. The latter prevent jamming of the output with too high an ore level, and protect the conveyor from impact of lumps with too low an ore level. Motion detectors assure that the conveyor is moving. Control applied to crusher systems including conveyors can facilitate use of mobile crushers in quarries and mines, since these can be controlled remotely by computer with reduced labor.

The objective of crusher control is usually to maximize crusher throughput at some specified product size, without overloading the crusher. Usually only three variables can be adjusted: feed rate, crusher opening, and feed size in the case of a secondary crusher. Four modes of control for a crusher are: (1) Setting overload control,

where the gape setting is fixed except that it opens when overload occurs. A hardness change during high throughput can cause a power overload on the crusher, which control should protect against. (2) Constant power setting control, which maximizes throughput. (3) Pressure control, which provides settings that give maximum crusher force, and hence, also throughput. (4) Feeding-rate control, for smooth operation. Setting control influences mainly product size and quality, while feed control determines capacity. Flow must also be synchronized with the feed requirements of downstream processes such as ball mills, and improved crusher efficiency can reduce the load on the more costly downstream grinding.

**ROLL CRUSHERS**

Once popular for coarse crushing, these devices long ago lost favor to gyratory and jaw crushers because of their poorer wear characteristics with hard rocks. Roll crushers are still commonly used for both primary and secondary crushing of coal and other friable rocks such as oil shale and phosphate. The roll surface is smooth, corrugated, or toothed, depending on the application. *Smooth rolls* tend to wear ring-shaped corrugations that interfere with particle nipping, although some designs provide a mechanism to move one roll from side to side to spread the wear. *Corrugated rolls* give a better bite to the feed, but wear is still a problem. *Toothed rolls* are still practical for rocks of not too high silica content, since the teeth can be regularly resurfaced with hard steel by electric-arc welding. Toothed rolls are frequently used for crushing coal and chemicals. For further details, see edition 6 of this handbook.

The **capacity** of roll crushers is calculated from the ribbon theory, according to the following formula:

$$Q = dLs/2.96 \tag{20-38}$$

where *Q* = capacity, cm<sup>3</sup>/min; *d* = distance between rolls, cm; *L* = length of rolls, cm; and *s* = peripheral speed, cm/min. The denominator becomes 1728 in engineering units for *Q* in cubic feet per minute, *d* and *L* in inches, and *s* in inches per minute. This gives the theoretical capacity and is based on the rolls' discharging a continuous, solid uniform ribbon of material. The actual capacity of the crusher depends on roll diameter, feed irregularities, and hardness and varies between 25 and 75 percent of theoretical capacity.

Sturtevant two-roll crushers are available in capacities from 2 to 30 hp (1.5 to 22 kW). The gap is controlled by a hand-wheel. Rolls are hard-surfaced for wear resistance.

**TABLE 20-12 Cone Crusher Capacity in Open Circuit, ton/h\***

Mill	Feed opening +, in.	Motor hp	r/min	Closed-Side Discharge Setting, in							
				¼	⅜	½	¾	1	1.5	2	
HP200	¾–7	150	1200	85	110	150	190	220	200		
HP500	¾–12	450	900	180	230	290	390	445	540	605	
HP700	1½–14	600	850	300	370	425	600	675	845	975	
MP1000	5–18	1000		600	750	900	1100	1200	1800	2400	

\*Nordberg Inc.—assumes feed weighing 100 lb/ft<sup>3</sup> and with a work index of 13. Range covered by short-head and standard versions.

**TABLE 20-13 Cone Crusher Capacity in Closed-Circuit, ton/h\***

Mill	Top Size of Product from Screen (98% passing), in											
	¼		⅜		½		¾		1		1½	
	A	B	A	B	A	B	A	B	A	B	A	B
HP200	65	90	80	115	115	165	140	200	160	230	180	265
HP500	135	195	175	250	220	315	280	405	335	465	380	545
HP700	215	310	275	390	215	445	425	610	480	680	590	850
MP1000	320	450	980	720	630	800	840	1100	1000	1200		

\*Nordberg Inc. Assumes feed weighing 100 lb/ft<sup>3</sup> and with a work index of 13. A—Net finished product from screen. B—Recirculating load.

## ROLL PRESS

A novel comminution device, the **roll press**, has achieved commercial success [Schoenert, *International J. Mineral Processing*, **22**, 401–412 (1988)]. It is used for fine crushing, replacing the function of a coarse-ball mill or of tertiary crushers. Unlike ordinary roll crushers which crush individual particles, the roll press is choke fed and acts on a thick stream or ribbon of feed. Particles are crushed mostly against other particles, so wear is very low. Energy efficiency is also greater than in ball mills.

The product is in the form of agglomerated slabs. These are broken up either in a ball mill or an impact or hammer mill running at a speed too slow to break individual particles. Some materials may even deagglomerate from the handling that occurs in conveyors. Product-size distributions are shown in Fig. 20-25. Note that the press can handle a hard rock like quartz. Pressure in Fig. 20-25 is the calculated force-per-unit contact area in the nip. A large proportion of fines is produced, but a fraction of coarse material survives. This makes recycle necessary. From experiments to grind cement clinker  $\sim 80 \mu\text{m}$ , as compression is increased from 100 to 300 MPa, the required recycle ratio decreases from 4 to 2.8. The energy required per ton of throughput increases from 2.5 to 3.5 kWh/ton. These data are for a 200-mm diameter pilot-roll press.

Status of 150 installations in the cement industry are reviewed [Strasser et al., *Rock Products*, **92**(5), 60–72 (1989)]. In cement-clinker milling, wear is usually from 0.1 to 0.8 g/ton, and for cement raw materials it is between 0.2 and 1.2 g/ton, whereas it may be 20- to 40-in ball mills. New surface of 100 to 130  $\text{cm}^2/\text{g}$  is produced with cement. The size of the largest feed particles should not exceed  $0.04 \times$  roll diameter ( $D$ ) according to Schoenert (loc. cit.). However, it has been found [Wuestner et al., *Zement-Kalk-Gips*, **41**(7), 345–353 (1987); English edition, 207–212] that particles as large as 3–4 times the roll gap may be fed to an industrial press. Particles receive preliminary breakage at the top of the nip.

The hybrid circuit in Fig. 20-26 has proven most versatile, and can increase capacity of an existing ball-mill circuit by 30 to 100 percent. Recycling the rock as in the hybrid flow sheet reduces the need for coarse-ball milling.

Roll presses are now manufactured by most cement-equipment manufacturers, for example Krupp-Polysius AG. For drives up to 1200 kW they are equipped with V-belt drives, allowing speed to be changed. Rolls in one particular crusher are 48 inches (1200 mm) in diameter and 30 inches (700-mm) wide and each weighs 90 tons. Machines with up to 2500 kW installed power and 1000 ton/h (900

tonne/h) capacity have been installed. The largest presses can supply feed for four or five ball mills.

Operating experience (Wuestner et al., loc. cit.) has shown that roll diameters about 1 m are preferred, as a compromise between production rate and stress on the equipment. The press must be operated choke fed, with a substantial depth of feed in the hopper; otherwise it will act like an ordinary roll crusher.

The advent of the roll press has greatly improved the economy of cement milling. More information is given later under cement.

## IMPACT BREAKERS

Impact breakers include heavy-duty hammer crushers and rotor impact breakers. Fine hammer mills are described in a subsequent subsection.

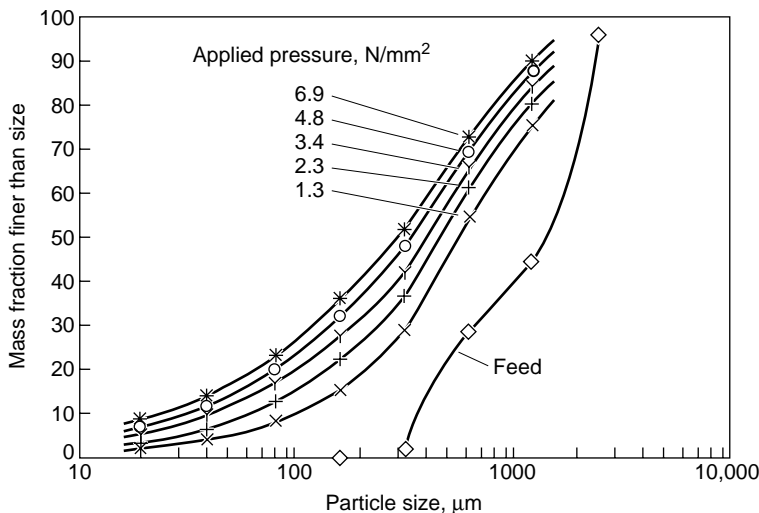
Not all rocks shatter well by impact. Impact breaking is best suited for the reduction of relatively nonabrasive and low-silica-content materials such as limestone, dolomite, anhydrite, shale, and cement rock, the most popular application being on limestone.

**Hammer Crusher** (Fig. 20-27) Pivoted hammers are mounted on a horizontal shaft, and crushing takes place by impact between the hammers and breaker plates. Heavy-duty hammer crushers are frequently used in the quarrying industry, for processing municipal solid waste, and scrap automobiles.

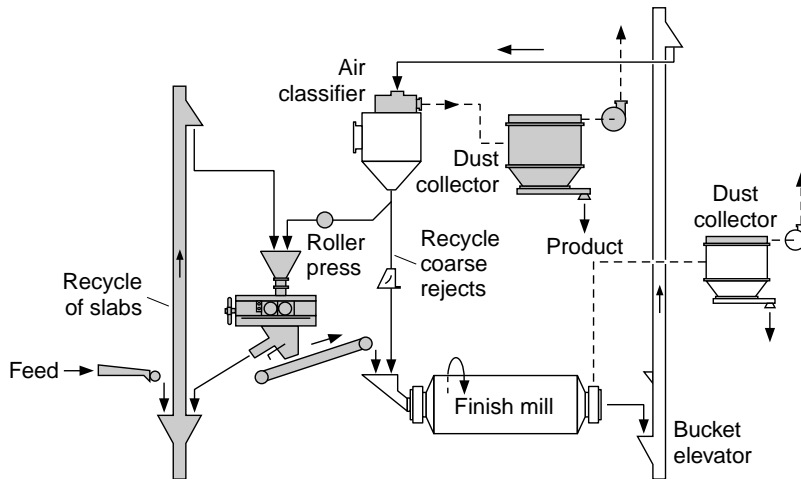
These crushers are of two types, with and without grates or screens. The bottom of the **Pennsylvania reversible impactor** (Fig. 20-27) is open, and the sized material passes through almost instantaneously. Particles acquire high velocities, and this leads to little control on particle size and a much higher proportion of fines than slow-speed crushers. A product-size distribution curve (*Handbook of Crushing*, Pennsylvania Crusher Corp, 1994) shows the following for crushing of minus 10-in subbituminous coal from Wyoming: 92 percent minus 2 in, 48 percent minus 0.53 in, 15 percent minus 10 mesh/in.

In the second type of mill (Fig. 20-28), a cylindrical grating is provided beneath the rotor for product discharge. Some hammer crushers are symmetrically designed so that the direction of rotation can be reversed to distribute wear evenly on the hammer and breaker plates. When such a **Pennsylvania nonreversible hammermill** is used for reduction, material is broken first by impact against hammers and then by rubbing action (attrition) against screen bars. Performance data of Pennsylvania reversible hammer mills are shown in Table 20-14.

*Sturtevant Inc.* produces three sizes of screen-type hammermills with 5 to 50 hp (4 to 37 kW) capacity, suitable for recycle of glass and



**FIG. 20-25** Size distribution of roll-press products. Feed is quartz, 300–2500  $\mu\text{m}$ , dry. [Schoenert, *International J. Mineral Processing*, **22**, 401–412 (1988).]



**FIG. 20-26** Hybrid flow sheet to combine a roll press and ball mill with a classifier. (Conroy, 31st IEEE Cement Industry Technical Conference, 509–542, 1988. Copyright IEEE.)

wastes, and for mineral processing. **Jeffrey hammermills** (Jeffrey Div, Indresco Inc.) are available with screen grates having capacities from 50 to 140 ton/h (135 to 350 Mg/h) for a product with top size 1.75 in (45 mm). The screenless, reversible type is also available.

Each hammer may weigh several hundred kilograms. Speed varies between 500 to 1800 r/min, depending on the size of the machine.

**Rotor Impactors** The rotor of these machines is a cylinder to which is affixed a tough steel bar. Breakage can occur against this bar or on rebound from the walls of the device. Free impact breaking is the principle of the rotor breaker, and it does not rely on pinch crushing or attrition grinding between rotor hammers and breaker plates.

The result is a high reduction ratio and elimination of secondary and tertiary crushing stages. The investment cost may be a third of that for a two-stage jaw and gyratory crusher plant producing 180 Mg/h (200 tons/h) and half for a plant crushing 540 Mg/h (600 tons/h) [Godfrey, *Quarry Managers' J.*, 405–416 (October 1964)].

By adding a screen on a portable mounting, a complete, compact mobile crushing plant of high capacity and efficiency for use in any location is provided.

The peripheral speed of the rotors manufactured by *KHD Humboldt Wedag* is 34 m/sec; the 52-ton rotor can handle a lump as large as 8 ton. Controllers stop the feeder if rotor speed drops below 75 per-

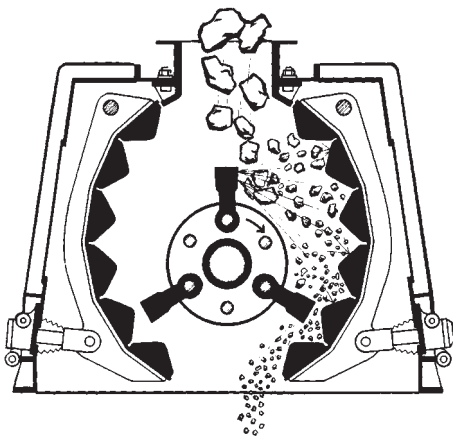
cent of normal [Schaefer and Gallus, *Zement-Kalk-Gips*, 41(10), 486–492 (1988); English ed., 277–280].

*Pennsylvania Crusher Corp.* offers a variety of impactor types: granulators, Bradford breakers, roll crushers, and jaw crushers. (See Table 20-15.)

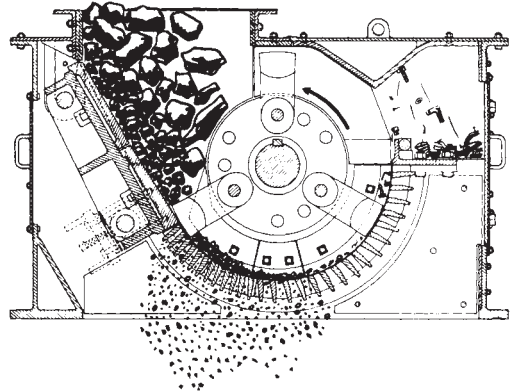
The **ring-type granulator** (*Pennsylvania Crusher Corp.*) features a rotor assembly with loose crushing rings, held outwardly by centrifugal force, which chop the feed. It is suitable for highly friable materials which may give excessive fines in an impact mill. For example, bituminous coal is ground to a product below 2 cm ( $\frac{3}{4}$  in). They have also been successfully used to grind abrasive quartz to sand size, due to the ease of replacement of the ring impact elements.

**Cage Mills** The **Stedman disintegrator** (*Stedman Machine Co.*), commonly referred to as a cage mill, is used for crushing quarry rock, phosphate rock, and fertilizer and for disintegrating clays, colors, press cake, and bones. Cages of one, two, three, four, six, and eight rows, with bars of special alloy steel, revolving in opposite directions, produce a powerful impact action that pulverizes many materials. (See Fig. 20-29.)

The life of a cage may be a few months and may produce 9000 Mg (10,000 tons) of quarry rock. A gray-iron cage is used for alumina grinding, with metal particles removed magnetically. The advantage of



**FIG. 20-27** Reversible impactor. (*Pennsylvania Crusher Corp.*)



**FIG. 20-28** Nonreversible hammermill (*Pennsylvania Crusher Corp.*)

TABLE 20-14 Performance Data for Reversible Hammer Mills

Model no.	Rotor dimensions, in	Maximum feed size, in	Maximum speed, r/min	hp	Capacity, tons/h
505	30 × 30	2½	1200	100–200	40–60
605	36 × 30	4	1200	200–300	80–100
708	42 × 48	8	900	300–550	140–180
815	48 × 90	10	900	900–1200	330–400
1014	60 × 84	12	720	1100–1500	450–500
1217	72 × 102	14	600	1550–2000	620–685
1221	72 × 126	14	600	1900–2500	760–850

NOTE: To convert inches to centimeters, multiply by 2.54; to convert horsepower to kilowatts, multiply by 0.746; and to convert tons per hour to megagrams per hour, multiply by 0.907.

TABLE 20-15 Performance of Dual-Rotor Impact Breakers

Model no.	Feed opening, in	Speed, r/min	hp	Hammer weight, lb	Product size, in	Capacity, tons/h
3648	36 × 48	550–990	250–300	300	2	300
4850	48 × 50	550–990	300–400	400	3	500
5462	54 × 62	480–750	400–500	500	4–5	700
6072	60 × 72	300–600	500–600	600	5–6	1200

To convert pounds to kilograms, multiply by 0.4535; to convert inches to centimeters, multiply by 2.54; to convert horsepower to kilowatts, multiply by 0.746; and to convert tons per hour to megagrams per hour, multiply by 0.907.

multiple-row cages is the achievement of a greater reduction ratio in a single pass.

These features and the low cost of the mills make them suitable for medium-scale operations where complicated circuits cannot be justified. The maximum feed size is 20 cm (8 in), and the product size may be as fine as 325 mesh.

**Prebreakers** Aside from the normal problems of grinding, there are special procedures and equipment for breaking large masses of feed to smaller sizes for further grinding. There is the breaking or shredding of bales, as with rubber, cotton, or hay, in which the compacted mass does not readily come apart. There also is often caking in bags of plastic or hygroscopic materials which were originally fine. Although crushers are sometimes used, the desired size-reduction ratio often is not obtainable. Furthermore, a lower capital investment may result through choosing a less rugged device which progressively attacks the large mass to remove only small amounts at a time. In structure such a device comprises a toothed rotating shaft in a casing.

*Prater Industries, Inc.*, offers a double roll with heavy-duty teeth as a precrusher feeder. The **Mikro roll crusher** (*Hosokawa Micron*

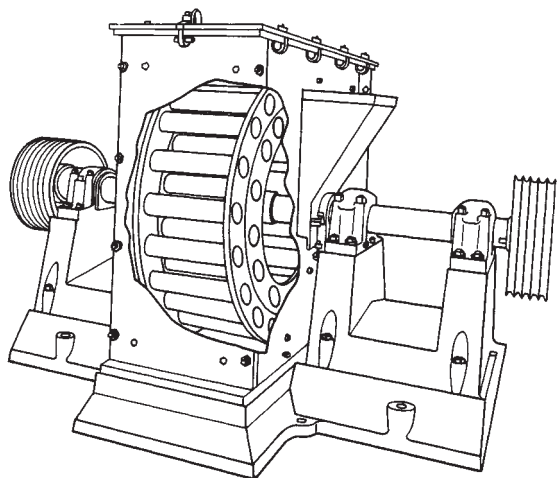


FIG. 20-29 Two-cage disintegrator. (Stedman Machine Co.)

*Powder Systems*) serves as grinder or prebreaker and is of similar type. The **Rietz prebreaker** differs somewhat from these.

**Precision Cutters and Slitters** Often it becomes desirable to reduce the size of a solid mass to regular smaller sizes.

Precision knife cutters differ from random cutting mills in that a feeder is synchronized with the knives. This ensures the exact size, whether it be slit widths in a sheet, fiber length from a strand, or both width and length from a sheet, as in dicing. In the **Giant dicing cutter**, the sheet stock is first slit lengthwise with opposing sets of circular knives. The slit strands then pass between pressure rolls to a rotary cutter which operates against an adjustable bed knife. Capacities range up to 18 Mg/h (20 tons/h), with sheet stock up to 60 cm (24 in) wide.

## PAN CRUSHERS

**Design and Operation** The pan crusher (Fig. 20-30) consists of one or more grinding wheels or mullers revolving in a pan; the pan may remain stationary and the mullers be driven, or the pan may be driven while the mullers revolve by friction. The mullers are made of tough alloys such as Ni-Hard. Iron scrapers or plows at a proper angle feed the material under the mullers.

The **Chambers dry pan** (*Bonnot Co.*) uses air cylinders to regulate the grinding pressure under each of the muller tires from 33,000 to 90,000 N (7500 to 20,000 lb).

The pan bottom rotates and has a central solid crushing ring as well as an outer ring of screen plates with openings from 0.16 to 1.3 cm (⅛ to ½ in). In some instances a solid pan bottom is used in place of a perforated screen bottom, and the ground material is discharged through a slot in the rim.

**Performance** The dry pan is useful for crushing medium-hard and soft materials such as clays, shales, cinders, and soft minerals such as barites. Materials fed should normally be 7.5 cm (3 in) or smaller, and a product able to pass No. 4 to No. 16 sieves can be delivered, depending on the hardness of the material.

High reduction ratios with low power and maintenance are features of pan crushers.

The Chambers dry pan is available from 1.8 to 3 m (6 to 10 ft) pan diameter with mullers ranging from 0.71 to 1.6 m (28 to 62 in) in diameter with 13- to 46-cm (5- to 18-in) face. Power ranges from 11 to 75 kW (15 to 100 hp) or from 0.8 to 4 kW/Mg (1 to 5 hp/ton) of product. Production rate varies from 1 to 54 Mg/h (1 to 60 tons/h) according to pan size and hardness of material as well as fineness of feed and product.

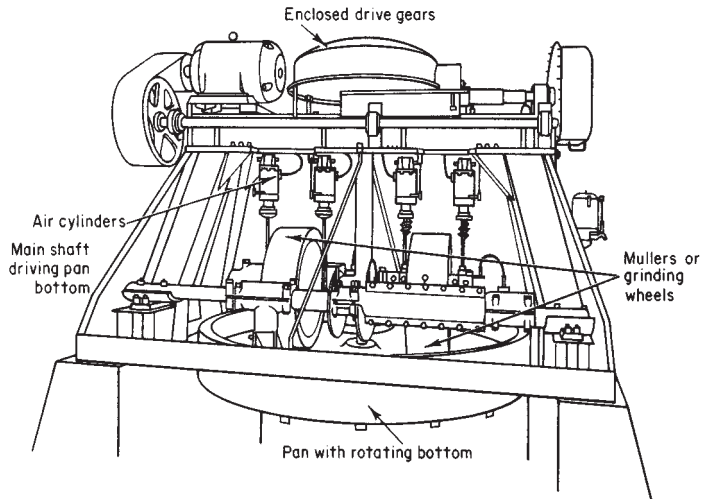


FIG. 20-30 Chambers 10-ft, 100-hp dry pan. (Bonnot Co.)

The **wet pan** is used for developing plasticity or molding qualities in ceramic feed materials. The abrasive and kneading actions of the mullers blend finer particles with the coarser particles as they are crushed (Greaves-Walker, *Am. Refract. Inst. Tech. Bull.* 64, 1937), and this is necessary so that a high packing density can be achieved to result in strength.

### TUMBLING MILLS

Ball, pebble, rod, tube, and compartment mills have a cylindrical or conical shell, rotating on a horizontal axis, and are charged with a grinding medium such as balls of steel, flint, or porcelain or with steel rods. The **ball mill** differs from the tube mill by being short in length; its length, as a rule, is not far from its diameter (Fig. 20-31). Feed to ball mills can be as large as 2.5 to 4 cm (1 to 1½ in) for very fragile

materials, although the top size is generally 1 cm (½ in). Most ball mills operate with a reduction ratio of 20 to 200:1. The largest balls are typically 13 cm (5 in) in diameter.

The **tube mill** is generally long in comparison with its diameter, uses smaller balls, and produces a finer product. The compartment mill consists of a cylinder divided into two or more sections by perforated partitions; preliminary grinding takes place at one end and finish grinding at the discharge end. These mills have a length-to-diameter ratio in excess of 2 and operate with a reduction ratio of up to 600:1. Rod mills deliver a more uniform granular product than other revolving mills while minimizing the percentage of fines, which are sometimes detrimental.

The **pebble mill** is a tube mill with flint or ceramic pebbles as the grinding medium and may be lined with ceramic or other nonmetallic liners. The **rock-pebble mill** is an autogenous mill in which the

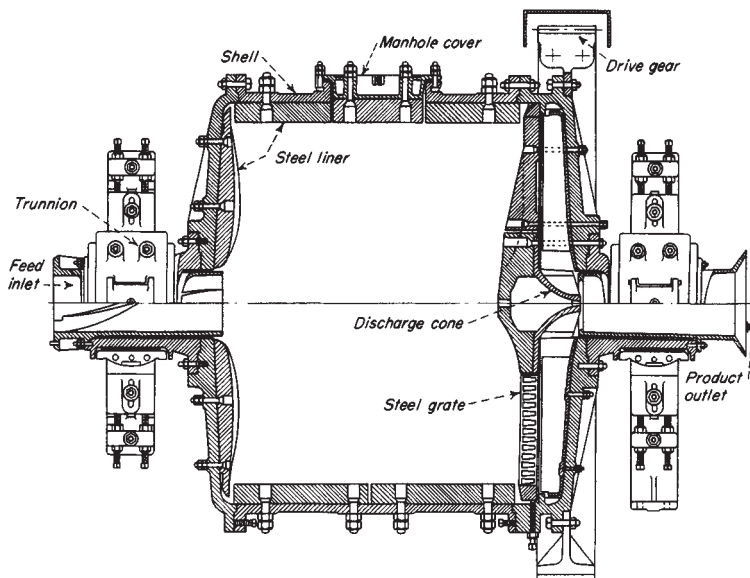


FIG. 20-31 Marcy grate-type continuous ball mill. (Allis Mineral Systems, Svedala Inc.)

medium consists of larger lumps scalped from a preceding step in the grinding flow sheet.

**Design** The conventional type of **batch mill** consists of a cylindrical steel shell with flat steel-flanged heads. Mill length is equal to or less than the diameter [Coghill, De Vaney, and O'Meara, *Trans. Am. Inst. Min. Metall. Pet. Eng.*, **112**, 79 (1934)]. The discharge opening is often opposite the loading manhole and for wet grinding usually is fitted with a valve. One or more vents are provided to release any pressure developed in the mill, to introduce inert gas, or to supply pressure to assist discharge of the mill. In dry grinding, the material is discharged into a hood through a grate over the manhole while the mill rotates. Jackets can be provided for heating and cooling.

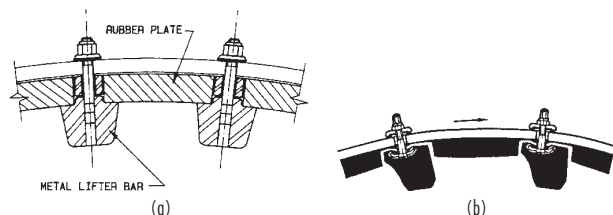
Material is fed and discharged through hollow trunnions at opposite ends of **continuous mills** (Fig. 20-31). A grate or diaphragm just inside the discharge end may be employed to regulate the slurry level in wet grinding and thus control retention time. In the case of **air-swept mills**, provision is made for blowing air in at one end and removing the ground material in air suspension at the same or other end.

Ball mills usually have **liners** which are replaceable when they wear. Optimum liner shapes which key the ball charge to the shell and prevent slippage are illustrated in Fig. 20-32. Special operating problems occur with smooth-lined mills owing to erratic slip of the charge against the wall. At low speeds the charge may **surge** from side to side without actually tumbling; at higher speeds tumbling with **oscillation** occurs. The use of lifters prevents this [Rose, *Proc. Inst. Mech. Eng. (London)*, **170**(23), 773-780 (1956)]. Power consumption in a smooth mill depends in a complex way on operating conditions such as feed viscosity, whereas it is more predictable in a mill with lifters [Kitchenier and Clarke, *Br. Chem. Eng.*, **13**(7), 991 (1968)].

Plant data on an 8-ft diameter rod mill showed that when smooth liners were replaced with lifter bars spaced 300 mm (12 in) apart, liner wear decreased by 13-fold, production increased 50 percent, and power per ton decreased by 34 percent [Howat and Verneulen, *Journal South African Institute Mining and Metallurgy*, **86**, 251-259 (July 1986)]. When a smooth-walled ball mill was fitted with lifter bars the production of  $-75 \mu\text{m}$  material increased 8 percent and the power/ton decreased 10 percent. Plant tests confirmed previous results [Meaders and McPherson, *Mining Engineering*, **16**, 81-84 (Sept. 1964)] that optimum lifter bar spacing is from 3 to 5 times bar height.

Liner wear increases with the size, hardness, and sharpness of feed more than with ball size. The hardness of manganese steel corresponds to softer types of ore, while Nihard is about the same as magnetite [Moore et al., *International J. of Mineral Processing*, **22**, 313-343 (1983)]. Quartz and pyrite are considerably harder than any metals used. Rubber, being resilient, is less affected by ore hardness, and therefore has the advantage with harder ores. Low-charge volume below 35 percent results in increased wear since the liners are not protected by a covering of ore. Several studies indicate that wear increases at least proportional to the square of mill speed in percent of critical.

Both all-rubber liners, and rubber liners with metal lifter bars are currently used in large ball mills [McTavish, *Mining Engineering*, **42**, 1249-1251 (Nov. 1990)]. Both types (Fig. 20-32) have rubber-liner plates, separated and held in place by lifter bars. Rubber liners have the following advantages: Abrasion and impact resistance, 15 percent



**FIG. 20-32** Types of ball-mill liners: (a) combination liner [McTavish, *Mining Engineering*, **42**, 11, 1249-1251 (1990) Exton Industries, Inc.]; (b) all-rubber liner [Moller and Brough, *Mining Engineering*, **41**, 8, 849-853 (1989) Skega Ltd.].

lower weight than steel, which makes replacement easier, lower noise, and tight sealing against the shell.

The dimensions and spacing of rubber lifter bars are critical to good operation and wear resistance. Figure 20-32 shows rubber lifters with a spacing formula recommended by Moller and Brough [*Mining Engineering*, **41**, 849-853 (Aug. 1989)]. Lifters must be at least as high as the ball radius, to key the ball charge and assure that the balls fall into the toe area of the mill [Powell, *International J. Mineral Processing*, **31**, 163-193 (1991)].

The flexibility of rubber is helpful in discharge grates. Each time the grate dips into the slurry it flexes, tending to work out particles stuck in the grate holes. Metal frames support the rubber while leaving areas with holes free to flex. The grate is backed up by lifter bars which lift the slurry into the discharge trommel.

Grinding balls can be made of forged steel, cast steel, or cast iron. (See under Wear for more information on alloys.)

*Pebble mills* are frequently lined with nonmetallic materials when iron contamination would harm a product such as a white pigment or cement. Belgian silex (silica) or porcelain block are popular linings. Silica linings and ball media have proved to wear better than other nonmetallic materials. The higher density of silica media increases the production capacity and power draft of a given mill.

Capacities of pebble mills are generally 30 to 50 percent of the capacity of the same size of ball mill with steel grinding media and liners; this depends directly on the density of the media.

Smaller mills, up to about  $0.19\text{-m}^3$  (50-gal) capacity, are made in one piece with a cover. U.S. Stoneware Co. makes these in wear-resistant Burundum-fortified ceramic and also makes larger three-piece units, in a metal protective case, up to  $0.8\text{-m}^3$  (210-gal) capacity. A handbook on pebble milling is available from Paul O. Abbe, Inc., Little Falls, NJ.

**Operation** **Cascading** and **catracting** are the terms applied to the motion of grinding media. The former applies to the rolling of balls or pebbles from top to bottom of the heap, and the latter refers to the throwing of the balls through the air to the toe of the heap.

The criterion by which the ball action in mills of various sizes may be compared is the concept of **critical speed**. It is the theoretical speed at which the centrifugal force on a ball in contact with the mill shell at the height of its path equals the force on it due to gravity:

$$N_c = 42.3/\sqrt{D} \quad (20-39)$$

where  $N_c$  is the critical speed, r/min, and  $D$  is diameter of the mill, m (ft), for a ball diameter that is small with respect to the mill diameter. The numerator becomes 76.6 when  $D$  is expressed in feet.

**Actual mill speeds** range from 65 to 80 percent of critical. It might be generalized that 65 to 70 percent is required for fine wet grinding in viscous suspension and 70 to 75 percent for fine wet grinding in low-viscosity suspension and for dry grinding of large particles up to 1-cm ( $1/2$ -in) size. The speeds might be increased by 5 percent of critical for un baffled mills to compensate for slip.

The chief factors determining the size of **grinding balls** are fineness of the material being ground and maintenance cost for the ball charge. A coarse feed requires a larger ball than a fine feed.

The need for a calculated ball-size feed distribution is open to question; however, methods have been proposed for calculating a rationed ball charge [Bond, *Trans. Am. Inst. Min. Metall. Pet. Eng.*, **153**, 373 (1943)].

The recommended optimum size of makeup rods and balls is [Bond, *Min. Eng.*, **10**, 592-595 (1958)]

$$D_b = \sqrt{\frac{X_f E_i}{K n_r}} \sqrt{\frac{\rho_s}{\sqrt{D}}} \quad (20-40)$$

where  $D_b$  = rod or ball diameter, cm (in);  $D$  = mill diameter, m (ft);  $E_i$  is the work index of the feed;  $n_r$  is speed, percent of critical;  $\rho_s$  is feed specific gravity; and  $K$  is a constant = 214 for rods and 143 for balls. The constant  $K$  becomes 300 for rods and 200 for balls when  $D_b$  and  $D$  are expressed in inches and feet respectively. This formula gives reasonable results for production-sized mills but not for laboratory mills. The ratio between the recommended ball and rod sizes is 1.23.



A graded charge of rods results from wear in a rod mill. **Rod diameter** may range from 10 to 2.5 cm (4 to 1 in), for example. A new rod load usually is patterned after a used one found to give good results. The maximum length of a rod mill appears to be 20 ft, because longer rods tend to twist and bend.

**Tumbling-Mill Circuits** Tumbling mills may be operated in **normal closed circuit**, as shown in Fig. 20-45 or 20-59, or in **reverse arrangement** in which the feed passes through the classifier before entering the mill (see secondary mill in Fig. 20-44 or 20-59).

**Material and Ball Charges** The load of a grinding medium can be expressed in terms of the percentage of the volume of the mill that it occupies; i.e., a bulk volume of balls half filling a mill is a 50 percent ball charge. The void space in a static bulk volume of balls is approximately 41 percent. Since the medium expands as the mill is rotated, the actual running volume is unknown.

Simple relationships govern the amount of balls and voids in the mill. The weight of balls =  $\rho_b \epsilon_b V_m$ , where  $\rho_b$  = bulk density of balls,  $g/cm^3$  ( $lb/ft^3$ );  $\epsilon_b$  = apparent ball filling fraction; and  $V_m$  = volume of mill =  $\pi D^2 L/4$ . Steel balls have a bulk density of approximately  $4.8 g/cm^3$  ( $300 lb/ft^3$ ); stone pebbles,  $1.68 g/cm^3$  ( $100 lb/ft^3$ ); and alumina balls,  $2.4 g/cm^3$  ( $150 lb/ft^3$ ).

The amount of material in a mill can be expressed conveniently as the ratio of its volume to that of the voids in the ball load. This is known as the **material-to-void ratio**. If the solid material and its suspending medium (water, air, etc.) just fill the ball voids, the M/V ratio is 1, for example. Grinding-media loads vary from 20 to 50 percent in practice, and M/V ratios are usually near 1.

The material charge of continuous mills called the **holdup** cannot be set directly but is indirectly determined by operating conditions. There is a maximum throughput rate that depends on the shape of the mill, the flow characteristics of the feed, the speed of the mill, and the type of feed and discharge arrangement. Above this rate the holdup increases unstably.

The holdup of material in a continuous mill determines the mean residence time, and thus the extent of grinding. Gupta et al. [*International J. Mineral Processing*, **8**, 345–358 (Oct. 1981)] analyzed published experimental data on a  $40 \times 40$ -cm grate discharge laboratory mill, and determined that holdup was represented by  $H_w = (4.020 - 0.176 WI)F_w + (0.040 + 0.01237 WI)S_w - (4.970 + 0.395 WI)$ , where WI is Bond work index based on 100 percent passing a 200-mesh sieve,  $F_w$  is the solids feed rate in kg/min, and  $S_w$  is weight percent solids in the feed. This represents experimental data for limestone, feldspar, sulfide ore, and quartz. The influence of WI is believed to be due to its effect on amount of fines present in the mill. Parameters that did not affect  $H_w$  are specific gravity of feed material, and feed size over the narrow range studied.

Sufficient data was not available to develop a correlation for overflow mills, but the data indicated a linear variation of  $H_w$  with  $F$  as well.

The mean residence time  $\tau$  (defined as  $H_w/F$ ) is the most important parameter, since it determines the time over which particles are exposed to grinding. Measurements on several industrial mills (Weller, *Automation in Mining Mineral and Metal Processing*, 3d IFAC Symposium, 303–309, 1980) (measured on the water, not the ore) showed that the maximum mill filling was about 40 percent, and the maximum flow velocity through the mill is 40 m/h.

Swaroop et al. [*Powder Technology*, **28**, 253–260 (Mar.–Apr. 1981)] found that the material holdup is higher and the vessel dispersion number  $D\tau/L^2$  (see subsection on Continuous Mill Simulation) is lower in the rod mill than in the ball mill under identical dimensionless conditions. This indicates that the known narrow-product-size distribution from rod mills is partly due to less mixing in the rod mill, in addition to different breakage kinetics.

The holdup in grate-discharge mills depends on the grate openings. Kraft et al. [*Zement-Kalk-Gips International*, **42**(7), 353–9 (1989); English edition, 237–9] measured the effect of various hole designs in wet milling. They found that slots tangential to the circumference gave higher throughput and therefore lower holdup in the mill. Total hole area had little effect until the feed rate was raised to a critical value (30 m/h in a mill 0.26 m diam  $\times$  0.6 m long); above this the larger area led to lower holdup. The open area is normally specified between 3 and 15 percent, depending on the number of grinding chambers and

other conditions. The slots should be 1.5 to 16 mm wide, tapered toward the discharge side by a factor of 1.5 to 2 to prevent blockage by particles.

**Dry versus Wet Grinding** The choice between wet and dry grinding is generally dictated by the end use of product. If the presence of liquid with the finished product is not objectionable or the feed is moist or wet, wet grinding generally is preferable to dry grinding, but power consumption, liner wear, and capital costs determine the choice. Other factors that influence choice are the performance of subsequent dry or wet classification steps, the cost of drying, and the capability of subsequent processing steps for handling a wet product.

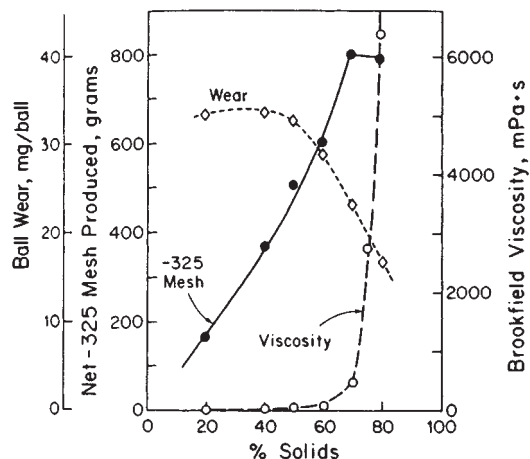
The net production in wet grinding in the Bond grindability test varies from 145 to 200 percent of that in dry grinding depending on mesh [Maxson, Cadena, and Bond, *Trans. Am. Inst. Min. Metall. Pet. Eng.*, **112**, 130–145, 161 (1934)]. Ball mills have a large field of application for wet grinding in closed circuit with size classifiers, which also perform advantageously wet.

In fine dry grinding, surface forces come into action to cause cushioning and ball coating with a less efficient use of energy. Grinding-media and liner-wear consumption per ton of ground product is lower for a dry-grinding system. However, power consumption for dry grinding is about 30 percent larger than for wet grinding. Dry grinding requires the use of dust-collecting equipment.

In **wet ball milling** the grinding rate increases with solids content up to 70 wt % (35 vol %), as Fig. 20-33 shows, due to pulp rheology. Examination of gouge marks indicated that most breakage was by impact of balls on particles rather than by abrasion.

The **rheological properties** of the slurry affect the grinding behavior in ball mills. Rheology depends on solids content, particle size, and mineral chemical properties [Kawatra and Eisele, *International J. Mineral Processing*, **22**, 251–259 (1988)]. Up to 50 percent solids by volume a mineral slurry exhibits dilatant behavior, i.e. shear stress increases more than proportionate to shear rate. Above 50 percent it becomes pseudoplastic, i.e., it exhibits a yield value (Austin, Klimpel, and Luckie, *Process Engineering of Size Reduction: Ball Milling*, AIME, 1984). Above the yield value the grinding rate decreases, and this is believed to be due to adhesion of grinding media to the mill wall causing centrifuging [Tangsatitkulchai and Austin, *Powder Technology*, **59**(4), 285–293 (1989)]. Maximum power draw and fines production are achieved when the solids content is just below that which produces the critical yield.

The solids concentration in a pebble-mill slurry should be high enough to give a slurry viscosity of at least 0.2 Pa·s (200 cP) for best grinding efficiency [Creyke and Webb, *Trans. Br. Ceram. Soc.*, **40**, 55



**FIG. 20-33** Effect of percent solids on the wear of mild steel balls, net weight of 325 mesh material produced, and pulp viscosity after grinding magnetic taconite for 60 min [Iwasaki et al., *International J. Mineral Processing*, **22**, 345–360 (1988).]

(1941)], but this may have been required to key the charge to the walls of the smooth mill used.

Since viscosity increases with amount of fines present, mill performance can often be improved by closed-circuit operation to remove fines. Chemicals such as surfactants allow the solids content to be increased without increasing the yield value of the pseudoplastic slurry, allowing a higher throughput. They may cause foaming problems downstream, however. Increasing temperature lowers the viscosity of water, which controls the viscosity of the slurry under high-shear conditions such as those encountered in the cyclone, but does not greatly affect chemical forces. Slurry viscosity can be most directly controlled by controlling solids content. To control viscosity it is necessary to measure the viscosity on line. Kawatra and Eisele (loc. cit.) have described viscometers that can measure viscosity of a flowing slurry stream with high-solids content. A satisfactory spindle type operates in an overflow reservoir of the slurry (Napier-Munn et al., DeBeers Diamond Research Laboratory, Johannesburg, 1985, in Kawatra and Eisele, loc. cit.). Vibrating and ultrasonic types can also be used.

A simple device [Montini and Moys, *J. South African Inst. Mining & Metallurgy*, **88**(6), 199–206 (1988)] measures slurry viscosity and hence percent solids within the mill. It consists of a bolt that passes through insulating washers in the shell. A measurement of electrical conduction is taken at a moment when the ball charge has just fallen away from the rotating shell. This measures the thickness of the slurry adhering to the vicinity of the bolt, which is related to the slurry viscosity. The device can distinguish among slurry concentrations of 60, 65, and 70 percent solids, and should be useful for computer control of viscosity in the mill.

**Feed and Discharge** Feed and discharge arrangements for ball and rod mills depend on their mode of operation. Various feed and discharge mechanisms are shown in Fig. 20-34.

**Mill feeders** attached to the feed trunnion of the conical mill and used to pass the feed into the mill without backspill are of several types. A feed chute is generally used for dry grinding, this consisting of an inclined chute which is sealed at the outer edge of the trunnion and down which the material slides to pass through the trunnion and into the mill. A screw feeder, consisting of a short section of screw conveyor which extends partway into the opening in the feed trunnion and conveys the material into the mill, may also be used when dry

grinding. For wet grinding, several different types of feeders are available: the scoop feeder, which is attached to and rotates with the mill trunnion and which dips into a stationary box to pick up the material and pass it into the mill; a drum feeder attached to and rotating with the feed trunnion, having a central opening into which the material is fed and an internal deflector or lifter to pass the material through the trunnion into the mill; or a combination drum and scoop feeder, in which the new feed to the mill is fed through the central opening of the drum while the scoop picks up the oversize being returned from a classifier to a scoop box well below the centerline of the mill.

Control of pulp level to obtain high-circulating load is accomplished by use of **grate-discharge mills**. In one case the grates allowed passage of sufficient pulp to maintain the circulating load at 400 percent (Duggan, *Min. Technol.*, Tech. Publ. 1456, March 1942).

**Mill Efficiencies** The controlling factors conceded to govern the ore-grinding efficiency of cylindrical mills are as follows:

1. Speed of mill affects capacity, also liner and ball wear, in direct proportion up to 65–75 percent of critical speed.
2. Ball charge equal to 35–50 percent of the mill volume gives the maximum capacity.
3. Minimum-size balls capable of grinding the feed give maximum efficiency.
4. Bar-type lifters are essential for smooth operation.
5. Material filling equal to ball-void volume is optimum.
6. Higher-circulating loads tend to increase production and decrease the amount of unwanted fine material.
7. Low-level or grate discharge with recycle from a classifier increases grinding capacity over the center or overflow discharge; but liner, grate, and media wear is higher.
8. Ratio of solids to liquids in the mill must be considered on the basis of slurry rheology.

Experimental evidence presented in a classic paper by Coghill and De Vaney ("Ball Mill Grinding," U.S. Bur. Mines Tech. Publ. 581, 1937) indicated that the efficiency of battered reject balls was about 11 percent less than that of new spherical balls. These and other results have been graphically presented (Rose and Sullivan, *Ball Rod and Tube Mills*, Chemical Publishing Co., NY, 1958).

**Selection of Mill** The selection of a ball- or rod-mill grinding unit is based on pilot-mill experiments, scaled up on the basis that production is proportional to energy input. When pilot experiments cannot be undertaken, performance is based on published data for similar types of materials, expressed in terms of either grindability or an energy requirement (see subsections "Grindability" and "Energy Laws"). Newer methods of sizing mills and determining operating conditions for optimum circuit performance are based on computer solutions of the grinding equations with values of rate and breakage functions determined from pilot or full-scale tests (see subsection "Simulation of Milling Circuits").

**Capacity and Power Consumption** One of the methods of mill sizing is based on the observation that the amount of grinding depends on the amount of energy expended, if one assumes comparable good practice of operation in each case. The energy applied to a ball mill is primarily determined by the size of mill and load of balls. Theoretical considerations show the net power to drive a ball mill to be proportional to  $D^{2.5}$ , but this exponent may be used without modification in comparing two mills only when operating conditions are identical [Gow, Guggenheim, Campbell, and Coghill, *Trans. Am. Inst. Min. Metall. Pet. Eng.*, **112**, 24 (1934)]. The net power to drive a ball mill was found to be

$$E = [(1.64L - 1)K + 1][(1.64D)^{3.5}E_2] \quad (20-41)$$

where  $L$  is the inside length of the mill, m (ft);  $D$  is the mean inside diameter of the mill, m (ft);  $E_2$  is the net power used by a 0.6- by 0.6-m (2- by 2-ft) laboratory mill under similar operating conditions; and  $K$  is 0.9 for mills less than 1.5 m (5 ft) long and 0.85 for mills over 1.5 m long. This formula may be used to scale up pilot-milling experiments in which the diameter and length of the mill are changed but the size of balls and the ball loading as a fraction of mill volume are unchanged. More accurate computer models are now available.

Morrell [*Trans. Instn. Min. Metall.*, Sect. C, **101**, 25–32 (1992)] established equations to predict power draft based on a model of the

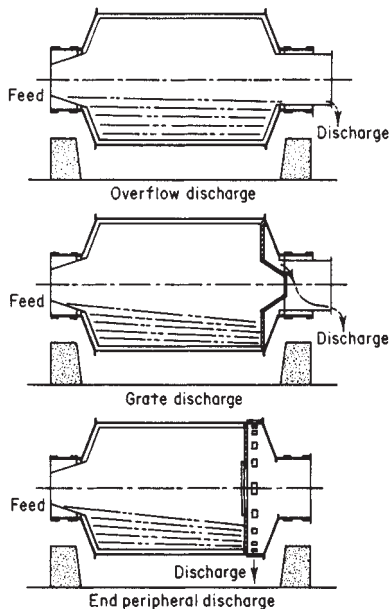


FIG. 20-34 Continuous ball-mill discharge arrangements for wet grinding.

shape of the rotating ball mass. Photographic observations from laboratory and plant-sized mills, including autogenous, semiautogenous and ball mills showed that the shape of the material charge could roughly be represented by angles that gave the position of the toe and shoulder of the charge. The power is determined by the angular speed and the torque to lift the balls. The resulting equations show that power increases rapidly with mill filling up to 35 percent, then varies little between 35 and 50 percent. Also, net power is related to mill diameter to an exponent less than 2.5. This agrees with Bond [Brit. Chem. Engr., 378-385 (1960)] who stated from plant experience that power increases with diameter to the 2.3 exponent or more for larger mills. Power input increases faster than volume, which varies with diameter squared. The equations can be used to estimate holdup for control of autogenous mills.

The gross power drawn by the mill is the net power plus the power drawn by the empty mill due to friction of its weight on the bearings.

**Motor and Drive** The ring motor is a low-frequency synchronous motor with its windings mounted directly on the mill shell. Hamdani and Zarif (Proc. IEEE Cement Industry Tech. Conference, 32d, 57-80, 1990) compared ring-motor cement mills with geared mills. Although the ring motor has higher initial cost, the operating cost is lower. In particular the downtime for maintenance is lower; the availability based on 20 years experience is >99 percent, while it is 89 percent with geared drives. Ring motors were said to become economically favorable over gear drives at sizes above 8500 hp [England, Power, 125(9), 111-2 (1981)].

Recent innovations [Knecht, IEEE Transactions on Industry Applications, 28(4), 962-969 (1992)] have improved the cost effectiveness and reliability of geared-mill designs as well. Slide-shoe bearings support the ends of the mill body and eliminate alignment problems caused by strain on the ends, and allow more compact end design. The bearing pads can be adjusted to compensate for deviations of the slide ring or settlement of the foundation, better than trunnion bearings.

One major requirement of gears is checking and adjusting to close tolerance the alignment of the girth gear and pinion which drives it. To avoid much of this effort, a self-adjusting pinion has been developed which is mounted in tilting bearings. Another improvement is the mounting of tandem-pinion gears in a common housing with the bearing system (Combiflex drive, Krupp Polysius AG), which further reduces maintenance problems. Maintenance is also reduced by covering the ring gear and using a circulating oil-lubrication system, instead of manually-applied grease.

Girth-gear drives can cause the concrete foundations to fail if not designed to resist harmonic vibrations (Saxer and Van der Heuvel, 31st IEEE Cement Industry Conference, 1989).

**Performance of Proprietary Equipment**

**Joy Denver Equipment Div** Manufactures a variety of grinding mills. Designs incorporate cast steel heads, heavy rolled steel shell, replaceable cast steel trunnions, hydraulic starting lubricator, inter-

nally lubricated trunnion bearings, hard iron trunnion linings, heavy-duty spherical self-aligning anti-friction roller bearings, reversible forged and machined drive pinions, and split construction, reversible mill gears. Sole plates are adjustable. Drive types include V-belt, gear reducer with air clutch or direct, and drum, scoop, scoop-drum or spout feeders. Grinding media may be rod with overflow, end peripheral or center peripheral discharge, or balls with overflow or grate discharge.

**Marcy Ball Mill** (Fig. 20-31; Mine and Smelter Div., Allis Mineral Processing Systems.) This is traditionally a grate-discharge mill, used to give a high throughput rate for a high circulating load in the wet and dry grinding of ores. The data in Table 20-16 must not be used for design but for orientation only. Mill design must be based on pilot experiments or other techniques previously discussed.

**Krupp Polysius AG Mineral Processing Systems** Provides rod- and tube-ball mills from 0.6 to 6 m diameter and up to 15.7 m long. Structural analyses are by computer methods. The patented slide-shoe design compensates for journal deformation, and hardened-steel spherical pads allow the shoes to pivot. Lubrication oil is provided at high pressure for startup/shutdown, and low pressure for continuous running. Drive can be by single pinion to 5,200 kW, twin pinion to 4,500 kW or higher, or gearless from 6,700 kW. Mill linings may be cast Cr-Mo steel alloy, or alloys with Ni for abrasion resistance. Rubber linings are fitted for many wet-grinding processes.

**Multicompartmented mills** feature grinding of coarse feed to finished product in a single operation, wet or dry. The primary grinding compartment carries large grinding balls or rods; one or more secondary compartments carry smaller media for finer grinding.

**STIRRED MEDIA MILLS**

Applications overlap with those of vibratory mills, described in the next group. Vibrational equipment is generally used for hard-grinding operations (ZrSiO<sub>4</sub>, SiO<sub>2</sub>, TiO<sub>2</sub>, Al<sub>2</sub>O<sub>3</sub>, etc.), while stirred grinders are mainly used for dispersion and soft grinding (dyes, clays, CaCO<sub>3</sub>, biological cells, etc). Stirred mills are also called **sand mills** when Ottawa sand is used as media. Contamination and grinder-body wear may be minimized in both types by the use of resilient coatings. Stirred mills use media 6 mm (¼ in.) in size or smaller, whereas vibratory mills use larger media for the same power input. Vibratory mills may grind dry, but most stirred mills are restricted to wet milling. Solids vary from 25 to 70 percent, depending on the feed size and rheology. Unlike in rotary-ball mills, some sedimentation may occur. The media filling ranges from 60 to 90 percent of apparent filling of the mill volume.

**Design** In stirred mills, a central paddle wheel or discid armature stirs the media at speeds from 100 to 1500 r/min. The media oscillate in one or more planes and commonly rotate very slowly.

In the **Attritor** (Union Process Inc.) a single vertical armature rotates several long radial arms. These are available in batch, continuous, and circulation types. Morehouse-Cowles media mills comprise a

**TABLE 20-16 Illustrative Performance of Marcy Ball Mills**

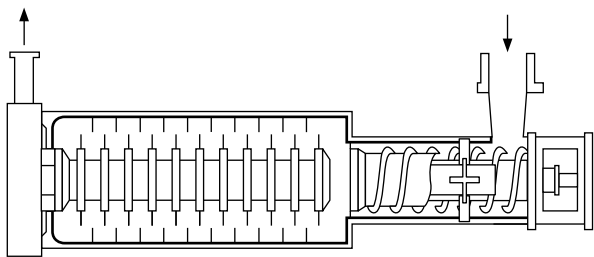
Size, ft.	Ball charge, tons	Hp. to run	Mill speed, r.p.m.	Capacity, tons/24 hr. (based on medium-hard ore)								
				No. 8 sieve*	No. 20 sieve	No. 35 sieve	No. 48 sieve	No. 65 sieve	No. 80 sieve	No. 100 sieve	No. 150 sieve	No. 200 sieve
				20% -200	35% -200	50% -200	60% -200	70% -200	80% -200	85% -200	93% -200	97% -200
3 × 2	0.85	5-7	35	19	15	12	10	8	6½	5	4	3
4 × 3	2.73	20-24	30	80	64	53	45	36	28	22	18	14
5 × 4	5.25	44-50	27	180	145	120	102	82	63	51	41	32
6 × 4½	8.90	85-95	24	375	300	250	210	170	135	105	85	66
7 × 5	13.10	135-150	22½	640	510	425	360	290	225	180	145	113
8 × 6	20.2	220-245	21	1100	885	735	625	500	390	310	250	195
9 × 7	30.0	345-380	20	1800	1450	1200	1020	815	635	505	410	315
10 × 10	56.50	700-750	18	3680	2960	2450	2100	1700	1325	1050	850	655
12 × 12	90.5	1260-1345	16.4	7125	5725	4750	4070	3290	2570	2035	1650	1275

\*Sieve through which substantially all the material can pass.

NOTE: To convert horsepower to kilowatts, multiply by 0.746; to convert tons to megagrams, multiply by 0.907; and to convert tons per 24 hours to megagrams per day, multiply by 0.907.

vertical tubular chamber with coaxial rotating disks, and an integral variable-flow diaphragm pump. Models are available from 5 to 100 hp for aqueous and solvent slurries. The Netzsch LME4 mill can be operated with a feed rate up to 100 L/hr [Kula and Schuette, *Biotechnology Progress*, **3**(1), 31–42 (1987)].

Figure 20-35 illustrates the Drais continuous stirred-media mill. The media are stirred by discs mounted on a central shaft. The advantage of horizontal machines is the elimination of gravity segregation of the feed. The feed slurry is pumped in at one end and discharged at the other, where the media are retained by a screen or array of closely spaced flat discs. The latter is useful with slurries having viscosity up to 50 Pa·s (50,000 cP), while screens are useful up to 1 Pa·s. Hydrodynamically shaped screen cartridges can accommodate media as fine as 0.2 mm. German manufacturers [Stadler et al., *Chemie-Ingenieur-Technik*, **62**(11), 907–915 (1990)] have produced mills of various shapes, primarily to aid separation of beads from product. When the mill body rotates with the screen at the axis, centrifugal force aids this separation.



**FIG. 20-35** Drais wet-grinding and dispersing system (U.S. patent 3,957,210) Draiswerke GmbH. [Stehr, International J. Mineral Processing, **22**(1–4), 431–444 (1988).]

Agitator discs are available in several forms: smooth, perforated, eccentric, and pinned. Effect of disc design has received limited study, but pinned discs are usually reserved for highly viscous materials.

Cooling water is circulated through a jacket and sometimes through the central shaft. The working speed of disc tips ranges from 5 to 15 m/sec, regardless of mill size.

The continuously stirred mill can be fed by screw feeders from several material bins simultaneously, thus blending uniform compositions, without incurring problems of transporting imperfectly blended or agglomerated mixtures. A series of mills may be used with decreasing media size and increasing rotary speed to achieve desired fine-particle size. No additional feed pumps are needed.

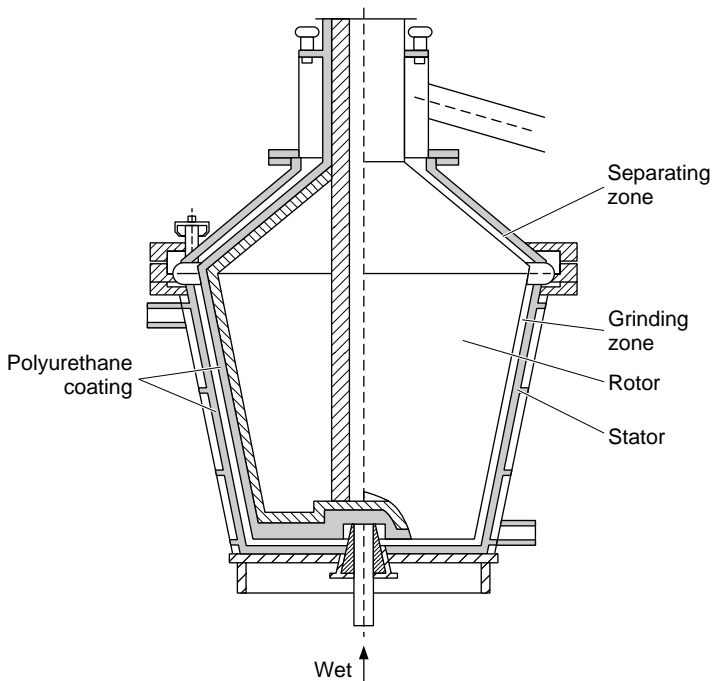
The **annular gap mill** shown in Fig. 20-36 is a variation of the bead mill. It has a high-energy input as shown in Fig. 20-37. It may be lined with polyurethane and operated in multipass mode to narrow the residence-time distribution and to aid cooling.

**Performance of Bead Mills** Materials processed in stirred-media mills are listed in Table 20-17. Variables affecting the milling process are listed below.

Stirred bead-mill process variables:

- Agitator speed
- Feed rate
- Size of beads
- Bead charge, percent of mill volume
- Cell concentration in feed
- Density of beads
- Temperature
- Design of blades
- Shape of mill chamber
- Residence time

The availability of more powerful, continuous machines has extended the possible applications to both lower- and higher-size ranges, from 5 to 200  $\mu\text{m}$  product size, and to feed size as large as 5 mm. The energy density may be 50 times larger than in tumbling-ball mills, so that a smaller mill is required (see Fig. 20-37). Mills range in size from 1 to 1000 L, with installed power up to 320 kW. Specific



**FIG. 20-36** Annular gap-bead mill (Welte Mahltechnik, GmbH.) [Kolb, Ceramic Forum International, **70**(5), 212–6 (1993)].

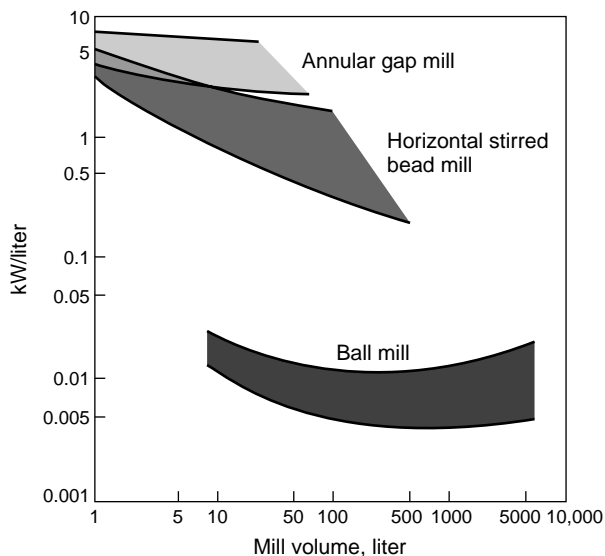


FIG. 20-37 Specific power of bead and ball mills [Kolb, Ceramic Forum International, 70(5), 212-6 (1993)].

power ranges from 10 to 200 or even 2000 kWh/tonne, with feed rates usually less than 1 tonne/h. Required energy can be scaled-up using dimensionless numbers, as shown in Fig. 20-38.

The nature of the media can influence the grinding rate. Table 20-18 lists some currently used media. Steel balls were more effective in the fine grinding of coal than glass balls [Mankosa et al., *Powder Technology*, 49(1), 75-82 (1986)], presumably because they have a higher density and greater impact energy than glass. There is also an optimum size of media, for coal about 20 times the size of the particle being ground. For large particles this appears to be related to the coefficient of friction which determines the nip angle. For small particles the capture zone is limited by the curvature of the bead, so that it is not feasible to reduce the size more than one order of magnitude with a given bead size. (For further examples see under Micas and Alumina.)

In vertical disc-stirred mills the media should be in a fluidized condition (White, *Media Milling*, Premier Mill Co., 1991). Particles can pack in the bottom if there is not enough stirring action or feed flow; or in the top if flow is too high. These conditions are usually detected by experiment.

A study of bead milling [Gao and Forsberg, *International J. Mineral Processing*, 32(1-2), 45-59 (1993)] was done in a continuous Drais mill of 6 L capacity having seven 120 × 10 mm horizontal discs. Twenty-seven tests were done with variables at three levels. Dolomite was fed with 2 m<sup>2</sup>/g surface area in a slurry ranging from 65 to 75 percent solids by weight, or 39.5 to 51.3 percent by volume. Surface area produced was found to increase linearly with grinding time or specific-energy consumption. The variables studied strongly affected milling rate; two extremes differed by a factor of 10. An optimum bead density for this feed material was 3.7. Evidently the discs of the chosen design could not effectively stir the more-dense beads. Higher slurry concentration above 70 wt % solids reduced the surface production per unit energy. The power input increased more than proportional to speed.

**Residence Time Distribution** Commercially available bead mills have a diameter-to-length ratio ranging from 1:2.5 to 1:3.5. The ratio is expected to affect the *residence time distribution* (RTD). A wide distribution results in overgrinding some feed and undergrinding another. Data from Kula and Schuette [*Biotechnology Progress*, 3(1), 31-42 (1987)] shows that in a Netzsch LME20 mill RTD extends from 0.2 to 2.5 times the nominal time, indicating extensive stirring. (See "Cell Disruption" under Applications.) The RTD is even more

TABLE 20-17 Materials Processed in Stirred-Media Mills (Stehr, *International J. Mineral Processing*, 22 1-4, 431-4, 1988).

Industry	Product
Paint & Lacquer	Primer coatings
	Lacquer
	Dispersion paints
Ink	Printing inks
	Dyestuffs
	Textile inks
	Pigment crudes activating
Chemical and pharmaceutical	Various
	High-grade ceramics
	Oxides for electric components
	Ferrites for permanent magnets
Electronics	Audio & Video coatings
	Limestone
	Fillers
	Paper coatings
Minerals	Flue gas desulfurization
	Kaolin
	Gypsum
	Alumina
Agrochemical	Precious metals liberation
	Pesticides
	Insecticides
	Herbicides
Foods	Fungicides
	Cocoa nibs
	Milk chocolate
	Peanuts
Biotechnology	Sesame
	Cell disruption
	Yeast disruption for enzyme extraction
	Rubber
Coal, energy	Dissolving polymers in solvents
	Coal-oil mixtures
	Coal-water slurry
	Gas turbine coal fuel
	Diesel coal fuel
	Fuel beneficiation, desulfurization

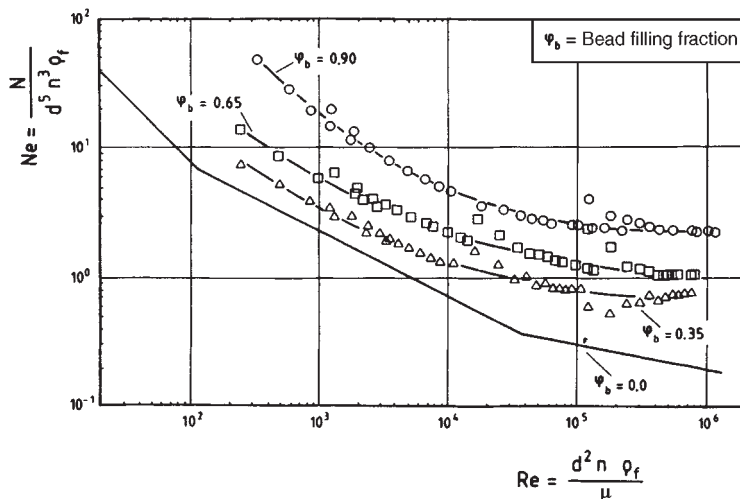
important when the objective is to reduce the top size of the product as Stadler et al. [*Chemie-Ingenieur-Technik*, 62(11), 907-915 (1990)] showed, because much of the feed received less than half the nominal residence time. A narrow RTD could be achieved by rapidly flowing material through the mill for as many as 10 passes.

## VIBRATORY MILLS

The dominant form of industrial vibratory mill is the type with two horizontal tubes, called the **horizontal tube mill**. These tubes are mounted on springs and given a circular vibration by rotation of a counterweight, shown in Fig. 20-39. Many feed flow arrangements are possible, adapting to various applications. Variations include polymer lining to prevent iron contamination, blending of several components, milling under inert gas and at high and low temperatures. An example is the Palla vibratory mill (ABB Raymond Div, *Combustion Engineering Inc.*).

The Vibro-Energy (Sweco, Inc.), a **vertical vibratory mill** (Fig. 20-40) has a mill body in a ring-shaped trough form but uses horizontal vibrations at a frequency of about 20 Hz of the contained media, usually alumina spheres or cylinders. Other characteristics appear in Table 20-19.

The vertical vibratory mill has good wear values and a low-noise output. It has an unfavorable residence-time distribution, since in continuous operation it behaves like a well-stirred vessel. Tube mills are better for continuous operation. The mill volume of the vertical mill cannot be arbitrarily scaled up because the static load of the upper media, especially with steel beads, prevents thorough energy introduction into the lower layers. Larger throughputs can therefore only be obtained by using more mill troughs, as in tube mills.



**FIG. 20-38** Newton number as a function of Reynolds number for a horizontal stirred bead mill, with fluid alone and with various filling fractions of 1-mm glass beads [Weit and Schwedes, *Chemical Engineering and Technology*, **10**(6), 398-404 (1987)]. ( $N$  = power input, W;  $d$  = stirrer disk diameter, m;  $n$  = stirring speed, 1/s;  $\mu$  = liquid viscosity, Pa·s;  $Q_f$  = feed rate, m<sup>3</sup>/s.)

The primary applications of vibratory mills are in fine milling of medium to hard minerals primarily in dry form, producing particle sizes of 1  $\mu$ m and finer. Throughputs are typically 10 to 20 t/hr. Grinding increases with residence time, active mill volume, the energy density and the vibration frequency, and media filling and feed charge. The amount of energy that can be applied limits the tube size to 600 mm, although one design reaches 1000 mm. Larger vibratory amplitudes are more favorable for comminution than higher frequency. The development of larger vibratory mills is unlikely in the near future because of excitation problems. This has led to the use of mills with as many as six grinding tubes.

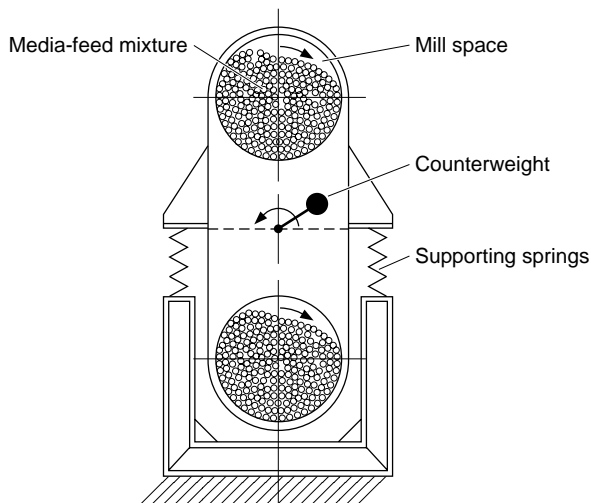
**Performance** The grinding-media diameter should preferably be 10 times that of the feed and should not exceed 100 times the feed diameter. To obtain improved efficiency when reducing size by several orders of magnitude, several stages should be used with different media diameters. As fine grinding proceeds, rheological factors alter the charge ratio, and power requirements may increase.

A variety of grinding media are available, as shown in Table 20-18. Size availability varies, ranging from 1.3 cm (1/2 in) down to 325 mesh (44  $\mu$ m).

Although there are no definitive data on media shape and grinding, ball-milling data indicate that spheres are the most effective shape. [Norris, *Trans. Inst. Min. Metall.*, **63**(567), 197-209 (1954)].

Although each machine has its peculiar characteristics and time requirements for various types of grinding, Fig. 20-40 illustrates some typical results obtained under optimum conditions for several materials.

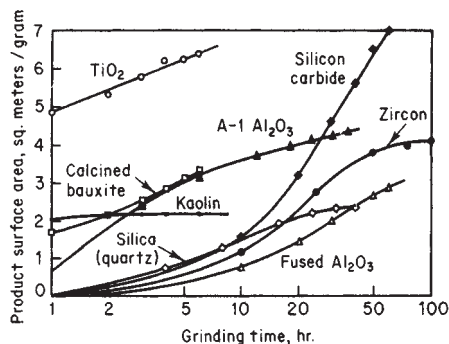
Advantages of vibratory mills are (1) simple construction and low-capital cost, (2) very fine product size attainable with large reduction



**FIG. 20-39** Two-tube vibratory mill. (Hoeffl, *Freiberger Forschungshefte A 750*, 125 pp., 1988.)

**TABLE 20-18 Media for Stirred and Vibratory Mills**  
(\* S = spheres, C = cylinders, I = irregular shapes)

Material	Common name	Density, g/cm <sup>3</sup>	Diameter, mm	Forms available*
Perfluoroethylene	Teflon	1.	—	C
Silicon dioxide	Ottawa sand	2.8	0.4-3.0	I
Annealed glass	Hard glass, unleaded	2.5	0.3-5.0	S
Annealed glass	Hard glass, leaded	2.9	0.3-5.0	S
Aluminum oxide	Alumina, Corundum	3.4	0.5-15.0	S,C,I
Zirconium silicate	Zircon	3.8	0.3-15.0	S,C,I
Zirconium oxide	Zirconia, Zircoa	5.4	0.5-3.0	S,C,I
Steel	Steel shot	7.6	0.2-15.0	S
Steel	Chrome steel	7.85	1.0-12.0	S



**FIG. 20-40** Vibratory-mill typical performance. (Sweco, Inc.)

**TABLE 20-19 Characteristics of Sweco Vibratory Mills**

Designation	Capacity	Typical sample charge, lb	Motor	Mill diameter, in
M-18	2.6 gal	5–20	¼	18
M-45	20 gal	50–200	5	45
M-60	70 gal	200–1000	10	60
M-80	182 gal	500–2000	40	80
DM-1	0.125 ft <sup>3</sup>	3–5	⅓	24
DM-3	0.5 ft <sup>3</sup>	20–60	1¼	30
DM-10	3 ft <sup>3</sup>	100–400	5	45
DM-20	65 ft <sup>3</sup>	200–800	10	60
DM-70	23 ft <sup>3</sup>	900–3000	40	95

NOTE: To convert gallons to cubic meters, multiply by  $3.785 \times 10^{-3}$ ; to convert pounds to kilograms, multiply by 0.4535; to convert horsepower to kilowatts, multiply by 0.746; and to convert inches to centimeters, multiply by 2.54.

ratio in a single pass, (3) good adaptation to many uses (4) Small space and weight requirements, (5) ease and low cost of maintenance. Disadvantages are (1) limited mill size and throughput, (2) vibration of the support and foundation, (3) high-noise output, especially when run dry.

**Residence Time Distribution** Hoeffl (Freiberger *Forschungshefte A*, 750, 119 pp., 1988) carried out the first investigations of residence time distribution and grinding on vibratory mills, and derived differential equations describing the motion. In vibratory horizontal-tube mills the mean axial transport velocity increases with increasing vibrational velocity, defined as the product  $r_s\Omega$ , where  $r_s$  = amplitude and  $\Omega$  = frequency. Apparently the media act as a filter for the feed particles, and are opened by vibrations. Nevertheless, good uniformity of transport is obtained, indicated by *vessel dispersion numbers*  $D\tau/L^2$  (see “Simulation of Milling Circuits” above) in the range 0.06 to 0.08 measured in limestone grinding under conditions where both throughput and vibrational acceleration are optimum.

The vibratory-tube mill is also suited to wet milling. In fine wet milling this narrow residence time distribution lends itself to a simple open circuit with a small throughput. But for tasks of grinding to colloid-size range, the stirred media mill has the advantage.

## NOVEL MEDIA MILLS

**Planetary Ball Milling** This is a method of increasing the gravitational force acting on balls in a ball mill. For example, refractory metals and carbides can be ground to 1 to 2.6  $\mu\text{m}$  in 5 to 20 min in an apparatus capable of applying a centrifugal force of 10 to 50 G. [Dobrovolskii, *Poroshk. Metall.*, 7(6), 1–7 (1967)].

**Pulverit** planetary mills are available from Geoscience Inc. High-speed planetary-ball mills can be used to perform rapid tests to simulate ball milling of materials [Vock, *DECHEMA-Monogr.*, 69, III-8 (1972)]. The size of high-speed mills will be much smaller than the size of same-capacity ball mills [Bradley, *S. Afr. Mech. Eng.*, 22, 129 (1972)].

## PARTICLE-SIZE CLASSIFIERS USED WITH GRINDING MILLS

Ball mills or tube mills can be operated in closed circuit with external air classifiers with or without air sweeping being employed. If air sweeping is employed, a cyclone separator may be placed between mill and classifier. (The principles of size reduction combined with size classification are discussed under “Characteristics of Size Classifiers.”) Likewise other types of grinding mill can be operated in closed circuit with external size classifiers (Fig. 20-12), as will be described at appropriate places on succeeding pages. However, many types of grinders are air-swept and are so closely coupled with their classifiers that the latter are termed internal classifiers.

**Dry Classifiers** Dry screens are used primarily in crusher circuits, since they are most effective down to 4 mesh. They can sometimes be used to 35 mesh. Examples are *Hammer* screens (W. S. Tyler, Inc.), *Rotex* screens (Rotex Inc.), and the *Vibro-Energy separator* (Sweco, Inc.).

Most dry-milling circuits use **air classifiers**. There are a number of types, but all use the principles of air drag and particle inertia, which

depend on particle size. The simplest type of air classifier is an elutriator. A countercurrent multielement elutriator is the *Zig-Zag classifier* (Hosokawa Micron Powder Systems Div.). The sharpness of separation increases with the number of elements. These devices are effective in the 30- to 80-mesh range.

Another type of classifier directs an air stream across a stream of the particles to be classified. An example is the radial-flow classifier (Kennedy Van Saun Corp.), which features adjustable elements to control the flow and classification. A further development on this principle is the Vari-Mesh classifier (Kennedy Van Saun Corp.), which controls classification by adjustable flow baffles. A change in direction of air flow is the operating principle of the reverse-flow Superfine classifier (Hosokawa Mineral Processing Systems).

**Rotating blades** are the main elements of several types of classifiers. The blades set up a centrifugal motion that tends to throw coarser particles outward. An example is the Mikro-ACM Pulverizer, in which an external fan forces air inwardly through the blades, carrying with it the fines. Centrifugal motion returns coarse particles to the hammers. The whizzer blades shown on the Raymond vertical mill (Fig. 20-49) have a similar centrifugal effect, throwing coarse particles to the wall of the chamber, where the lower boundary-layer air velocity allows them to fall back to the grinding zone.

Rotor blades also form an element of several external classifiers that are used in closed-circuit dry milling. These are generally called mechanical air separators or classifiers. Examples are the Whirlwind classifier (Sturtevant Inc.), the Gayco centrifugal separator (Universal Road Machinery Co. (see Fig. 20-41), and the whizzer separator (Raymond Division of Combustion Engineering Inc.).

Some mechanical air classifiers are designed so that the fine product must pass radially inward through rotor blades instead of spirally moving across them as with whizzer blades. Examples are the Mikron separator (Hosokawa Micron Powder Systems Div.), Sturtevant Side Draft separator, and the Majac classifier shown attached to the Majac jet mill (Fig. 20-55).

There are several mechanical air classifiers designed to operate in the superfine 10- to 90- $\mu\text{m}$  range. Two of these are the Mikroplex spiral air classifier MPVI (Hosokawa Micron Powder Systems Div.) and the classifier which is an integral part of the Hurricane pulverizer-classifier (ABB Raymond Div, Combustion Engineering Inc.) described under “Hammer Mills.” Others are the Majac classifier (Hosokawa Micron Powder Systems Div.), the Sturtevant Superfine Air Separator, and the Bradley RMC classifier. These also use a vane rotor, but operate at higher speed with higher power input and lower throughput.

**Performance** Deflector-type classifiers without rotating elements may give a product 85 percent through a 250- $\mu\text{m}$  sieve, although more typically they give a product 95 percent below 74  $\mu\text{m}$ . Mechanical air classifiers with rotating elements can give a product from 85 percent through 250  $\mu\text{m}$  to as fine as 99.9 percent below 44  $\mu\text{m}$ . The single whizzer is designed for operation where finenesses range to about 95 percent passing 74  $\mu\text{m}$ , whereas the double-whizzer separator is intended for use where higher-finesness products, in the range of 99.9 percent or better passing 44  $\mu\text{m}$ , are required. Sizes of mechanical air classifiers range from 1 to 7 m (3 to 24 ft) in diameter, with power requirements from 2 to 450 kW (3 to 600 hp). Superfine types can give a product 98 percent through 10  $\mu\text{m}$ .

Typical separation efficiency curves of an air classifier versus particle size are given in Fig. 20-14. The amount of top size in the fines may be very low, but there is typically 10 to 30 percent fines in the coarse product; that is, the low end of the curve tends to flatten out at 10 to 30 percent. In addition, the separation at the cut size is typically a gradual curve. Data of this sort, which are needed to evaluate closed-circuit mill performance, are seldom available. See subsection on characteristics of size classifiers for a testing method.

The Sturtevant air separator (Sturtevant Inc.) incorporates a hydraulic mechanism to adjust the width of the ring baffle over the spinner blades, which allows adjusting the separation curve within limits, at some cost in production rate. For example, the residue on 74- $\mu\text{m}$  screen can be varied from 1 to 20 percent, with a production rate shown in Table 20-20 for cement rock.

An improved version of the Raymond classifier sends all the air to the product-collector cyclone, returning only solids. This improves

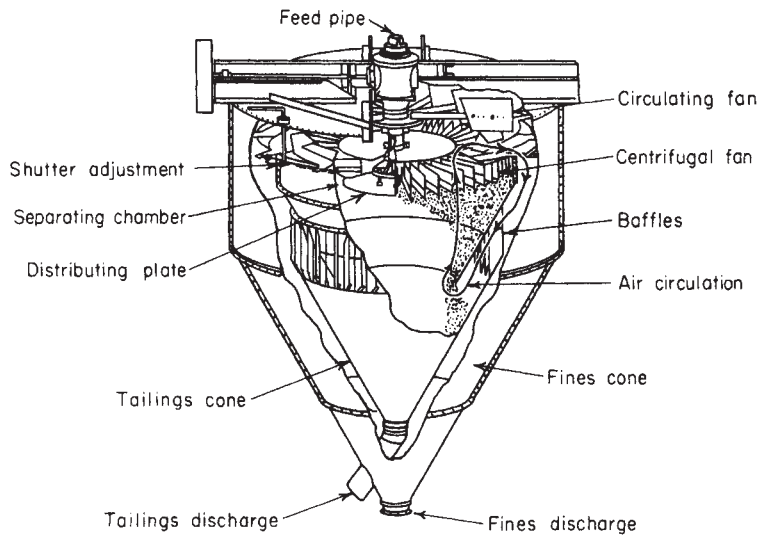


FIG. 20-41 Typical centrifugal separator.

fines production, since air returned with coarse material otherwise carries fines.

**Wet Classifiers** Closed-circuit wet milling is the rule in large-scale operations because of its greater production and economy. The simplest wet classifier is a **settling basin** arranged so that the fines do not have time to settle but are drawn off while the thickened coarse product is raked to a central discharge. Examples are the Hardinge Hydro-Classifier and the Dorr thickener. For classification near micrometer size a **continuous centrifuge** such as the Sharpless super-centrifuge or the Bird centrifuge is effective. The separation is not sharp in settlers, and the large space requirement is a detraction. **Rake classifiers** and **screw classifiers** are described in Sec. 21. The action is countercurrent, so separation of coarse grains is more effective. Examples are the Hardinge countercurrent (screw) classifier (Fig. 20-42) and the Dorr-Oliver rake classifier (Fig. 20-43). Typical circuits used with these classifiers in cement- and ore-processing plants are shown in Figs. 20-43 and 20-44. **Hydrocyclones** have become the most popular wet classifiers in ore operations owing to their compact design and economy of operation. Control is effected by feeding at a constant rate from a sump, in which the liquid level is maintained by varying water addition as the slurry feed rate varies (see Fig. 20-45).

In the 1930s there were attempts to use **screens** for wet closed-circuit milling, but operating cost was prohibitive. Recently screens have been developed that are practical for mill circuits. The first of these was the Dutch State Mines screen, which has the screen cloth on a curved incline, with the dilute slurry flowing over and through it. Because of the angle of attack, the effective opening is smaller than the physical opening, so blinding does not occur, but the separation is less sharp.

The use of rubber screen cloths also solves problems of blinding [Wessel, *Aufbereit. Tech.*, 8(2), 53-62; (5), 167-80; (8), 417-428 (1967);

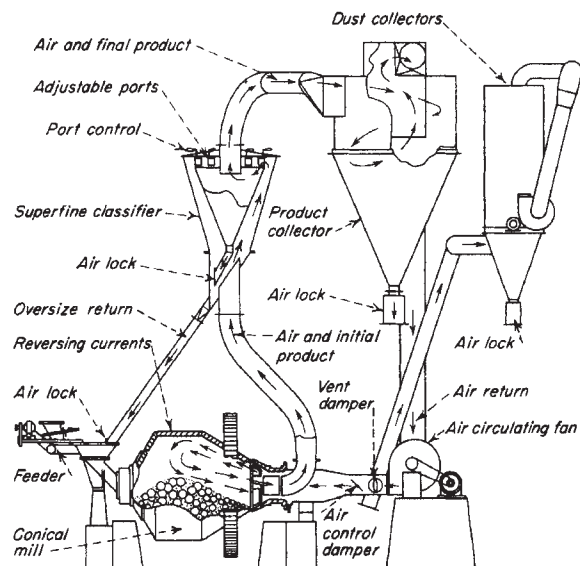


FIG. 20-42 Hardinge conical mill with reversed-current air classifier.

TABLE 20-20 Production Rate of Sturtevant Air Separator at 74  $\mu$ m

Separator diameter		Fines production	
m	ft	Mg/h	ton/h
0.9	3	0.4-1.0	0.4-1.1
2.5	8	3-9	3-10
4.3	14	15-40	17-45
6.1	20	77-210	85-230
8.0	26	180-450	200-500

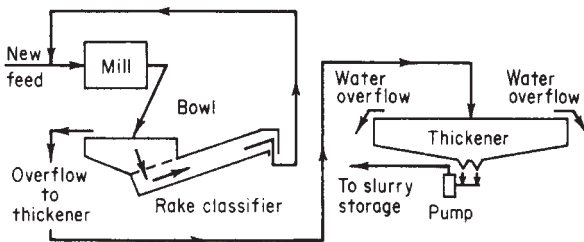


FIG. 20-43 Single-stage closed-circuit wet-grinding system. [Tonry, *Pit Quarry* (February-March 1959).]



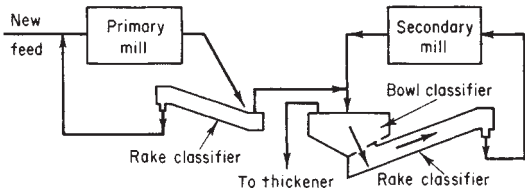


FIG. 20-44 Two-stage closed-circuit wet-grinding system. [Tonry, Pit Quarry (February–March 1959).]

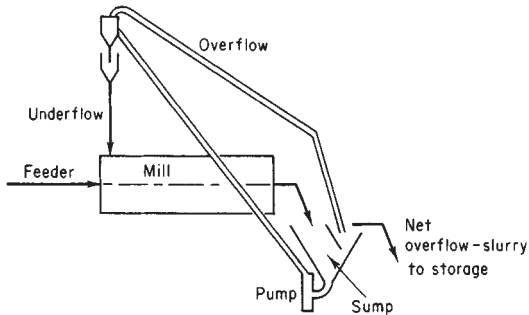


FIG. 20-45 Closed-circuit wet grinding with liquid-solid cyclone. [Tonry, Pit Quarry (February–March 1959).]

Michel, *Min. Mag. (London)*, annual review issue (5), 189–193, 207 (1968)]. An upper layer of rubber is perforated with fine slots for particle sizes from 0.2 to 2.5 mm., and this is supported by a lower layer with coarse holes. The vibration rate is 2500 to 3000 cycles/min. The advantage of screens over other classifiers is that a considerably sharper separation can be effected, and less fines are returned to the mill. Screen separation is considerably less than perfect, although there are few published data. The selectivity of a screen depends on the screen opening size and the feed rate, as well as other variables. A semiempirical model for an inclined vibratory screen [Karra, *CIM Bulletin*, 167–171 (Apr. 1979); *Proc. 14th International Mining Congress*, Toronto, III(6), 1–614; King, *International J. Mineral Processing*, 29(3–4), 249–265 (1990)] includes factors for these effects.

## HAMMER MILLS

Hammer mills for fine pulverizing and disintegration are operated at high speeds. The rotor shaft may be vertical or horizontal, generally the latter. The shaft carries hammers, sometimes called beaters. The hammers may be T-shaped elements, stirrups, bars, or rings fixed or pivoted to the shaft or to disks fixed to the shaft. The grinding action results from **impact** and **attrition** between lumps or particles of the material being ground, the housing, and the grinding elements. A cylindrical screen or grating usually encloses all or part of the rotor. The fineness of product can be regulated by changing rotor speed, feed rate, or clearance between hammers and grinding plates, as well as by changing the number and type of hammers used and the size of discharge openings.

The **screen or grating discharge** for a hammer mill serves as an internal classifier, but its limited area does not permit effective usage when small apertures are required. A larger external screen may then be required.

The feed must be nonabrasive with a hardness of 1.5 or less. The mill is capable of taking 2-cm (¾-in) feed material, depending on the size of the feed throat, and reducing it to a product substantially all able to pass a No. 200 sieve. For producing materials in the fine-size range, it may be operated in conjunction with external air classifiers. Such an arrangement is shown in Figs. 20-12 or 20-42. A number of machines have internal air classifiers.

**Hammer Mills without Internal Air Classifiers** The **Mikro-Pulverizer** (Fig. 20-46) (Hosokawa Micron Powder Systems Div.) is a close-clearance, screen discharge, high-speed, controlled sealed-feed hammer mill used for a wide range of nonabrasive materials, the major applications being sugar, carbon black, chemicals, pharmaceuticals, plastics, dyestuffs, dry colors, and cosmetics. For performance see Table 20-21. Speeds, types of hammers, feed devices, housing variations, and perforations of screens are all varied to fit applications, with the result that finenesses and character of grind cover a wide range. Some of the grinds are as fine as 99.9 percent through a 325-mesh screen. Feed material should usually be down to 4 cm (1½ in) or finer. If feed is larger, an auxiliary crusher may be required, preferably as a separate unit, because synchronization is difficult since the crusher has larger capacities than the pulverizer. Tie-in is possible with careful regulation of relative speeds of crusher and feed screw or screws.

A replaceable liner for the mill housing cover is made with multiple serrations. Hammer tips can be provided with tungsten carbide inserts for greatest wear resistance or with Hastellite tipping. An air-injector feeder can be supplied to project the feed particles directly in front of the hammer tips, to provide a more direct blow and thus increase mill efficiency. Cinematographic studies show that otherwise the particles receive a glancing blow from hammers. Wet feed can be charged with feed screws or pumps for wet grinding. Mikro-Pulverizers are made in five sizes shown in Table 20-21, plus a 150-hp size. The smallest size is the Bantam, which is widely used in laboratories for development and pilot work. Results will indicate in a qualitative way what may be expected of full-scale production units.

The **Imp pulverizer** (Raymond Division, Combustion Engineering Inc.) is an air-swept hammer mill. This machine is made in many sizes from the smallest, using 18 kW (25 hp), to the largest size, with six rows of hammers and requiring 700 kW (1000 hp) to drive it. The machines are equipped with a hopper below which is the star feeder, actuated by a pawl-and-ratchet mechanism. The Imp mill is generally used as part of an air-swept classifying circuit such as shown in Fig. 20-42. Any type of classifier can be used, depending on the application. Any solid material with a top size of 1 in. that is softer than 2 on the Moh scale can be processed to a fineness ranging from 1000 to 45 μm.

The **Blue Streak dual-screen pulverizer** (Prater Industries, Inc.) is used for the grinding of resins, chemical salts, plastic scrap, food products, and similar materials to a granular uniform powder of No. 30 or No. 40 sieve fineness. Feed enters opposite ends of the rotor and undergoes three stages of size reduction by hammers of decreasing size. Two perforated screens cover more than 70 percent of the area of the final sizing drum through which the product passes.

The **Atrita pulverizer** (Riley Stoker Corp.) is available in several single and duplex types. Capacities vary from 3400 to 25,000 kg/h (7500 to 54,000 lb/h). The coal is carried in a pin mill where most of the pulverizing is done, followed by a recycling classifier.

Hot air can be introduced into the machine for drying the coal. Air at 150°C dries coal with 8 percent moisture down to about 1 percent.

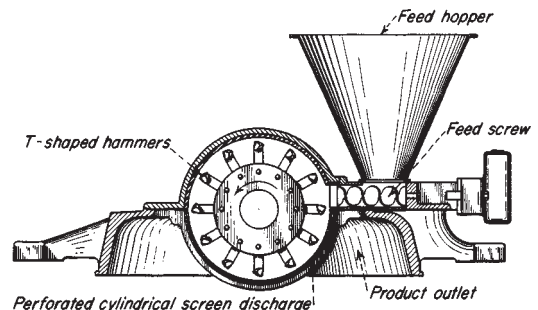


FIG. 20-46 Mikro-Pulverizer hammer mill. (Hosokawa Micron Powder Systems Div.)

TABLE 20-21 Mikro-Pulverizer Performance

Size	Rotor diam., in.	Max. r.p.m.	Hp.	Avg. capacities, lb./hr.		
				6X sugar	Clay-graphite water slurry	Pigments and colors (dry)
Bantam	5	16,000	¾-1	75-100	75-100	70-90
1	8	9,600	3-5	350-550	550	300-500
2	12	6,900	7½-15	800-1500	750-1600	800-2000
3	18	4,600	20-40	2000-4500	4500	2500-4500
4	24	3,450	40-100	4000-9000	7000	4500-7000

NOTE: To convert inches to centimeters, multiply by 2.54; to convert horsepower to kilowatts, multiply by 0.746; and to convert pounds per hour to kilograms per hour, multiply by 0.4535.

The **Aero pulverizer** (*Foster Wheeler Corp.*) is used for coal, pitch, and coke, blowing the ground material directly into the furnace. The housing is divided into two or three short cylindrical pulverizing chambers.

Hot gases can be introduced to dry the fuel being pulverized. Refractory material such as tramp iron is removed in the first pulverizing chamber and eliminated through a tramp-iron pocket.

**Disintegrator** The Rietz machine (Fig. 20-47) consists of a rotor running inside a 360° screen enclosure. The rotor includes a number of hammers designed to run at fairly close clearance relative to the inside of the cylindrical screen enclosing the disintegration chamber. The hammers are normally fixed rigidly to the shaft by keyways, pins, or welding, but swing hammers are used when indicated.

**Rietz disintegrators** are supplied in three types. *In-line disintegrators* (RI series) are designed for in-line installation, in which they function without impeding the process flow. Their primary applications are the mixing, delumping, and dissolving of fluids, slurries, and pastes and the grinding and separation of high-fiber solids.

*Angle disintegrators* (RA and RP series) are used for the fine pulping of many food products and for fine dispersion and homogenizing in the food and chemical industries. *Vertical disintegrators* (RD series) are used for dry pulverizing, wet grinding to produce slurries or pastes, shredding, defibrizing, and the fine pulping of soft fruits and vegetables.

Rietz disintegrators are normally supplied in rotor diameters from 10 to 60 cm (4 to 24 in.), with rotational speeds to produce hammer tip speeds in ranges of 300 to 6700 m/min (1000 to 22,000 ft/min) and power ranges from 0.4 to 150 kW (½ to 200 hp). Higher speeds and higher power are available. AC variable-frequency drives can eliminate belts and provide easier variation of speed. Models are available

in various materials of construction and in highly sanitary, easy-cleaning models or heavy-duty industrial construction (Table 20-22).

**Fitz mills** (*Fitzpatrick Co.*) consist of several series of hammer mills in configurations adapted to a variety of uses in food processing. There are high-speed screen hammer mills with flat hammers for impact, and narrow hammers or sharp hammers for tough plastic or fibrous materials. There are long, small-diameter rotating mills for processing pastes and two-shaft toothed masticators. There are also single-roll toothed choppers and shredders with fixed knives.

*Prater Industries, Inc.*, manufactures narrow swing-hammer screened mills for oilseeds and fibrous materials.

**Turbo pulverizers** and **turbo mills** (*Pallmann Pulverizer Co.*) combine the action of hammer and attrition mills, finding special application for grinding plastic materials that would be softened under high-energy warm-mill conditions.

**Pin Mills** In contrast to peripheral hammers of the rigid or swing types, there is a class of high-speed mills having pin breakers in the grinding circuit. These may be on a rotor with stator pins between circular rows of pins on the rotor disk, or they may be on rotors operating in opposite directions, thereby securing an increased differential of speed. See also the Mikro-ACM pulverizer described later.

**Fine impact mills** (*Hosokawa Micron Powder Systems Div.*) are high-speed impact mills with one stationary and one rotating stud disk. The mills are operated without a sieve and hence can be used with materials that tend to block (see Fig. 20-48). The **Contraplex wide chamber** is a similar mill with both disks rotating. It is suitable for grinding materials that tend to form deposits or for greasy, heat-sensitive products. These mills are used in the grinding of food, pesticides, pigments, and soft minerals, the wet grinding of PVC suspensions, and the crushing of cacao beans, etc. A laboratory model is also available.

**Entoletter impact mills** (*Entoletter, Inc.*) and the **Simpactor impact Mill** (*Sturtevant Inc.*) are a class of vertical-shaft devices in which feed at the shaft is caused to move rotationally and is thrown outward from the rotor to impact on an outer ring. Pin-type structures have been found effective; and in these the pins on the rotor do primary breakage, while the outer ring of pins gives further reduction. A wide range of speeds is employed, the higher ones being used for fine pulverizing. These mills grind a great variety of free-flowing or semi-free-flowing substances. Among these are plastics, rubber, grain and flour, coal, clay, slag, and salts. In some cases, external classification is required to remove oversize for return to the mill, or the mill may be combined with a classifier that contains no driven elements. Plastic materials are embrittled by liquid nitrogen or other suitable refrigerants to reduce their elasticity. For the highest speeds, the stator pins are mounted on a ring which is moving in reverse rotation to the central rotor.

**Hammer Mills with Internal Air Classifiers** The rotating components of the Raymond **vertical mill** are carried on its vertical shaft. They are the grinding element, double-whizzer classifier, and fan, as shown in Fig. 20-49. This mill has a hammer-tip speed of 7600 m/min (25,000 ft/min), so that it is effective for finer grinding than the Imp mill, which has a tip speed of 6400 m/min (21,000 ft/min).

The fine product is carried in the air stream through the fan and discharge port and separated by a cyclone collector into a suitable container.

Machines are available with rotor diameters of 45.7 and 88.9 cm (18 and 35 in.), driven by 15- and 110-kW (20- and 150-hp) motors respectively. The larger mill is directly connected to a vertical motor. Normal rotor speed for the 45.7-cm (18-in) Raymond vertical mill is 6000 r/min and 3600 r/min for the 88.9-cm (35-in) machine.

The field of application of the Raymond vertical mill is the production of soft materials that range in size from those having 99 percent passing a 44- $\mu$ m sieve to those having 99 percent smaller than 15  $\mu$ m, depending on the state of aggregation of the feed. A production rate of 227 kg/h (500 lb/h) is achieved with a chemical in a 45.7-cm (18-in) machine, consuming 13.4 kW (18 hp) when the product is substantially smaller than 15  $\mu$ m. In a talc operation on a 88.9-cm (35-in) machine requiring 110 kW (150 hp), a production rate of 320 kg/h (700 lb/h) is obtained. At a production rate of 2250 kg/h (5000 lb/h), a sample of the product leaves only a trace of talc on a No. 325 testing sieve.

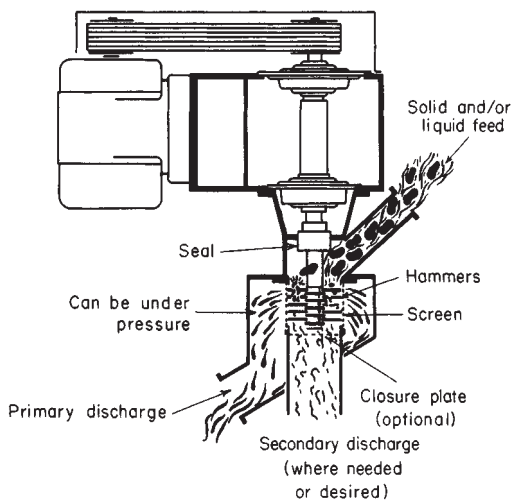


FIG. 20-47 Rietz disintegrator. (Rietz Div. Hosokawa Bepex Corp.)

**TABLE 20-22 Performance of Rietz Disintegrators**

Model	Rotor diam., in.	Max. r.p.m.	Hp. range	Screen perforation, in.	Typical applications	
					Material	Capacity
RA-1	4	16,000	½-5	⅛-¼	General lab use	1-10 lb./min.
RP-6	6	3,600	1-20	⅜	Horseradish	300 lb./hr.
RI-2	6 or 8	5,000	3-20	⅛	Detergent delumping	100 gal./min.
RD-8	8	8,400	3-20	⅛	Color coat	3600 lb./hr.
RA-2	8 or 12	8,400	3-20	⅛	Meat, cooked	3000-5000 lb./hr.
RP-8	8	3,600	10-60	¼	Blood de clotting	20 gal./min.
RD-12	12	7,200	15-50	¼-¾	Polystyrene	3000-10,000 lb./hr.
RA-3	12 or 18	6,500	10-75	⅜	Corn, heated	350 lb./min.
RP-12	12	3,600	20-75	⅜	Asbestos-cement slurry	200 gal./min.
RD-18	18	3,600	30-150	⅜	Chemical-fertilizer delumping	15 tons/hr.
RP-18	18	3,600	25-100	¼	Animal fat (90°F.)	15,000 lb./hr.
RD-24	24	3,600	75-400	1	Wood-chip shredding	30 tons/hr.
RI-4	24	3,600	50-200	¼	Bagasse depithing	30 tons/hr. (dry)

Maximum horsepower depends upon maximum speed.

RA and RP models are normally supplied with stainless-steel contact parts.

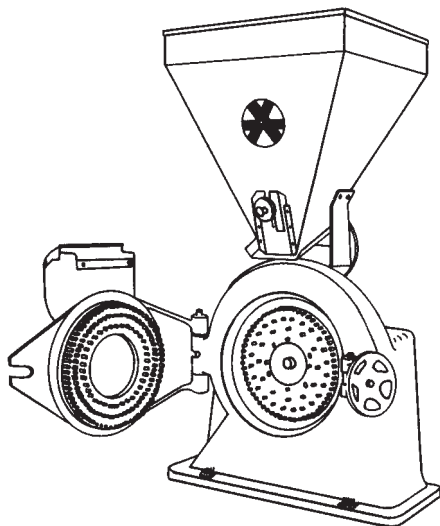
Some disintegrators are available for operation under pressure.

Screens are available in various sizes and types of perforations down to 0.006 in.

NOTE: To convert inches to centimeters, multiply by 2.54; to convert horsepower to kilowatts, multiply by 0.746; and to convert pounds per hour to kilograms per hour, multiply by 0.4535.

The **Mikro-ACM pulverizer** is a pin mill with the feed being carried through the rotating pins and recycled through an attached vane classifier. The classifier rotor is separately driven through a speed control which may be adjusted independently of the pin-rotor speed. Oversize particles are carried downward by the internal circulating air stream and are returned to the pin rotor for further reduction. The constant flow of air through the ACM maintains a reasonable low temperature which makes it ideal for handling heat-sensitive materials. Typical capacities are given in Table 20-23. The mill is built in eight sizes: model 2 to model 400 with drive motor from 5 to 400 hp and production rates from 0.2 to 36 times the rate in Table 20-26.

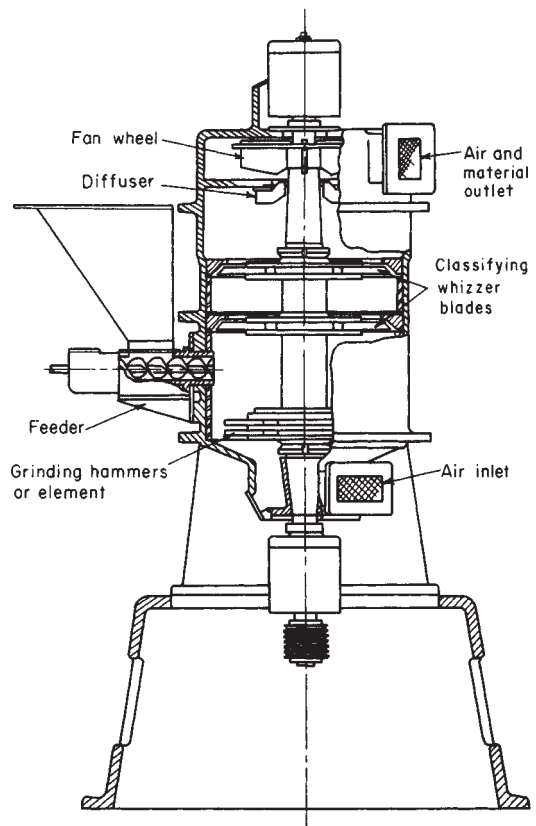
The **Pulvocron** (*Hosokawa Bepex Corp.*) employs one or more beater plates, around the periphery of which are attached rigid hammers of hard metal. It is driven within a casing at clearances of small fractions of an inch, the periphery of which is generally V-cut. The grinding ring has provision for cooling with liquid in direct contact with its periphery. Feed enters around the driving shaft and is broken by breaker plates. It then travels to a classifying chamber, in which is a separately driven and controlled rotor with vanes. See Table 20-24.



**FIG. 20-48** Fine-impact mill. (*Hosokawa Micron Powder Systems Div.*)

## RING-ROLLER MILLS

Ring-roller mills (Fig. 20-50) are equipped with rollers that operate against grinding rings. Pressure may be applied with heavy springs or by centrifugal force of the rollers against the ring. Either the ring or the rollers may be stationary. The grinding ring may be in a vertical



**FIG. 20-49** Raymond vertical mill. (*Raymond Division, Combustion Engineering Inc.*)

**TABLE 20-23 Test Results on Model 10 Mikro-ACM Pulverizer**

Material	Fineness, d <sub>97</sub> , μm		Output, lb/h
	Feed	Product	
Alumina	45	11	519
Calcined coke	3000	79	315
Clay	850	45	750
Cocoa/sugar	300	44	100
Corn starch	105	62	300
Dextrose	1200	75	700
Diatomaceous earth	70	35	800
Graphite	150	45	250
Herbicide	150	45	790
Kaolin	200	9.6	600
Limestone	6000	45	360
Phenolic resin	9000	75	1140
Starch	25000	180	400
Sugar	450	75	1000
Sugar	450	30	850
Talc	43	12	80
Titanium dioxide	6000	30	1000
Wood flour	2000	125	40
Xanthan gum	6000	180	70

NOTE: 100 mesh = 150 μm; 200 mesh = 75 μm; 325 mesh = 45 μm

**TABLE 20-24 Performance of the 20-in Pulvocron**

Material	Particle analysis, by weight	Capacity, lb./hr.	Hp.
Sucrose	97.5% minus 325 mesh	1800	60
Sodium chloride	99.4% minus 100 mesh	3600	50
	99.95% minus 325 mesh	160	45
Urea-formaldehyde and melamine molding compounds	99.2% minus 80 mesh	1600	45
Paraformaldehyde	99.7% minus 325 mesh	1300	40
Casein	99% minus 80 mesh	650	50
Corn flour	88% minus 200 mesh	800	35
Soy flakes	95% minus 200 mesh	2000	60
Sterols	100% minus 5 μ	700	60
Lactose	98.5% minus 200 mesh	1200	40
Alumina, hydrated	99% minus 325 mesh	700	30
Cinnamon	99.7% minus 60 mesh	1000	50

NOTE: To convert pounds per hour to kilograms per hour, multiply by 0.4535; to convert horsepower to kilowatts, multiply by 0.746.

or a horizontal position. Ring-roller mills are also referred to as ring-roll mills or roller mills or medium-speed mills. The ball-and-ring and bowl mills are types of ring-roller mill.

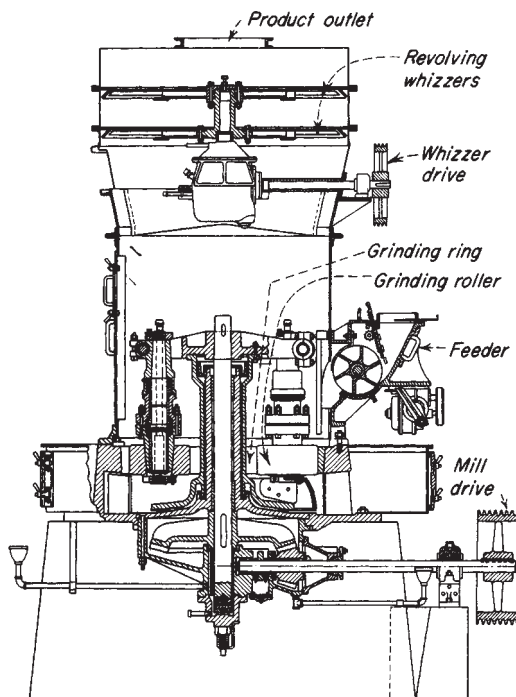
Ring-roller mills are more energy efficient than ball mills or hammer mills. The energy to grind coal to 80 percent passing 200 mesh was determined (Luckie and Austin, *Coal Grinding Technology—A Manual for Process Engineers*) as: ball mill—13 hp/ton; hammer mill—22 hp/ton; roller mill—9 hp/ton.

Ring-roller mills should be distinguished from roller mills. Paint roll mills are described under "Disk Attrition Mills," and flour roll mills under "Cereals and Other Vegetable Products."

**Ring-Roller Mills without Internal Classification** Known examples are no longer produced.

**Ring Mills with Internal Screen Classification** The grinding action of the Hercules (*Bradley Pulverizer Co.*) is that of three rolls that are revolved around and against a die to create grinding pressures of approximately 100 MPa (15,000 lb/in<sup>2</sup>). It can produce minus-20-mesh agricultural limestone or phosphate rock from minus-5-cm (-2-in) feed. The material is discharged from the grinding chamber through a surrounding screen. Capacity is relatively high, being 23 to 45 Mg/h (25 to 50 tons/h) of average-hardness dry limestone. Other product sizes may be obtained by changing the screen aperture.

The B & W pulverizer, Type E, consists of a single row of balls operating between a rotating bottom ring and a stationary top ring. Externally adjusted springs apply pressure to the top ring to give the required loading for proper pulverizing. In operation wet raw coal is



**FIG. 20-50** Raymond high-side mill with an internal whizzer classifier. (ABB Raymond Div., Combustion Engineering Inc.)

admitted inside the ball row and is fed through the grinding elements by centrifugal force. The Type E pulverizer is particularly suited to the direct firing of rotary kilns and industrial furnaces when close temperature control is required and long periods of continuous operation are essential. It is built in 17 sizes with capacities up to 12.6 Mg/h (14 tons/h) or more.

The Raymond ring-roller mill (Fig. 20-50) is of the internal air-classification type. The base of the mill carries the grinding ring, rigidly fixed in the base and lying in the horizontal plane. Underneath the grinding ring are tangential air ports through which the air enters the grinding chamber. A vertical shaft driven from below carries the roller journals. Centrifugal force urges the pivoted rollers against the ring. The raw material from the feeder drops between the rolls and ring and is crushed. Both centrifugal air motion and plows move the coarse feed to the nips. The air entrains fines and conveys them up from the grinding zone, providing some classification at this point. An air classifier is also mounted above the grinding zone to return oversize.

The method of classification used with Raymond mills depends on the fineness desired. If a medium-fine product is required (up to 85 or 90 percent through a No. 100 sieve), a single-cone air classifier is used. This consists of a housing surrounding the grinding elements with an outlet on top through which the finished product is discharged. This is known as the low-side mill. For a finer product and when frequent changes in fineness are required, the whizzer-type classifier is used. This type of mill is known as the high-side mill.

The Raymond ring-roll mill with internal air classification is used for the large-capacity fine grinding of most of the softer nonmetallic minerals. Materials with a Mohs-scale hardness up to and including 5 are handled economically on these units. Typical natural materials handled include barites, bauxite, clay, gypsum, magnesite, phosphate rock, iron oxide pigments, sulfur, talc, graphite, and a host of similar materials. Many of the manufactured pigments and a variety of chemicals are pulverized to high fineness on such units. Included are such materials as calcium phosphates, sodium phosphates, organic insecticides, powdered cornstarch, and many similar materials. When properly operated under suction, these mills are entirely dust-free and

automatic. They are available in nine basic sizes. Connected power ranges from 10 to 400 kW (15 to 600 hp). Capacities range from 0.5 to 450 Mg/h (0.5 to 50 tons/h), depending upon nature of material and exact fineness of grind.

The **Bradley pneumatic** (air-swept type) **Hercules mills** (*Bradley Pulverizer Co.*) are centrifugal ring-roll-type pulverizing mills which can be fitted with either two or three rolls. These mills are suitable for the pulverization of many materials to produce as coarse as 98 percent minus-20 mesh to as fine as 99.5 percent minus-325 mesh. The size of the pulverized product can be varied by adjusting the fineness selector mounted on top of the mill. Capacities range from 225 kg/h (500 lb/h) to 90 Mg/h (100 tons/h). When combined with the superfine *Bradley RMC classifier*, this mill can make a product finer than 11  $\mu$ m.

The **Williams ring-roller mill** (*Williams Patent Crusher & Pulverizer Co.*) is an air-swept mill with integral classifier of the rotating-blade type (the *Spinner air classifier*) or a double-cone type. The fluid-bed roller mill system has jets to introduce hot air into the bed of coal in the mill to dry it.

Of similar design is the **Raymond VR mill**, which is designed to run with hot gases to simultaneously dry and grind. It accepts feed as large as 3 in.

The **MBF pulverizer** (*Foster Wheeler Corp.*) for coal grinding also has three grinding rollers pivoted off the grinding housing. These pulverizers are commonly used in the utility industry, and capacities of up to 80 Mg/h (90 tons/h) are available.

**Bowl Mills** In the Raymond bowl mill the journals that carry the grinding rollers are stationary while the grinding ring rotates. The grinding pressure is produced by means of springs, which may be adjusted to give the required pressure, and the distance between the rollers and the ring may be set to a predetermined clearance. The rollers do not touch the ring, there being no metal-to-metal contact.

## DISK ATTRITION MILLS

The disk or attrition mill is a modern counterpart of the early buhrstone mill. Stones are replaced by steel disks mounting interchangeable metal or abrasive grinding plates rotating at higher speeds, thus permitting a much broader range of application. They have a place in the grinding of tough organic materials, such as wood pulp and corn grits. Grinding takes place between the plates, which may operate in a vertical or a horizontal plane. One or both disks may be rotated; if both, then in opposite directions. The assembly, comprising a shaft, disk, and grinding plate, is called a **runner**. Feed material enters a chute near the axis, passes between the grinding plates, and is dis-

charged at the periphery of the disks. The grinding plates are bolted to the disks; the distance between them is adjustable.

The **Andritz-Sprout-Bauer attrition mill** (Fig. 20-51) is available in single- and double-runner models with 30- to 91-cm- (12- to 36-in.-) diameter disks and with power ranging up to 750 kW (1000 hp). By the use of a variety of plates and shell constructions these units are represented in such applications as coarse granulating, pulverizing, and shredding.

In general, single-runner mills are used for the same purposes as double-runner mills, excepting that they will accept a coarser feedstock, their range of reduction for a given material is more limited, and they offer correspondingly higher outputs at lower power. While spike-tooth plates can be used in certain applications to simulate hammer-mill action, they are more generally applied to specialized tasks involving tearing, shredding, or controlled shattering, as in dehulling, and in wet corn-milling, where the germ must be separated from the starchy part and the hulls. The performance data presented in Table 20-25 typify the applications of the attrition mill.

**Buhrstone mills** are attrition mills with hard circular stones serving as grinding media, generally French, American, Esopus buhrstones, or rock emery. Buhrstone mills are still employed for grinding special cereals and grains. Feed enters the mill through a center hole in one of the stones. It is distributed between the stone faces and ground while working its way to the periphery.

## DISPERSION AND COLLOID MILLS

When the problem is to disrupt lightly bonded clusters or agglomerates, a new aspect of fine grinding enters. This may be illustrated by the breakdown of pigments to incorporate them in liquid vehicles in the making of paints, and the disruption of biological cells to release soluble products. Purees, food pastes, pulps, and the like are processed by this type of mill. Dispersion is also associated with the formation of emulsions which are basically two-fluid systems. Syrups, sauces, milk, ointments, creams, lotions, and asphalt and water-paint emulsions are in this category.

Mills employed for dispersion and colloidal operations operate on the principle of high-speed fluid shear. They produce dispersed droplets of fine size, around 3 to 5  $\mu$ m.

Paint-grinding roller mills (Fig. 20-52) consist of two to five smooth rollers (sometimes called rolls) operating at differential speeds. A paste is fed between the first two, or low-speed, rollers and is discharged from the final, or high-speed, roller by a scraping blade. The paste passes from the surface of one roller to that of the next because of the differential speed, which also applies shear stress to the film of

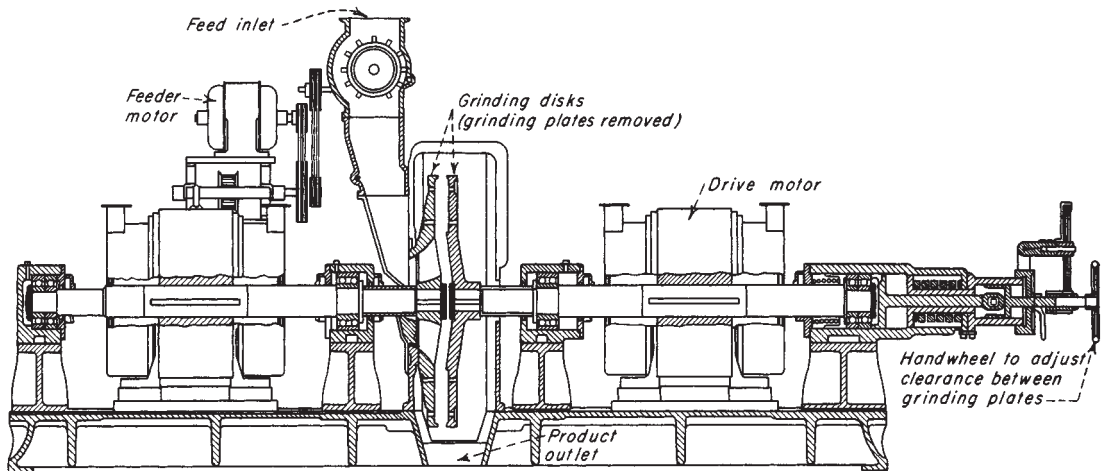


FIG. 20-51 Double-runner attrition mill. (Andritz-Sprout-Bauer Inc.)

TABLE 20-25 Performance of Disk Attrition Mills

Material	Size-reduction details	Unit*	Capacity lb./hr.	Hp.
Alkali cellulose	Shredding for xanthation	B	4,860	5
Asbestos	Fluffing and shredding	C	1,500	50
Bagasse	Shredding	B	1,826	5
Bronze chips	1/4 in. to No. 100 sieve size	A	50	10
Carnauba wax	No. 4 sieve to 65% < No. 60 sieve	D	1,800	20
Cast-iron borings	1/4 in. to No. 100 sieve	A	100	10
Cast-iron turnings	1/4 in. to No. 100 sieve	E	500	50
Coconut shells	2 x 2 x 1/4 in. to 5/100 sieve	B	1,560	17
	5/100 sieve to 43% < No. 200 sieve	D	337	20
Cork	2/201 sieve to 20/120 < No. 200 sieve	D	145	15
Corn cobs	1 in. to No. 10 sieve	F	1,500	150
Cotton seed oil and solvent	Oil release from 10/200 sieve product	B	2,400	30
Mica	4 x 4 x 1/4 in. to 3/60 sieve	B	2,800	6
	8/60 to 75% < 60/200 sieve	D	510	7.5
Oil-seed cakes (hydraulic)	1 1/2 in. to No. 16 sieve	F	15,000	100
Oil-seed residue (screw press)	1 in. to No. 16 sieve size	F	25,000	100
Oil-seed residue (solvent)	1/4 in. to No. 16 sieve	F	35,000	100
Rags	Shredding for paper stock	B	1,440	11
Ramie	Shredding	B	820	10
Sodium sulfate	35/200 sieve to 80/325 sieve	B	11,880	10
Sulfite pulp sheet	Fluffing for acetylation, etc.	C	1,500	50
Wood flour	10/50 sieve to 35% < 100 sieve	D	130	15
Wood rosin	4 in. max. to 45% < 100 sieve	B	7,200	15

\*A—8 in. single-runner mill D—20 in. double-runner mill

B—24 in. single-runner mill E—24 in. double-runner mill

C—36 in. single-runner mill F—36 in. double-runner mill

†2/20, or smaller than No. 2 and larger than No. 20 sieve size.

NOTE: To convert inches to centimeters, multiply by 2.54; to convert pounds per hour to kilograms per hour, multiply by 0.4535; and to convert horsepower to kilowatts, multiply by 0.746.

material passing between the rollers. Roller-mill technique and action have been studied by Hummel [*J. Oil Colour Chem. Assoc.*, 270–277 (June 1950)], and the breakup of agglomerates in this mill has been discussed by Kreckel [*Chem. Ing. Tech.*, 38(3), 229 (1966)].

Colloid mills which are employed for dispersion or for emulsification fall into four main groups: the hammer or turbine, the smooth-surface disk, the rough-surface type, and valve or orifice devices.

A mathematical analysis of the action in Kady and other colloid mills checks well with experimental performance [Turner and McCarthy, *Am. Inst. Chem. Eng. J.*, 12(4), 784 (1966)]. Various models of the Kady mill have been described, and capacities and costs given by Zimmerman and Lavine [*Cost Eng.*, 12(1), 4–8 (1967)]. Energy requirements differ so much with the materials involved that other devices are often used to obtain the same end. These include high-speed stirrers, turbine mixers, bead mills, and vibratory mills. In some cases, sonic devices are effective.

The concentration of energy in mills of this class is high, and there is a considerable amount of heating. This is materially reduced by use

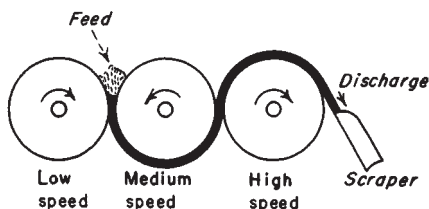


FIG. 20-52 Roller mill for paint grinding.

of a cooling-water jacket. In other cases, as when emulsions are made hot, the jacket is employed for heating.

The **Morehouse mill** (*Morehouse Industries, Inc.*) is a high-speed disk type of mill (Fig. 20-53). The undispersed phase is fed at the top and passes between converging disks, being thrown outward at the periphery.

In the **Premier Mill** the rotor is shaped like the frustrum of a cone, similar to that in Fig. 20-53. Surfaces are smooth, and adjustment of the clearance can be made from 25 μm (0.001 in) upward. A small impeller helps to feed material into the rotor gap. The mill is jacketed for temperature control. Direct-connected liquid-type mills are available with 15- to 38-cm (6- to 15-in) rotors. These mills operate at 3600 r/min at capacities up to 2 m<sup>3</sup>/h (500 gal/h). They are powered with up to 28 kW (40 hp). Working parts are made of Invar alloy, which does not expand enough to change the grinding gap if heating occurs. The rotor is faced with Stellite or silicon carbide for wear resistance. For pilot-plant operations, the Premier Mill is available with 7.5- and 10-cm (3- and 4-in) rotors. These mills are belt-driven and operate at 7200 to 17,000 r/min with capacities of 0.02 to 2 m<sup>3</sup>/h (5 to 50 gal/h).

The **Charlotte mill** (*Chemicolloid Corp.*) also employs high speed of rotation with the fluid flowing between a grooved conical rotor and a corresponding grooved conical stator. Clearance between them is regulated by an external calibrated adjustment device. Laboratory model W-10 operates at 0.75 kW (1 hp) with a capacity of 4 to 190 L/h (1 to 50 gal/h). Sanitary models are available for processing foodstuffs.

The **APV Gaulin colloid mill** has a smooth rotor, shaped like a discus.

A **high-pressure valve homogenizer** such as the Gaulin and Rannie (APV Gaulin Group) forces the suspension through a narrow orifice. The equipment has two parts: a high-pressure piston pump and a homogenizer valve [Kula and Schuette, *Biotechnology Progress*, 3(1), 31–42 (1987)]. The pump in production machines may have up to 6 pistons. The valve, illustrated in Fig. 20-54, opens at a preset or adjustable value, and the suspension is released at high velocity (300 m/sec) and impinges on an impact ring. The flow changes direction twice by 90 degrees, resulting in turbulence. Machines studied so far compress up to 60 Mpa, but higher pressures are becoming available. For machines with feed rates greater than 2000 L/h and pressures up to 100 Mpa tungsten carbide or special ceramics are used for the valve components to reduce erosion. There is also a 2-stage valve, but it has been shown better to expend all the pressure across a single stage.

The temperature of the suspension increases about 2.5°C per 10 Mpa pressure drop. Therefore intermediate cooling is required for

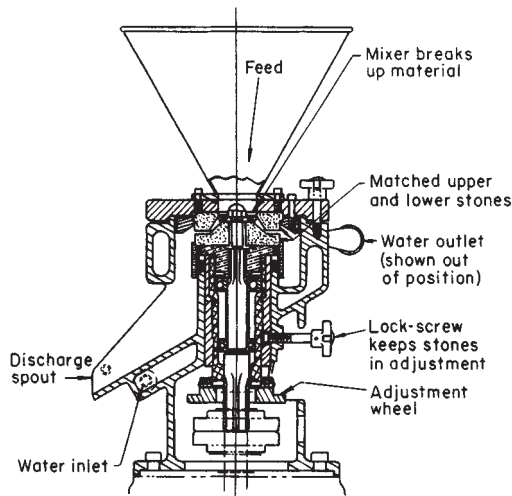


FIG. 20-53 Model M colloid mill. (*Morehouse Industries, Inc.*)

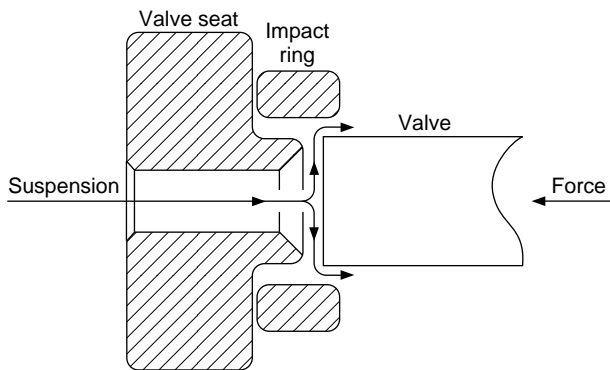


FIG. 20-54 Details of valve seat of the Gaulin high-pressure homogenizer, type CD.

multiple passes. In the Gaulin M3 homogenizer operated with a feed rate of 400 L/h and a pressure of 55 Mpa around 6000 kcal/hr have to be removed by a cooling system.

These units have been used to disrupt bacterial cells for release of enzymes. (See "Cell Disruption.")

### FLUID-ENERGY OR JET MILLS

A detailed description of mills of this type has been presented by Gossett [*Chem. Process.* (Chicago), **29**(7), 29 (1966)]. **Fluid-energy mills** may be classified in terms of the nature of the mill action. In one class of mills, the fluid energy is admitted in fine high-velocity streams at an angle around a portion or all of the periphery of a grinding and classifying chamber. In this class are the Micronizer, jet pulverizer, Reductionizer, Jet-O-Mizer, and others of somewhat similar structure. In the other class the fluid streams convey the particles at high velocity into a chamber where two streams impact upon each other. The **Majac** and the **Fluidized-Bed Jet** mills are in this class. Whether the particles are conveyed with the jet or are intercepted by jets, there is a high-energy release and a high order of turbulence which causes the particles to grind upon themselves and to be ruptured. Not all the particles are fully ground; so it is necessary to carry out a classifying operation and to return the oversize for further grinding. Most of these mills utilize the energy of the flowing-fluid stream to effect a centrifugal classification. The Majac mill differs, using a mechanical air classifier.

The **Micronizer** (*Sturtevant Inc.*) consists of a shallow circular grinding chamber in which the material to be pulverized is acted upon by a number of gaseous fluid jets issuing through orifices spaced around the periphery of the chamber. The rotating gas must discharge at the center, carrying the fines with it, while the coarse particles are thrown toward the wall, where they are subjected to further reduction by impact from particles entrained by incoming jets.

The action in these mills has been studied photographically and mathematically [Rumpf, *Chem. Ing. Techn.*, **32**(3), 129-135; (5), 335-342 (1960); *AT&S translations*, 668GJ, 844GJ].

Micronizer mills are constructed in nine standard sizes from 5 to 107 cm (2 to 42 in) in diameter, with capacities from 250 g/h to 1.8 Mg/h ( $\frac{1}{2}$  lb/h to 2 tons/h). The feed size should be smaller than 1 cm ( $\frac{1}{4}$  in). Production rate, fluid consumption, and fineness figures are shown in Table 20-26.

The **jet pulverizer** (*Jet Pulverizer Co.*) is another mill of the shallow-pan, angle-jet, and radial-inward-classification type, like the Micronizer.

The **Jet-O-Mizer** (*Fluid Energy Processing & Equipment Co.*) is one of a group employing a hollow elongated torus which is placed vertically. The operating principle is similar to that of the Micronizer, with the feed entering tangentially to the whirling fluid stream and the fines leaving centrally.

TABLE 20-26 Micronizer Performance\*

Material	Product average size, $\mu\text{m}$	Feed		Fluid consumption, g fluid/g solid	
		Size sieve no.	Rate, lb/h	Air	Steam
Ceylon graphite	2	3	200	—	8.5
Cryolite	3	60	900	—	4.0
Limestone	3.5	80	1000	—	4.0
Hard talc	3.5	20	1000	—	4.0
Silica gel	5.5	8	500	—	3.5
Soft talc	6.5	20	1800	—	2.5
Barite	3.5	40	1800	—	2.2
Bituminous coal	2	10	1300	—	1.2
Copal resin	5	2	600	—	7.5
Wolframite ore	5.5	10	800	5.6	—
Sulfur	3.5	3	1300	3.5	—

\**Ind. Eng. Chem.*, **38**, 672 (1946). To convert pounds per hour to kilograms per hour, multiply by 0.4535.

**Trost air mills** from *Colt Industries* are available in five sizes. The smallest mill (Gem T) is a research unit and can be used for fine-grinding studies. Capacities of 1 to 2300 kg/h (2 to 5000 lb/h) are available. Air-flow rates vary from 0.2 to 28 m<sup>3</sup>/min (6.5 to 1000 ft<sup>3</sup>/min).

The **Majac jet pulverizer** (*Hosokawa Micron Powder Systems Div.*) is an opposed-jet type with a mechanical classifier (Fig. 20-55). Fineness is controlled primarily by the classifier speed and the amount of fan air delivered to the classifier, but other effects can be achieved by variation of nozzle pressure, distance between the muzzles of the gun barrels, and position of the classifier disk. These pulverizers are available in 30 sizes, operated on quantities of compressed air ranging from approximately 0.6 to 13.0 m<sup>3</sup>/min (20 to 4500 ft<sup>3</sup>/min). In most applications, the economics of the use of this type of jet pulverizer becomes attractive in the range of 98 percent through 200 mesh or finer.

Materials illustrated in Table 20-27 are shown because of their wide range and type.

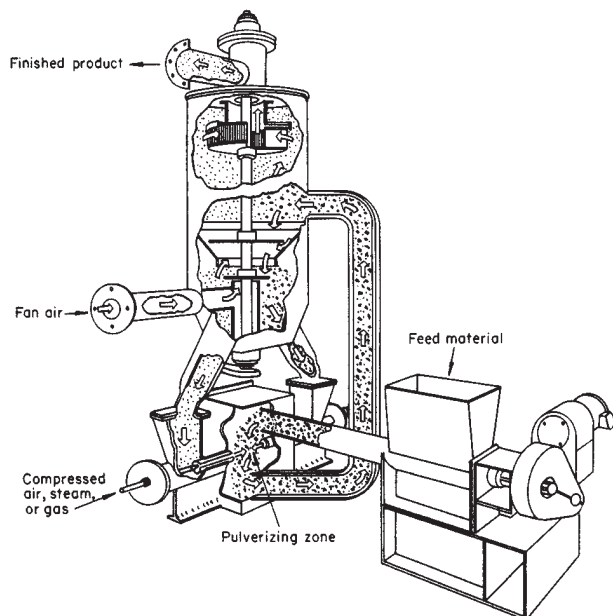


FIG. 20-55 Majac jet pulverizer. (*Hosokawa Micron Powder Systems Div.*)

TABLE 20-27 Majac Jet Pulverizer Capacities\*

Material	Finished particle size	Mill size	Production, lb h	Grinding fluid used
Alumina	-325 mesh, 3 $\mu\text{m}$ average	15	12,000	6300 lb/h steam at 100 psig, 750°F.
Coal, bituminous	90%, -325 mesh	20	8,000	3000 ft <sup>3</sup> /min air at 100 psig, 70°F.
Diphenyl phthalate	-325 mesh, 20-30 $\mu\text{m}$ maximum, 4.2 $\mu\text{m}$ average	2-6	435	300 ft <sup>3</sup> /min air at 100 psig, 70°F.
Feldspar, silica	99%, -200 mesh	15	8,500	1350 ft <sup>3</sup> /min air at 100 psig, 800°F.
Graphite	90%, -10 $\mu\text{m}$	8.5-2.5	50	75 ft <sup>3</sup> /min air at 100 psig, 70°F.
Mica	95%, -325 mesh	8	1,600	720 ft <sup>3</sup> /min air at 100 psig, 800°F.
Rare-earth ore	60%, -1 $\mu\text{m}$	8-15	400	720 ft <sup>3</sup> /min air at 100 psig, 800°F.

\*°C = (°F - 32)  $\times$   $\frac{5}{9}$ . To convert pounds per hour to kilograms per hour, multiply by 0.4535; to convert pounds per square inch gauge to kilopascals, multiply by 7.0.

**Fluidized-bed opposed-jet mills** (*Hosokawa Micron Powder Systems Div.*) differ from the Majac mill in that powder is not fed into the jets, but the jets impinge into a chamber which contains suspended powder. The powder is entrained into the jets. This eliminates wear on the nozzles, and reduces contamination. Otherwise, construction and applications are similar to the Majac mill. The fluidized-bed level is maintained a few inches above the jets. The Fluidized-bed mill is available in 13 sizes with air volumes ranging from 50 to 11,000 m<sup>3</sup>/h. One application is for toner grinding.

## NOVEL METHODS

Only once in 15 years does a truly novel method of size reduction become successful. The roll press is a truly successful example of a novel mill, and stirred-bead mills are older mills that have reached a new state of development. Many more methods are proposed and studied; some of these are described below. The information may be useful to judge other novel methods that may be proposed.

**Avoiding Size Reduction** Since size reduction is a difficult and inefficient operation, it is sometimes better to avoid it and use another approach. Thus rather than make large crystals and then grind them, one may be able to precipitate or crystallize material in the desired fine size. It may even be possible to control the process to give a more narrow size distribution than would be possible by size reduction.

In the case of lactose manufacture, crystals of uniform size are produced by first grinding part of a previous batch and taking a quantity with the required number of particles, then introducing these as seed crystals into a solution that is gradually cooled with gentle stirring. Variation in size of the seed crystals does not affect the size of the product crystals.

Some materials that are prepared in the molten state are converted advantageously to flake form by cooling a thin layer continuously on the surface of a rotating drum. Another way is to spray cool from the melt, using a spray dryer with cold air. Thus, massive cooling and subsequent pulverizing are avoided. See the Index for details of these other methods.

Ultrafine powders can be prepared in high-temperature plasmas. Particles below 1  $\mu\text{m}$  and larger particles with unusual surface structures are formed according to Waldie [*Trans. Inst. Chem. Eng.*, **48**(3), T90 (1970)]. Energy costs are discussed.

Bond [*Min. Eng. (London)*, **60**(1), 63-64 (1968)] reviewed attempts to induce breakage without wastefully applying pressure and concluded that inherent practical limitations have been found for the following methods: spinning particles, resonant vibration, electrohydraulic crushing, induction heating, sudden release of gas pressure, and chisel-effect breakers. For a review of more recent efforts, see edition 6 of this handbook.

## CRUSHING AND GRINDING PRACTICE

### CEREALS AND OTHER VEGETABLE PRODUCTS

**Flour and Feed Meal** The roller mill is the traditional machine for grinding wheat and rye into high-grade flour. A typical mill used for this purpose is fitted with two pairs of rolls, capable of making two separate reductions. After each reduction the product is taken to a bolting machine or classifier to separate the fine flour, the coarse product being returned for further reduction. Feed is supplied at the top, where a vibratory shaker spreads it out in a thin stream across the full width of the rolls.

Rolls are made with various types of corrugation. Two standard types are most generally used: the dull and the sharp, the former mainly on wheat and rye, and the latter for corn and feed. Under ordinary conditions, a sharp roll is used against a sharp roll for very tough wheat, a sharp fast roll against a dull slow roll for moderately tough wheat, a dull fast roll against a sharp slow roll for slightly brittle wheat, and a dull roll against a dull roll for very brittle wheat. The speed ratio usually is 2½:1 for corrugated rolls and 1¼:1 for smooth rolls. By examining the marks made on the grain fragments it has been concluded (Scott, *Flour Milling Processes*, Chapman & Hall, London, 1951) that the differential action of the rolls actually can open up the berry and strip the endosperm from the hulls.

High-speed hammer or pin mills result in some *selective grinding*. Such mills combined with air classification can produce fractions with controlled protein content. An example of such a combination is a Bauer hurricane hammer mill combined with the Alpine Mikroplex superfine classifier. Flour with different protein content is needed for

the baking of breads and cakes, and these types of flour were formerly available only by selection of the type of wheat, which is limited by growing conditions prevailing in particular locations [Wichser, *Milling*, **3**(5), 123-125 (1958)].

**Soybeans, Soybean Cake, and Other Pressed Cakes** After granulation on rolls the granules are generally treated in presses or solvent extracted to remove the oil. The product from the presses goes to attrition mills or flour rolls and then to bolters, depending upon whether the finished product is to be a feed meal or a flour.

The method used for grinding pressed cakes depends upon the nature of the cake, its purity, residual oil, and moisture content. If the whole cake is to be pulverized without removal of fibrous particles, it may be ground in a hammer mill with or without air classification. A 15-kW (20-hp) hammer mill with an air classifier, grinding pressed cake, had a capacity of 136 kg/h (300 lb/h), 90 percent through No. 200 sieve; a 15-kW (20-hp) screen-hammer mill grinding to 0.16-cm (¼-in) screen produced 453 kg/h (1000 lb/h). In many cases the hammer mill is used merely as a preliminary disintegrator, followed by an attrition mill. Typical performance of the attrition mill is given in Table 20-25. A finer product may be obtained in a hammer mill in closed circuit with an external screen or classifier.

High-speed hammer mills are extensively used for the grinding of soya flour. For example, the Raymond Imp mill with an air classifier is used, primarily with solvent-extracted soya.

**Starch and Other Flours** Grinding of starch is not particularly difficult, but precautions must be taken against explosions; starches must not come in contact with hot surfaces, sparks, or flame when sus-

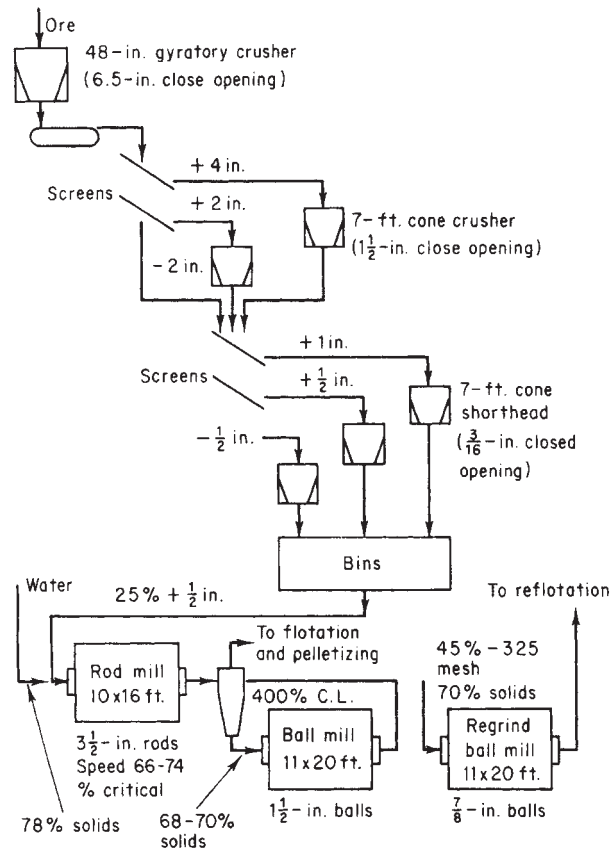


pended in air. See "Properties of Solids: Safety" for safety precautions. When a product of medium fineness is required, a hammer mill of the screen type is employed. Potato flour, tapioca, banana, and similar flours are handled in this manner. For finer products a high-speed impact mill such as the Entoleter pin mill is used in closed circuit with bolting cloth, an internal air classifier, or vibrating screens.

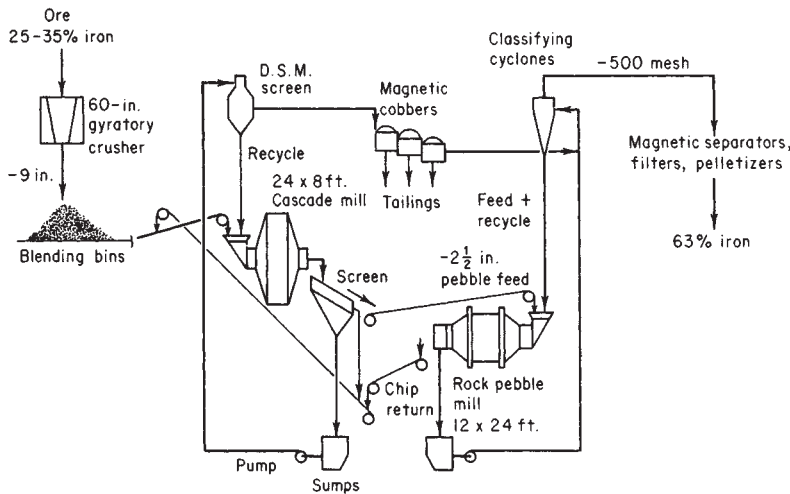
**ORES AND MINERALS**

**Metalliferous Ores** The most extensive grinding operations are done in the ore-processing and cement industries. Grinding is one of the major problems in milling practice and one of the main items of expense. Mill manufacturers, operators, and engineers find it necessary to compare grinding practice in one plant with that of another, attempting to evaluate circuits and practices (Arbiter, *Milling in the Americas*, 7th International Mineral Processing Congress, Gordon and Breach, New York, 1964). Direct-shipping ores are high in metal assay, and require only preliminary crushing before being fed to a blast furnace or smelter. As these high-grade ores have been depleted, it has become necessary to concentrate ores of lower mineral value. The native copper ores of Michigan have given way to porphyry copper ores of the southwest. Initially the deposits containing 2 to 4 percent copper were worked, but now ores of 0.40 percent must be processed by grinding and flotation or leaching. The effectiveness of closed-circuit milling with wet classifiers reopened the Iron Range of Minnesota by permitting economic beneficiation of taconite iron ores, which contain up to two-thirds hard cherty gangue. By grinding, magnetic separation or froth flotation and pelletizing, a blast-furnace feed is produced that is more uniform and gives a higher iron yield than the direct-shipping ores.

Three types of milling circuits are used in large ore-processing plants [Allis Chalmers, *Engineering & Mining J.*, 181(6), 69-171 (1980)]. (1) Three stages of gyratory crushers, followed by a wet rod mill followed by a ball mill (Fig. 20-56). This combination has high-power efficiency and low steel consumption, but higher-investment cost because rod mills are limited in length to 20 ft by potential tangling of the rods. (2) Similar crusher equipment followed by one or two stages of large ball mills. One stage may suffice if product size can be as coarse as 65 mesh. This circuit has lower capital cost but higher energy and wear costs. (3) One stage of gyratory crusher followed by large-diameter semiautogenous ball mills followed by a second stage of autogenous or ball mills (Fig. 20-57). The advantage of autogenous mills is reduction of ball-wear costs, but power costs are at least 25 percent greater, because



**FIG. 20-56** Ball- and rod-mill circuit. Simplified flow sheet of the Cleveland-Cliffs Iron Co. Republic mine iron-ore concentrator. To convert inches to centimeters, multiply by 2.54; to convert feet to centimeters, multiply by 30.5. (Johnson and Bjorne, *Milling in the Americas*, Gordon and Breach, New York, 1964.)



**FIG. 20-57** Autogenous mill circuit. Simplified flow diagram of the Cleveland-Cliffs Iron Co. Empire iron-mine concentrator with two autogenous wet-grinding stages. To convert inches to centimeters, multiply by 2.54; to convert feet to centimeters, multiply by 30.5.

irregular-shaped media are less effective than balls. A fourth circuit using the roll press has been widely accepted in the cement industry (see "Roll Press" and "Cement Industry"), and could be used in other mineral plants. It could replace the last stage of crushers and the first stage of ball or rod mills, at substantially reduced power and wear.

A flow sheet for one iron ore process is shown in Fig. 20-56. For the grinding of softer copper ore the rod mill might be eliminated, both coarse-crushing and ball-milling ranges being extended to fill the gap.

**Autogenous milling** of iron and copper ores has been widely accepted. When successful, this method results in economies due to elimination of media wear. Probably another reason for efficiency is the use of higher circulating loads and better classification. These improvements resulted from the need to use larger-diameter mills to obtain grinding with rock media that have a lower density than steel balls. The major difficulty is in arranging the crushing circuits and the actual mining so as to assure a steady supply of large ore lumps to serve as grinding media. With rocks that are too friable this cannot be achieved.

With other ores there has been a problem of buildup of intermediate-sized particles, but this has been solved either by adding a small load of steel balls, thus converting to a semiautogenous grinding system (SAG), or by sending the scalped intermediate-sized particles through a cone crusher. A flow sheet for a typical wet autogenous circuit is shown in Fig. 20-57.

**Nonmetallic Minerals** Dry and wet grinding processes are used. **Dry grinding** is less expensive than wet grinding in the coarser sizes because a dry product is obtained without a final drying step. Dry grinding is carried out with ball, pebble, roller, and hammer mills with closed-circuit air classification. The product may be 99.8 percent through a 325-mesh sieve. Jet mills can produce a product in the range 5 to 15  $\mu\text{m}$ , but at greater cost.

**Wet processes** use continuous ball and pebble mills, stirred and vibratory media mills, and pug mills. Wet processes take advantage of more effective classification in water, using bowl and cone classifiers, hydroseparators, thickeners, continuous centrifuges and cyclones, vacuum filters, and rotary, tray, or tunnel dryers. After drying, the cake generally has to be broken up in some type of disintegrator or pulverizer unless it was spray-dried. The objective of a process may be to obtain many grades of the same material by tying classifiers and

screens into the grinding system to remove various-sized products. Choice of equipment generally depends on (1) hardness and (2) contaminations. Capacity of any system decreases rapidly with increasing fineness of the material; this applies particularly to nonmetallics, for which extreme fineness is usually required.

**Clays and Kaolins** Because of declining quality of available clay deposits, beneficiation is becoming more required [Uhlig, *Ceramics Forum International*, 67(7-8), 299-304 (1990), English and German text]. Beneficiation normally begins with a size-reduction step, not to break particles but to dislodge adhering clay from coarser impurities. In **dry processes** this is done with low-energy impact mills.

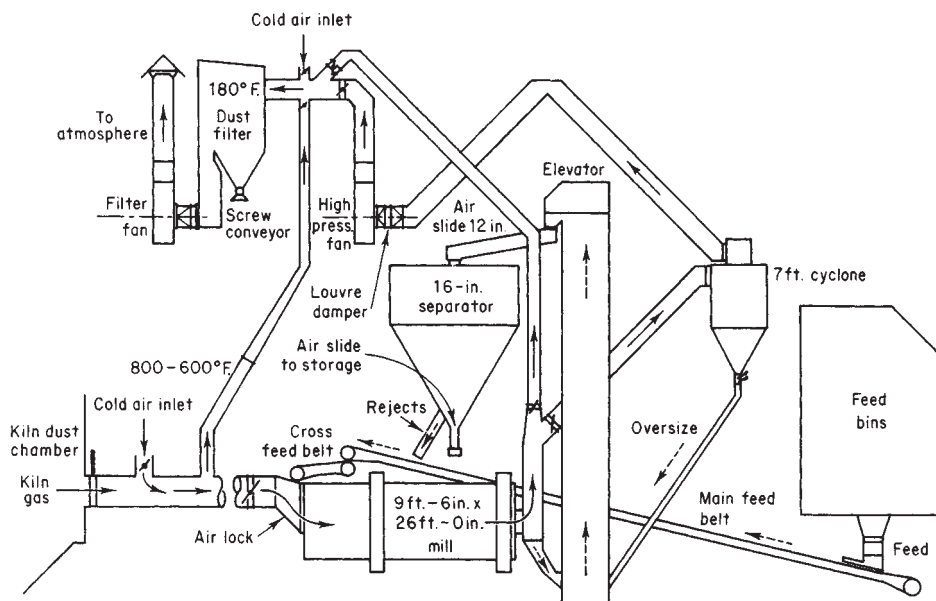
Mined clay with 22 percent moisture is broken up into pieces of less than 5 cm (2 in) in a rotary impact mill without screen, and fed to a rotary gas-fired kiln for drying (see Fig. 20-58). The moisture content is then 8 to 10 percent, and this material is fed to a mill, usually a Raymond ring-roll mill with an internal whizzer classifier or a pan mill. Hot gases introduced to the mill complete the drying while the material is being pulverized to the required fineness.

To grind 3.2 Mg/h (3½ tons/h) of a raw clay, power consumption will be about 75 kW (100 hp), and it takes about 31 m<sup>3</sup> (1100 ft<sup>3</sup>) of natural gas 3.7 MJ/m<sup>3</sup> (1000 Btu/ft<sup>3</sup>) to dry the clay from 10 percent moisture down to about 1 percent. The product is used in paint pigments and rubber fillers.

Larger amounts of clay are being produced in dry powdered form [Anon., *Ceramics Forum International*, 67(7-8), 330-4 (1990)]. After grinding, the clay is agglomerated to a flowable powder with water mist in a balling drum.

In the **wet process**, the clay is masticated in a pug mill to break up lumps and then dispersed with a dispersing aid and water to make a 40 percent solids slip of low viscosity. A high-speed agitator such as a Cowles dissolver is used for this purpose. Sands are settled out, and then the clay is classified into two size fractions in either a Hydrosorter or a continuous Sharples or Bird centrifuge. The fine fraction, with sizes of less than 1  $\mu\text{m}$ , is used as a pigment and for paper coating, while the coarser fraction is used as a paper filler.

A process for upgrading kaolin by grinding in a stirred bead mill has been reported (Stanczyk and Feld, *U.S. Bur. Mines Rep. Invest.* 6327 and 6694, 1965). By this means the clay particles are delaminated, and the resulting platelets give a much improved surface on coated paper.



**FIG. 20-58** Combined drying-grinding system using ball-mill and hot kiln exhaust gases. To convert inches to centimeters, multiply by 2.54; to convert feet to centimeters, multiply by 30.5;  $^{\circ}\text{C} = (^{\circ}\text{F} - 32) \times 5/9$ . [Tonry, Pit Quarry (February-March 1959).]

**Talc and Soapstone** Generally these are easily pulverized. Certain fibrous and foliated talcs may offer greater resistance to reduction to impalpable powder, but these are no longer produced because of their asbestos content.

Talc milling is largely a grinding operation accompanied by air separation. Most of the industrial talcs are dry-ground. Dryers are commonly employed to predry ahead of the milling operation because the wet material reduces mill capacity by as much as 30 percent.

Conventionally, in talc milling, rock taken from the mines is crushed in primary and then in secondary crushers to at least 1.25 cm (½ in) and frequently as fine as 0.16 cm (⅙ in).

Ring-roll mills with internal air separation are widely used for the large-capacity fine grinding of the softer talcs. High-speed hammer mills with internal air separation are also an outstanding success on some of the softer high-purity talcs for very fine fineness.

The mills in the western United States, in which generally are ground softer talcs than those of New York, have simple flow sheets. Single-stage crushing is employed, and the talc is merely ground in Raymond roller mills in closed circuit with air separators.

For a ring-roller mill receiving 2.54-cm (1-in) feed, production rates range from 1360 to 2720 kg/h (3000 to 6000 lb/h) for 60-kW (80-hp) grinding to 99 to 99.5 percent able to pass a No. 200 sieve.

Talcs of extreme fineness and high surface area are rapidly attaining industrial importance and are used for various purposes in the paint, paper, plastics, and rubber industries.

**Carbonates and Sulfates** Carbonates include limestone, calcite, marble, marls, chalk, dolomite, and magnesite; the most important sulfates are barite, celestite, anhydrite, and gypsum; these are used as fillers in paint, paper, and rubber. (Gypsum and anhydrite are discussed below as part of the cement, lime, and gypsum industries.)

A Raymond 5057 ring-roller mill pulverizing fluorspar produces 4500 kg (10,000 lb) of product per hour 95 percent minus 200 mesh with 104 kW (140-hp) operating power, or 26 kWh/Mg (23.4 kWh/ton). Fluorspar is also ground in continuous-tube mills with classification.

**Silica and Feldspar** These are ground in silex-lined mills with flint balls (see Table 20-28). At a mine near Cairo, Illinois, silica is successively crushed prior to ball-milling in American rotary impact mills having loose crushing rings made of hard alloy steel. The rings are easily replaced as they wear.

Feldspar for the ceramic and chemical industries is ground finer than for the glass industry. A feldspar mill is described in U.S. Bur. Mines Cir. 6488, 1931. It uses pebble mills with a Gayco air classifier.

Table 20-28 gives the results obtained with Hardinge pebble mills, grinding several siliceous refractory materials.

**Asbestos and Mica** Asbestos is no longer mined in the United States because of the severe health hazard, but it is still mined and processed in Canada. See previous editions of this handbook for process descriptions.

The micas, as a class, are difficult to grind to a fine powder; one exception is disintegrated schist, in which the mica occurs in minute flakes. For dry grinding, hammer mills equipped with an air-transport system are generally used. Maintenance is often high. It has been established that the method of milling has a definite effect on the par-

ticle characteristics of the final product. Dry grinding of mica is customary for the coarser sizes down to 100 mesh. Micronized mica, produced by high-pressure steam jets, is considered to consist of highly delaminated particles.

Conditions for grinding micas and kaolin in a Drais stirred-bead mill were investigated [Sivamohan and Vachot, *Powder Technology*, **61**(2), 119–129 (1990)]. Muscovite with a high aspect ratio of 50:1 imparts strength and electrical breakdown resistance to molded-plastic parts. A feed material with  $d_{90}$  of 180  $\mu$ m and aspect ratio 3:1 was ground in 1 to 10 passes with 4 min residence time. It gave aspect ratio as high as 27:1 and  $d_{50}$  of 8  $\mu$ m with the longest grinding times. Glass beads of 0.3 and 0.8 mm diameter had the same effect. Pulp density of 12 wt % gave better grinding rate than 25 percent. Low-dispersant concentration of 0.35 wt % was best.

Wollastonite with an aspect ratio of 15:1 is useful as a replacement for asbestos and as a high-strength filler for plastics. The feed material with  $d_{90}$  of 45  $\mu$ m was similarly ground. Beads of 0.3 mm gave faster grinding than 0.8 mm beads, and these corresponded to a bead-particle-size ratio of 19, confirming other results.

**Refractories** Refractory bricks are made from fireclay, alumina, magnesite, chrome, forsterite, and silica ores. These materials are crushed and ground, wetted, pressed into shape, and fired. To obtain the maximum brick density, furnishes of several sizes are prepared and mixed. Thus a magnesia brick may be made from 40 percent coarse, 40 percent middling, and 20 percent fines. Theorems have been proposed for calculating weight ratios of sizes to produce maximum packing density of powder mixtures [Lewis and Goldman, *J. Am. Ceram. Soc.*, **49**(6), 323 (1966)]. Preliminary crushing is done in jaw or gyratories, intermediate crushing in pan mills or ring rolls, and fine grinding in open-circuit ball mills. Since refractory plants must make a variety of products in the same equipment, pan mills and ring rolls are preferred over ball mills because the former are more easily cleaned.

Sixty percent of refractory magnesite is made synthetically from Michigan brines. When calcined, this material is one of the hardest refractories to grind. Gyratory crushers, jaw crushers, pan mills, and ball mills are used.

Alumina produced by the Bayer process is precipitated and then calcined [Krawczyk, *Ceramic Forum International*, **67**(7–8), 342–8 (1990)]. Aggregates are typically 20 to 70  $\mu$ m, and have to be reduced. The standard product is typically made in continuous dry ball or vibratory mills to give a product  $d_{50}$  size of 3–7  $\mu$ m, 98 percent finer than 45  $\mu$ m. The mills are lined with wear-resistant alumina blocks, and balls or cylinders are used with an alumina content of 80–92 percent. The products containing up to 96 percent  $Al_2O_3$  are used for bricks, kiln furniture, grinding balls and liners, high voltage insulators, catalyst carriers, etc.

Ultrafine grinding is carried out batchwise in vibratory or ball mills, either dry or wet. The purpose of batch operation is to avoid the residence time distribution which would pass less-ground material through a continuous mill. The energy input is 20–30 times greater than for standard grinding, with inputs of 1300–1600 kWh/ton compared to 40–60. Jet milling is also used, followed by air classification, which can reduce top size below 8  $\mu$ m.

**TABLE 20-28 Grinding Refractory Siliceous Materials in Pebble Mills**

	Feldspar	Silica sand	Enamel frit	Grog
Size of mill	8' × 60"	8' × 48"	4½' × 16"	5' × 22"
Feed size	2"	20 mesh	¼"	1½"
Size of product	99% through No. 200 sieve	98% through No. 325 sieve	97% through No. 100 sieve	95% through No. 10 sieve
Capacity, tons/hr	1.75	1.25	0.225	5
Power for mill, hp	68	58	8.5	28
Power for auxiliaries, hp	21	20		
Pebble load, lb	10,000	12,000	2000	2800
Speed of mill, r.p.m.	22	18	30	30
Moisture, %	1	1	0	1
Type of classifier	Hardinge	Air	Trommel screen on mill	
Lining and grinding mediums		Flint blocks and flint pebbles	Steel	

NOTE: To convert feet to centimeters, multiply by 30.5; to convert inches to centimeters, multiply by 2.54; to convert tons per hour to megagrams per hour, multiply by 0.907; and to convert horsepower to kilowatts, multiply by 0.746.

Among new mill developments, annular-gap bead mills and stirred bead mills are being used. These have a high cost, but result in a steep particle-size distribution when used in multipass mode [Kolb, *Ceramic Forum International*, 70(5), 212-216 (1993)]. Costs for fine grinding typically exceed the cost of raw materials. Products are used for high-performance ceramics.

Silicon carbide grains were reduced from 100-200 mesh to 80 percent below 1 µm in a version of stirred bead mill, using 20-30 mesh silicon carbide as media (Hoyer, Report Investigations U.S. Bureau Mines 9097, 9 pp., 1987).

**Crushed Stone and Aggregate** In-pit crushing is increasingly being used to reduce the rock to a size that can be handled by a conveyor system. In quarries with a long, steep haul, conveyors may be more economic than trucks. The primary crusher is located near the quarry face, where it can be supplied by shovels, front-end loaders or trucks. The crusher may be fully mobile or semimobile. It can be of any type listed below. The choices depend on individual quarry economics, and are described by Faulkner [*Quarry Management and Products*, 7(6), 159-168 (1980)].

Primary crushers used are jaw, gyratory, impact, and toothed roll crushers. Impact mills are limited to limestone and softer stone. With rocks containing more than 5 percent quartz, maintenance of hammers may become prohibitive. Gyratory and cone crushers dominate the field for secondary crushing of hard and tough stone. Rod mills have been employed to manufacture stone sand when natural sands are not available.

Crushed stone for road building must be relatively strong and inert, and must meet specifications regarding size distribution and shape. Both size and shape are determined by the crushing operation. Table 20-29 lists specifications for a few size ranges.

The purpose of these specifications is to produce a mixture where the fines fill the voids in the coarser fractions, thus to increase load-bearing capacity. (See "Refractories" above.)

Sometimes a product that does not meet these requirements must be adjusted by adding a specially crushed fraction. No crushing device available will give any arbitrary size distribution, and so crushing with a small reduction ratio and recycle of oversize is practiced when necessary.

The claim of various crushers to produce a cubical product is exaggerated. However, there are differences. If an impact mill is designed to apply an excess of energy at each blow, then production of slivers can be avoided but a larger amount of fines is produced.

A survey of research on product shape and size distribution (**grading**) was given by Rösslein [translation by Shergold, *Quarry Managers J.*, 207-222 (October 1946)]. The main study involved tests on 30 jaw crushers, with shapes of over 1 million particles being measured. Concerning **particle shape**, there is a tendency for hard rocks to produce more numerous flaky chippings than soft rocks. The size of feed to a crusher does not affect the shape of products. With jaw crushers, the largest and finest sizes contain the highest proportion of flaky pieces, but even the intermediate sizes are irregular. An increase in the reduction ratio of jaw crushers increases the flakiness of the product.

Smooth jaws produce more numerous flaky pieces than corrugated jaws. Curved jaws produce less fines but more numerous flaky particles. Crusher speed has little effect. The presence of material too small to be crushed has a deleterious effect on the shape of products. Secondary crushers with a small reduction ratio can improve the shape of primary crushed material, but secondary crushers are not inherently different from primary crushers. Slotted screens can remove flaky particles from the product. Impact crushers produce fewer flaky particles than any other type.

Grading of the product (i.e., size distribution) depends on the discharge opening, which is difficult to measure and adjust owing to wear of the plates in a jaw crusher. Size of feed and wear of plates do not affect grading significantly. Table 20-10 relates sizes of product to crusher settings.

**FERTILIZERS AND PHOSPHATES**

Many of the materials used in the fertilizer industry are pulverized, such as those serving as sources for calcium, phosphorus, potassium, and nitrogen. The most commonly used for their lime content are limestone, oyster shells, marls, lime, and, to a small extent, gypsum. Limestone is generally ground in hammer mills, ring-roller mills, and ball mills. Fineness required varies greatly from No. 10 sieve to 75 percent through No. 100 sieve.

**Oyster Shells and Lime Rock** Operating characteristics for hammer mills grinding oyster shells and burned lime for agricultural purposes are given in Table 20-30.

**Phosphates** Phosphate rock is generally ground for one of two major purposes: for direct application to the soil or for acidulation with mineral acids in the manufacture of fertilizers. Because of larger capacities and fewer operating-personnel requirements, plant installations involving production rates over 900 Mg/h (100 tons/h) have used ball-mill grinding systems. Ring-roll mills are used in smaller applications. Rock for direct use as fertilizer is usually ground to various specifications, ranging from 40 percent minus 200 mesh to 70 percent minus 200 mesh. For manufacture of normal and concentrated superphosphates the fineness of grind ranges from 65 percent minus 200 mesh to 85 percent minus 200 mesh.

Grindability of phosphate rocks from different areas varies widely; in Table 20-31 typical work-index data are shown.

Grinding-media wear in phosphate ball-mill grinding systems ranges from 5 to 25 g/Mg (0.05 to 0.20 lb/ton) ground; ball-mill liners show an average consumption of 2.5 to 100 g/Mg (0.01 to 0.05 lb/ton) ground.

**Inorganic salts** often do not require fine pulverizing, but they frequently become lumpy. In such cases, they are passed through a double-cage mill or some type of hammer mill.

**Basic slag** is often used as a source of phosphorus. Its grinding resistance depends largely upon the way in which it has been cooled, slowly cooled slag generally being more easily pulverized. The most common method for grinding basic slag is in a ball mill, followed by a tube mill or a compartment mill. Both systems may be in closed circuit with an air classifier. A 2.1- by 1.5-m (7- by 5-ft) mill, requiring

**TABLE 20-29 Selected Standard Sizes of Coarse Aggregate\***

Size number	Nominal size, square openings	Amounts finer than each laboratory sieve (square openings), percent by weight																	
		4 in	3½ in	3 in	2½ in	2 in	1½ in	1 in	¾ in	½ in	⅜ in	No. 4 (4760 µm)	No. 8 (2380 µm)	No. 16 (1190 µm)	No. 50 (297 µm)	No. 100 (149 µm)			
1	3½ to 1½ in.	100	90 to 100	—	25 to 60	—	0 to 15	—	0 to 5	—	—	—	—	—	—	—	—	—	—
2	2½ to 1½ in.	—	—	100	90 to 100	35 to 70	0 to 15	—	0 to 5	—	—	—	—	—	—	—	—	—	—
3	2 to 1 in.	—	—	—	100	90 to 100	35 to 70	0 to 15	—	0 to 5	—	—	—	—	—	—	—	—	—
4	1½ to ¾ in.	—	—	—	—	100	90 to 100	20 to 55	0 to 15	—	0 to 5	—	—	—	—	—	—	—	—
5	1 to ½ in.	—	—	—	—	—	100	90 to 100	20 to 55	0 to 10	0 to 5	—	—	—	—	—	—	—	—
6	¾ to ⅜ in.	—	—	—	—	—	—	100	90 to 100	20 to 55	0 to 15	0 to 5	0 to 5	—	—	—	—	—	—
7	½ in. to No. 4	—	—	—	—	—	—	—	100	90 to 100	40 to 70	0 to 15	0 to 5	0 to 5	—	—	—	—	—
8	⅜ in. to No. 8	—	—	—	—	—	—	—	—	100	85 to 100	10 to 30	0 to 10	0 to 5	0 to 5	—	—	—	—
9	No. 4 to No. 16	—	—	—	—	—	—	—	—	—	100	85 to 100	10 to 40	0 to 10	0 to 5	0 to 5	—	—	—

\*ASTM Standards on Mineral Aggregates and Concrete, March 1956.

NOTE: To convert inches to centimeters, multiply by 2.54.

**TABLE 20-30 Operating Data for Grinding Oyster Shells and Burned Lime in Hammer Mills**

Type of mill	Material	Size, in.	Capacity, tons/hr.	Hp.
Jeffrey	Oyster shells	15 × 8	0.5-0.75	8
		20 × 12	1-1.5	12
		24 × 18	2-3	20
		30 × 24	4-5	30
		36 × 24	8-10	40
Stedman	Burned lime	12 × 9	1.5	8
		20 × 12	4	20
		24 × 20	8	40
		30 × 30	12	60
		36 × 36	20	100

NOTE: To convert inches to centimeters, multiply by 2.54; to convert tons per hour to megagrams per hour, multiply by 0.907; and to convert horsepower to kilowatts, multiply by 0.746.

**TABLE 20-31 Ball-Mill Grindability of Various Phosphate Rocks**

Rock type	Calcium phosphate content, %	Work index, kw-hr/ton
Central Florida, pebble	68	14.5-16.5
North Florida, pebble	72	18.0-21.0
North Carolina, calcined concentrate	62-67	14.2-18.0
Central Florida, concentrate	72-74	16.0-23.0
Morocco	80-82	10.1-23.6
Idaho		19.0-24.7

NOTE: To convert kilowatthours per ton to kilowatthours per megagram, multiply by 1.1.

94 kW (125 hp), operating with a 4.2-m (14-ft) 22.5-kW (30-hp) classifier, gave a capacity of 4.5 Mg/h (5 tons/h) from the classifier, 95 percent through a No. 200 sieve. Mill product was 68 percent through a No. 200 sieve, and circulating load 100 percent.

**CEMENT, LIME, AND GYPSUM**

**Portland-cement** manufacture requires grinding on a very large scale and entails a large use of electric power. Raw materials consist of sources of lime, alumina, and silica and range widely in properties, from crystalline limestone with silica inclusions to wet clay. Therefore a variety of crushers are needed to handle these materials. Typically a crushability test is conducted by measuring the product size from a laboratory impact mill on core samples [Schaefer and Gallus, *Zement-Kalk-Gips*, 41(10), 486-492 (1988); English ed., 277-280]. Abrasiveness is measured by weight loss of the hammers. The presence of 5 to 10 percent silica can result in an abrasive rock, but only if the silica grain size exceeds 50 μm. Silica inclusions can also occur in soft rocks. The presence of sticky clay will usually result in handling problems, but other rocks can be handled even if moisture reaches 20 percent.

If the rock is abrasive, the first stage of crushing may use gyratory or jaw crushers, otherwise a rotor-impact mill. Their reduction ratio is only 1:12 to 1:18, so they often must be followed by a hammer mill, or they can feed a roll press. Rotor crushers have become the dominant primary crusher for cement plants because of the characteristics. All of these types of crushers may be installed in moveable crusher plants.

In the grinding of raw materials, two processes are used: the dry process in which the materials are dried to less than 1 percent moisture and then ground to a fine powder, and the wet process in which the grinding takes place with addition of water to the mills to produce a slurry. The two processes are used about equally in the United States.

**Dry-Process Cement** After crushing, the feed may be ground from a size of 5 to 6 cm (2 to 2½ in) to a powder of 75 to 90 percent passing a 200-mesh sieve in one or several stages.

The first stage, reducing the material size to approximately 20 mesh, may be done in vertical, roller, ball-race, or ball mills. The last-

named rotate from 15 to 18 r/min and are charged with grinding balls 5 to 13 cm (2 to 5 in) in diameter. The second stage is done in tube mills charged with grinding balls of 2 to 5 cm (¾ to 2 in).

Frequently ball and tube mills are combined into a single machine consisting of two or three compartments, separated by perforated-steel diaphragms and charged with grinding media of different size. Rod mills are hardly ever used in cement plants. The compartments of a tube mill may be combined in various circuit arrangements with classifiers, as shown in Fig. 20-59.

A dry-process plant has been described by Bergstrom [*Rock Prod.*, 59-62 (August 1968)].

**Wet-Process Cement** Ball, tube, and compartment mills of essentially the same construction as for the dry process are used for grinding. Water or clay slip is added at the feed end of the initial grinder, together with the roughly proportioned amounts of limestone and other components.

In modern installations wet grinding is sometimes accomplished in ball mills alone, operating with excess water in closed circuit with classifiers and hydroseparators.

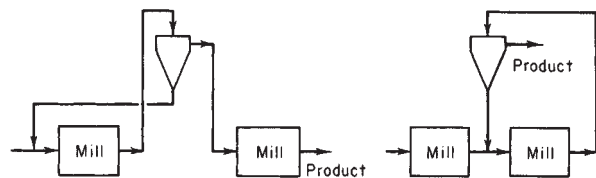
Figures 20-43 to 20-44 illustrate single-stage and two-stage closed-circuit wet-grinding systems. The circuits of Fig. 20-59 may also be used as a closed-circuit wet-grinding system incorporating a liquid-solid cyclone as the classifier.

A wet-process plant making cement from shale and limestone has been described by Bergstrom [*Rock Prod.*, 64-71 (June 1967)]. There are separate facilities for grinding each type of stone. The ball mill operates in closed circuit with a battery of Dutch State Mines screens. Material passing the screens is 85 percent minus 200 mesh. The entire process is extensively instrumented and controlled by computer. Automatic devices sample crushed rock, slurries, and finished product for chemical analysis by X-ray fluorescence. Mill circuit feed rates and water additions are governed by conventional controllers.

**Finish-Grinding of Cement Clinker** Typically the hot clinker is first cooled and then ground in a compartment mill in closed circuit with an air classifier. To crush the clinkers, balls as large as 5 in may be needed in the first compartment. A roll press added before the ball mill can reduce clinkers to a fine size, and thus reduce the load on the ball mills. The main reasons for adding a roll press has been to increase capacity of the plant, and lower cost.

Installation of roll presses in several cement plants is described (31st IEEE Cement Industry Technical Conference, 1989). Considerable modification of the installation was required because of the characteristics of the press. A roll press is a constant throughput machine, and the feed rate cannot easily be reduced to match the rate accepted by the ball mill that follows it. Several mills attempted to control the rate by increasing the recycle of coarse rejects from the air classifier, but the addition of such fine material was found to increase the pull-in capacity of the rolls, for example from 180 to 250 t/hr. With the resulting high recycle ratio of 5:1 the roll operation became unstable, and power peaks occurred. Deaeration of fines occurs in the nip, and this also interferes with feeding fines to the rolls. In some plants these problems were overcome by recirculating slabs of product directly from the roll discharge (Fig. 20-26). In other cases the rolls were equipped with variable speed drives to allow more versatile operation when producing several different grades/finenesses of cement. The roll press was found to be 2.5 times as efficient as the ball mill, in terms of new surface per unit energy.

Tests showed that the slab from pressing of clinker at 120 bar and 20 percent recycle contained 97 percent finer than 2.8 mm, and 39



**FIG. 20-59** Two cement-milling circuits. [For others, see Tonry, Pit Quarry (February-March 1959).]

percent finer than 48  $\mu\text{m}$ . Current operation is at 160 bar. The wear was small; after 4000 h operation and 1.5 million tons of throughput the wear rate was less than 0.1 g per ton, or 0.215 g/ton of finished cement. There is some wear of the working parts of the press, requiring occasional maintenance. The press is controlled by four control loops. The main control adjusts the gates that control slab recycle. Since this adjustment is sensitive, the level in the feed bin is controlled by adjusting the clinker-feed rate to assure choke-feed conditions. Hydraulic pressure is also controlled. Separator-reject rate is fixed. The investment cost was only \$42,000 per ton of increased capacity. Energy savings is 15 kWh/ton. This together with off-peak power rates results in energy cost savings of \$500,000/yr.

**Particle-Size Control** The strength of cements varies with fineness to which it is ground, and also with size distribution, which affects particle packing. Controlling the particle-size distribution of cements to achieve a higher packing density can give higher strengths, (Helmuth, 23rd IEEE Cement Industry Technical Conference, 1981, 33 pp.). See subsection "Refractories" for further discussion of particle packing.

There have been efforts to take advantage of the greater energy efficiency and lower cost of the roll press for product grinding [Wuestner et al., *Zement-Kalk-Gips*, 41(7), 345-353 (1987); English ed., 207-212]. However, the much steeper size distribution [Tamashige, 32d IEEE Cement Industry Technical Conference, 319-340 (1990)], requires a fine size that results in greatly increased water requirement and very rapid setting, which are unacceptable. Also, insufficient heat is generated to dehydrate the gypsum component [Rosemann et al., *Zement-Kalk-Gips*, 42(4), 165-9 (1987); English ed., 141-3]. It has also been found that the impact deagglomerators tried so far did not completely break up agglomerates as well as a ball mill. Thus there is room for further improvements in developing ways to optimize cement particle-size distribution.

**Lime** Lime used for agricultural purposes generally is ground in hammer mills. It includes burnt, hydrated, and raw limestone. When a fine product is desired, as in the building trade and for chemical manufacture, ring-roller mills, ball mills, and certain types of hammer mills are used.

**Gypsum** When gypsum is calcined in rotary kilns, it is first crushed and screened. After calcining it is pulverized. Tube mills are usually used. These impart plasticity and workability. Occasionally such calcined gypsum is passed through ring-roller mills ahead of the tube mills.

## COAL, COKE, AND OTHER CARBON PRODUCTS

**Bituminous Coal** The grinding characteristics of bituminous coal are affected by impurities contained, such as inherent ash, slate, gravel, sand, and sulfur balls. The grindability of coal is determined by grinding it in a standard laboratory mill and comparing the results with the results obtained under identical conditions on a coal selected as a standard. This standard coal is a low-volatile coal from Jerome Mines, Upper Kittanning bed, Somerset County, Pennsylvania, and is assumed to have a grindability of 100. Thus a coal with a grindability of 125 could be pulverized more easily than the standard, while a coal with a grindability of 70 would be more difficult to grind. (Grindability and grindability methods are discussed under "Properties of Solids.")

**Anthracite** Anthracite is harder to reduce than bituminous coal. It is pulverized for foundry-facing mixtures in ball mills or hammer mills followed by air classifiers. Only to a lesser extent is it used for fuel in powdered form.

A 3- by 1.65-m (10-ft by 66-in) Hardinge mill in closed circuit with an air classifier as shown in Fig. 20-42, grinding 4-mesh anthracite with 3.5 percent moisture, produced 10.8 Mg/h (12 tons/h), 82 percent through No. 200 sieve. The power required for the mill was 278 kW (370 hp); for auxiliaries, 52.5 kW (70 hp); speed of mill, 19 r/min; ball load, 25.7 Mg (28.5 tons). Data for a similar pilot circuit are given in Table 20-32 (Saner, U.S. Bur. Mines Rep. Invest. 7170, 1968).

Anthracite for use in the manufacture of electrodes is calcined, and the degree of calcination determines the grinding characteristics. Calcined anthracite is generally ground in ball and tube mills or ring-roller mills equipped with air classification. A Raymond high-side ring-roller mill grinding calcined anthracite for electrode manufacture has a capac-

**TABLE 20-32 Closed-Circuit Continuous Grinding of Anthracite in an Air-Swept Ball Mill**

Production rate, lb/h	Mean product size, $\mu\text{m}$	Circulating load, %	Recirculated material, $-37 \mu\text{m}$ , %	Energy, kWh/ton
19.8	7.3	277	42	330
23.0	6.6	283	59	280
27.0	6.1	757	31	246

NOTE: To convert pounds per hour to kilograms per hour, multiply by 0.454; to convert kilowatts per ton to kilowatts per megagram, multiply by 1.1.

ity of 2.1 Mg/h (4600 lb/h) for a product fineness of 76 percent passing a No. 200 sieve and 52.5-kW (70-hp) power requirement.

**Coke** The grinding characteristics of coke vary widely. By-product coke is hard and abrasive, while certain foundry and retort coke is extremely hard to grind. For certain purposes it may be necessary to produce a uniform granule with minimum fines. This is best accomplished in rod or ball mills in closed circuit with screens. Hourly capacity of a 1.2- by 3-m (4- by 10-ft) rod mill with screens, operating on by-product-coke breeze, was 8.1 Mg (9 tons), 100 percent through No. 10 sieve, and 73 percent on No. 200 sieve; power requirement, 30 kW (40 hp).

Petroleum coke is generally pulverized for the manufacture of electrodes; ring-roller mills with air classification and tube mills are generally used. A No. 5057 Raymond ring-roller mill gave an hourly output of 3.8 tons, 78.5 percent through No. 200 sieve, with 67 kW (90 hp).

**Other Carbon Products Pitch** may be pulverized as a fuel or for other commercial purposes; in the former case the unit system of burning is generally employed, and the same equipment is used as described for coal. Grinding characteristics vary with the melting point, which may be anywhere from 50 to 175°C.

**Natural graphite** may be divided into three grades in respect to grinding characteristics: flake, crystalline, and amorphous. Flake is generally the most difficult to reduce to fine powder, and the crystalline variety is the most abrasive. Graphite is ground in ball mills, tube mills, ring-roller mills, and jet mills with or without air classification. Beneficiation by flotation is an essential part of most current procedures.

Majac jet-pulverizer performance on natural graphite is given in Table 20-27. Graphite for pencils has 47, 83, 91, and 94 percent by weight smaller than 4, 9, 18, and 31  $\mu\text{m}$  respectively.

Artificial graphite has been ground in ball mills in closed circuit with air classifiers. For lubricants the graphite is ground wet in a paste in which water is eventually replaced by oil. The colloid mill is used for production of graphite paint.

**Mineral black**, a shale sometimes erroneously called "rotten stone," contains a large amount of carbon and is used as a filler for paints and other chemical operations. It is pulverized and classified with the same equipment as shale, limestone, and barite.

**Bone black** is sometimes ground very fine for paint, ink, or chemical uses. A tube mill often is used, the mill discharging to a fan which blows the material to a series of cyclone collectors in tandem.

**Decolorizing carbons** of vegetable origin should not be ground too fine. Standard fineness varies from 100 percent through No. 30 sieve to 100 percent through No. 50, with 50 to 70 percent on No. 200 sieve as the upper limit. Ball mills, hammer mills, and rolls, followed by screens, are used. When the material is used for filtering, a product of uniform size must be used.

**Charcoal** usually is ground in hammer mills with screen or air classification. For absorption of gases it is usually crushed and graded to about No. 16 sieve size. Care should be taken to prevent it from igniting during grinding.

**Gilsonite** sometimes is used in place of asphalt or pitch. It is easily pulverized and is generally reduced on hammer mills with air classification.

## CHEMICALS, PIGMENTS, AND SOAPS

**Colors and Pigments Dry colors and dyestuffs** generally are pulverized in hammer mills (see Table 20-21 or 20-23). The jar mill or

a large pebble mill is often used for small lots. There is a special problem with some dyes which are coarsely crystalline. These are ground to the desired fineness with hammer or jet mills using air classification to limit the size. Synthetic mineral pigments are usually fine agglomerates. They may be disintegrated with hammer or jet mills without elaborate pregrinding. A 1.5- by 0.4-m (4.5-ft by 16-in) Hardinge conical mill in closed circuit with classifier, grinding 50-mesh iron oxide with 33 percent moisture for the paint trade, showed a capacity of 22.5 Mg/day (25 tons/day), 100 percent through No. 200 sieve. Power consumption was 15 kW (20 hp), mill speed 30 r/min, ball load 1800 kg (4000 lb). The conditions necessary for dispersing pigments in paint by means of steel-ball mills have been investigated [Fischer, *Ind. Eng. Chem.*, **33**(12), 1465-1472 (1941)]. Other examples for iron pigments are given in Table 20-33.

Easily dispersible colors are not ordinarily ground fine, since they are subsequently processed in a liquid medium in pebble mills, rolls, or colloid mills. There is, however, a tendency to grind them wet with a dispersing agent, then drying and pulverizing, after which they are easily dispersed in the vehicle in which they are used.

**White pigments** are the basic commodities processed in large quantities. Titanium dioxide is the most important. The problem of cleaning the mill between batches does not exist as with different colors. These pigments are finish-ground to sell as dry pigments using mills with air classification. For the denser, low-oil-absorption grades, roller and pebble mills are employed. For looser, fluffier products, hammer and jet mills are used. Often a combination of the two mill actions is used to set the finished quality. Jet-mill performance for a number of extenders is given in Table 20-26.

**Lead Oxides** Lead litharge containing 25 to 30 percent free lead is required for storage-battery plates. It is processed on Raymond Imp mills. They have the ability to produce litharge that has a desired low density of 1.1 to 1.3 g/cm<sup>3</sup> (18 to 22 g/in<sup>3</sup>). A 56-kW (75-hp) unit produces 860 kg/h (1900 lb/h) of material having this density.

The processing of **diatomite** is unique, since its particle-size control is effected by calcination treatments and air classification.

**Chemicals** The fineness obtainable with a hammer mill on rock salt and chemicals is given in Tables 20-23 and 20-24.

**Sulfur** The ring-roller mill can be used for the fine grinding of sulfur. Inert gases are supplied instead of hot air (see "Properties of Solids: Safety" for use of inert gas). Performance of a Raymond No. 5057 ring-roller mill is given in Table 20-34. The total cost might be 3 to 4 times the power cost and include labor, inert gas, maintenance, and fixed charges.

**Soaps** Soaps in a finely divided form may be classified as soap powder, powdered soap, and chips or flakes. The term "soap powder" is applied to a granular product, No. 12 to No. 16 sieve size with a certain amount of fines, which is produced in hammer mills with perforated or slotted screens.

The oleates and erucates are best pulverized by multicage mills; laurates and palmitates, in cage mills and also in hammer mills if particu-

**TABLE 20-34 Grinding Sulfur**

Fineness, % through No. 325 sieve	Capacity, tons/hr.	Power, kw.-hr./ton
90	6.0	13.7
95	5.0	16.4
99	3.5	23.4
99.9	2.5	32.7

NOTE: To convert tons per hour to megagrams per hour, multiply by 0.907; to convert kilowatthours per ton to kilowatthours per megagram, multiply by 1.1.

larly fine division is not required; stearates may generally be pulverized in multicage mills, screen mills, and air-classification hammer mills.

## ORGANIC POLYMERS

The grinding characteristics of various resins, gums, waxes, hard rubbers, and molding powders depend greatly upon their softening temperatures. When a finely divided product is required, it is often necessary to use a water-jacketed mill or a pulverizer with an air classifier in which cooled air is introduced into the system. Hammer and cage mills are used for this purpose. Some low-softening-temperature resins can be ground by mixing with 15 to 50 percent by weight of dry ice before grinding. Refrigerated air sometimes is introduced into the hammer mill to prevent softening and agglomeration [Dorris, *Chem. Metall. Eng.*, **51**, 114 (July 1944)].

Most **gums and resins**, natural or artificial, when used in the paint, varnish, or plastic industries, are not ground very fine, and hammer or cage mills will produce a suitable product. Typical performance of the disk attrition mill is given in Table 20-25. Roll crushers will often give a sufficiently fine product.

The Raymond ring-roll mill with its internal air separation is widely used to pulverize **phenolformaldehyde resins**. The usual fineness of grind is finer than 99 percent minus 200 mesh. Air at 4°C (40°F) is usually introduced into the mill to limit temperature rise. A typical 3036 Raymond mill using 34 kW (45 hp) will produce better than 900 kg/h (2000 lb/h) at 99 percent minus 200 mesh.

**Hard rubber** is one of the few combustible materials which is generally ground on heavy steam-heated rollers. The raw material passes to a series of rolls in closed circuit with screens and air classifiers. Farrel-Birmingham rolls are used extensively for this work. There is a differential in the roll diameters. The motor should be separated from the grinder by a fire wall.

Specifications for **molding powders** vary widely, from a No. 8 to a No. 60 sieve product; generally the coarser products are No. 12, 14, or 20 sieve material. Specifications usually prescribe a minimum of fines (below No. 100 and No. 200 sieve). Molding powders are produced with hammer mills, either of the screen type or equipped with air classifiers.

The following materials may be ground at ordinary temperatures if only the regular commercial fineness is required: amber, arabac, tragacanth, rosin, olibanum, gum benzoïn, myrrh, guaiaicum, and montan wax. If a finer product is required, hammer mills or attrition mills in closed circuit, with screens or air classifiers, are used.

## PROCESSING WASTE

In flowsheets for processing *municipal solid waste* (MSW), the objective is to separate the waste into useful materials, such as scrap metals, plastics, and *refuse-derived fuels* (RDF). Usually size reduction is the first step, followed by separations with screens or air classifiers, which attempt to recover concentrated fractions [Savage and Diaz, *Proceedings ASME National Waste Processing Conference*, Denver, Colo., 361-373 (1986)]. Many installed circuits proved to be ineffective or not cost-effective, however. Begnaud and Noyon [*Bicycle*, **30**(3), 40-41 (1989)] concluded from a study of French operations that milling could not grind selectively enough to separate different materials.

Size reduction uses either hammer mills or blade cutters (shredders). Hammer mills are likely to break glass into finer sizes making it hard to separate. Better results may be obtained in a flowsheet where size reduction follows separation (Savage, Seminar on the Application

**TABLE 20-33 Grinding Iron Oxides in a Ring-Roller Mill**

Material	Fineness	Capacity, lb./hr.	Total hp.-hr./ton
Raw sienna	99% through No. 200 sieve	5950	23.5
Burnt sienna	99.5% through No. 200 sieve	5800	22.1
Raw umber	99% through No. 200 sieve	5200	26.9
Burnt umber	99.5% through No. 200 sieve	5400	25.9
Natural ocher	99.9% through No. 200 sieve	4500	31.0
Iron oxide (ore)	99% through No. 325 sieve	3100	45.0
Iron oxide (precipitated)	99.9% through No. 325 sieve	1800	72.5

NOTE: To convert pounds per hour to kilograms per hour, multiply by 0.4535; to convert horsepower-hours per ton to kilowatthours per megagram, multiply by 0.82.

of U.S. Water and Air Pollution Control Technology to Korea, Korea, May 1989).

The energy requirement for reducing MSW to 90 percent passing 10 cm is typically 6 kWh/ton, or 50 kWh/ton for passing 1 cm. Wear is also a major cost, and wear rates are shown in Fig. 20-60. The maximum capacity of commercially available hammer mills is about 100 ton/h.

### CRYOGENIC GRINDING

This is a process used for recovering recycled materials [Biddulph, *Chemical Engineering*, **87**(3), 93-96 (1980)]. This process permits efficient separation of materials in cases where some materials in a mixture become brittle, while others do not, and it also reduces crusher energy requirements. Examples are rubber crumb recovered in a pure state from scrap tires, which has found uses including road and sports surfaces and polymer fillers. Stripping of polymeric insulation from copper wires occurs when the chilled material is passed through crushing rolls. The Inchscrap process shreds chilled baled automobiles, magnetically separating pure steel and other components. Biddulph (loc. cit.) presents graphs for design of a heat-transfer tunnel using liquid nitrogen. Countercurrent flow of the gas also extracts the latent heat of the nitrogen. The process can be economic

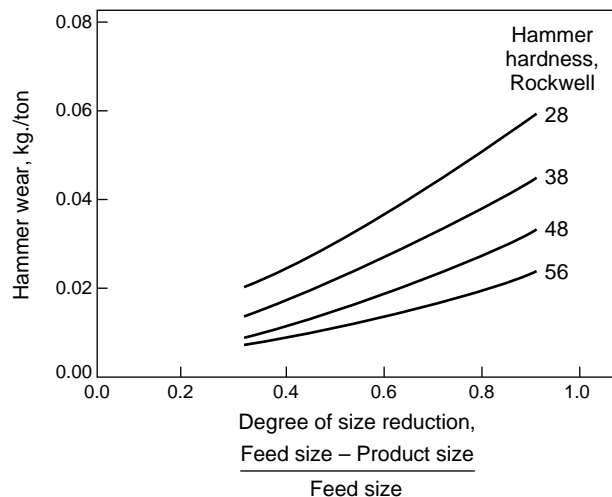


FIG. 20-60 Hammer wear as a consequence of shredding municipal solid waste. (Savage and Diaz, *Proceedings ASME National Waste Processing Conference, Denver, CO, 361-373, 1986.*)

## PRINCIPLES OF SIZE ENLARGEMENT

**GENERAL REFERENCES:** Ennis & Litster, *The Science & Engineering of Granulation Processes*, Blackie Academic Ltd., 1997. Ennis (ed.), *Proceedings of the First International Particle Technology Forum, Vol. 1, AIChE, Denver, 1994*. Ennis, *Powder Technology*, **88**, 203 (1996). Kapur, *Adv. Chem. Eng.*, **10**, 55, 1978. Kristensen, *Acta Pharm. Suec.*, **25**, 187, 1988. Pietsch, *Size Enlargement by Agglomeration*, John Wiley & Sons Ltd., Chichester, 1992. Randolph & Larson, *Theory of Particulate Processes*, Academic Press, Inc., San Diego, 1988. Stanley-Wood, *Enlargement and Compaction of Particulate Solids*, Butterworth & Co. Ltd., 1983. Ball et al., *Agglomeration of Iron Ores*, Heinemann, London, 1973. Capes, *Particle Size Enlargement*, Elsevier, New York, 1980. King, "Tablets, Capsules and Pills," in *Remington's Pharmaceutical Sciences*, Mack Pub. Co., Easton, Pa., 1970. Knepper (ed.), *Agglomeration*, Interscience, New York, 1962. Mead (ed.), *Encyclopedia of Chemical Process Equipment*, Reinhold, New York, 1964. Pietsch, *Roll Pressing*, Heyden, London, 1976. Sastry (ed.), *Agglomeration 77*, AIIME, New York, 1977. Sauchelli (ed.), *Chemistry and*

where the added value of the recovered product ranges from a few cents to 15 cents/kg.

Results for cryogrinding of polymers in an opposed-jet laboratory mill are given by [Haesse, *Kunststoffe-German Plastics*, **70**(12), 9-10 (1980)].

### CELL DISRUPTION

Mechanical disruption is the most practical first step in the release and isolation of proteins and enzymes from microorganisms on a commercial scale. The size-reduction method must be gently tuned to the strength of the organisms to minimize formation of fine fragments that interfere with subsequent clarification by centrifugation or filtration. Typically, fragments as fine as 0.3  $\mu\text{m}$  are produced. High-speed stirred-bead mills and high-pressure homogenizers have been applied for cell disruption [Kula and Schuette, *Biotechnology Progress*, **3**(1), 31-42 (1987)].

There are two limiting cases in operation of bead mills for disruption of bacterial cells. When the energy imparted by collision of beads is insufficient to break all cells, the rate of breakage is proportional to the specific energy imparted [Bunge et al., *Chemical Engineering Science*, **47**(1), 225-232 (1992)]. On the other hand, when the energy is high due to higher speed above 8 m/sec, larger beads above 1 mm, and low concentrations of 10 percent, each bead impact has more than enough energy to break any cells that are captured, which causes problems during subsequent separations.

The strength of cell walls differs among bacteria, yeasts, and molds. The strength also varies with the species and the growth conditions, and must be determined experimentally. Beads of 0.5 mm are typically used for yeast and bacteria. Recommended bead charge is 85 percent for 0.5 mm beads, and 80 percent for 1 mm beads [Schuette et al., *Enzyme Microbial Technology*, **5**, 143 (1983)].

Residence-time distribution is important in continuous mills. Further data are given in the above references.

While the above discussion centered on the rate of disruption, the objective is usually to attain at least 90 percent release of the valuable protein from the cells. Cell disruption with protein solubilization is considered to be first order in amount of protein remaining [Currie et al., *Biotechnol. Bioeng.*, **14**, 725 (1972)]:

$$(R_m - R)/R_m = \exp(-kt)$$

where R is residual protein, and  $R_m$  is maximum protein removable.

Valve homogenizers have been used to disrupt cells and release soluble components (Pandolf, *Cell Disruption by Homogenization*, APV Gaulin, 1993). The cell disruption is believed due to the sudden pressure drop, although impact may also be a cause [Brookman, *Biotechnol. Bioeng.*, **16**, 371 (1974); Engler and Robinson, *Biotechnol. Bioeng.*, **23**, 765 (1981)]. The release of glycose-6-phosphate dehydrogenase from *Saccharomyces cerevisiae* is linear with pressure beginning at 200 bar and reaches 40 percent at 550 bar in the Gaulin M3 unit.

*Technology of Fertilizers*, Reinhold, New York, 1960. Sherrington and Oliver, *Granulation*, Heyden, London, 1981.

### SCOPE AND APPLICATIONS

**Size enlargement** is any process whereby small particles are gathered into larger, relatively permanent masses in which the original particles can still be distinguished. The term encompasses a variety of unit-operations or processing techniques dedicated to particle agglomeration. **Agglomeration** is the formation of aggregates through the sticking together of feed and/or recycle material. These processes can be loosely broken down into **agitation** and **compression** methods. Although terminology is industry specific, agglomeration by agitation will be referred to as **granulation**. Here, a particulate feed is



introduced to a process vessel and is agglomerated, either batchwise and continuously, to form a granulated product. Agitative processes include fluid-bed, pan (or disc), drum, and mixer granulators. The feed typically consists of a mixture of solid ingredients, referred to as a **formulation**, which includes an active or key ingredient, binders, diluents, flow aids, surfactants, wetting agents, lubricants, fillers, or end-use aids (e.g., sintering aids, colors or dyes, taste modifiers). The agglomeration can be induced in several ways. A solvent or slurry can be atomized onto the bed of particles which either coats the particle or granule surfaces promoting agglomeration, or the spray drops can form small nuclei in the case of a powder feed which subsequently can agglomerate. The solvent or slurry may contain a binder, or solid binder may be present as one component of the feed. Alternatively, the solvent may induce dissolution and recrystallization in the case of soluble particles. Slurries often contain the same particulate matter as the dry feed, and granules may be formed, either completely or partially, as the droplets solidify in flight prior to reaching the particle bed. **Spray-drying** is an extreme case with no further, intended agglomeration taking place after granule formation. Agglomeration may also be induced by heat, which either leads to controlled **sintering** of the particle bed or induces sintering or partial melting of a binder component of the feed, e.g., a polymer.

An alternative approach to size enlargement is by **compression agglomeration**, where the mixture of particulate matter is fed to a compression device which promotes agglomeration due to pressure. Either continuous sheets of solid material are produced or some solid form such as a **briquette** or **tablet**. Heat or cooling may be applied, and reaction may be induced as for example with sintering. Carrier fluids may be present, either added or induced by melting, in which case the product is **wet extruded**. Continuous compaction processes include roll presses, briquetting machines, and extrusion, whereas batch-like processes include tableting. Some processes operate in a semicontinuous fashion, such as ram extrusion.

At the level of a manufacturing plant, the size-enlargement process involves several peripheral, unit operations such as milling, blending, drying or cooling, and classification, referred to generically as an **agglomeration circuit** (Fig. 20-61). In addition, more than one

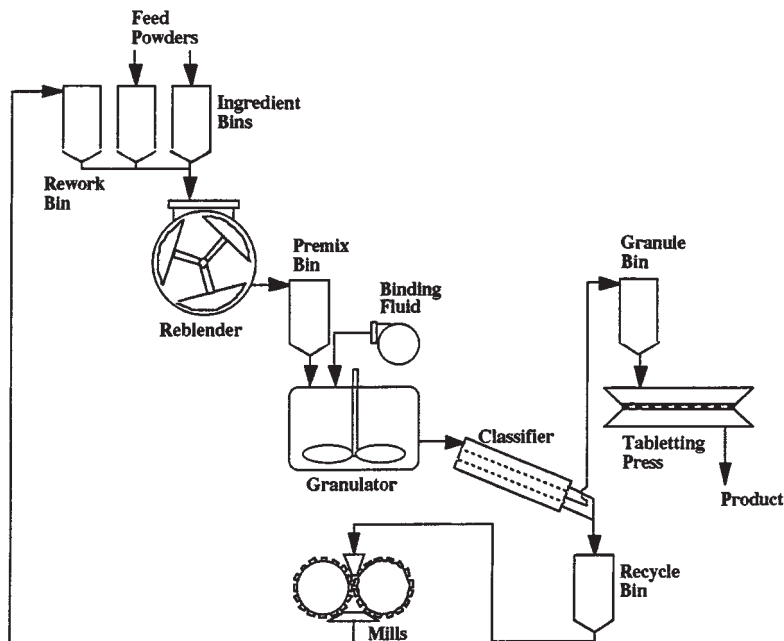
agglomeration step may be present as in the case of a pharmaceutical process which often involves both an agitative-granulation technique followed by the compressive technique of tableting.

Numerous benefits result from size-enlargement processes, as will be appreciated from Table 20-35. A wide variety of size-enlargement methods are available; a classification of these is given in Table 20-36.

## APPROACHING THE DESIGN OF SIZE-ENLARGEMENT PROCESSES

**Agglomeration Kinetics** A change in particle size of a particulate material due to agglomeration is akin to a change in chemical species, and so analogies exist between agglomeration and chemical kinetics and the unit operations of size enlargement and chemical reaction. The performance of a **granulator** or **compactor** may be described by the **extent of agglomeration** of a species, typically represented by a loss in number of particles. Let  $(x_1, x_2, \dots, x_n)$  represent a list of attributes such as average particle size, porosity, strength, surface properties, and any generic quality metric and associated variances. Alternatively,  $(x_1, x_2, \dots, x_n)$  might represent the concentrations or numbers of certain size or density classes, just as in the case of chemical reactors. The proper design of a chemical reactor or an **agglomerator** then relies on understanding and controlling the evolution (both time and spatial) of the feed vector  $\mathbf{X}$  to the desired product vector  $\mathbf{Y}$ . Inevitably, the reactor or granulator is contained within a larger plant-scale process chain, or **manufacturing circuit**, with overall plant performance being dictated by the interactions between individual unit operations. For successful plant design and operation, there are four natural levels of scrutiny (Fig. 20-62). Conceptually, the design of chemical reactors and agglomeration processes differ in that the former deals with chemical transformations whereas the latter deals primarily with **physical transformations** with the mechanisms or rate processes of agglomeration controlled by a set of key **physicochemical interactions**.

**Granulation Rate Processes** Granulation is controlled by four key rate processes. These include wetting, coalescence or growth, consolidation, and breakage (Fig. 20-63). Initial **wetting** of the particles by the binding fluid is strongly influenced by spray or fluid distri-



**FIG. 20-61** A typical agglomeration circuit utilized in the processing of pharmaceutical or agricultural chemicals involving both granulation and compression techniques. Reprinted from *Granulation and Coating Technologies for High-Value-Added Industries*, Ennis and Litster (1996) with permission of E & G Associates. All rights reserved.

**TABLE 20-35 Objectives of Size Enlargement**

Production of useful structural forms, as in pressing of intricate shapes in powder metallurgy.
Provision of a defined quantity for dispensing and metering, as in agricultural chemical granules or pharmaceutical tablets.
Elimination of dust handling hazards or losses, as in briquetting of waste fines.
Improved product appearance, or product renewal.
Reduced caking and lump formation, as in granulation of fertilizer.
Improved flow properties, as in granulation of pharmaceuticals for tableting or ceramics for pressing.
Increased bulk density for storage.
Creation of non-segregating blends of powder ingredients, as in sintering of fines for steel or agricultural chemical granules.
Control of solubility, as in instant food products.
Control of porosity and surface-to-volume ratio, as with catalyst supports.
Improvement of heat transfer characteristics, as in ores or glass for furnace feed.
Removal of particles from liquid, as with polymer additives which induce clay flocculation.

Reprinted from *Granulation and Coating Technologies for High-Value-Added Industries*, Ennis and Litster (1996) with permission of E & G Associates. All rights reserved.

bution as well as feed-formulation properties. Often wetting agents such as surfactants are carefully chosen to enhance poorly wetting feeds. In the **coalescence** or **growth** stage, partially wetted primary particles and larger nuclei coalesce to form granules composed of several particles. The term **nucleation** is typically applied to the initial coalescence of primary particles in the immediate vicinity of the larger-wetting drop, whereas the more general term of **coalescence**

refers to the successful collision of two granules to form a new larger granule. Nucleation is promoted from some initial distribution of moisture, such as a drop or from the homogenization of a fluid feed to the bed, as with high-shear mixing. The nucleation process is strongly linked with the wetting stage. As granules grow, they become consolidated by the compaction forces of the bed due to agitation. This **consolidation** stage strongly influences final granule porosity, and therefore end-use properties such as granule strength or dispersability. Formed granules may be particularly susceptible to **breakage** if they are inherently weak or if flaws develop during drying. The final size distribution and other end-use properties of the product are determined by the complex interaction of all these rate processes acting simultaneously.

**Compaction Rate Processes** The performance of compaction techniques is controlled by the ability of the particulate phase to uniformly transmit stress and the relationship between applied stress and the compaction and strength characteristics of the final compacted particulate phase. The general area of study relating compaction and stress transmission is referred to as **powder mechanics** (Brown & Richards, *Principles of Powder Mechanics*, Pergamon Press Ltd., Oxford, 1970).

**Process versus Formulation Design** The end-use properties of the agglomerated material are controlled by agglomerate size and porosity. Granule structure may also influence properties. To achieve a desired **product quality** as defined by metrics of end-use properties, size and porosity may be manipulated by changes in either process **operating** or product **material variables** (Fig. 20-63). The first approach is the realm of traditional **process engineering**, whereas the second is **product engineering**. Both approaches are

**TABLE 20-36 Size-Enlargement Methods and Application**

Method	Product size (mm)	Granule density	Scale of operation	Additional comments	Typical applications
Tumbling granulators Drums Discs	0.5 to 20	Moderate	0.5–800 ton/hr	Very spherical granules	Fertilizers, iron ore, non-ferrous ore, agricultural chemicals
Mixer granulators Continuous high shear (e.g. Shugi mixer)	0.1 to 2	Low to high	Up to 50 ton/hr	Handles very cohesive materials well, both batch and continuous	Chemicals, detergents, clays, carbon black
Batch high shear (e.g. paddle mixer)	0.1 to 2	High	Up to 500 kg batch		Pharmaceuticals, ceramics
Fluidized granulators Fluidized beds Spouted beds Wurster coaters	0.1 to 2	Low (agglomerated) Moderate (layered)	100–900 kg batch 50 ton/hr continuous	Flexible, relatively easy to scale, difficult for cohesive powders, good for coating applications	Continuous: fertilizers, inorganic salts, detergents Batch: pharmaceuticals, agricultural chemicals, nuclear wastes
Centrifugal granulators	0.3 to 3	Moderate to high	Up to 200 kg batch	Powder layering and coating applications	Pharmaceuticals, agricultural chemicals
Spray methods Spray drying	0.05 to 0.5	Low		Morphology of spray dried powders can vary widely	Instant foods, dyes, detergents, ceramics
Prilling	0.7 to 2	Moderate			Urea, ammonium nitrate
Pressure compaction Extrusion Roll press Tablet press Molding press Pellet mill	>0.5 >1 10	High to very high	Up to 5 ton/hr Up to 50 ton/hr Up to 1 ton/hr	Very narrow size distributions, very sensitive to powder flow and mechanical properties	Pharmaceuticals, catalysts, inorganic chemicals, organic chemicals, plastic preforms, metal parts, ceramics, clays, minerals, animal feeds
Thermal processes Sintering	2 to 50	High to very high	Up to 100 ton/hr	Strongest bonding	Ferrous & non-ferrous ores, cement clinker, minerals, ceramics
Liquid systems Immiscible wetting in mixers Sol-gel processes Pellet flocculation	<0.3	Low	Up to 10 ton/hr	Wet processing based on flocculation properties of particulate feed	Coal fines, soot and oil removal from water Metal dicarbide, silica hydrogels Waste sludges and slurries

Reprinted from *Granulation and Coating Technologies for High-Value-Added Industries*, Ennis and Litster (1996) with permission of E & G Associates. All rights reserved.

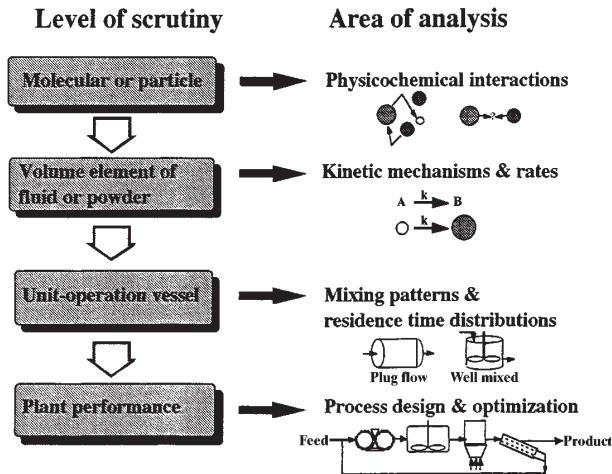


FIG. 20-62 Comparisons of levels of analysis of chemical reaction and size-enlargement processes. Reprinted from *Granulation and Coating Technologies for High-Value-Added Industries*, Ennis and Litster (1996) with permission of E & G Associates. All rights reserved.

critical and must be integrated to achieve a desired end point in product quality. Operating variables are defined by the chosen agglomeration technique and peripheral processing equipment. In addition, the choice of agglomeration technique dictates the mixing pattern of the vessel. Material variables include parameters such as binder viscosity, surface tension, particle-size distribution and friction, and the adhesive properties of the solidified binder. Material variables are specified by the choice of ingredients, or **product formulation**. Both operating and material variables together define the kinetic mechanisms and

rate constants of wetting, growth, consolidation, attrition, and powder flow. Overcoming a given size-enlargement problem often requires changes in both processing conditions and in product formulation.

**PRODUCT CHARACTERIZATION**

Powders are agglomerated to modify physical or physicochemical properties. Effective measurement of agglomerate properties is vital. However, many tests are industry specific and take the form of empirical indices based on standardized protocols. Such tests as described below are useful for quality control if used with care. However, since they often reflect an end use rather than a specifically defined agglomerate property, they often are of little developmental utility for recommending process or formulation changes. Significant improvements have been made in the ability to measure real agglomerate properties. Key agglomerate properties are **size**, **porosity**, and **strength** and their associated distributions. These properties directly affect end-use attributes of the product such as attrition resistance, flowability, bulk-solid permeability, wettability and dispersibility, appearance, or active-agent release rate.

**Size** Agglomerate **mean size** and **size distribution** are both important properties. (See subsection "Particle-Size Measurement.") For granular materials, sieve analysis is the most common sizing technique. Care is needed in sizing wet granules. Handling during sampling and sieving can cause changes to the size distribution through coalescence or breakage. Sieves are also easily blinded. Snap freezing the granules with liquid nitrogen prior to sizing overcomes these problems [Hall, *Chem. Eng. Sci.*, **41**, 187 (1986)]. On-line or in-line measurement of granules as large as 9 mm is now available by laser diffraction techniques, making improved granulation control schemes possible [Ogunnaikie et al., *I.E.C. Fund.*, 1997].

**Porosity and Density** There are three important densities of granular or agglomerated materials: **bulk density**  $\rho_b$  (related to the volume occupied by the bulk solid), the apparent or **agglomerate density**  $\rho_a$  (related to the volume occupied by the agglomerate including internal porosity) and the true or **skeletal-solids density**  $\rho_s$ . These densities are related to the each other and the interagglomerate **voidage**  $\epsilon_b$  and the intra-agglomerate **porosity**  $\epsilon_g$ :

$$\epsilon_b = 1 - \frac{\rho_b}{\rho_s}; \epsilon_g = 1 - \frac{\rho_a}{\rho_s} \quad (20-42)$$

Bulk density is easily measured from the volume occupied by the bulk solid and is a strong function of sample preparation. True density is measured by standard techniques using liquid or gas pycnometry. Apparent (agglomerate) density is difficult to measure directly. Hinkley et al. [*Int. J. Min. Proc.*, **41**, 53-69 (1994)] describe a method for measuring the apparent density of wet granules by kerosene displacement. Agglomerate density may also be inferred from direct measurement of true density and porosity using Eq. (20-42).

Agglomerate porosity can be measured by gas adsorption or mercury porosimetry. However, any breakage or compression of the granules under high pressure during porosimetry can invalidate the results.

**Strength of Agglomerates** **Agglomerate bonding mechanisms** may be divided into five major groups [Rumpf, in Knepper (ed.), *Agglomeration*, op. cit., p. 379]. More than one mechanism may apply during a given size-enlargement operation. (In addition, see Krupp [*Adv. Colloid. Int. Sci.*, **1**, 111 (1967)] for a review of adhesion mechanisms.)

**Solid bridges** can form between particles by the sintering of ores, the crystallization of dissolved substances during drying as in the granulation of fertilizers, and the hardening of bonding agents such as glue and resins.

**Mobile liquid binding** produces cohesion through interfacial forces and capillary suction. Three states can be distinguished in an assembly of particles held together by a mobile liquid (Fig. 20-64). Small amounts of liquid are held as discrete lens-shaped rings at the points of contact of the particles; this is the **pendular state**. As the liquid content increases, the rings coalesce and there is a continuous network of liquid interspersed with air; this is the **funicular state**. When all the pore spaces in the agglomerate are completely filled, the **capillary state** has been reached. When a mobile liquid bridge fails, it con-

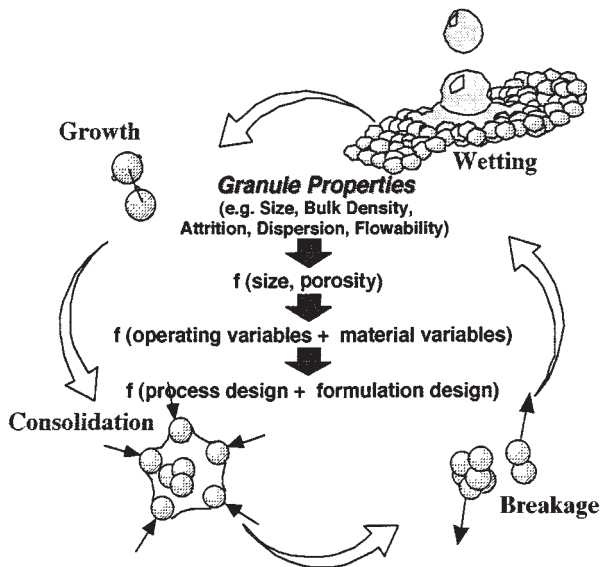


FIG. 20-63 The rate processes of agitative agglomeration, or granulation, which include powder wetting, granule growth, granule consolidation, and granule attrition. These processes combined control granule size and porosity, and they may be influenced by formulation or process-design changes. Reprinted from *Granulation and Coating Technologies for High-Value-Added Industries*, Ennis and Litster (1996) with permission of E & G Associates. All rights reserved.

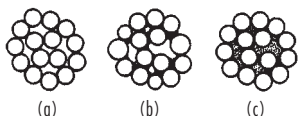


FIG. 20-64 Three states of liquid content for an assembly of spherical particles. (a) Pendular state. (b) Funicular state. (c) Capillary state. [Newitt and Conway-Jones, *Trans. Inst. Chem. Eng. (London)*, **36**, 422 (1958).]

stricts and divides without fully exploiting the adhesion and cohesive forces in the bridge in the absence of viscous effects. Binder viscosity markedly increases the strength of the pendular bridge due to dynamic lubrication forces, and aids the transmission of adhesion. For many systems, viscous forces outweigh interfacial capillary effects, as demonstrated by Ennis et al. [*Chem. Eng. Sci.*, **45**, 3071 (1990)].

In the limit of high viscosity, **immobile liquid bridges** formed from materials such as asphalt or pitch fail by tearing apart the weakest bond. Then adhesion and/or cohesion forces are fully exploited, and binding ability is much larger.

**Intermolecular and electrostatic forces** bond very fine particles without the presence of material bridges. Such bonding is responsible for the tendency of particles less than about 1  $\mu\text{m}$  diameter to form agglomerates spontaneously under agitation. With larger particles, however, these short-range forces are insufficient to counterbalance the weight of the particle, and adhesion does not occur without applied pressure. High compaction pressures act to plastically flatten interparticle contacts and substantially enhance short-range forces.

**Mechanical interlocking** of particles may occur during the agitation or compression of, for example, fibrous particles, but it is probably only a minor contributor to agglomerate strength in most cases.

For an agglomerate of equal-sized spherical particles (Rumpf, loc. cit., 379), the tensile strength is

$$\sigma_T = \frac{9}{8} \frac{1 - \epsilon_g}{\epsilon_g} \frac{H}{d^2} \quad (20-43)$$

where  $H$  is the individual bonding force per point of contact and  $d$  is the size of particles making up the granule. For other bonding mechanisms, Fig. 20-65 indicates values of tensile strength to be expected in various size enlargement processes. In particular, it should be noted that viscous mechanisms of binding (e.g., adhesives) can exceed capillary effects in determining agglomerate strength.

**Strength Testing Methods** Compressed agglomerates often fail in **tension** along their diameter. This is the basis of the commonly used measurement of **crushing strength** of an agglomerate as a method to assess tensile strength. However, the brittle failure of a granule depends on the flaw distribution as well as the inherent tensile strength of bonds as given by the Griffith crack theory. [Lawn, *Fracture of Brittle Solids*, 2d ed., Cambridge University Press, 1975] Therefore, it is more appropriate to characterize granule strength by **fracture toughness**  $K_{IC}$  [Kendall, *Nature*, **272**, 710 (1978)]; See also subsections "Size Reduction: Properties of Solids" and "Breakage".

Several strength-related indices are measured in different industries which give some measure of resistance to attrition. These tests do not measure strength or toughness directly, but rather the size distribution of fragments after handling the agglomerates in a defined way. The handling could be repeated drops, tumbling in a drum, fluidizing, circulating in a pneumatic conveying loop, etc. These indices should only be used for quality control if the test procedure simulates the actual handling of the agglomerates during processing and transportation.

**Flow Property Tests** **Flowability** of the product granules can be characterized by **unconfined yield stress** and **angle of friction** by

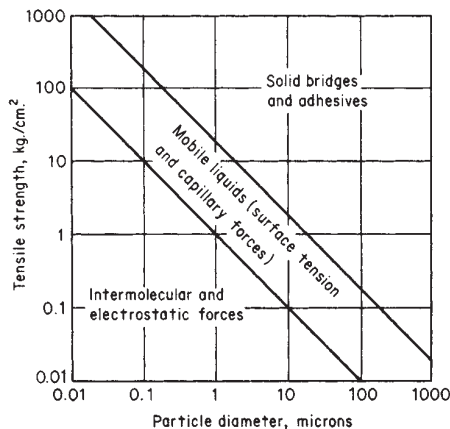


FIG. 20-65 Theoretical tensile strength of agglomerates. [Adapted from Rumpf, "Strength of Granules and Agglomerates," in Knepper (ed.), *Agglomeration*, Wiley, New York, 1962.]

shear-cell tests as used generally for bulk solids (see subsection "Powder Mechanics and Powder Compaction" and also Section 21, Solids Transport and Storage). **Caking** refers to deterioration in the flow properties of the granules due to chemical reaction or hygroscopic effects. Caking tests as used for fertilizer granules consist of two parts (Bookey and Raistrick, in Sauchelli (ed.), *Chemistry and Technology of Fertilizers*, p. 454). A cake of the granules is first formed in a compression chamber under controlled conditions of humidity, temperature, etc. The crushing strength of the cake is then measured to determine the degree of caking.

**Redispersion Tests** Agglomerated products are often **redispersed** in a fluid by a customer. Examples include the dispersion of fertilizer granules in spray-tank solutions or of tablets within the gastrointestinal tract of the human body. The mechanisms comprising this redispersion process of product **wetting**, agglomerate **disintegration**, and final **dispersion** are related to interfacial properties (For details, see subsection "Wetting"). There are a wide range of industry-specific empirical indices dealing with redispersion assessment.

**Disintegration height tests** consist of measuring the length required for complete agglomerate disintegration in a long, narrow tube. Small fragments may still remain after initial agglomerate disintegration. The residual of material which remains undispersed is measured by a related test, or **long-tube sedimentation test**. The residual undispersed material is reported by the level in the bottom tip of the tube. A variation of this test is the **wet screen test**, which measures the residual remaining on a fine mesh screen (e.g., 350 mesh) following pouring the beaker solution through the screen.

**Tablet-disintegration tests** consist of cyclical immersion in a suitable dissolving fluid of pharmaceutical tablets contained in a basket. Acceptable tablets disintegrate completely by the end of the specified test period (*United States Pharmacopeia*, 17th rev., Mack Pub. Co., Easton, Pa., 1965, p. 919).

**Permeability** **Bulk solid permeability** is important in the iron and steel industry where gas-solid reactions occur in the sinter plant and blast furnace. It also strongly influences compaction processes where entrapped gas can impede compaction, and solids-handling equipment where restricted gas flow can impede product flowability. The permeability of a granular bed is inferred from measured pressure drop under controlled gas-flow conditions.

## AGGLOMERATION RATE PROCESSES

**GENERAL REFERENCES:** Adetayo *et al.*, *Powder Tech.*, **82**, 37 (1995). Brown & Richards, *Principles of Powder Mechanics*, Pergamon Press (1970). Carson & Marinelli, *Chemical Eng.*, April (1994). Ennis & Litster, *The Science & Engineering of Granulation Processes*, Blackie Academic Ltd., 1997. Ennis *et al.*, *Powder Tech.*, **65**, 257 (1991). Ennis & Sunshine, *Tribology International*, **26**, 319 (1993). Ennis (ed.), *Proceedings of the First International Particle Technology Forum*, Vol. 1, AIChE, Denver, 1994. Ennis, *Powder Technology*, **88**, 203 (1996). Kristensen, *Acta Pharm. Suec.*, **25**, 187, 1988. Lawn, *Fracture of Brittle Solids*, 2nd ed., Cambridge University Press, 1975. Owens & Wendt, *J. Appl. Polym. Sci.*, **13**, 1741 (1969). Pan *et al.*, *Dynamic Properties of Interfaces & Association Structure*, American Oil Chem. Soc. Press (1995). Parfitt (ed.), *Dispersion of Powders in Liquids*, Elsevier Applied Science Publishers Ltd., 1986.

## WETTING

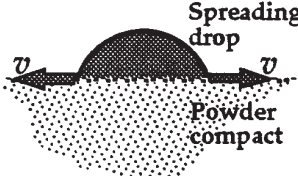
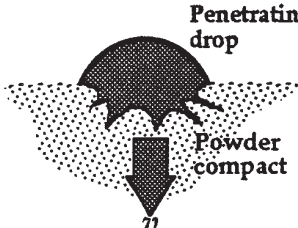

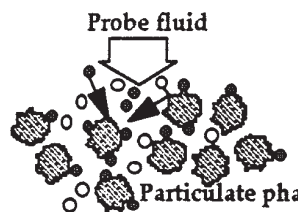
The initial distribution of binding fluid can have a pronounced influence on the size distribution of seed granules, or **nuclei**, which are formed from fine powder. Both the final **extent** of and the **rate** at

which the fluid wets the particulate phase are important. For a poor wetting fluid, a substantial portion of the powder remains ungranulated. When the size of a particulate feed material is larger than drop size, wetting dynamics controls the distribution of coating material which has a strong influence on the later stages of growth. Wetting phenomena also influence redistribution of individual ingredients within a granule, drying processes, and redispersion of granules in a fluid phase (e.g., agricultural chemicals and pharmaceutical products).

**Methods of Measurement** Methods of characterizing the rate process of wetting include four approaches as illustrated in Table 20-37. The first considers the ability of a drop to spread across the powder. This approach involves the measurement of a **contact angle** of a drop on a powder compact. The contact angle is a measure of the affinity of the fluid for the solid as given by the Young-Dupré equation, or

$$\gamma^{sv} - \gamma^{sl} = \gamma^{lv} \cos \theta \quad (20-44)$$

**TABLE 20-37 Methods of Characterizing Wetting Dynamics of Particulate Systems\***

Mechanism of wetting	Characterization method
 <p>Spreading of drops on powder surface</p> <p><b>Spreading drop</b></p> <p><b>Powder compact</b></p>	<p><b>Contact angle goniometer</b></p> <ul style="list-style-type: none"> <li>Contact angle</li> <li>Drop height or volume</li> <li>Spreading velocity</li> </ul> <p><b>References:</b> Kossen &amp; Heertjes, <i>Chem. Eng. Sci.</i>, <b>20</b>, 593 (1965). Pan <i>et al.</i>, <i>Dynamic Properties of Interfaces &amp; Association Structure</i>, American Oil Chem. Soc. Press (1995)</p>
 <p>Penetration of drops into powder bed</p> <p><b>Penetrating drop</b></p> <p><b>Powder compact</b></p>	<p><b>Washburn test</b></p> <ul style="list-style-type: none"> <li>Rate of penetration by height or volume</li> </ul> <p><b>Bartell cell</b></p> <ul style="list-style-type: none"> <li>Capillary pressure difference</li> </ul> <p><b>References:</b> Parfitt (ed.), <i>Dispersion of Powders in Liquids</i>, Elsevier Applied Science Publishers Ltd., 1986. Washburn, <i>Phys. Rev.</i>, <b>17</b>, 273 (1921). Bartell &amp; Osterhof, <i>Ind. Eng. Chem.</i>, <b>19</b>, 1277 (1927).</p>
 <p>Penetration of particles into fluid</p> <p><b>Particle</b></p> <p><b>Drop surface</b></p> <p><b>time</b></p>	<p><b>Flotation tests</b></p> <ul style="list-style-type: none"> <li>Penetration time</li> <li>Sediment height</li> <li>Critical solid surface energy distribution</li> </ul> <p><b>References:</b> R. Ayala, Ph.D. Thesis, Chem. Eng., Carnegie Mellon Univ. (1985). Fuerstaneau <i>et al.</i>, <i>Colloids &amp; Surfaces</i>, <b>60</b>, 127 (1991). Vargha-Butler, <i>et al.</i>, <i>Colloids &amp; Surfaces</i>, <b>24</b>, 315 (1987).</p>
 <p>Chemical probing of powder</p> <p><b>Probe fluid</b></p> <p><b>Particulate phase</b></p>	<p><b>Inverse gas chromatography</b></p> <ul style="list-style-type: none"> <li>Preferential adsorption with probe gases</li> </ul> <p><b>Electrokinetics</b></p> <ul style="list-style-type: none"> <li>Zeta potential and charge</li> </ul> <p><b>Surfactant adsorption</b></p> <ul style="list-style-type: none"> <li>Preferential adsorption with probe surfactants</li> </ul> <p><b>References:</b> Lloyd <i>et al.</i> (eds.), ACS Symposium Series <b>391</b>, ACS, Washington D.C. (1989). Aveyard &amp; Haydon, <i>An Introduction to the Principles of Surface Chemistry</i>, Cambridge Univ. Press (1973). Shaw, <i>Introduction to Colloid &amp; Surface Chemistry</i>, Butterworths &amp; Co. Ltd. (1983).</p>

where  $\gamma^{sv}$ ,  $\gamma^{sl}$ ,  $\gamma^{lv}$  are the solid-vapor, solid-liquid, and liquid-vapor interfacial energies, respectively, and  $\theta$  is the contact angle measured through the liquid as illustrated in Fig. 20-66. When the solid-vapor interfacial energy exceeds the solid-liquid energy, the fluid wets the solid with a contact angle less than  $90^\circ$ . In the limit of  $\gamma^{sv} - \gamma^{sl} \geq \gamma^{lv}$ , the contact angle equals  $0^\circ$  and the fluid **spreads** on the solid. The extent of wetting is controlled by the group  $\gamma^{lv} \cos \theta$  which is referred to as **adhesion tension**. Sessile drop studies of contact angle can be performed on powder compacts in the same way as on planar surfaces. Methods involve (1) direct measurement of the contact angle from the tangent to the air-binder interface, (2) solution of the Laplace-Young equation involving the contact angle as a boundary condition, or (3) indirect calculations of the contact angle from measurements of e.g., drop height (Ennis & Litster, *The Science & Engineering of Granulation Processes*, Blackie Academic Ltd., 1997). The compact can either be saturated with the fluid for static measurements, or dynamic measurements may be made through a computer-imaging goniometer [Pan et al., *Dynamic Properties of Interfaces & Association Structure*, American Oil Chem. Soc. Press (1995)].

For granulation processes, the dynamics of wetting are often crucial, requiring that powders be compared on the basis of a short time scale, **dynamic contact angle**. Important factors are the physical nature of the powder surface (particle size, pore size, porosity, environment, roughness, pretreatment). Powders which are formulated for granulation often are composed of a combination of ingredients. The dynamic wetting process is therefore influenced by the rates of ingredient dissolution and surfactant adsorption and desorption kinetics. [Pan et al., loc. cit.].

The second approach to characterize wetting considers the ability of the fluid to penetrate a powder bed. It involves the measurement of the extent and rate of fluid rise by capillary suction into a column of powder, better known as the **Washburn test**. Considering the powder to consist of capillaries of radius  $R$ , the equilibrium height of rise  $h_e$  is determined by equating capillary and gravimetric pressures, or

$$h_e = \frac{2\gamma^{lv} \cos \theta}{\Delta\rho g R} \quad (20-45)$$

where  $\Delta\rho$  is the fluid density with respect to air,  $g$  is gravity, and  $\gamma^{lv} \cos \theta$  is the adhesion tension as before. In addition to the equilibrium height of rise, the dynamics of penetration can be equally important. Ignoring gravity and equating viscous losses with the capillary pressure, the rate ( $dh/dt$ ) and dynamic height of rise  $h$  are given by

$$\frac{dh}{dt} = \frac{R\gamma^{lv} \cos \theta}{4\mu h}, \quad \text{or} \quad h = \sqrt{\left[ \frac{R\gamma^{lv} \cos \theta}{2\mu} \right] t} \quad (20-46)$$

where  $t$  is time and  $\mu$  is binder-fluid viscosity. [Parfitt (ed.), *Dispersion*

of Powders in Liquids, Elsevier Applied Science Publishers Ltd., 10 (1986).] The grouping of terms in brackets involves the material properties which control the dynamics of fluid penetration, namely average pore radius, or **tortuosity**  $R$  (related to particle size and void distribution of the powder), adhesion tension, and binder viscosity.

The contact angle or adhesion tension of a binder solution with respect to a powder can be determined from the slope of the penetration profile. Washburn tests can also be used to investigate the influence of powder preparation on penetration rates. The **Bartell cell** is related to the Washburn test except that adhesion tension is determined by a variable gas pressure which opposes penetration. [Bartell & Osterhof, *Ind. Eng. Chem.*, **19**, 1277 (1927).]

The contact angle of a binder-particle system is not itself a primary thermodynamic quantity, but rather a reflection of individual interfacial energies [Eq. (20-44)] which are a function of the molecular interactions of each phase with respect to one another. An interfacial energy may be broken down into its **dispersion** and **polar** components. These components reflect the chemical character of the interface, with the polar component due to hydrogen bonding and other polar interactions and the dispersion component due to van der Waals interactions. These components may be determined by the wetting tests described here, where a variety of solvents are chosen as the wetting fluids to probe specific molecular interactions as described by Zisman [Contact Angle, Wettability, & Adhesion, *Advances in Chemistry Series*, ACS, **43**, 1 (1964)]. These components of interfacial energy are strongly influenced by trace impurities which often arise in crystallization of the active ingredient, or other forms of processing such as grinding, and they may be modified by judicious selection of **surfactants**. [R. Ayala, Ph.D. Thesis, *Chem. Eng.*, Carnegie Mellon Univ. (1985).] Charges may also exist at interfaces. In the case of solid-fluid interfaces, these may be characterized by **electrokinetic** studies [Shaw, *Introduction to Colloid & Surface Chemistry*, Butterworths & Co. Ltd. (1983)].

The total solid-fluid interfacial energy (i.e., both dispersion and polar components) is also referred to as the **critical solid-surface energy** of the particulate phase. It is equal to the surface tension of a fluid which *just* wets the solid with zero-contact angle. This property of the particle feed may be determined by a third approach to characterize wetting, involving the penetration of particles into a series of fluids of varying surface tension. [R. Ayala, Ph.D. Thesis, *Chem. Eng.*, Carnegie Mellon Univ. (1985).]; Fuerstaneau et al., *Colloids & Surfaces*, **60**, 127 (1991).] The critical surface energy may also be determined from the variation of sediment height with the surface tension of the solvent. [Vargha-Butler, et al., *Colloids & Surfaces*, **24**, 315 (1987).] Distributions in surface energy and its components often exist in practice, and these may be determined by the wetting measurements described here.

**Examples of the Impact of Wetting** Wetting dynamics has a pronounced influence on the initial nuclei distribution formed from fine powder. The influence of powder-contact angle on the average size of nuclei formed in fluid-bed granulation is illustrated in Fig. 20-67 where contact angle of the powder with respect to water was varied by changing the weight ratios of the ingredients of lactose and salicylic acid, which are hydrophilic and hydrophobic, respectively. [Aulton & Banks, *Proceedings of Powder Technology in Pharmacy Conference*, Powder Advisory Centre, Basel, Switzerland (1979).] Aulton et al. [*J. Pharm. Pharmacol.*, **29**, 59P (1977)] also demonstrated the influence of surfactant concentration on shifting nuclei size due to changes in adhesion tension.

The effect of fluid-penetration rate and the extent of penetration on granule-size distribution for drum granulation was shown by Gluba et al. [*Powder Hand. & Proc.*, **2**, 323 (1990).] Increasing penetration rate increased granule size and decreased asymmetry of the granule-size distribution.

**Controlling Wetting** Table 20-38 summarizes typical changes in material & operating variables which are necessary to improve wetting uniformity. Also listed are appropriate routes to achieve these changes in a given variable through changes in either the formulation or in processing. Improved wetting uniformity generally implies a tighter granule-size distribution and improved-product quality due to a better-controlled manufacturing process. Eqs. (20-44) to (20-46), shown previously, provide the basic trends of the effect of material variables on both wetting dynamics and wetting extent.

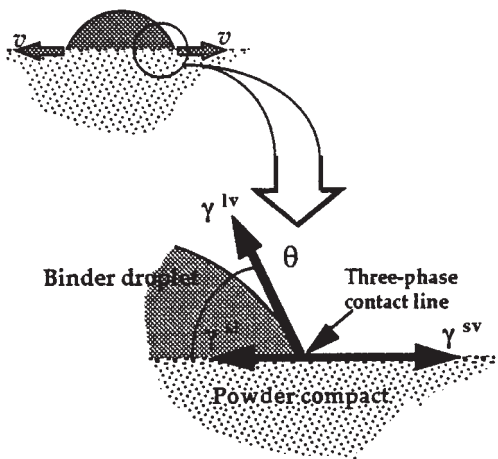
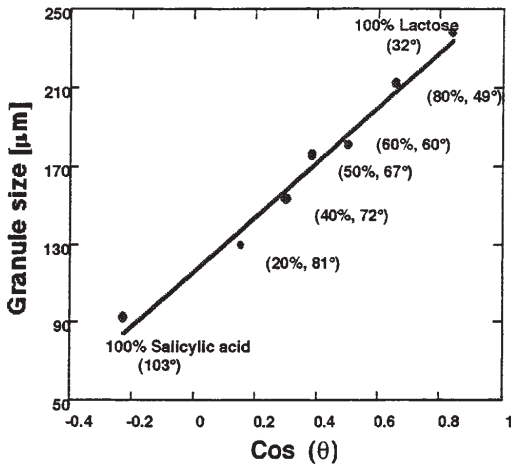


FIG. 20-66 Contact angle on a powder surface, where  $\gamma^{sv}$ ,  $\gamma^{sl}$ ,  $\gamma^{lv}$  are the solid-vapor, solid-liquid, and liquid-vapor interfacial energies, and  $\theta$  is the contact angle measured through the liquid.



**FIG. 20-67** The influence of contact angle on nuclei size formed in fluid-bed granulation of lactose/salicylic acid mixtures. Formulations ranged from hydrophobic (100% salicylic acid) to hydrophilic (100% lactose). Powder contact angle  $\theta$  was determined by gonimetry and percent lactose of each formulation is given in parentheses. [Aulton & Banks, Proceedings of Powder Technology in Pharmacy Conference, Powder Advisory Centre, Basel, Switzerland (1979).]

Since drying occurs simultaneously with wetting, the effect of drying can substantially modify the expected impact of a given process variable and this should not be overlooked. In addition, simultaneously drying often implies that the *dynamics* of wetting are far more important than the *extent*.

Adhesion tension should be maximized to increase the rate and extent of both binder spreading and binder penetration. Maximizing adhesion tension is achieved by minimizing contact angle and maximizing surface tension of the binding solution. These two aspects work against one another as surfactant is added to a binding fluid, and in general, there is an optimum surfactant concentration which must be determined for the formulation (R. Ayala, loc. cit.). In addition, surfactant type influences adsorption and desorption kinetics at the three-phase contact line. An inappropriate choice of surfactant can lead to Marangoni interfacial stresses which slow the dynamics of wetting [Pan et al., loc. cit.]. Additional variables which influence adhesion tension include (1) impurity profile and particle habit/morphology typically controlled in the particle-formation stage such as crystallization, (2) temperature of granulation, and (3) technique of grinding, which is an additional source of impurity as well.

Decreases in binder viscosity enhance the rate of both binder spreading and binder penetration. The prime control over the viscosity of the binding solution is through binder concentration. Therefore, liquid loading and drying conditions strongly influence binder viscosity. For processes *without* simultaneous drying, binder viscosity generally decreases with increasing temperature. For processes *with* simultaneous drying, however, the dominantly observed effect is that lowering temperature lowers binder viscosity and enhances wetting due to decreased rates of drying and increased liquid loading.

Changes in particle-size distribution affect the pore distribution of the powder. Large pores between particles enhance the *rate* of binder penetration, whereas they decrease the final *extent*. In addition, the particle-size distribution affects the ability of the particles to pack within the drop as well as the final degree of saturation [Waldie, *Chem. Engin. Sci.*, **46**, 2781 (1991)].

The drop distribution and spray rate of binder fluid have a major influence on wetting. Generally, finer drops will enhance wetting as well as the distribution of binding fluid. The more important question, however, is how large may the drops be or how high of a spray rate is

**TABLE 20-38 Controlling Wetting In Granulation Processes\***

Typical changes in material or operating variables which improve wetting uniformity	Appropriate routes to alter variable through formulation changes	Appropriate routes to alter variable through process changes
Increase adhesion tension. Maximize surface tension. Minimize contact angle.	Alter surfactant concentration or type to maximize adhesion tension and minimize Marangoni effects. Precoat powder with wettable monolayers, e.g., coatings or steam.	Control impurity levels in particle formation. Alter crystal habit in particle formation. Minimize surface roughness in milling.
Decrease binder viscosity.	Lower binder concentration. Change binder. Decrease any diluents and polymers which act as thickeners.	Raise temperature for processes without simultaneous drying. Lower temperature for processes with simultaneous drying since binder concentration will decrease due to increased liquid loading. This effect generally offsets inverse relationship between viscosity and temperature.
Increase pore size to increase rate of fluid penetration. Decrease pore size to increase extent of fluid penetration.	Modify particle size distribution of feed ingredients.	Alter milling, classification or formation conditions of feed if appropriate to modify particle size distribution.
Improve spray distribution.	Improve atomization by lowering binder fluid viscosity.	Increase wetted area of the bed per unit mass per unit time by increasing the number of spray nozzles, lowering spray rate, increase air pressure or flow rate of two-fluid nozzles.
Increase solids mixing.	Improve powder flowability of feed.	Increase agitation intensity (e.g., impeller speed, fluidization gas velocity, or rotation speed).
Minimize moisture buildup & losses.	Avoid formulations which exhibit adhesive characteristics with respect to process walls.	Maintain spray nozzles to avoid caking and nozzle drip. Avoid spray entrainment in process air streams, and spraying process walls.

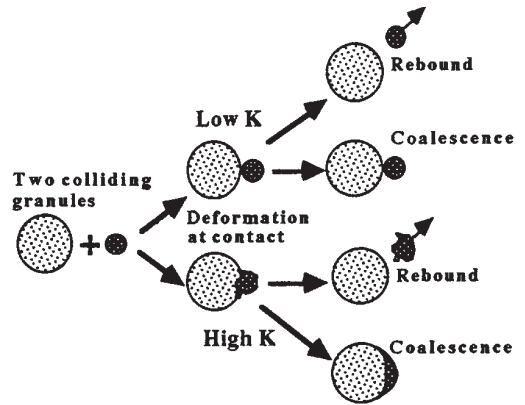
\* Reprinted from *Granulation and Coating Technologies for High-Value-Added Industries*, Ennis and Litster (1996) with permission of E & G Associates. All rights reserved.

possible. The answer depends on the wetting propensity of the feed. If the liquid loading for a given spray rate exceeds the ability of the fluid to penetrate and spread on the powder, maldistribution in binding fluid will develop in the bed. This maldistribution increases with increasing spray rate, increasing drop size, and decreasing spray area (due to, e.g., bringing the nozzle closer to the bed or switching to fewer nozzles). The maldistribution will lead to large granules on the one hand and fine ungranulated powder on the other. In general, the width of the granule-size distribution will increase and generally the average size will decrease. Improved spray distribution can be aided by increases in agitation intensity (e.g., mixer impeller or chopper speed, drum rotation rate, or fluidization gas velocity) and by minimizing moisture losses due to spray entrainment, dripping nozzles, or powder caking on process walls.

**GROWTH AND CONSOLIDATION**

The evolution of the granule-size distribution of a particulate feed in a granulation process is controlled by several mechanisms, as illustrated in Table 20-39. These include the **nucleation** of fine powder to form initial primary granules, the **coalescence** of existing granules and the **layering** of raw material onto previously formed nuclei or granules. Granules may simultaneously be compacted by **consolidation** and reduced in size by **breakage**. There are strong interactions between these rate processes. Dominant mechanisms of growth and consolidation are dictated by the relationship between critical particle properties and operating variables as well as by mixing, size distribution, and the choice of processing.

**Growth Physics and Contact Mechanics** In order for two colliding granules to coalesce rather than break up, the **collisional kinetic energy** must first be dissipated to prevent rebound as illustrated in Fig. 20-68. In addition, the strength of the bond must resist any subsequent breakup forces due to **bed agitation intensity**. The ability of the granules to **deform** during processing increases the bonding or **contact area** thereby dissipating breakup forces and has a large effect on growth rate. From a balance of binding and separating forces and torque acting within the area of granule contact, Ouchiya & Tanaka [*I & EC Proc. Des. & Dev.*, **21**, 29 (1982)] derived a **critical limit of size** above which coalescence becomes impossible, given by



**FIG. 20-68** Mechanisms of granule coalescence for low- and high-deformability systems. Rebound occurs for average granule sizes greater than the critical granule size  $D_c$ .  $K$  = deformability.

$$D_c = (AQ^3\zeta^2K^{3/2}\sigma_T)^{1/[4-(3/2)\eta]} \quad (20-47)$$

$K$  is **deformability**, a proportionality constant relating the maximum compressive force  $Q$  to the deformed-contact area,  $A$  is a constant with units of  $(L^3/F)$  which relates granule volume to impact compression force and  $\sigma_T$  is the **tensile strength** of the granule bond [see Eq. (20-43)]. The parameters  $\zeta$  and  $\eta$  depend on the deformation mechanism acting within the contact area, with their values bounded by the cases of complete plastic or complete elastic deformation. For plastic deformation,  $\zeta = 1$ ,  $\eta = 0$ , and  $K \propto 1/H$  where  $H$  is hardness. For elastic, Hertzian deformation,  $\zeta = 2/3$ ,  $\eta = 2/3$ , and  $K \propto (1/E^*)^{2/3}$  where  $E^*$  is reduced elastic modulus. Granule deformation is generally dominated by **inelastic** behavior of the contacts during collision, with such deformation treated by the area of **inelastic contact mechanics**. [Johnson, *Contact Mechanics*, Cambridge University Press (1985).]

The value  $D_c$  represents a harmonic **average** granule size. Therefore, it is possible for the collision of two large granules to be unsuccessful, their average being beyond this critical size, whereas the collision of a large and small granule leads to successful coalescence.  $D_c$  is a strong function of moisture, as illustrated in Fig. 20-69 by the marked increase in average granule size with moisture which is related to deformability.

Granules are compacted as they collide due to bed agitation intensity. This process of **granule consolidation** expels pore fluid to the granule surface, thereby increasing local liquid saturation in the contact area of colliding granules. This surface fluid (1) increases the tensile strength of the liquid bond  $\sigma_T$ , and (2) increases surface plasticity and deformability  $K$ . Equation (20-47) shows that these factors generally increase the extent of granule growth, particularly for systems of low deformability. In such **low-deformability systems**, growth is largely controlled by the extent of this fluid layer. For **deformable systems**, however, the combined effect of these increases is more complex. Deformability  $K$  is related to both the **yield strength** of the material  $\sigma_y$ , i.e., the ability of the material to resist stresses, and the ability of the surface to be strained without degradation or rupture of the granule, with this maximum allowable **critical deformation strain** denoted by  $(\Delta L/L)_c$ . Figure 20-70 illustrates the stress-strain behavior of cylindrical compact agglomerates during compression as a function of liquid saturation, with **strain** denoted by  $\Delta L/L$ . In general, high deformability  $K$  requires low yield strength  $\sigma_y$  and high critical strain  $(\Delta L/L)_c$ . For this formulation, increasing moisture increases deformability by lowering interparticle frictional resistance which also increases mean granule size (Fig. 20-69).

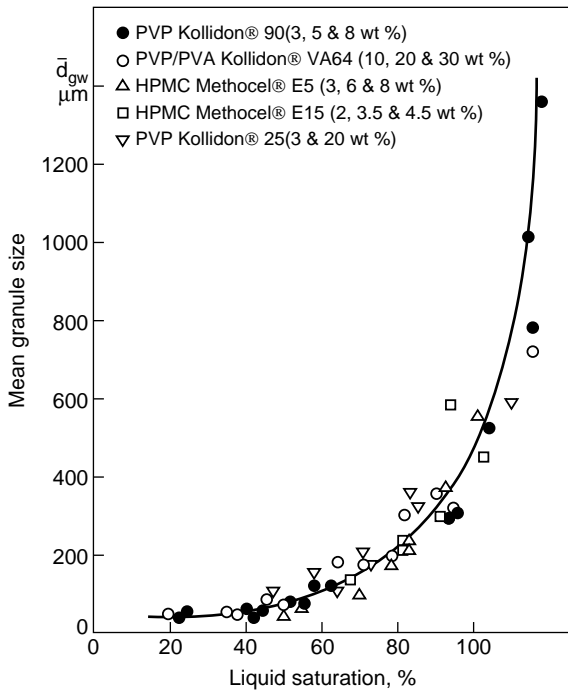
**Effect of Equipment Mechanical Variables** The importance of deformability to the growth process depends on **bed agitation intensity** in comparison to the strength of the formed granules for agitative granulation processes. **Low agitation intensity** processes include fluid-bed, drum, and pan granulators. **High agitation intensity** processes include pin and plow shear-type mixers, and high-shear

**TABLE 20-39 Growth and Breakage Mechanisms in Granulation Processes**

Granule growth		Granule breakage	
<b>Nucleation</b> $j\rho_1 \rightarrow P_j$ 		<b>Shatter</b> $P_j \rightarrow j\rho_1$ 	
<b>Coalescence</b> $P_i + P_j \rightarrow P_{i+j}$ 		<b>Fragmentation</b> $P_j \rightarrow P_j + P_{i-j}$ 	
<b>Layering</b> $P_i + j\rho_1 \rightarrow P_{i+j}$ 		<b>Wear</b> $P_i \rightarrow P_{i-j} + j\rho_1$ 	
<b>Abrasion transfer</b> $P_i + P_j \rightarrow \begin{cases} P_{i+1} + P_{j-1} \\ P_{i-1} + P_{j+1} \end{cases}$ 			
<b>Free fines</b> $P_1$ 		<b>Working unit</b> $P_i$ 	

After Sastry and Fuerstenau in *Agglomeration '77*, Sastry (ed.), AIME, New York, 381 (1977).





**FIG. 20-69** Effect of moisture as a percentage of granule saturation on mean granule diameter, indicating the marked increase in granule deformability with increased moisture. Mean granule diameter is a measure of the critical limit of size  $D_c$ . Granulation of calcium hydrogen phosphate with aqueous binder solutions in a Filder PMAT 25 VG high-shear mixer. [Ritala et al., *Drug Dev. & Ind. Pharm.*, **14**(8), 1041 (1988).]

mixers involving choppers. Bed agitation intensity and compaction pressure are controlled by **mechanical variables** of the process such as fluid-bed excess gas velocity or mixer-impeller speed. Agitation intensity controls the relative **collisional velocities** of granules within the process and therefore growth, breakage, consolidation, and final-product density. Figure 20-71 summarizes typical characteristic velocities, agitation intensities and compaction pressures, and product-relative densities achieved for a variety of size-enlargement processes.

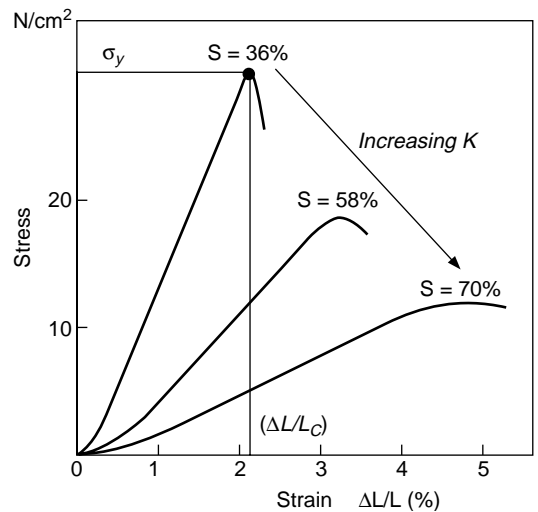
**Low-Agitation Intensity Growth** For low-agitation processes, consolidation of the granules occurs at a much slower rate than growth, and granule deformation can be ignored to a first approximation. The growth process can be modeled by the collision of two rigid granules each coated by a liquid layer of thickness  $h$ . The probability of successful coalescence is governed by a dimensionless **Stokes number**  $St$  given by

$$St = \frac{4\rho u_0 d}{9\mu} \quad (20-48)$$

where  $u_0$  is the relative collisional velocity of the granules,  $\rho$  is granule density,  $d$  is the harmonic average of granule diameter, and  $\mu$  is the solution phase binder viscosity. The Stokes number represents the ratio of initial collisional kinetic energy to the energy dissipated by viscous lubrication forces, and it is one measure of normalized bed agitation energy. (The granule Stokes number is akin to the particle Reynolds number in two-phase systems.) Successful growth by coalescence or layering requires that

$$St < St^* \quad \text{where} \quad St^* = \left(1 + \frac{1}{e_r}\right) \ln(h/h_a) \quad (20-49)$$

where  $St^*$  is a critical Stokes number representing the energy required for rebound. The binder layer thickness  $h$  is related to liquid loading,  $e_r$  is the coefficient of restitution of the granules and  $h_a$  is a

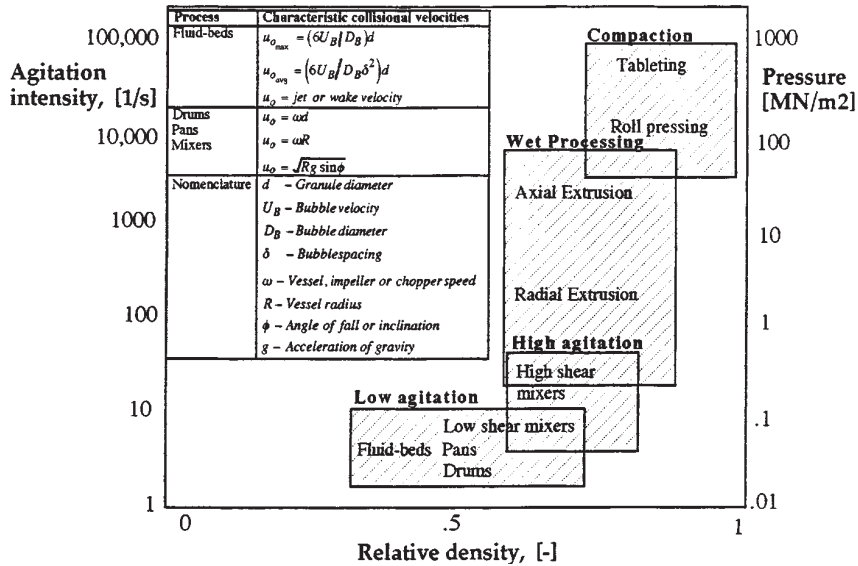


**FIG. 20-70** The influence of moisture as a percentage of sample saturation  $S$  on granule deformability. Here, deformation strain ( $\Delta L/L$ ) is measured as a function of applied stress, with the peak stress and strain denoted by tensile strength  $\sigma_y$  and critical strain ( $\Delta L/L_c$ ) of the material. Dicalcium phosphate with a 15 wt % binding solution of PVP/PVA Kollidon® VA64. [Holm et al., *Powder Tech.*, **43**, 213 (1985).] With kind permission from Elsevier Science SA, Lausanne, Switzerland.

measure of surface roughness or asperities. The critical condition given by Eq. (20-49) controls the growth of low-deformability systems (Fig. 20-68). [Ennis et al., *Powder Tech.*, **65**, 257 (1991).]

Both the **binder solution viscosity**  $\mu$  and the granule density are largely properties of the feed. Binder viscosity is also a function of local temperature, collisional strain rate (for non-Newtonian binders) and binder concentration. It can be controlled as discussed above through judicious selection of binding and surfactant agents and measured by standard rheological techniques. [Bird et al., *Dynamics of Polymeric Liquids*, vol. 1, John Wiley & Sons, Inc. (1977)]. The **collisional velocity** is a function of process design and operating variables, and is related to bed agitation intensity and mixing. Possible choices of  $u_0$  are summarized in Fig. 20-71. Note that  $u_0$  is an interparticle collisional velocity, which is not necessarily the local average granular flow velocity.

Three regimes of granule growth may be identified for low-agitation intensity processes [Ennis et al., *Powder Tech.*, **65**, 257 (1991)]. For small granules or high binder viscosity lying within a **noninertial regime** of granulation, all values of  $St$  will lie below the critical value  $St^*$  and therefore all granule collisions result in successful growth provided binder is present. Growth rate is independent of granule kinetic energy, particle size, and binder viscosity (provided other rate processes are constant). Distribution of binding fluid then controls growth, and this is strongly coupled with the rate process of wetting. (See subsection "Wetting.") As granules grow in size, their collisional momentum increases, leading to localized regions in the process where  $St$  exceeds the critical value  $St^*$ . In this **inertial regime** of granulation, granule size, binder viscosity, and collision velocity determine the proportion of the bed in which granule rebound is possible. Increases in binder viscosity and decreases in agitation intensity increase the extent of granule growth. When the spatial average of  $St$  exceeds  $St^*$ , growth is balanced by granule disruption or breakup, leading to the **coating regime** of granulation. Growth continues by coating of granules by binding fluid alone. Transitions between granulation regimes depends on bed hydrodynamics. As demonstrated by Ennis et al. [*Powder Tech.*, **65**, 257 (1991)], granulation of an initially fine powder may exhibit characteristics of all three granulation regimes as time progresses, since  $St$  increases with increasing granule size. Implications and additional examples regarding the regime analysis are highlighted by Ennis [*Powder Tech.*, **88**, 203 (1996).]



**FIG. 20-71** Classification of agglomeration processes by agitation intensity and compaction pressure. Relative density is with respect to primary particle density and equals  $(1 - \epsilon)$  where  $\epsilon$  is the solid volume fraction. Reprinted from *Granulation and Coating Technologies for High-Value-Added Industries*, Ennis and Litster (1996) with permission of E & G Associates. All rights reserved.

**High-Agitation Intensity Growth** For high-agitation processes involving high-shear mixing granule deformability and plastic deformation can no longer be neglected as they occur at the same rate as granule growth. Typical growth profiles for high-shear mixers are illustrated in Fig. 20-72. Two stages of growth are evident, which reveal the possible effects of binder viscosity and impeller speed. The *initial, non-equilibrium stage of growth* is controlled by granule deformability, and is of most practical significance in manufacturing. Increases in  $St$  due to lower viscosity or higher impeller speed increase the rate of growth as shown in Fig. 20-72, since the system becomes more deformable and easier to knead into larger-granule structures. These effects are contrary to what is predicted from the Stokes analysis based on rigid, elastic granules.

Growth continues until disruptive and growth forces are balanced in the process. This last *equilibrium stage of growth* represents a balance between dissipation and collisional kinetic energy, and so increases in  $St$  decrease the final granule size, as expected from the Stokes analysis. Note that the equilibrium-granule diameter decreases with the inverse square root of the impeller speed, as it should based on  $St = St^*$  with  $u_0 = d \cdot (du/dx) = \omega d$ . The Stokes analysis is used to determine the effect of operating variables and binder viscosity on equilibrium growth, where disruptive and growth forces are balanced.

In the early stages of growth for high-shear mixers, the Stokes analysis in its present form is inapplicable. Freshly formed, uncompacted granules are easily deformed, and as growth proceeds and consolidation of granules occur, they will surface harden and become more resistant to deformation. This increases the importance of the elasticity of the granule assembly. Therefore, in later stages of growth, older granules approach the ideal Stokes model of rigid, elastic collisions. For these reasons, the Stokes approach has had reasonable success in providing an overall framework with which to compare a wide variety of granulating materials [Ennis, *Powder Tech.*, **88**, 203 (1996)]. In addition, the Stokes number controls in part the degree of deformation occurring during a collision since it represents the importance of collision kinetic energy in relation to viscous dissipation, although the exact dependence of deformation on  $St$  is presently unknown.

**Extent of Noninertial Growth** Growth by coalescence in granulation processes may be modeled by the population balance. (See the

Modeling and Simulation subsection.) It is necessary to determine both the mechanism and kernels which describe growth. For fine powders within the noninertial regime of growth, all collisions result in successful coalescence provided binder is present. Coalescence occurs via a random, size-independent kernel which is only a function of liquid loading  $y$ , or

$$\beta(u, v) = k = k^* f(y) \quad (20-50)$$

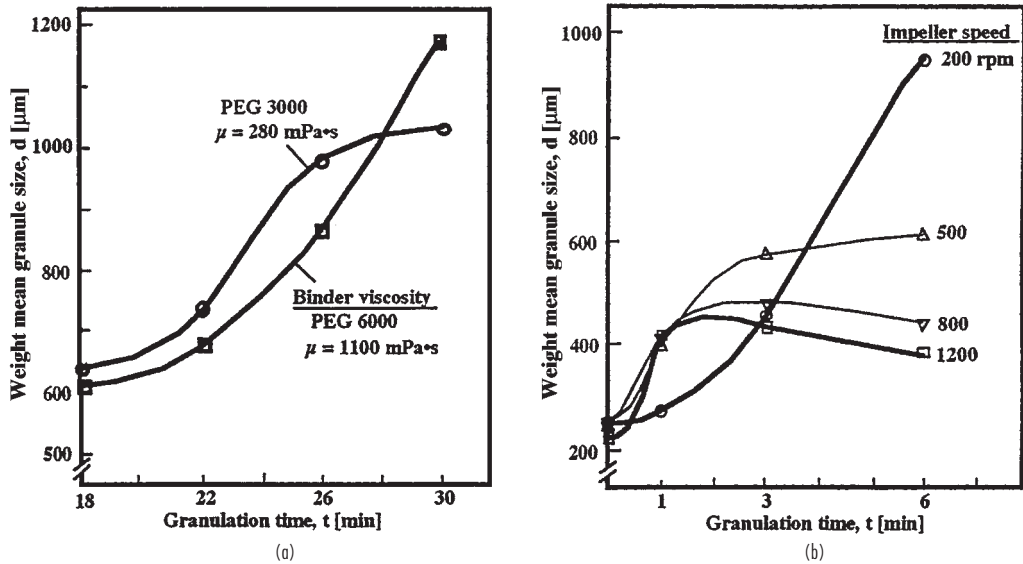
The dependence of growth on liquid loading  $f(y)$  strongly depends on wetting properties. For random growth, it may be shown that the average granule size increases exponentially with time, or  $d = d_0 e^{kt}$ , and that the **maximum extent** of granulation  $(kt)_{\max}$  occurring within the noninertial regime is given by

$$(kt)_{\max} = 6 \ln \left( \frac{St^*}{St_0} \right) \quad (20-51)$$

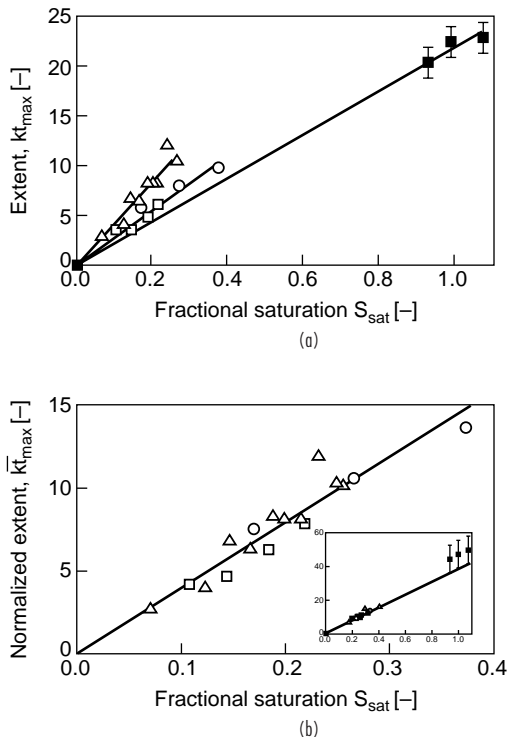
$$(kt)_{\max} \propto \ln \left( \frac{\mu}{\rho u_0 d_0} \right) \quad (20-52)$$

$St_0$  is the Stokes number based on initial nuclei diameter  $d_0$  [Adetayo et al., *Powder Tech.*, **82**, 37 (1995)]. Extent  $(kt)_{\max}$  depends logarithmically on binder viscosity and inversely on agitation velocity. Maximum granule size depends linearly on these variables. Also,  $(kt)_{\max}$  has been observed to depend linearly on liquid loading  $y$ . Therefore, the maximum granule size depends exponentially on liquid loading. Fig. 20-73 illustrates this normalization of extent  $(kt)_{\max}$  for the drum granulation of limestone and fertilizers.

**Determination of  $St^*$**  The extent of growth is controlled by some limit of granule size, either reflected by the critical Stokes number  $St^*$  or by the critical limit of granule size  $D_c$ . There are three possible methods to determine this critical limit. The first involves measuring the critical rotation speed for the survival of a series of liquid-binder drops during drum granulation [Ennis, Ph.D. Thesis (1990)]. A second refined version involves measuring the survival of granules in a couette-fluidized shear device [Tardos & Khan, AICHE Annual Meeting, Miami (1995)]. Both the onset of granule deformation and complete granule rupture are determined from the dependence of granule shape and the number of surviving granules,



**FIG. 20-72** Granule diameter as a function of time for high-shear mixer granulation, illustrating the influence of deformability on growth behavior. (a) 10-liter vertical high-shear melt granulation of lactose with liquid loading of 15 wt % binder and impeller speed of 1400 rpm for two different viscosity grades of polyethylene glycol binders. [Schaefer *et al.*, Drug Dev. & Ind. Pharm., **16**(8), 1249 (1990)]. (b) 10-liter vertical high-shear mixer granulation of dicalcium phosphate with 15 wt % binder solution of PVP/PVA Kollidon® VA64, liquid loading of 16.8 wt % and chopper speed of 1000 rpm for varying impeller speed. [Schaefer *et al.*, Pharm. Ind., **52**(9), 1147 (1990).]



**FIG. 20-73** (a) Maximum extent of noninertial growth  $(kt)_{\text{max}}$  as a function of fractional saturation of the powder feed  $S_{\text{sat}}$  for drum granulation, and (b) maximum extent normalized for differences in  $St_0$ . Feed powders: ammonium sulfate (O); monoammonium phosphate ( $\square$ ); diammonium phosphate ( $\Delta$ ); limestone ( $\blacksquare$ ). [Adetayo *et al.*, Powder Tech., **82**, 37 (1995).] With kind permission from Elsevier Science SA, Lausanne, Switzerland.

respectively, on shear rate. Granule breakdown and deformation are controlled by a generalization of  $St$ , or a yield number  $Y$  given by

$$Y = \frac{\rho u_0^2}{\tau_y} = \frac{\rho (du_0/dx)^2 d^2}{\tau_y} \quad (20-53)$$

Viscosity has been replaced by a generalized form of plastic deformation controlled by a yield stress  $\tau_y$ , which may be determined by compression experiments. Compare with Eq. (20-48). The critical shear rate describing complete granule rupture defines  $St^*$ , whereas the onset of deformation and the beginning of granule breakdown defines an additional critical value  $St^y$ .

The last approach is to measure the deviation in the growth-rate curve from random exponential growth [Adetayo & Ennis, *AICHE J.*, (1997)]. The deviation from random growth indicates a value of  $w^*$ , or the **critical granule diameter** at which noninertial growth ends. This value is related to  $D_c$ . (See the Modeling and Simulation subsection for further discussion.)

**Consolidation** Consolidation of granules determines **granule porosity**, and hence **granule density**. Granules may consolidate over extended times and achieve high densities if there is no simultaneous drying to stop the consolidation process. The extent and rate of consolidation are determined by the balance between the collision energy and the granule resistance to deformation. Decreasing feed-particle size decreases the rate of consolidation due to the high specific surface area and low permeability of fine powders. The effects of binder viscosity and liquid content are complex and interrelated. For low-viscosity binders, consolidation *increases* with liquid content, but for high-viscosity binders consolidation *decreases* with increasing liquid content (see Fig. 20-74). The exact effect of liquid content and binder viscosity is determined by the balance between viscous dissipation and particle frictional losses and is difficult to predict [Iveson *et al.*, *Powder Tech.*, (1996)]. Increasing agitation intensity increases the degree of consolidation by increasing the energy of collision and compaction.

**Controlling Growth and Consolidation** Table 20-40 summarizes typical changes in material & operating variables which maximize granule growth and consolidation. Also listed are appropriate routes to achieve these changes in a given variable through changes in either the formulation or in processing. Growth and consolidation of

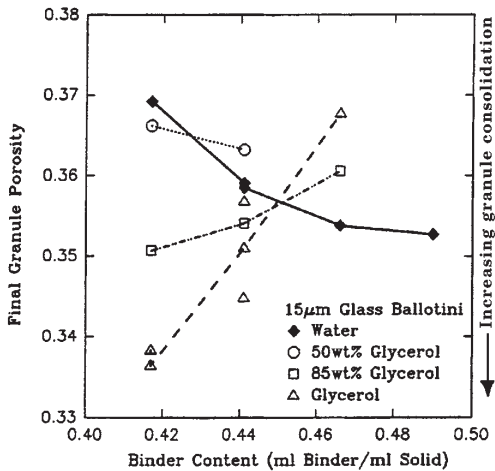


FIG. 20-74 Effect of binder viscosity and liquid content on final granule porosity for the drum granulation of 15 µm glass ballotini. Decreasing granule porosity corresponds to increasing extent of granule consolidation. [Iveson et al., Powder Tech., 88, 15 (1996).] With kind permission from Elsevier Science SA, Lausanne, Switzerland.

granules are strongly influenced by *St*. Increasing *St* increases energy with respect to dissipation during deformation of granules. Therefore, the rate of growth for deformable systems (e.g., deformable formulation or high-shear mixing) and the rate of consolidation of granules generally increases with increasing *St*. *St* may be increased by de-

creasing binder viscosity or increasing agitation intensity. Changes in binder viscosity may be accomplished by formulation changes (e.g., the type or concentration of binder) or by operating temperature changes. In addition, simultaneous drying strongly influences the effective binder concentration and viscosity. The maximum extent of growth increases with decreasing *St* and increased liquid loading, as reflected by Eqs. (20-50) and (20-51). Increasing particle size also increases the rate of consolidation, and this can be modified by upstream milling or crystallization conditions.

**BREAKAGE**

A granule is a nonuniform physical composite possessing certain macroscopic mechanical properties, such as a generally anisotropic yield stress, as well as an inherent flaw distribution. Hard materials may fail in tension (see brittle fracture under size reduction), with the breaking strength being much less than the inherent tensile strength of bonds because of the existence of flaws. [Lawn, *Fracture of Brittle Solids*, 2d ed., Cambridge University Press (1975).] Bulk breakage tests of granule strength measure both the inherent bond strength of granule as well as its flaw distribution. [Bemros & Bridgwater, *Powder Tech.*, 49, 97 (1987).] In addition, the mechanism of granule breakage (Table 20-39) is a strong function of materials properties of the granule itself as well as the type of loading imposed by the test conditions. Ranking of product-breakage resistance by ad hoc tests may be test specific, and in the worst case differ from actual process conditions. Standardized mechanical tests should be employed instead to measure material properties which minimize the effect of flaws and loading conditions under well-defined geometries of internal stress, as described below.

**Fracture Properties** Fracture toughness defines the stress distribution in the body just before fracture and is given by

$$K_{Ic} = Y\sigma_f\sqrt{\pi c} \tag{20-54}$$

TABLE 20-40 Controlling Growth and Consolidation in Granulation Processes\*

Typical changes in material or operating variables which maximize growth and consolidation	Appropriate routes to alter variable through formulation changes	Appropriate routes to alter variable through process changes
Rate of growth (low deformability): Increase rate of nuclei formation  Increase collision frequency  Increase residence time Rate of growth (high deformability): Decrease binder viscosity  Increase agitation intensity  Increase particle density Increase rate of nuclei formation, collision frequency & residence time, as above for low deformability systems.	Improve wetting properties. (See "Wetting" subsection.) Increase binder distribution.  Decrease binder concentration or change binder. Decrease any diluents and polymers which act as thickeners.	Increase spray rate and number of drops.  Increase mixer impeller or drum rotation speed or fluid-bed gas velocity. Increase batch time or lower feed rate.  Decrease operating temperature for systems with simultaneous drying. Otherwise increase temperature. Increase mixer impeller or drum rotation speed or fluid-bed gas velocity.
Extent of growth: Increase binder viscosity  Decrease agitation intensity  Decrease particle density Increase liquid loading  Rate of consolidation: Decrease binder viscosity Increase agitation intensity Increase particle density Increase particle size	Increase binder concentration, change binder, or add diluents and polymers as thickeners.  As above for high deformability systems. Particle size and friction strongly interact with binder viscosity to control consolidation. Feed particle size may be increased and fine tail of distribution removed.	Increase operating temperature for systems with simultaneous drying. Otherwise decrease temperature. Decrease mixer impeller or drum rotation speed or fluid-bed gas velocity.  Extent observed to increase linearly with moisture.  As above for high deformability systems. In addition, increase compaction forces by increasing bed weight, or altering mixer impeller or fluid-bed distributor plate design. Size is controlled in milling and particle formation.

Reprinted from *Granulation and Coating Technologies for High-Value-Added Industries*, Ennis and Litster (1996) with permission of E & G Associates. All rights reserved.

where  $\sigma_f$  is the applied fracture stress,  $c$  is the length of the crack in the body, and  $Y$  is a calibration factor introduced to account for different body geometries. (Lawn, loc. cit.)

The elastic stress cannot exceed the **yield stress** of the material, implying a region of local yielding at the crack tip. Nevertheless, to apply the simple framework of linear elastic fracture mechanics, Irwin [*J. Applied Mechanics*, **24**, 361 (1957)] proposed that this **process zone size**  $r_p$  be treated as an *effective* increase in crack length  $\delta c$ . Fracture toughness is then given by

$$K_c = Y\sigma_f\sqrt{\pi(c + \delta c)} \quad \text{with} \quad \delta c \sim r_p \quad (20-55)$$

The process zone is a measure of the yield stress or plasticity of the material in comparison to its brittleness. Yielding within the process zone may take place either plastically or by diffuse microcracking, depending on the brittleness of the material. For plastic yielding,  $r_p$  is also referred to as the **plastic zone size**.

The **critical strain energy release rate**  $G_c$  is the energy equivalent to fracture toughness, first proposed by Griffith [*Phil. Trans. Royal Soc.*, **A221**, 163 (1920)]. They are related by

$$G_c = K_c^2/E \quad (20-56)$$

**Fracture Measurements** In order to ascertain fracture properties in any reproducible fashion, very specific test geometry must be used since it is necessary to know the stress distribution at predefined, induced cracks of known length. Three traditional methods are (1) the **three-point bend test**, (2) **indentation fracture testing**, and (3) **Hertzian contact compression** between two spheres of the material (See fracture under size reduction). In the case of the three-point bend test, toughness is determined from the variance of fracture stress on induced crack length, as given by Eq. (20-55) where  $\delta c$  is initially taken as zero and determined in addition to toughness. (Ennis & Sunshine, *Tribology International*, **26**, 319 (1993).) In the case of indentation fracture, one determines **hardness**  $H$  from the area of the residual plastic impression and fracture toughness from the lengths of cracks propagating from the indent as a function of indentation load  $F$  [Johansson & Ennis, *Proceedings of the First International Particle Technology Forum*, vol. 2, AICHe, Denver, 178 (1994).] Hardness is a measure of the yield strength of the material. Toughness and hardness in the case of indentation are given by

$$K_c = \beta\sqrt{\frac{E}{H}}\frac{F}{c^{3/2}} \quad \text{and} \quad H \sim \frac{F}{A} \quad (20-57)$$

Table 20-41 compares typical fracture properties of agglomerated materials. Fracture toughness  $K_c$  is seen to range from 0.01 to 0.06 MPa·m<sup>1/2</sup>, less than that typical for polymers and ceramics, presumably due to the high agglomerate voidage. Critical strain energy release rates  $G_c$  from 1 to 200 J/m<sup>2</sup>, typical for ceramics but less than that for polymers. Process zone sizes  $\delta c$  are seen to be large and of the order of 0.1–1 mm, values typical for polymers. Ceramics on the other hand typically have process zone sizes less than 1 μm. Critical displacements required for fracture may be estimated by the ratio  $G_c/E$ , which is an indication of the **brittleness** of the material. This value was of the order of 10<sup>-7</sup>–10<sup>-8</sup> mm for polymer-glass agglomerates, similar to polymers, and of the order of 10<sup>-9</sup> mm for herbicide bars, similar to ceram-

ics. In summary, granulated materials behave similar to brittle ceramics which have small critical displacements and yield strains but also similar to ductile polymers which have large process or plastic zone sizes.

**Mechanisms of Breakage** The process zone plays a large role in determining the mechanism of granule breakage (Table 20-39). [Ennis & Sunshine, loc. cit.] Agglomerates with process zones small in comparison to granule-size break by a brittle-fracture mechanism into smaller fragments, or **fragmentation** or **fracture**. On the other hand for agglomerates with process zones of the order of their size, there is insufficient volume of agglomerate to concentrate enough elastic energy to propagate gross fracture during a collision. The mechanism of breakage for these materials is one of **wear**, **erosion**, or **attrition** brought about by diffuse microcracking. In the limit of very weak bonds, agglomerates may also **shatter** into small fragments or primary particles.

Each mechanism of breakage implies a different functional dependence of breakage rate on material properties. For the case of **abrasive wear** of ceramics due to surface scratching by loaded indentors, Evans & Wilshaw [*Acta Metallurgica*, **24**, 939 (1976)] determined a volumetric wear rate  $V$  of

$$V = \frac{d_i^{1/2}}{A^{1/4}K_c^{3/4}H^{1/2}} P^{5/4}l \quad (20-58)$$

where  $d_i$  is indenter diameter,  $P$  is applied load,  $l$  is wear displacement of the indenter and  $A$  is apparent area of contact of the indenter with the surface. Therefore, wear rate depends inversely on fracture toughness. For the case of fragmentation, Yuregir et al. [*Chem. Eng. Sci.*, **42**, 843 (1987)] have shown that the fragmentation rate of organic and inorganic crystals is given by

$$V \sim \frac{H}{K_c^2} \rho u^2 a \quad (20-59)$$

where  $a$  is crystal length,  $\rho$  is crystal density, and  $u$  is impact velocity. Note that hardness plays an opposite role for fragmentation than for wear, since it acts to concentrate stress for fracture. Fragmentation rate is a stronger function of toughness as well.

Drawing on analogies with this work, the breakage rates by wear  $B_w$  and fragmentation  $B_f$  for fluid-bed processing should be of the forms:

$$B_w = \frac{d_0^{1/2}}{K_c^{3/4}H^{1/2}} h_b^{5/4}(U - U_{mf}) \quad (20-60)$$

$$B_f \sim \frac{H}{K_c^2} \rho(U - U_{mf})^2 a \quad (20-61)$$

where  $d$  is granule diameter,  $d_0$  is primary particle diameter,  $(U - U_{mf})$  is fluid-bed excess gas velocity, and  $h_b$  is bed height. Fig. 20-75 illustrates the dependence of erosion rate on material properties for granules undergoing a wear mechanism of breakage, as governed by Eq. (20-60).

**Controlling Breakage** Table 20-42 summarizes typical changes in material & operating variables which are necessary to minimize breakage. Also listed are appropriate routes to achieve these changes in a given variable through changes in either the formulation or in processing. Both fracture toughness and hardness are strongly influenced by the compatibility of the binder with the primary particles, as well as the elastic/plastic properties of the binder. In addition, hardness and toughness increase with decreasing voidage and are influenced by

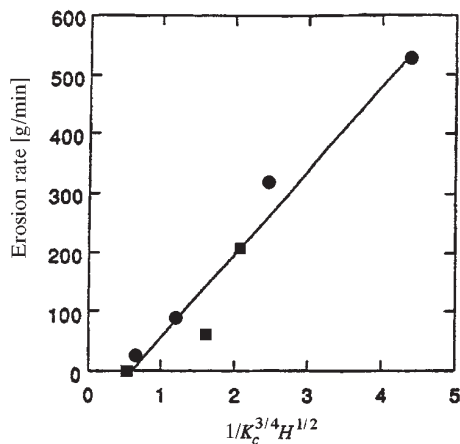
**TABLE 20-41 Fracture Properties of Agglomerated Materials\***

Material	$K_c$ (MPa·m <sup>1/2</sup> )	$G_c$ (J/m <sup>2</sup> )	$\delta c$ (μm)	$E$ (MPa)	$G_c/E$ (m)
Bladex 60™†	0.070	3.0	340	567	5.29e-09
Bladex 90™†	0.014	0.96	82.7	191	5.00e-09
Glean™†	0.035	2.9	787	261	1.10e-08
Glean Aged™†	0.045	3.2	3510	465	6.98e-09
CMC-Na (M)‡	0.157	117.0	641	266	4.39e-07
Klucel CF‡	0.106	59.6	703	441	1.35e-07
PVP 360K‡	0.585	199.0	1450	1201	1.66e-07
CMC 2% 1kN‡	0.097	16.8	1360	410	4.10e-08
CMC 2% 5kN‡	0.087	21.1	1260	399	5.28e-08
CMC 5% 1kN‡	0.068	15.9	231	317	5.02e-08

\*Ennis & Sunshine, *Tribology International*, **26**, 319 (1993)

†DuPont corn herbicides

‡50 μm glass beads with polymer binder



**FIG. 20-75** Fluid-bed erosion or wear rate as a function of granule material properties.  $K_c$  is fracture toughness and  $H$  is hardness as measured by three-point bend tests. [Ennis & Sunshine, *Tribology International*, **26**, 319 (1993).]

previous consolidation of the granules (see subsection of Growth and Consolidation). While the direct effect of increasing gas velocity and bed height is to increase breakage of dried granules, increases in these variables may also act to increase consolidation of wet granules, lower voidage, and therefore lower the final-breakage rate. Granule structure also influences breakage rate, e.g., a layered structure is less prone to breakage than a raspberry-shaped agglomerate. However, it

may be impossible to compensate for extremely low toughness by changes in structure. Measurements of fracture properties help define expected breakage rates for a product and aid product development of formulations.

## POWDER MECHANICS & POWDER COMPACTION

The ability of powders to freely flow, easily compact, and maintain strength during stress unloading determines the success of compaction techniques of agglomeration. These attributes are strongly influenced by mechanical properties of the feed. [Brown & Richards, *Principles of Powder Mechanics*, Pergamon Press (1970).] The flow properties summarized below are also relevant to the design of bulk powder handling systems such as feeders and hoppers [see Section 21 & Carson & Marinelli, *Chemical Eng.*, April (1994)].

**Powder Mechanics Measurements** As opposed to fluids, powders may withstand applied shear stress similar to a bulk solid due to **interparticle friction**. As the applied shear stress is increased, the powder will reach a maximum sustainable shear stress  $\tau$ , at which point it yields or flows. This limit of shear stress  $\tau$  increases with increasing applied normal load  $\sigma$ , with the functional relationship being referred to as a **yield locus**. A well-known example is the Mohr-Coulomb yield locus, or

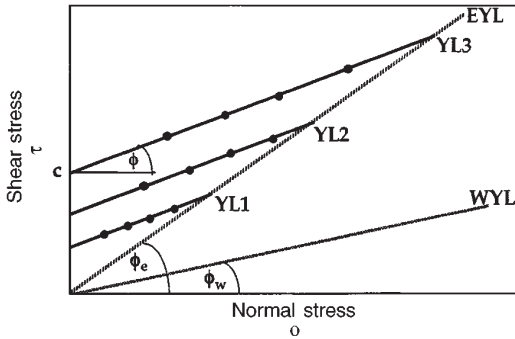
$$\tau = c + \mu\sigma = c + \sigma \tan \phi \quad (20-62)$$

Here,  $\mu$  is the coefficient of internal friction,  $\phi$  is the internal angle of friction, and  $c$  is the shear strength of the powder in the absence of any applied normal load. The yield locus of a powder may be determined from a **shear cell**, which typically consists of a cell composed of an upper and lower ring. The normal load is applied to the powder vertically while shear stresses are measured while the lower half of the cell is either translated or rotated [Carson & Marinelli, loc. cit.]. Over-

**TABLE 20-42 Controlling Breakage in Granulation Processes\***

Typical changes in material or operating variables which minimize breakage	Appropriate routes to alter variable through formulation changes	Appropriate routes to alter variable through process changes
Increase fracture toughness Maximize overall bond strength Minimize agglomerate voidage	Increase binder concentration or change binder. Bond strength strongly influenced by formulation and compatibility of binder with primary particles.	Decrease binder viscosity to increase agglomerate consolidation by altering process temperatures (usually decrease for systems with simultaneous drying). Increase bed-agitation intensity (e.g., increase impeller speed, increase bed height) to increase agglomerate consolidation. Increase granulation-residence time to increase agglomerate consolidation, but minimize drying time.
Increase hardness to reduce wear Minimize binder plasticity Minimize agglomerate voidage	Increase binder concentration or change binder. Binder plasticity strongly influenced by binder type.	See above effects which decrease agglomerate voidage.
Decrease hardness to reduce fragmentation Maximize binder plasticity Maximize agglomerate voidage	Change binder. Binder plasticity strongly influenced by binder type.  Apply coating to alter surface hardness.	Reverse the above effects to increase agglomerate voidage.
Decrease load to reduce wear	Lower-formulation density.	Decrease bed-agitation and compaction forces (e.g., mixer impeller speed, fluid-bed height, bed weight, fluid-bed excess gas velocity, drum rotation speed).
Decrease contact displacement to reduce wear		Decrease contacting by lowering mixing and collision frequency (e.g., mixer impeller speed, fluid-bed excess gas velocity, drum rotation speed).
Decrease impact velocity to reduce fragmentation	Lower-formulation density.	Decrease bed-agitation intensity (e.g., mixer impeller speed, fluid-bed excess gas velocity, drum rotation speed). Also strongly influenced by distributor-plate design in fluid-beds, or impeller and chopper design in mixers.

\* Reprinted from *Granulation and Coating Technologies for High-Value-Added Industries*, Ennis and Litster (1996) with permission of E & G Associates. All rights reserved.



**FIG. 20-76** The yield loci of a powder, reflecting the increased shear stress required for flow as a function of applied normal load. YL1 through YL3 represent yield loci for increasing previous compaction stress. EYL and WYL are the effective and wall yield loci, respectively.

compacted powders dilate when sheared, and the ability of powders to change volume with shear results in the powder's shear strength  $\tau$  being a strong function of previous compaction. There are therefore a series of *yield loci* (YL) as illustrated in Fig. 20-76 for increasing previous **compaction stress**. The individual yield loci terminate at a critical state of stress, which when joined together form the *effective yield locus* (EYL) which typically passes through the stress-strain origin, or

$$\tau = \mu_e \sigma = \sigma \tan \phi_e \quad (20-63)$$

This line represents the critical shear stress that a powder can withstand which has not been over or underconsolidated, i.e., the stress typically experienced by a powder which is in a constant state of shear. When sheared powders also experience friction along a wall, this relationship is described by the wall yield locus, or

$$\tau = \mu_w \sigma = \sigma \tan \phi_w \quad (20-64)$$

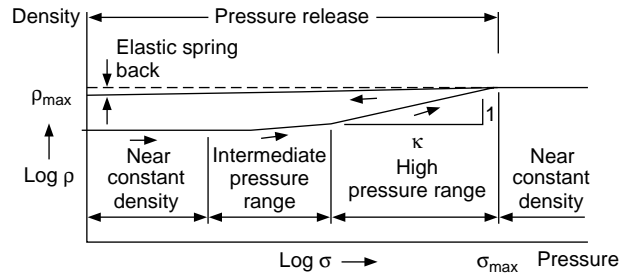
The angles  $\phi_e$  and  $\phi_w$  are the **effective angle** and **wall angle of friction**, respectively.

A powder's strength increases significantly with increasing previous compaction. The relationship between the unconfined yield stress  $f_c$ , or a powder's strength, and compaction pressure  $\sigma_c$ , is described by the powder's **flow function FF**. The flow function is the paramount characterization of powder strength and flow properties, and it is calculated from the yield loci determined from shear cell measurements. [Jenike, *Storage and Flow of Solids*, Univ. of Utah, *Eng. Exp. Station Bulletin*, no. 123, November (1964). See also Sec. 21 on storage bins, silos, and hoppers.]

**Compact Density** Compact strength depends on the number and strength of interparticle bonds (Eq. 20-43) created during consolidation, and both generally increase with increasing compact density. Compact density is in turn a function of the maximum pressure achieved during compaction. The **mechanisms of compaction** have been discussed by Cooper & Eaton [J. *Am. Ceramic Soc.*, **45**, 97 (1962)] in terms of two largely independent, probabilistic processes. The first is the filling of large holes with particles from the original size distribution. The second is the filling of holes smaller than the original particles by **plastic flow** or **fragmentation**. Additional, possible mechanisms include the low pressure elimination of arches and cavities created during die filling due to wall effects, and the final high-pressure consolidation of the particle phase itself. As these mechanisms manifest themselves over different pressure ranges, four stages of compression are generally observed in the compressibility diagram when density is measured over a wide pressure range (Fig. 20-77). The slope of the intermediate- and high-pressure regions is defined as  $1/\kappa$  where  $\kappa$  is the **compressibility** of the powder. The density at an arbitrary pressure  $\sigma$  is given by a compaction equation of the form

$$\rho = \rho_0 \left[ \frac{\sigma}{\sigma_0} \right]^{1/\kappa} \quad (20-65)$$

where  $\rho_0$  is the density at an arbitrary pressure or stress  $\sigma_0$ . For a complete review of compaction equations, see Kawakita & Lüdde [Powder



**FIG. 20-77** Compressibility diagram of a typical powder illustrating four stages of compaction.

*Tech.*, **4**, 61 (1970/71)] and Hersey et al. [*Proceedings of First International Conf. of Compaction & Consolidation of Particulate Matter*, Brighton, 165 (1972)].

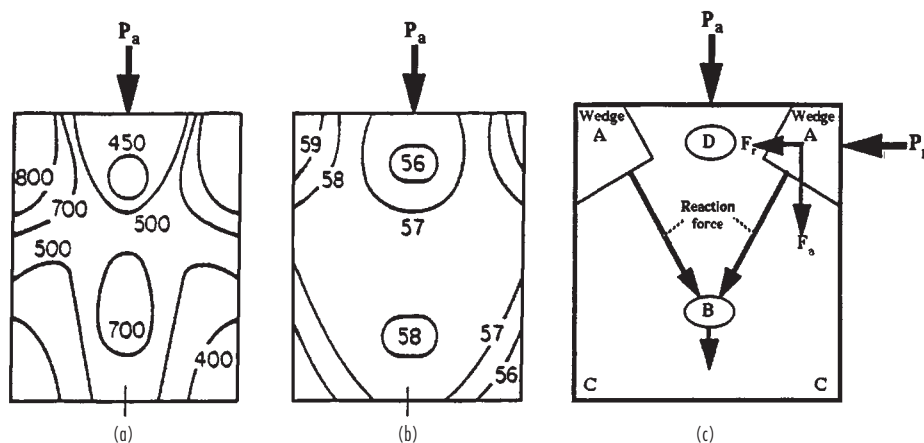
**Transmission of Forces** As pressure is applied to a powder in a die or roll press, various zones in the compact are subjected to differing intensities of pressure and shear. Compaction stress decreases with axial distance from the applied pressure [Strijbos *et al.*, *Powder Tech.*, **18**, 187 & 209 (1977)] due to **frictional properties** of the powder and die wall. For example, the axial pressure experienced within a cylindrical die with an applied axial load  $\sigma_0$  may be estimated to a first approximation by

$$\sigma_z = \sigma_0 e^{-(4\mu_w \lambda \phi_e / D)z} \quad (20-66)$$

where  $D$  is die diameter,  $z$  is axial distance from the applied load,  $\lambda$  is the ratio of radial to axial pressure given by  $\lambda \approx K_0 = (1 - \sin \phi_e) / (1 + \sin \phi_e)$ , and  $\mu_w$  and  $\phi_e$  are the wall friction coefficient and effective angle of friction defined above (Eqs. 20-63 and 64). Typical pressure and density distributions for uniaxial compaction are shown in Fig. 20-78. High- and low-density annuli are apparent along the die corners, with a dense axial core in the lower part of the compact and a low-density core just below the moving upper punch. These density variations are due to the formation of a dense conical wedge acting along the top punch (A) with a resultant force directed toward the center of the compact (B). The wedge is densified to the greatest extent by the shearing forces developed by the axial motion of the upper punch along the stationary wall, whereas the corners along the bottom stationary die are densified the least (C). The lower axial core (B) is densified by the wedge, whereas the upper low-density region (D) is shielded by the wedge from the full axial compressive force. These variations in compact density lead to local variations in strength as well as differential zones of expansion upon compact unloading, which in turn can lead to flaws in the compact.

**Compact Strength** Both **particle size** and **bond strength** control final compact strength (Eq. 20-43). Although particle surface energy and elastic deformation play a role, **plastic deformation** at particle contacts is likely the major mechanism contributing to large **permanent** bond formation and successful compaction in practice. Figure 20-79 illustrates the strength of mineral compacts of varying hardness and size cut. To obtain significant strength, Benbow [*Enlargement & Compaction of Particulate Solids*, Stanley-Wood (ed.), Butterworths, 169 (1983)] found that a **critical yield pressure** must be exceeded which was independent of size but increased linearly with particle hardness. Strength also increases linearly with compaction pressure, with the slope inversely related to particle size. Similar results were obtained by others for ferrous powder, sucrose, sodium chloride, and coal [Hardman & Lilly, *Proc. Royal Soc. A.*, **333**, 183 (1973)]. Particle hardness and elasticity may be characterized directly by nanoindentation [Johnson & Ennis, *Proceedings of the First International Particle Technology Forum*, vol. 2, AIChE, Denver, 178 (1994)].

The development of flaws and the loss of interparticle bonding during decompression substantially weaken compacts (see breakage subsection). **Delamination** during load removal involves the fracture of the compact into layers, and it is induced by strain recovery in excess of the elastic limit of the material which cannot be accommodated by



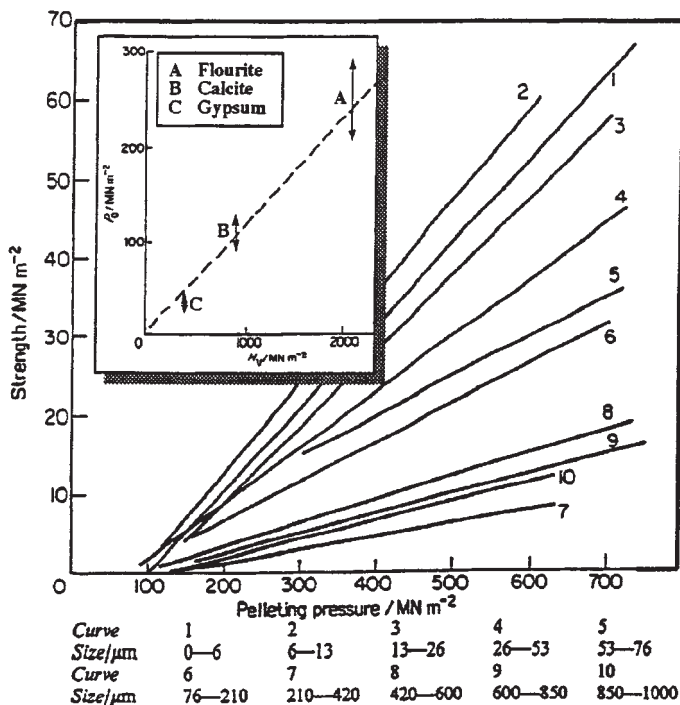
**FIG. 20-78** Reaction in compacts of magnesium carbonate when pressed ( $P_a = 671 \text{ kg/cm}^2$ ). (a) Stress contour levels in kilograms per square centimeter. (b) Density contours in percent solids. (c) Reaction force developed at wedge responsible for stress and density patterns. [Train, Trans. Inst. Chem. Eng. (London), **35**, 258 (1957).]

plastic flow. Delamination also occurs during compact ejection, where the part of the compact which is clear of the die elastically recovers in the radial direction while the lower part remains confined. This differential strain sets up shear stresses causing fracture along the top of the compact referred to as **capping**.

**Hiestand Tableting Indices** Likelihood of failure during decompression depends on the ability of the material to relieve elastic stress by plastic deformation without undergoing brittle fracture, and this is time dependent. Those which relieve stress rapidly are less

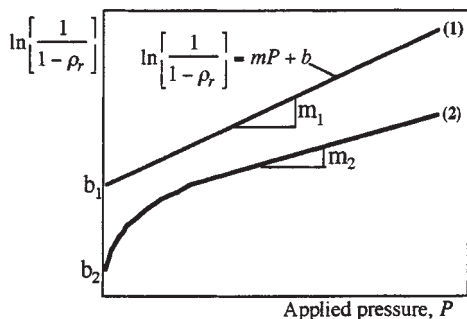
likely to cap or delaminate. Hiestand & Smith [*Powder Tech.*, **38**, 145 (1984)] developed three pharmaceutical **tableting indices**, which are applicable for general characterization of powder compactability. The **strain index** (SI) is a measure of the elastic recovery following plastic deformation, the **bonding index** (BI) is a measure of plastic deformation at contacts and bond survival, and the **brittle fracture index** (BFI) is a measure of compact brittleness.

**Compaction Cycles** Insight into compaction performance is gained from direct analysis of pressure/density data over the cycle of



**FIG. 20-79** Effect of pelleting pressure on axial crushing strength of compacted calcite particles of different sizes demonstrating existence of a critical yield pressure. Inset shows the effect of hardness on critical yield pressure. [Benbow, Enlargement and Compaction of Particulate Solids, Stanley-Wood (ed.), Butterworths, 169 (1983).]





**FIG. 20-80** Heckel profiles of the unloaded relative compact density for (1) a material densifying by pure plastic deformation, and (2) a material densifying with contributions from brittle fragmentation and particle rearrangement.

axial compact compression and decompression. Figure 20-80 illustrates typical **Heckel profiles** for plastic and brittle deforming materials which are determined from density measurements of *unloading* compacts. The slope of the curves gives an indication of the yield pressure of the particles. The contribution of fragmentation and rearrangement to densification is indicated by the low-pressure deviation from linearity. In addition, elastic recovery contributes to the degree of hysteresis which occurs in the *at-pressure* density curve during compression followed by decompression. [Doelker, *Powder Technology & Pharmaceutical Processes*, Chulia et al. (eds.), Elsevier, 403 (1994).]

**Powder Feeding** Bulk density control of feed materials and reproducible powder feeding are crucial to the smooth operation of

compaction techniques. In the case of pharmaceutical tableting, reproducible tablet weights with variations of less than 2 percent are required. Feeding problems are most acute for direct powder-filling of compression devices, as opposed to granular feeds. **Flowability data** developed from shear cell measurements are invaluable in designing machine hoppers for device filling. In addition, complex-ure feeding systems have been developed to aid filling and ensure uniform bulk density. Lubricants or glidants such as fumed silica and talc are also added in small amounts to improve flow properties. These additives act to modify coefficients of friction of the particulate feed.

**Controlling Powder Compaction** Compaction properties of powders are generally improved by altering flow properties. In particular, stress transmission improves with either low wall-friction angle or raising the internal angle of friction of the powder. **Internal lubricants** may be mixed with the feed material to be compacted. They may aid stress transmission by reducing the wall angle of friction angle of the material, but may also weaken bonding properties and the unconfined yield stress of the powder. **External lubricants** are applied to the die surface. They reduce sticking to the die and aid stress transmission by reducing the wall angle of friction of the material.

**Binders** improve the strength of compacts through increased plastic deformation or chemical bonding. They may be classified as **matrix type**, **film type**, and **chemical**. Komarek [*Chem. Eng.*, 74(25), 154 (1967)] provides a classification of binders and lubricants used in the tableting of various materials.

Particle properties such as size, shape, elastic/plastic properties, and surface properties are equally important. Their direct effect, however, is difficult to ascertain without thorough particle characterization. Generally, friction coefficients decrease with decreasing particle hardness. Increasing particle size and decreasing the spread of the size distribution lowers powder friction, thereby aiding stress transmission. However, increasing particle size may also lower compact strength, as described by Eq. (20-43).

## SIZE ENLARGEMENT EQUIPMENT AND PRACTICE

**GENERAL REFERENCES:** Ball et al., *Agglomeration of Iron Ores*, Heinemann, London, 1973. Capes, *Particle Size Enlargement*, Elsevier, New York, 1980. Ennis & Litster, *The Science & Engineering of Granulation Processes*, Blackie Academic Ltd., 1997. Knepper (ed.) *Agglomeration*, Interscience, New York, 1962. Kristensen, *Acta Pharm. Suec.*, 25, 187, 1988. Pietsch, *Size Enlargement by Agglomeration*, John Wiley & Sons Ltd., Chichester, 1992. Pietsch, *Roll Pressing*, Heyden, London, 1976. Sastry (ed.), *Agglomeration 77*, AIME, New York, 1977. Sherrington & Oliver, *Granulation*, Heyden, London, 1981. Stanley-Wood, *Enlargement and Compaction of Particulate Solids*, Butterworth & Co. Ltd., 1983.

Particle size enlargement equipment can be classified into several groups, with advantages, disadvantages, and applications summarized in Table 20-36. Comparisons of bed-agitation intensity, compaction pressures, and product bulk density for selected agglomeration processes are highlighted above in Fig. 20-71.

Particle size terminology is industry specific. In the following discussion, particle size enlargement in tumbling, mixer and fluidized-bed granulators is referred to as **granulation**. Granulation includes **pelletization** or **balling** as used in the iron-ore industry, but does not include the breakdown of compacts as used in some tableting industries. The term pelleting or pelletization will be used for extrusion processes only.

### TUMBLING GRANULATORS

In **tumbling granulators**, particles are set in motion by the tumbling action caused by the balance between gravity and centrifugal forces. The most common types of tumbling granulators are **disc** and **drum** granulators. Their use is widespread, including the iron-ore industry (where the process is sometimes called **balling** or **wet pelletization**), fertilizer manufacture, agricultural chemicals and pharmaceuticals.

Tumbling granulators generally produce granules in the size range 1 to 20 mm and are not suitable for making granules smaller than 1

mm. Granule density generally falls between that of fluidized-bed and mixer granulators (Fig. 20-71), and it is difficult to produce highly porous agglomerates in tumbling granulators. Tumbling equipment is also suitable for coating large particles, but it is difficult to coat small particles, as growth by coalescence of the seed particles is hard to control.

Drum and disc granulators generally operate in **continuous feed** mode. A key advantage to these systems is the ability to run at large scale. Drums with diameters up to four meters and throughputs up to 100 ton/hr are widely used in the mineral industry.

**Disc Granulators** Figure 20-81 shows the elements of a **disc granulator**. It is also referred to as a **pelletizer** in the iron-ore industry or a **pan granulator** in the agricultural chemical industry. The equipment consists of a rotating, tilted disc or pan with a rim. Solids and wetting agents are continuously added to the disc. A coating of the feed material builds up on the disc and the thickness of this layer is controlled by scrapers or a plow, which may oscillate mechanically. The surface of the pan may also be lined with expanded metal or an abrasive coating to promote proper lifting and cascading of the particulate bed, although this is generally unnecessary for fine materials. Solids are typically fed by either volumetric or gravimetric feeders. Gravimetric feeding generally improves granulation performance due to smaller fluctuations in feed rates which act to disrupt rolling action in the pan. Wetting fluids which promote growth are generally applied by a series of single-fluid spray nozzles distributed across the face of the bed. Solids feed and spray nozzle locations have a pronounced effect on granulation performance and granule structure.

Variations of the simple pan shape include (1) an outer reroll ring which allows granules to be simultaneously coated or densified without further growth, (2) multisteped sidewalls, and (3) a pan in the form of a truncated cone (Capes, *Particle Size Enlargement*, Elsevier, 1980).

The required disc-rotation speed is given in terms of the **critical speed**, i.e., the speed at which a single particle is held stationary on

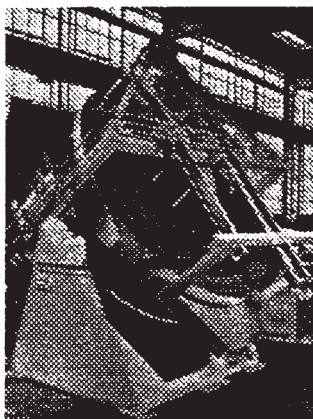
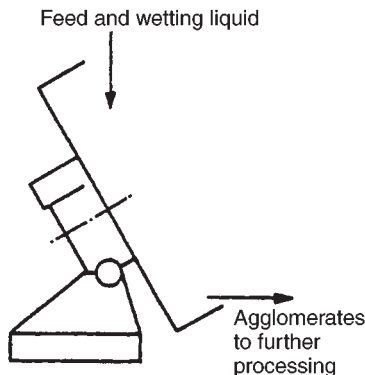


FIG. 20-81 A typical disc granulator (*Capes, Particle Size Enlargement, Elsevier, 1980*).



the rim of the disc due to centripetal forces. The critical speed  $N_c$  is given by:

$$N_c = \sqrt{\frac{g \sin \phi}{2\pi^2 D}} \quad (20-67)$$

where  $g$  is the gravitational acceleration,  $\phi$  is the angle of the disc to the horizontal, and  $D$  is the disc diameter. The typical operating range for discs is 50 to 75 percent of critical speed, with angles  $\phi$  of 45–55°. This range ensures a good tumbling action. If the speed is too low, sliding will occur. If the speed is too high, particles will be thrown off the disc or openings develop in the bed, allowing spray blowthrough and uneven buildup on the disc bottom. Proper speed is influenced by flow properties of the feed materials in addition to granulation performance.

Discs range in size from laboratory models 30 cm in diameter up to production units of 10 meters in diameter with throughputs of 100 ton/hr. Figure 20-82 shows throughput capacities for discs of varying diameter for different applications and formulation feed densities. When scaling up from laboratory or pilot tests it is usual to keep the

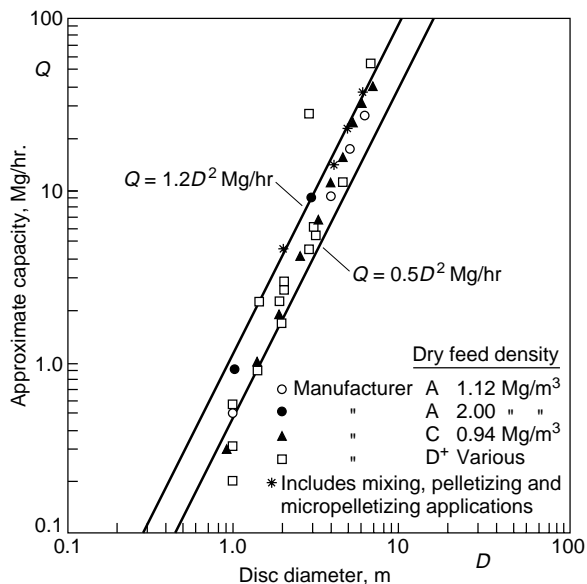


FIG. 20-82 Capacity of inclined disc granulators of varying diameter and formulation feed densities. (*Capes, Particle Size Enlargement, Elsevier, 1980*.)

same disc angle and fraction of critical speed. Power consumption and throughput are approximately proportional to the square of disc diameter, and disc height is typically 10–20 percent of diameter. It should be emphasized that these relationships are best used as a guide and in combination with actual experimental data on the system in question in order to indicate the approximate effect of scale-up.

A key feature of disc operation is the inherent **size classification** (Fig. 20-83). Product overflows from the **eye** of the tumbling granules where the large granules are segregated. The overflow size distribution is narrow compared to drum granulators, and discs typically operate with little or no pellet recycle. Due to this segregation, positioning of the feed and spray nozzles is key in controlling the balance of granulation-rate processes.

Total holdup and granule residence time distribution vary with changes to operating parameters which affect granule motion on the disc. Total holdup (mean residence time) increases with decreasing pan angle, increasing speed and increasing moisture content. The residence time distribution for a disc lies between the mixing extremes of plug flow and completely mixed. Increasing the disc angle narrows the residence time distribution. Several mixing models for disc granulators have been proposed (see Table 20-58 in modeling and simulation subsection). One to two-minute residence times are common.

**Drum Granulators** Granulation drums are common in the metallurgical and fertilizer industries and are primarily used for very large throughput applications (see Table 20-43). In contrast to discs, there is no output size classification and high recycle rates of off-size product are common. As a first approximation, granules can be considered to flow through the drum in plug flow, although backmixing to some extent is common.

A granulation drum consists of an inclined cylinder which may be either open-ended or fitted with annular retaining rings. Feeds may

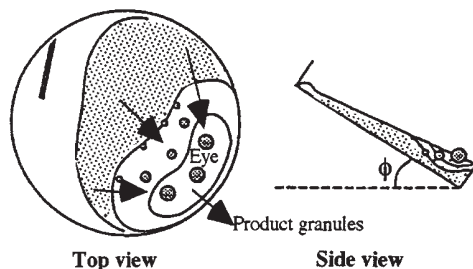


FIG. 20-83 Granule segregation on a disc granulator, illustrating a size-classified granular bed sitting on ungranulated feed powder. Reprinted from *Granulation and Coating Technologies for High-Value-Added Industries*, Ennis and Litster (1996) with permission of E & G Associates. All rights reserved.

**TABLE 20-43 Characteristics of Large-Scale Granulation Drums\***

Diameter, (ft)	Length, (ft)	Power, (hp)	Speed, (rpm)	Approximate capacity, (ton/hr)†
Fertilizer granulation				
5	10	15	10–17	7.5
6	12	25	9–16	10
7	14	30	9–15	20
8	14	60	20–14	25
8	16	75	20–14	40
10	20	150	7–12	50
Iron-ore balling				
9	31	60	12–14	54
10	31	60	12–14	65
12	33	75	10	98

\*Capes, *Particle Size Enlargement*, Elsevier (1980)

†Capacity excludes recycle. Actual drum throughput may be much higher.

NOTE: To convert feet to centimeters, multiply by 30.48; to convert tons/hr to megagrams per hour, multiply by 0.907; and to convert horsepower to kilowatts, multiply by 0.746.

be either premoistened by mixers to form granule nuclei, or liquid may be sprayed onto the tumbling bed via nozzles or distributor-pipe systems. Drums are usually tilted longitudinally a few degrees from the horizontal (0–10°) to assist flow of granules through the drum. The critical speed for the drum is calculated from Eq. 20-67 with  $\phi = 80$ –90°. To achieve a cascading, tumbling motion of the load, drums operate at lower fractions of critical speed than discs, typically 30–50% of  $N_c$ . Scrapers of various designs are often employed to control buildup of the drum wall. Holdup in the drum is between 10 and 20% of the drum volume. Drum length ranges from 2–5 times diameter, and power and capacity scale with drum volume. Holdup and mean residence time are controlled by drum length, with difficult systems requiring longer residence times than those that agglomerate readily. One to five-minute residence times are common.

A variation of the basic cylindrical shape is the multicone drum which contains a series of compartments formed by annular baffles [Stirling, in Knepper (ed.), *Agglomeration*, Interscience, New York, 1962].

Drum granulation plants often have significant recycle of undersize, and sometimes crushed oversize granules. Recycle ratios between 2:1 and 5:1 are common in iron-ore balling and fertilizer granulation circuits. This large recycle stream has a major effect on circuit operation, stability, and control. A surge of material in the recycle stream affects both the moisture content and the size distribution in the drum. Surging and limit-cycle behavior are common. There are several possible reasons for this, including:

1. A shift in controlling mechanism from coalescence to layering when the ratio of recycled pellets to new feed changes [Sastri and Fuerstenau, *Trans. Soc. Mining Eng., AIME*, **258**, 335–340 (1975)].

2. Significant changes in the moisture content in the drum due to recycle fluctuations (recycle of dry granules in fertilizer granulation) [Zhang et al., *Control of Particulate Processes IV* (1995)].

In many cases, plants simply live with these problems. However, use of modern model-based control schemes in conjunction with improved methods for on-line moisture and particle size analysis can help overcome these effects [Ennis (ed.), *Powder Tech.*, **82** (1995); Zhang et al., *Control of Particulate Processes IV* (1995)].

**Granulation Rate Processes and Effect of Operating Variables** Granulation rate processes have been discussed in detail above (see “Agglomeration Rate Processes”). Nucleation, coalescence, consolidation, and layering are all important processes in tumbling granulation. In tumbling granulators, the growth processes are complex for a number of reasons:

1. Granules remain wet and can deform and consolidate. The behavior of a granule is therefore a function of its history.

2. Different granulation behavior is observed for broad- and narrow-size distributions.

3. There is often complex competition between growth mechanisms.

**Consolidation** of the granules in tumbling granulators directly determines granule density and porosity. Since there is typically no in situ drying to stop the consolidation process, granules consolidate over extended times. Increasing size, speed, and angle of drums and discs will increase the rate of consolidation. Increasing residence time through lower feed rates will increase the extent of consolidation. With disc granulators, residence time can also be increased by increasing bed depth (controlled by bottom inserts), raising disc speed, or lowering disc angle. With drum granulators, residence time can be influenced by internal baffling.

Growth rate is very sensitive to liquid content for narrow initial-size distributions, with increases in liquid content for fine powders leading to an approximate exponential increase in granule size. For low-viscosity liquids, granulation occurs when very close to the saturation of the granule. This leads to the following equation to estimate moisture requirements [Capes, *Particle Size Enlargement*, Elsevier (1980)]:

$$w = \frac{\epsilon \rho_l}{\epsilon \rho_l + (1 - \epsilon) \rho_s}$$

$$w = \frac{1}{1 + 1.85(\rho_s/\rho_l)}; d_p < 30 \mu\text{m} \quad (20-68)$$

$$w = \frac{1}{1 + 2.17(\rho_s/\rho_l)}; d_p > 30 \mu\text{m}$$

where  $w$  is the weight fraction of the liquid,  $\epsilon$  is the porosity of the close-packed material,  $\rho_s$  is true particle density,  $\rho_l$  is liquid density, and  $d_p$  is the average size of the feed material. Equation (20-68) is suitable for preliminary mass-balance requirements for liquid binders with similar properties to water. If possible, however, the liquid requirements should be measured in a balling test on the material in question, since unusual packing and wetting effects, particle internal porosity, and solubility, air inclusions, etc. may cause error. Approximate moisture requirements for balling several materials are given in Table 20-44. In addition, for materials containing soluble constituents, such as fertilizer formulations, the total solution-phase ratio controls growth, and not simply the amount of binding fluid used.

When fines are recycled, as in iron ore, sinter feed, or fertilizer drum granulation, they are rapidly granulated and removed from the

**TABLE 20-44 Moisture Requirements for Granulating Various Materials**

Raw material	Approximate size of raw material, less than indicated mesh	Moisture content of balled product, wt % H <sub>2</sub> O
Precipitated calcium carbonate	200	29.5–32.1
Hydrated lime	325	25.7–26.6
Pulverized coal	48	20.8–22.1
Calcined ammonium metavanadate	200	20.9–21.8
Lead-zinc concentrate	20	6.9–7.2
Iron pyrite calcine	100	12.2–12.8
Specular hematite concentrate	150	8.0–10.0
Taconite concentrate	150	8.7–10.1
Magnetic concentrate	325	9.8–10.2
Direct-shipping open-pit iron ores	10	10.3–10.9
Underground iron ore	¼ in.	10.4–10.7
Basic oxygen converter fume	1 $\mu$	9.2–9.6
Raw cement meal	150	13.0–13.9
Fly ash	150	24.9–25.8
Fly ash-sewage sludge composite	150	25.7–27.1
Fly ash-clay slurry composite	150	22.4–24.9
Coal-limestone composite	100	21.3–22.8
Coal-iron ore composite	48	12.8–13.9
Iron ore-limestone composite	100	9.7–10.9
Coal-iron ore-limestone composite	14	13.3–14.8

\*Dravo Corp.

distribution up to some critical size, which is a function of both moisture content and binder viscosity. Changing the initial-size distribution changes the granule porosity and hence moisture requirements [Adetayo et al., *Chem. Eng. Sci.*, **48**, 3951 (1993)]. Since recycle rates in drum systems are high, differences in size distribution between feed and recycle streams are one source of the limit-cycle behavior observed in practice.

Growth by layering is important for the addition of fine powder fed to recycled well-formed granules in drum granulation circuits and for disc granulators. In each case, layering will compete with nuclei formation and coalescence as growth mechanisms. Layered growth leads to a smaller number of larger, denser granules with a narrower-size distribution than growth by coalescence. Layering is favored by a high ratio of pellets to new feed, low moisture and positioning powder feed to fall onto tumbling granules.

**Granulator-Dryers for Layering and Coating** Some designs of tumbling granulators also act as dryers specifically to encourage layered growth or coating and discourage coalescence or agglomeration, e.g., the fluidized-drum granulator [Anon, *Nitrogen*, **196**, 3–6 (1992)]. These systems have drum internals designed to produce a falling curtain of granules past an atomized feed solution or slurry. Layered granules are dried by a stream of warm air before circulating through the coating zone again. Applications are in fertilizer and industrial chemicals manufacture. Analysis of these systems is similar to fluidized-bed granulator dryers.

In the pharmaceutical industry, pan granulators are still widely used for coating application. Pans are suitable for coating only relatively large granules or tablets. For smaller particles, the probability of coalescence is too high.

**Relative Merits of Disc versus Drum Granulators** The principal difference between disc and drum granulators is the classifying action of the disc, resulting in disc granulators having narrower exit-granule-size distributions than drums. This alleviates the need for product screening and recycle for disc granulators in some industries with only moderate-size specifications. For industries with tighter specifications, however, recycle rates are rarely more than 1:2 compared to drum recycle rates often as high as 5:1. The classified mixing action of the disc affects product bulk density, growth mechanisms, and granule structure as well. Generally, drum granulators produce denser granules than discs. Control of growth mechanisms on discs is complex, since regions of growth overlap and mechanisms compete. Both layered and partially agglomerated structures are therefore possible in disc granulators.

Other advantages claimed for the disc granulator include low equipment cost, sensitivity to operating controls, and easy observation of the granulation/classification action, all of which lend versatility in agglomerating many different materials. Dusty materials and chemical reactions such as the ammoniation of fertilizer are handled less readily in the disc granulator than in the drum.

Advantages claimed for the drum granulator over the disc are greater capacity, longer retention time for materials difficult to agglomerate or of poor flow properties, and less sensitivity to upsets in the system due to the damping effect of a large, recirculated load. Disadvantages are high recycle rates which can promote limit-cycle behavior or degradation of properties of the product.

## MIXER GRANULATORS

**Mixer granulators** contain an agitator to mix particles and liquid to cause granulation. In fact, mixing any wet solid will cause some granulation, even if unintentionally. Mixer granulators have a wide range of applications including pharmaceutical, agrochemical, and detergent (Table 20-36), and they have the following advantages:

- They can process plastic, sticky materials.
- They can spread viscous binders.
- They are less sensitive to operating conditions than tumbling granulators.
- They can produce small (<2 mm) high-density granules.

Power and maintenance costs are higher than for tumbling granulators. Outside of high-intensity continuous systems (e.g., the Schugi in-line mixer), mixers are not feasible for very large throughput applications if substantial growth is required. Granules produced in mixer granulators may not be as spherical as those produced in tumbling granulators, and are generally denser due to higher-agitation intensity (see Fig. 20-71). Control of the amount of liquid phase and the intensity and duration of mixing determine agglomerate size and density. Due to greater compaction and kneading action, generally less liquid phase is required in mixers than in tumbling granulation.

**Low-Speed Mixers** **Pug mills** and **paddle mills** are used for both batch and continuous applications. These devices have horizontal troughs in which rotate central shafts with attached mixing blades of bar, rod, paddle, and other designs. (See Sec. 19.) The vessel may be of single- or double-trough design. The rotating blades throw material forward and to the center to achieve a kneading, mixing action. Characteristics of a range of pug mills available for fertilizer granulation are given in Table 20-45. These mills have largely been replaced by tumbling granulators in metallurgical and fertilizer applications, but they are still used as a premixing step for blending very different raw materials e.g., filter cake with dry powder.

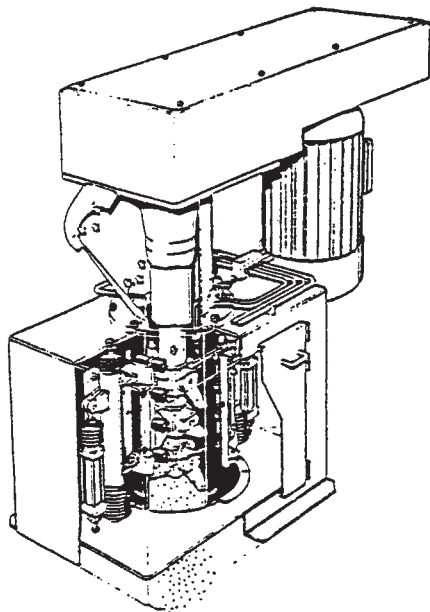
**Batch planetary mixers** are used extensively in the pharmaceutical industry for powder granulation. A typical batch size of 100 to 200 kg has a power input of 10 to 20 kW. Mixing times in these granulators are quite long (20 to 40 min).

**High-Speed Mixers** **High-speed mixers** include continuous-shaft mixers and batch high-speed mixers. **Continuous-shaft mixers** have blades or pins rotating at high speed on a central shaft. Both horizontal and vertical shaft designs are available. Examples include the vertical **Schugi mixer** (Fig. 20-84) and the horizontal **pin or peg**

TABLE 20-45 Characteristics of Pug Mixers for Fertilizer Granulation\*

Model	Material bulk density, lb/ft <sup>3</sup>	Approximate capacity, tons/h	Size (width × length), ft	Plate thickness, in	Shaft diameter, in	Speed, r/min	Drive, hp
A	25	8	2 × 8	¼	3	56	15
	50	15	2 × 8	¼	3	56	20
	75	22	2 × 8	¼	3	56	25
	100	30	2 × 8	¼	3	56	30
B	25	30	4 × 8	¾	4	56	30
	50	60	4 × 8	¾	4	56	50
	75	90	4 × 8	¾	4	56	75
	100	120	4 × 8	¾	5	56	100
C	25	30	4 × 12	¾	5	56	50
	50	60	4 × 12	¾	5	56	100
	75	90	4 × 12	¾	6	56	150
	100	120	4 × 12	¾	6	56	200
	125	180	4 × 12	¾	7	56	300

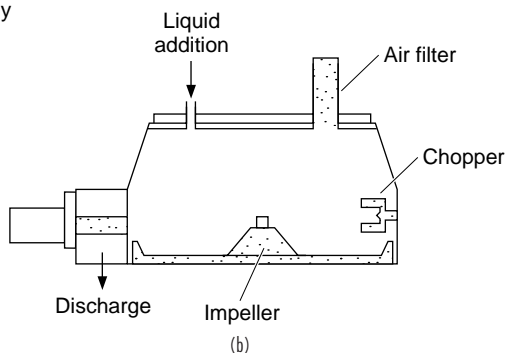
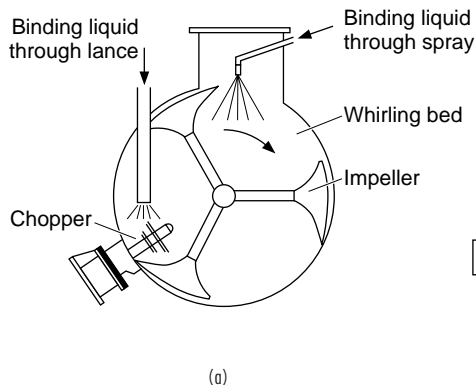
\*Feeco International, Inc. To convert pounds per cubic foot to kilograms per cubic meter, multiply by 16; to convert tons per hour to megagrams per hour, multiply by 0.907; to convert feet to centimeters, multiply by 30.5; to convert inches to centimeters, multiply by 2.54; and to convert horsepower to kilowatts, multiply by 0.746.



**FIG. 20-84** The Schugi Flexomix<sup>®</sup> vertical high-shear continuous granulator. Shaft speeds range from 100–3500 rpm, capacities from 0.1 to 200 megagrams per hour, and power requirements from 1–100 kW. (Courtesy of Hosokawa Micron Australia Pty. Ltd.)

**mixers.** These mixers operate at high speed (200 to 3500 rpm) to produce granules of size 0.5 to 1.5 mm with a residence time of a few seconds. Schugi capacities may range up to 50 tons/hr. Typical plant capacities of lower-shear peg mixers are 10–20 tons/hr [Capes, *Particle Size Enlargement*, 1980]. Examples of applications include detergents, agricultural chemicals, clays, ceramics, and carbon black.

Batch high-shear mixer granulators are used extensively in the pharmaceutical industry. Plow-shaped mixers rotate on a horizontal shaft at 60 to 800 rpm. Separate high-speed cutters or choppers rotate at much higher speed (500 to 3500 rpm) and are used to limit the maximum granule size. Granulation times of the order 5–10 mins are common, which includes both wet massing and granulation stages operating at low and high impeller speed, respectively. Several designs with both vertical and horizontal shafts are available (Fig. 20-85). Popular designs include horizontal Lödige and vertical Diosna, Fielder, and Gral granulators [Schaefer, *Acta. Pharm. Sci.*, **25**, 205 (1988)].



**FIG. 20-85** (a) Horizontal and (b) vertical high-shear mixer granulators for pharmaceutical granule preparation for subsequent tableting.

**Granulation-Rate Processes and Effect of Operating Variables** Granule deformation is important due to the higher agitation intensity existing in high-shear mixers as compared with tumbling granulators (see Fig. 20-71 and “Growth and Consolidation: High Agitation Intensity Growth”). As deformability is linked to granule saturation and interparticle, frictional forces, consolidation and growth are highly coupled as illustrated in Fig. 20-86 where continued growth is associated with continued compaction and decreases in granule porosity. Impeller shaft power intensity has been used both as a rheological tool to characterize formulation deformability as well as a control technique to judge granulation end-point. [See Kristensen et al., *Acta. Pharm. Sci.*, **25**, 187 (1988) and Holm et al., *Powder Tech.*, **43**, 225 (1985).]

**Scale-Up and Operation** Scale-up of pharmaceutical mixer granulators is difficult because geometric similarity is often not preserved. Kristensen recommends constant relative swept volume ratio  $\dot{V}_R$  as a scale-up parameter defined as:

$$\dot{V}_R = \frac{\dot{V}_{\text{imp}}}{V_{\text{tot}}} \quad (20-69)$$

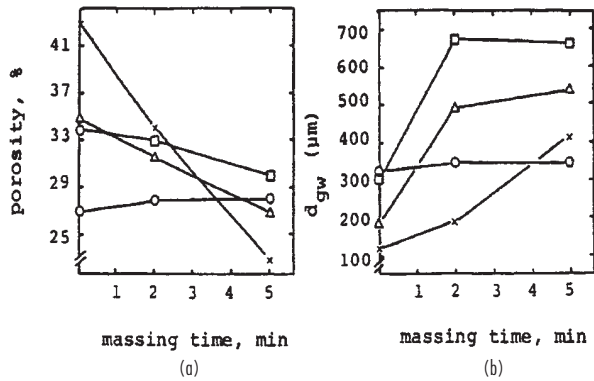
where  $\dot{V}_{\text{imp}}$  is the volume rate swept by the impeller and  $V_{\text{tot}}$  is the total volume of the granulator. Depending on mixer design, relative swept volume may decrease significantly with scale [Schaefer, loc. cit.] requiring increases in impeller speed with scale-up. In general, scale-up leads to poorer liquid distribution, higher-porosity granules and wider granule-size distributions. Required granulation time may increase with scale, though this depends on the importance of consolidation kinetics as discussed above.

Power dissipation can lead to temperature increases of up to 40°C in the mass. Note that evaporation of liquid as a result of this increase needs to be accounted for in determining liquid requirements for granulation. Liquid should be added through an atomizing nozzle to aid uniform liquid distribution in many cases. In addition, power intensity (kW/kg) has been used with some success to judge granulation end point and for scale-up, primarily due to its relationship to granule deformation [Holm loc. cit.]. Swept volume ratio is a preliminary estimate of expected power intensity.

## FLUIDIZED-BED AND RELATED GRANULATORS

In fluidized granulators (**fluidized beds** and **spouted beds**), particles are set in motion by air, rather than by mechanical agitation. Applications include fertilizers, industrial chemicals, agricultural chemicals, pharmaceutical granulation, and a range of coating processes. Fluidized granulators produce either high-porosity granules due to the agglomeration of powder feeds or high-strength layered granules due to coating of seed particles or granules by liquid feeds.

Figure 20-87 shows a typical production-size **batch** fluid-bed granulator. The air-handling unit dehumidifies and heats the inlet air. Heated fluidization air enters the processing zone through a distribu-



**FIG. 20-86** Relationship between consolidation and growth kinetics in high-shear mixer granulators. Effect of wet-massing time on intragranular porosity (a) and granule size (b) in a high-shear mixer, Fielder PMAT 25 VG. Impeller speed: 250 rpm. Chopper speed: 3000 rpm. Starting materials: Lactose, o; Dicalcium phosphate, x. Dicalcium phosphate/cornstarch 85/15 w/wt %:  $\Delta$ . Dicalcium phosphate/cornstarch 55/45 w/wt %: h [Kristensen *et al.*, *Acta Pharm. Sci.*, **25**, 187 (1988).]

tor which also supports the particle bed. Liquid binder is sprayed through an air-atomizing nozzle located above, in, or below the bed. Bag filters or cyclones are needed to remove dust from the exit air. Other fluidization gases such as nitrogen are also used in place of or in combination with air to avoid potential explosion hazards due to fine powders.

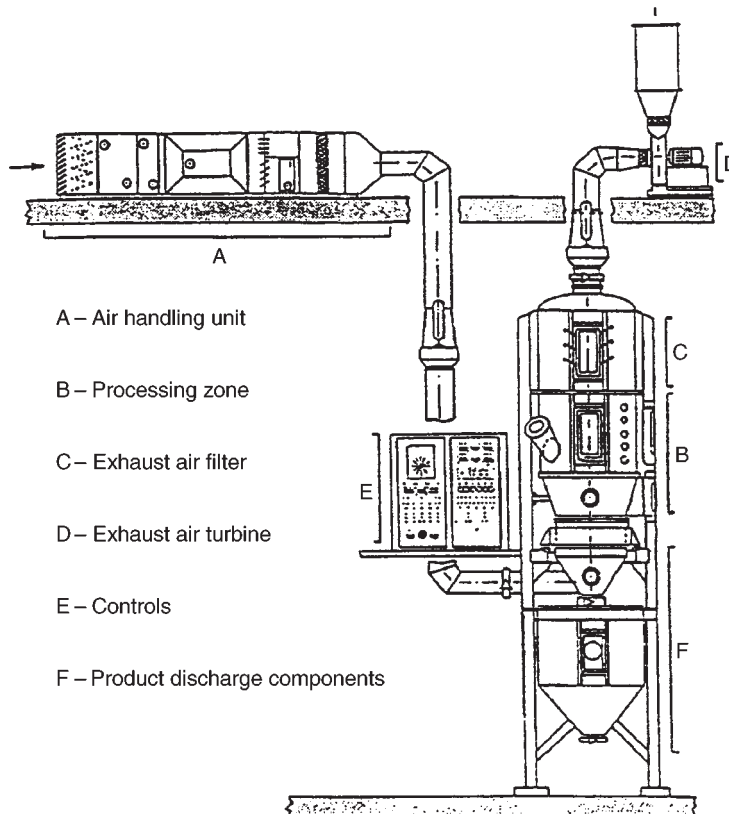
**Continuous** fluid-bed granulators are used in the fertilizer and detergent industries. For fertilizer applications, near-size granules are recycled to control the granule size distribution. Dust is not recycled directly, but first remelted or slurried in the liquid feed.

Advantages of fluidized-beds over other granulation systems include high-volumetric intensity, simultaneous drying and granulation, high heat and mass-transfer rates, and robustness with respect to operating variables on product quality. Disadvantages include the effect of high operating costs with respect to air handling and dust containment, and the potential of defluidization due to uncontrolled growth.

**Hydrodynamics** The hydrodynamics of fluidized beds is covered in detail in Sec. 17. Only aspects specifically related to particle size enlargement are discussed here. Granular product from fluidized beds are generally **group B** or **group D** particles under Geldart's powder classification. However, for batch granulation, the bed may initially consist of a **group A** powder. For granulation, fluidized beds typically operate in the range  $1.5U_{mf} < U < 5U_{mf}$  where  $U_{mf}$  is the minimum fluidization velocity and  $U$  is the operating superficial gas velocity. For batch granulation, the gas velocity may need to be increased significantly during operation to maintain the velocity in this range as the bed particle size increases.

For group B and D particles, nearly all the excess gas velocity ( $U - U_{mf}$ ) flows as bubbles through the bed. The flow of bubbles controls particle mixing, attrition, and elutriation. Therefore, elutriation and attrition rates are proportional to excess gas velocity. Readers should refer to Sec. 17 for important information and correlations on Geldart's powder classification, minimum fluidization velocity, bubble growth and bed expansion, and elutriation.

**Mass and Energy Balances** Due to the good mixing and heat-transfer properties of fluidized beds, the exit-gas temperature is assumed to be the same as the bed temperature. Fluidized bed gran-



**FIG. 20-87** Fluid-bed granulator for batch processing of powder feeds. [Ghebre-Selassie (*ed.*), *Pharmaceutical Pelletization Technology*, Marcel Dekker (1989).]

ulators also act simultaneously as dryers and therefore are subject to the same mass and energy-balance limits as driers, namely:

1. The concentration of solvent of the atomized binding fluid in the exit air cannot exceed the saturation value for the solvent in the fluidizing gas at the bed temperature.

2. The supplied energy in the inlet air must be sufficient to evaporate the solvent and maintain the bed at the desired temperature.

Both these limits restrict the maximum rate of liquid feed or binder addition for given inlet gas velocity and temperature. The liquid feed rate may be further restricted to avoid excess coalescence or quenching.

**Granulation Rate Processes and Effect of Operating Variables** Table 20-46 summarizes the typical effect of feed properties (material variables) and operating variables on fluidized-bed granulation. Due to the range of mechanisms operating simultaneously, the combined effect of these variables can be complex. "Rules of thumb" for operation are very dependent on knowing the dominant granulation mechanisms or rate processes. Understanding individual rate processes allows at least semiquantitative analysis to be used in design and operation. See Tables 20-38, 20-40, and 20-42 on controlling the individual granulation rate processes of wetting, coalescence and consolidation, and breakage, respectively.

Competing mechanisms of growth include layering which results in dense, strong granules with a very tight size distribution and coalescence which results in raspberry-like agglomerates of higher voidage. Growth rates range from 10–100  $\mu\text{m hr}^{-1}$  to 100–2000  $\mu\text{m hr}^{-1}$  for growth by layering and coalescence, respectively.

Air atomizing nozzles are commonly used to control the droplet-size distribution independently of the liquid feed rate and to minimize the chances of **defluidization** due to uncontrolled growth or large droplets.

**Equipment Operation** Spray nozzles suffer from caking on the outside and clogging on the inside. When the nozzle is below the bed surface, fast capture of the liquid drops by bed particles, as well as scouring of the nozzle by particles, prevents caking. Blockages inside the nozzle are also common, particularly for slurries. The nozzle design should be as simple as possible and provision for in situ cleaning or easy removal is essential.

The formation of large, wet agglomerates that dry slowly is called **wet quenching**. Large agglomerates defluidize, causing channeling and poor mixing, ultimately leading to shutdown. Sources of wet quenching include high liquid-spray rates, large spray droplets, or dripping nozzles. **Dry quenching** (uncontrolled coalescence) is the formation and defluidization of large, stable, dry agglomerates, which also may ultimately lead to shutdown. Early detection of quenching is important. The initial stages of defluidization are detected by monitoring the bed temperature just above the distributor. A sudden increase (dry quenching) or decrease (wet quenching) indicates the onset of bed defluidization. Wet quenching is avoided by reducing the liquid

feed rate and improving the nozzle operation. In situ jet grinding is sometimes used to limit the maximum stable size of dry agglomerates.

Control is accomplished by monitoring bed temperature, as well as granule size and density of samples. Temperature is controlled best by adjusting the liquid feed rate. For batch granulation, the fluidizing air velocity must be increased during the batch. **Bed pressure fluctuations** can be used to monitor the quality of fluidization and to indicate when gas velocity increases are required. In addition, intermittent sampling systems may be employed with **on-line size analyzers** to monitor granule size. There is no simple heuristic to control the final-granule-size distribution (batch) or exit-granule-size distribution (continuous). A good knowledge of the granulation processes combined with model-based control schemes can be used to fix the batch time (batch), or adjust the seed-granule recycle (continuous) to maintain product quality.

**Scale-up** of fluid-bed granulators relies heavily on pilot-scale tests. The pilot-plant fluid bed should be at least 0.3 meters in diameter so that bubbling rather than slugging fluidization behavior occurs. Key in scale-up is the increase in agitation intensity with increasing bed height. In particular, granule density and attrition resistance increase linearly with operating bed height whereas the rate of granule dispersion decreases.

**Draft Tube Designs and Spouted Beds** A **draft tube** is often employed to regulate particle circulation patterns. The most common design is the **Wurster** draft tube fluid bed employed extensively in the pharmaceutical industry, usually for coating and layered growth applications. The **Wurster coater** uses a bottom positioned spray, but other variations are available (Table 20-47).

The **spouted-bed granulator** consists of a central high-velocity **spout** surrounded by a **moving bed annular region**. (See Sec. 17.) All air enters through the orifice at the base of the spout. Particles entrained in the spout are carried to the bed surface and rain down on the annulus as a fountain. Bottom-sprayed designs are the most common. Due to the very high gas velocity in the spout, granules grow by layering only. Therefore, spouted beds are good for coating applications. However, attrition rates are also high, so the technique is not suited to weak granules. Spouted beds are well suited to group D particles and are more tolerant of nonspherical particles than a fluid bed. Particle circulation is better controlled than in a fluidized bed, unless a draft tube design is employed. Spouted beds are difficult to scale past two meters in diameter.

The liquid spray rate to a spouted bed may be limited by agglomerate formation in the spray zone causing spout collapse [Liu & Litster, *Powder Tech.*, **74**, 259 (1993)]. The maximum liquid spray rate increases with increasing gas velocity, increasing bed temperature, and decreasing binder viscosity (see Fig. 20-88). The maximum liquid flow rate is typically between 20 and 90 percent of that required to saturate the exit air, depending on operating conditions. Elutriation of fines from spouted-bed granulators is due mostly to the attrition of newly layered material, rather than spray drying. The elutriation rate is proportional to the kinetic energy in the inlet air (see Eq. 20-71).

**TABLE 20-46 Effect of Variables on Fluidized-Bed Granulation\***

Operating or material variable	Effect of increasing variable
Liquid feed or spray rate	Increase size and spread of granule-size distribution Increase granule density and strength Increase chance of defluidization due to quenching
Liquid droplet size	Increase size and spread of granule size distribution
Gas velocity	Increase attrition and elutriation rates (major effect) Decrease coalescence for inertial growth No effect on coalescence for noninertial growth Increase granule consolidation and density
Bed height	Increase granule density and strength
Bed temperature	Decrease granule density and strength
Binder viscosity	Increase coalescence for inertial growth No effect on coalescence for noninertial growth Decrease granule density
Particle or granule size	Decrease chance of coalescence Increase required gas velocity to maintain fluidization

\* Reprinted from *Granulation and Coating Technologies for High-Value-Added Industries*, Ennis and Litster (1996) with permission of E & G Associates. All rights reserved.

## CENTRIFUGAL GRANULATORS

In the pharmaceutical industry, a range of centrifugal granulator designs are used. In each of these, a horizontal disc rotates at high speed causing the feed to form a rotating **rope** at the walls of the

**TABLE 20-47 Sizes & Capacities of Wurster Coaters\***

Bed diameter, inches	Batch size, kg
7	3–5
9	7–10
12	12–20
18	35–55
24	95–125
32	200–275
46	400–575

\* Ghebre-Sellasie (ed.), *Pharmaceutical Pelletization Technology*, Marcel Dekker (1989).

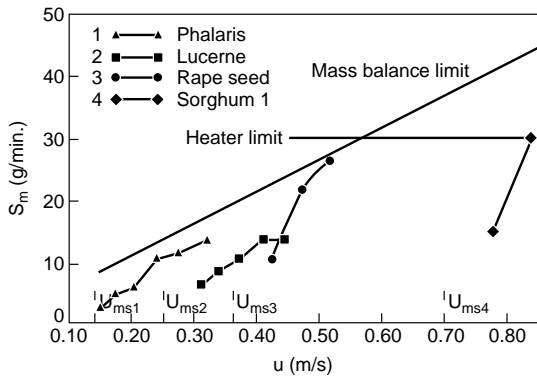


FIG. 20-88 Effect of gas velocity on maximum liquid rate for a spouted-bed seed coater. [Liu & Liltner, *Powder Tech.*, **74**, 259 (1993).] With kind permission from Elsevier Science SA, Lausanne, Switzerland.

vessel (see Fig. 20-89). There is usually an allowance for drying air to enter around the edge of the spinning disc. Applications of such granulators include spherulization of extruded pellets, dry-powder layering of granules or sugar spheres, and coating of pellets or granules by liquid feeds.

**Centrifugal Designs** Centrifugal granulators tend to give denser granules or powder layers than fluidized beds and more spherical granules than mixer granulators. Operating costs are reasonable but capital cost is generally high compared to other options. Several types are available including the **CF granulator** (Fig. 20-89) and **rotary fluidized-bed** designs which allow high gas volumes and therefore significant drying rates (Table 20-48). CF granulator capacities range from 3–80 kg with rotor diameters of .36–1.3 meters and rotor speeds of 45–360 rpm [Ghebre-Selassie (ed.), *Pharmaceutical Pelletization Technology*, Marcel Dekker, (1989)].

**Particle Motion and Scale-Up** Very little fundamental information is published on centrifugal granulators. Qualitatively, good operation relies on maintaining a smoothly rotating **stable rope** of tumbling

particles. Operating variables which affect the particle motion are disc speed, peripheral air velocity, and the presence of baffles.

For a given design, good rope formation is only possible for a small range of disc speeds. If the speed is too low, a rope does not form. If the speed is too high, very high attrition rates can occur. Scale-up on the basis of either **constant peripheral speed** ( $DN = \text{const.}$ ), or **constant Froude number** ( $DN^2 = \text{const.}$ ) is possible. Increasing peripheral air velocity and baffles helps to increase the rate of rope turnover. In designs with tangential powder or liquid feed tubes, additional baffles are usually not necessary. The motion of particles in the equipment is also a function of the frictional properties of the feed, so the optimum operating conditions are feed specific.

**Granulation Rate Processes** Possible granulation processes occurring in centrifugal granulators are extrudate breakage, consolidation, rounding (spherulization), coalescence, powder layering and coating, and attrition. Very little information is available about these processes as they occur in centrifugal granulators, however, similar principles from tumbling and fluid-bed granulators will apply.

## SPRAY PROCESSES

Spray processes include **spray driers**, **prilling towers**, and **flash driers**. Feed solids in a fluid state (solution, gel, paste, emulsion, slurry, or melt) are dispersed in a gas and converted to granular solid products by heat and/or mass transfer. In spray processes, the size distribution of the particulate product is largely set by the drop size distribution, i.e., **nucleation** is the dominant granulation process. Exceptions are where fines are recycled to coalesce with new spray droplets and where spray-dried powders are rewet in a second tower to encourage agglomeration. For spray drying, a large amount of solvent must be evaporated whereas prilling is a spray-cooling process. Fluidized or spouted bed must be used to capture nucleated fines as hybrid granulator designs, e.g., the **fluid-bed spray dryer**.

Product diameter is small and bulk density is low in most cases, except prilling. Feed liquids must be pumpable and capable of atomization or dispersion. Attrition is usually high, requiring fines recycle or recovery. Given the importance of the droplet-size distribution, nozzle design and an understanding of the fluid mechanics of drop formation are critical. In addition, heat and mass-transfer rates during

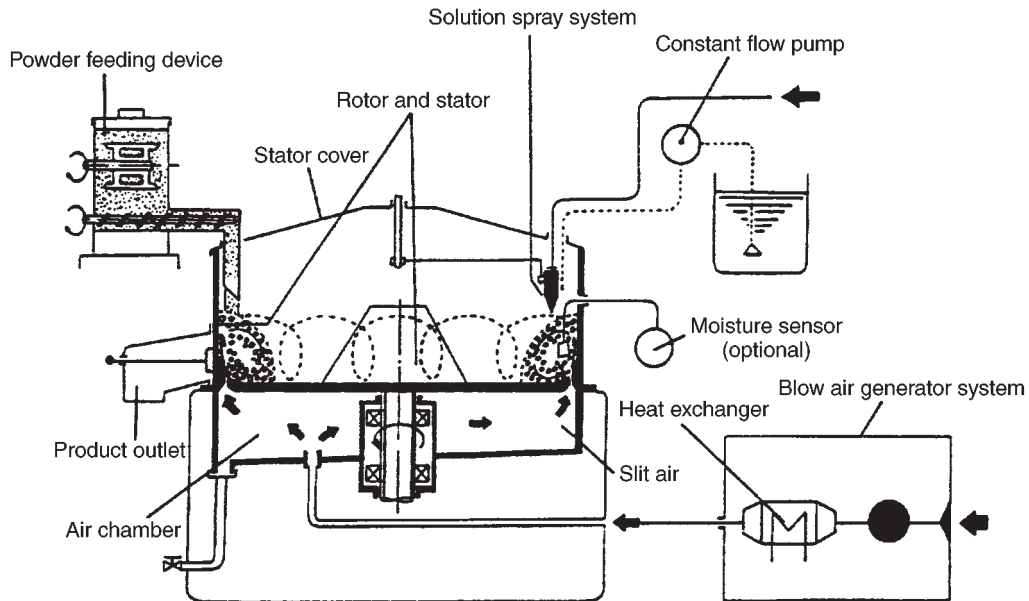


FIG. 20-89 Schematic of a CF granulator. [Ghebre-Selassie (ed.), *Pharmaceutical Pelletization Technology*, Marcel Dekker (1989).]



**TABLE 20-48 Specifications of Glatt Rotary Fluid-Bed Granulators\***

Parameter	15	60	200	500
Volume, liters	45	220	670	1560
Fan				
Power, kW	11	22	37	55
Capacity, m <sup>3</sup> /hr	1500	4500	8000	12000
Heating capacity, kW	37	107	212	370
Diameter, m	1.7	2.5	3.45	4.0

\*Glatt Company, in Ghebre-Selassie (ed.), *Pharmaceutical Pelletization Technology*, Marcel Dekker (1989).

drying can strongly effect the particle morphology, of which a wide range of characteristics are possible.

**Spray Drying** Detailed descriptions of spray dispersion dryers, together with application, design, and cost information, are given in Sec. 17. Product quality is determined by a number of properties such as particle form, size, flavor, color, and heat stability. Particle size and size distribution, of course, are of greatest interest from the point of view of size enlargement.

In general, particle size is a function of atomizer-operating conditions and also of the solids content, liquid viscosity, liquid density, and feed rate. Coarser, more granular products can be made by increasing viscosity (through greater solids content, lower temperature, etc.), by increasing feed rate, and by the presence of binders to produce more agglomeration of semidry droplets. Less-intense atomization and spray-air contact also increase particle size, as does a lower exit temperature, which yields a moister (and hence a more coherent) product. This latter type of spray-drying agglomeration system has been described by Masters and Stoltze [*Food Eng.*, 64 (February 1973)] for the production of instant skim-milk powders in which the completion of drying and cooling takes place in vibrating conveyors (see Sec. 17) downstream of the spray dryer.

**Prilling** The prilling process is similar to spray drying and consists of spraying droplets of liquid into the top of a tower and allowing these to fall against a countercurrent stream of air. During their fall the droplets are solidified into approximately spherical particles or prills which are up to about 3 mm in diameter, or larger than those formed in spray drying. The process also differs from spray drying since the droplets are formed from a melt which solidifies primarily by cooling with little, if any, contribution from drying. Traditionally, ammonium nitrate, urea, and other materials of low viscosity and melting point and high surface tension have been treated in this way. Improvements in the process now allow viscous and high-melting point materials and slurries containing undissolved solids to be treated as well.

The design of a prilling unit first must take into account the properties of the material and its sprayability before the tower design can proceed. By using data on the melting point, viscosity, surface tension, etc., of the material, together with laboratory-scale spraying tests, it is possible to specify optimum temperature, pressure, and orifice size for the required prill size and quality. Tower sizing basically consists of specifying the cross-sectional area and the height of fall. The former is determined primarily by the number of spray nozzles necessary for the desired production rate. Tower height must be sufficient to accomplish solidification and is dependent on the heat-transfer characteristics of the prills and the operating conditions (e.g., air temperature). Because of relatively large prill size, narrow but very tall towers are used to ensure that the prills are sufficiently solid when they reach the bottom. Table 20-49 describes the principal characteristics of a typical prilling tower.

Theoretical calculations are possible to determine tower height with reasonable accuracy. Simple parallel streamline flow of both droplets and air is a reasonable assumption in the case of prilling towers compared with the more complex rotational flows produced in spray dryers. For velocity of fall, see, for example, Becker [*Can. J. Chem.*, 37, 85 (1959)]. For heat transfer, see, for example, Kramers [*Physica*, 12, 61 (1946)]. Specific design procedures for prilling towers are available in the *Proceedings of the Fertilizer Society (England)*; see Berg and Hallie, no. 59, 1960; and Carter and Roberts, no. 110, 1969.

Recent developments in nozzle design have led to drastic reductions

**TABLE 20-49 Some Characteristics of a Typical Prilling Operation\***

Tower size		
Prill tube height, ft	130	
Rectangular cross section, ft	11 by 21.4	
Cooling air		
Rate, lb/h	360,000	
Inlet temperature	Ambient	
Temperature rise, °F	15	
Melt		
Type	Urea	Ammonium nitrate
Rate, lb/h	35,200 (190 lb H <sub>2</sub> O)	43,720 (90 lb H <sub>2</sub> O)
Inlet temperature, °F	275	365
Prills		
Outlet temperature, °F	120	225
Size, mm	Approximately 1 to 3	

\*HPD Incorporated. To convert feet to centimeters, multiply by 30.5; to convert pounds per hour to kilograms per hour, multiply by 0.4535; °C = (°F - 32) ÷ 1.8.

in the required height of prilling towers. However, such nozzle designs are largely proprietary and little information is openly available.

**Flash Drying** Special designs of pneumatic-conveyor dryers, described in Sec. 17 can handle filter and centrifuge cakes and other sticky or pasty feeds to yield granular size-enlarged products. The dry product is recycled and mixed with fresh, cohesive feed, followed by disintegration and dispersion of the mixed feed in the drying-air stream.

## PRESSURE COMPACTION PROCESSES

The success of compression agglomeration depends on the effective utilization and transmission of the applied external force and on the ability of the material to form and maintain interparticle bonds during pressure compaction (or consolidation) and decompression. Both these aspects are controlled in turn by the geometry of the confined space, the nature of the applied loads and the physical properties of the particulate material and of the confining walls. (See the section on Powder Mechanics and Powder Compaction.)

Pressure compaction is carried out in two classes of equipment. These are **confined-pressure devices** (molding, piston, tableting, and roll presses), in which material is directly consolidated in closed molds or between two opposing surfaces; and **extrusion devices** (pellet mills, screw extruders), in which material undergoes considerable shear and mixing as it is consolidated while being pressed through a die. See Table 20-36 for examples of uses. Product densities and applied pressures are substantially higher than agitative agglomeration techniques, as shown in Fig. 20-71.

**Piston and Molding Presses** Piston or molding presses are used to create uniform and sometimes intricate compacts, especially in powder metallurgy and plastics forming. Equipment comprises a mechanically or hydraulically operated press and, attached to the platens of the press, a two-part mold consisting of top (male) and bottom (female) portions. The action of pressure and heat on the particulate charge causes it to flow and take the shape of the cavity of the mold. Compacts of metal powders are then sintered to develop metallic properties, whereas compacts of plastics are essentially finished products on discharge from the molding machine.

**Tableting Presses** Tableting presses are employed in applications having strict specifications for weight, thickness, hardness, density, and appearance in the agglomerated product. They produce simpler shapes at higher production rates than do molding presses. A single-punch press is one that will take one station of tools consisting of an upper punch, a lower punch, and a die. A rotary press employs a rotating round die table with multiple stations of punches and dies. Older rotary machines are single-sided; that is, there is one fill station and one compression station to produce one tablet per station at every revolution of the rotary head. Modern high-speed rotary presses are double-sided; that is, there are two feed and compression stations to

TABLE 20-50 Characteristics of Tableting Presses\*

	Single-punch	Rotary
Tablets per minute	8-140	72-6000
Tablet diameter, in.	1/8-4	5/8-2 1/2
Pressure, tons	1 1/2-100	4-100
Horsepower	1/4-15	1 1/2-50

\*Browning, *Chem. Eng.*, **74**(25), 147 (1967).

NOTE: To convert inches to centimeters, multiply by 2.54; to convert tons to megagrams, multiply by 0.907; and to convert horsepower to kilowatts, multiply by 0.746.

produce two tablets per station at every revolution of the rotary head. Some characteristics of tableting presses are shown in Table 20-50.

For successful tableting, a material must have suitable flow properties to allow it to be fed to the tableting machine. Wet or dry granulation is used to improve the flow properties of materials. In the case of **wet granulation**, agitative granulation techniques such as fluidized beds or mixer granulators as discussed above are often employed.

In **dry granulation**, the blended dry ingredients are first densified in a heavy-duty rotary tableting press which produces "slugs" 1.9 to 2.5 cm (3/4 to 1 in) in diameter. These are subsequently crushed into particles of the size required for tableting. Predensification can also be accomplished by using a rotary compactor-granulator system. A third technique, direct compaction, uses sophisticated devices to feed the blended dry ingredients to a high-speed rotary press.

Excellent accounts of tableting in the pharmaceutical industry have been given by Kibbe [*Chem. Eng. Prog.*, **62**(8), 112 (1966)], Carstensen [*Handbook of Powder Science & Technology*, Fayed & Otten (eds.), Van Nostrand Reinhold Inc., **252** (1983)], Stanley-Wood (ed.) (loc. cit.), and Doelker (loc. cit.).

**Roll Presses** Roll presses compact raw material as it is carried into the gap between two rolls rotating at equal speeds (Fig. 20-90). The size and shape of the agglomerates are determined by the geometry of the roll surfaces. Pockets or indentations in the roll surfaces form briquettes the shape of eggs, pillows, teardrops, or similar forms from a few grams up to 2 kg (5 lb) or more in weight. Smooth or corrugated rolls produce a solid sheet which can be granulated or broken down into the desired particle size on conventional grinding equipment.

Roll presses can produce large quantities of materials at low cost, but the product is less uniform than that from molding or tableting presses. The introduction of the proper quantity of material into each of the rapidly rotating pockets in the rolls is the most difficult problem in the briquetting operation. Various types of feeders have helped to overcome much of this difficulty.

The impacting rolls can be either solid or divided into segments. Segmented rolls are preferred for hot briquetting, as the thermal expansion of the equipment can be controlled more easily.

Roll presses provide a **mechanical advantage** in amplifying the feed pressure  $P_0$  to some maximum value  $P_m$ . This maximum pressure

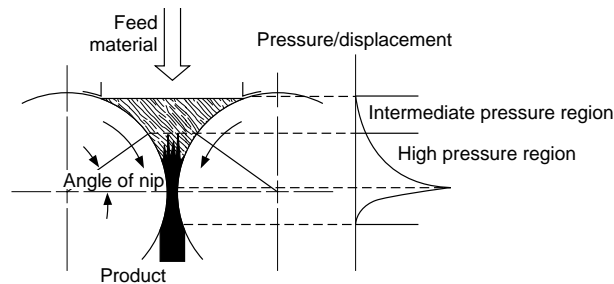


FIG. 20-90 Regions of compression in roll presses. Slippage and particle rearrangement occurs above the angle of nip, and powder compaction at high pressure occurs in the nonslip region below the angle of nip. Reprinted from *Granulation and Coating Technologies for High-Value-Added Industries*, Ennis and Lütser (1996) with permission of E & G Associates. All rights reserved.

$P_m$  and the roll compaction time control compact density. Generally speaking, as compaction time decreases (e.g., by increasing roll speed), the minimum necessary pressure for quality compacts increases. There may be an upper limit of pressure as well for friable materials or elastic materials prone to delamination.

Pressure amplification occurs in two regions of the press (Fig. 20-90). Above the **angle of nip**, sliding occurs between the material and roll surface as material is forced into the rolls, with intermediate pressure ranging from 1-10 psi. Energy is dissipated primarily through overcoming particle friction and cohesion. Below the angle of nip, no slip occurs as the powder is compressed into a compact and pressure may increase up to several thousand psi. Both these intermediate and high-pressure regions of densification are indicated in compressibility diagram of Fig. 20-77.

The overall performance of the press and its mechanical advantage ( $P_m/P_0$ ) depend on the mechanical and frictional properties of the powder. (See "Powder Mechanics and Powder Compaction" section.) For design procedures, see Johanson [*Proc. Inst. Briquet. Agglom. Bien. Conf.*, **9**, 17 (1965)]. Nip angle  $\alpha$  generally increases with decreasing compressibility  $\kappa$ , or with increasing roll friction angle  $\phi_w$  and effective angle of friction  $\phi_e$ . Powders which compress easily and have high-friction grip high in the rolls. The mechanical advantage pressure ratio ( $P_m/P_0$ ) increases and the time of compaction decreases with decreasing nip angle since the pressure is focused over a smaller roll area. In addition, the mechanical advantage generally increases with increasing compressibility and roll friction.

The most important factor that must be determined in a given application is the pressing force required for the production of acceptable compacts. Roll loadings (i.e., roll separating force divided by roll width) in commercial installations vary from 4.4 MN/m to more than 440 MN/m (1000 lb/in to more than 100,000 lb/in). Roll sizes up to 91 cm (36 in) in diameter by 61 cm (24 in) wide are in use.

The roll loading  $L$  is related to the maximum developed pressure and roll diameter by

$$L = \frac{F}{W} = \frac{1}{2} f P_m D \propto P_m D^{1/2} (h + d)^{1/2} \quad (20-70)$$

where  $F$  is the **roll-separating force**,  $D$  and  $W$  are the roll diameter and width,  $f$  is a **roll-force factor** dependent on compressibility  $\kappa$  and gap thickness as given in Fig. 20-91,  $h$  is the gap thickness and  $d/2$  is the pocket depth for briquette rolls. [Pietsch, *Size Enlargement by Agglomeration*, John Wiley & Sons Ltd., Chichester, 1992.] The maximum pressure  $P_m$  is established on the basis of required compact density and quality, and it is a strong function of roll gap distance and powder properties as discussed above, particularly compressibility.

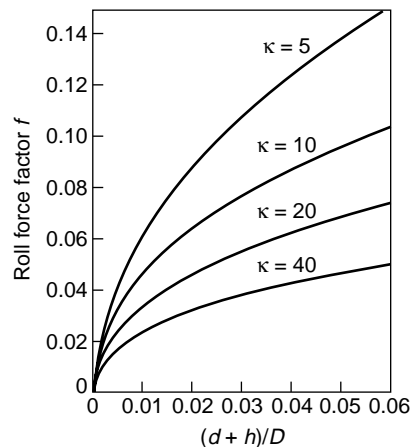


FIG. 20-91 Roll-force factor as a function of compressibility  $\kappa$  and dimensionless gap distance  $(d+h)/D$ . [Pietsch (ed.), *Roll Pressing*, Powder Advisory Centre, London (1987).]

Small variations in feed properties can have a pronounced effect on maximum pressure  $P_m$  and press performance. Roll presses are scaled on the basis of constant maximum pressure. The required roll loading increases approximately with the square root of increasing roll diameter or gap width.

The allowable roll width is inversely related to the required pressing force because of mechanical-design considerations. The throughput of a roll press at constant roll speed decreases as pressing force increases since the allowable roll width is less. Machines with capacities up to 45 Mg/h (50 tons/h) are available. Some average figures for the pressing force and energy necessary to compress a number of materials on roll-type briquette machines are given in Table 20-51. Typical capacities are given in Table 20-52.

During compression in the slip region, escaping air may induce flu-

idization or erratic pulsating of the feed. This effect, which is controlled by the permeability of the powder, limits the allowable roll speed of the press, and may also induce compact delamination. Increases in roll speed or decreases in permeability require larger feed pressures.

**Pellet Mills** Pellet mills operate on the principle shown in Fig. 20-92. Moist, plastic feed is pushed through holes in dies of various shapes. The friction of the material in the die holes supplies the resistance necessary for compaction. Adjustable knives shear the rodlike extrudates into pellets of the desired length. Although several designs are in use, the most commonly used pellet mills operate by applying power to the die and rotating it around a freely turning roller with fixed horizontal or vertical axis.

Pellet quality and capacity vary with properties of the feed such as

**TABLE 20-51 Pressure and Energy Requirements to Briquette Various Materials\***

Pressure range, lb./sq. in.	Approximate energy required, kw.-hr./ton	Type of material being briquetted or compacted		
		Without binder	With binder	Hot
Low 500–20,000	2–4	Mixed fertilizers, phosphate ores, shales, urea	Coal, charcoal, coke, lignite, animal feed, candy	Phosphate ores, urea
Medium 20,000–50,000	4–8	Acrylic resins, plastics, PVC, ammonium chloride, DMT, copper compounds, lead	Ferroalloys, fluorspar, nickel	Iron, potash, glass-making mixtures
High 50,000–80,000	8–16	Aluminum, copper, zinc, vanadium, calcined dolomite, lime, magnesia, magnesium carbonates, sodium chloride, sodium and potassium compounds	Flue dust, natural and reduced iron ores	Flue dust, iron oxide, natural and reduced iron ores, scrap metals
Very high >80,000	>16	Metal powders, titanium	—	Metal chips

\*Courtesy Bepex Corporation. To convert pounds per square inch to newtons per square meter, multiply by 6895; to convert kilowatthours per ton to kilowatthours per megagram, multiply by 1.1.

**TABLE 20-52 Some Typical Capacities (tons/h) for a Range of Roll Presses\***

Roll diameter, in	10	16	12	10.3	13	20.5	28	36
Maximum roll-face width, in	3.25	6	4	6	8	13.5	27	10
Roll-separating force, tons	25	50	40	50	75	150	300	360
Carbon								
Coal, coke		2	1		3	6	25	
Charcoal			8			13		
Activated					3	7		
Metal and ores								
Alumina					5	10	28	
Aluminum				2	4	8	20	
Brass, copper	0.5			1.5	3	6	16	
Steel-mill waste					5	10		
Iron				3	6	15	40	
Nickel powder					2.5	5.0		
Nickel ore						20	40	
Stainless steel				2	5	10		
Steel								25
Bauxite		1.5				10	20	
Ferrometals						10		
Chemicals								
Copper sulfate	0.5	1.5		1	3	6	15	
Potassium hydroxide				1	4	8		
Soda ash	0.5				3	6	15	
Urea	0.25					10		
DMT	0.25				2	6		
Minerals								
Potash						20	80	
Salt				2	5	9		
Lime					4	8	15	
Calcium sulfate							13	40
Fluorspar						5	10	28
Magnesium oxide						1.5	5	
Asbestos						1.5	3	
Cement						5		
Glass batch						5	12	

\*Courtesy Bepex Corporation. To convert inches to centimeters, multiply by 2.54; to convert tons to megagrams, multiply by 0.907; and to convert tons per hour to megagrams per hour, multiply by 0.907.

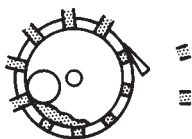


FIG. 20-92 Operating principle of a pellet mill.

moisture, lubricating characteristics, particle size, and abrasiveness, as well as die characteristics and speed. A readily pelleted material will yield about 122 kg/kWh [200 lb/(hp-h)] by using a die with 0.6-cm (1/4-in) holes. Some characteristics of pellet mills are given in Table 20-53.

**Screw Extruders** Screw extruders employ a screw to force material in a plastic state continuously through a die. If the die hole is round, a compact in the form of a rod is formed, whereas if the hole is a thin slit, a film or sheet is formed. Many other forms are also possible.

Basic types of extruders include axial end plate, radial screen, rotary cylinder or gear, and ram or piston. For a review, see Newton [*Powder Technology & Pharmaceutical Processes*, Chulia et al. (eds.), Elsevier, 391 (1994).]

Both wet and dry extrusion techniques are available, and both are strongly influenced by the frictional properties of the particulate phase and wall. In the case of wet extrusion, rheological properties of the liquid phase are equally important. See Pietsch [*Size Enlargement by Agglomeration*, John Wiley & Sons Ltd., Chichester, 346 (1992)] and Benbow et al. [*Chem. Eng. Sci.*, **422**, 2151 (1987)] for a review of design procedures for dry and wet extrusion, respectively.

A common use of screw extruders is in the forming and compounding of plastics. Table 20-54 shows typical outputs that can be expected per horsepower for various plastics and the characteristics of several popular extruder sizes.

Deairing pug-mill extruders which combine mixing, densification, and extrusion in one operation are available for agglomerating clays, catalysts, fertilizers, etc. Table 20-55 gives data on screw extruders for the production of catalyst pellets.

## THERMAL PROCESSES

Bonding and agglomeration by temperature elevation or reduction are applied either in conjunction with other size-enlargement processes or as a separate process. Agglomeration occurs through one or more of the following mechanisms:

1. Drying of a concentrated slurry or wet mass of fines
2. Fusion
3. High-temperature chemical reaction
4. Solidification and/or crystallization of a melt or concentrated slurry during cooling

**Sintering and Heat Hardening** In powder metallurgy compacts are sintered with or without the addition of binders. In ore processing the agglomerated mixture is either sintered or indurated. Sintering refers to a process in which fuel is mixed with the ore and burned on a grate. The product is a porous cake. Induration, or heat hardening, is accomplished by combustion of gases passed through

TABLE 20-53 Characteristics of Pellet Mills

Horsepower range	10–250
Capacity, lb/(hp-h)	75–300
Die characteristics	
Size	Up to 26 in inside diameter × approximately 8 in wide
Speed range	75–500 r/min
Hole-size range	1/16–1/4 in inside diameter
Rollers	As many as three rolls; up to 10-in diameter

NOTE: To convert horsepower to kilowatts, multiply by 0.746; to convert pounds per horsepower-hour to kilograms per kilowatt-hour, multiply by 0.6; and to convert inches to centimeters, multiply by 2.54.

TABLE 20-54 Characteristics of Plastics Extruders\*

Efficiencies		lb/(hp-h)	
Rigid PVC		7–10	
Plasticized PVC		10–13	
Impact polystyrene		8–12	
ABS polymers		5–9	
Low-density polyethylene		7–10	
High-density polyethylene		4–8	
Polypropylene		5–10	
Nylon		8–12	

Relation of size, power, and output			
hp	Diameter		Output, lb/h, low-density polyethylene
	in	mm	
15	2	45	Up to 125
25	2½	60	Up to 250
50	3½	90	Up to 450
100	4½	120	Up to 800

\*The *Encyclopedia of Plastics Equipment*, Simonds (ed.), Reinhold, New York, 1964.

NOTE: To convert inches to centimeters, multiply by 2.54; to convert horsepower to kilowatts, multiply by 0.746; to convert pounds per hour to kilograms per hour, multiply by 0.4535; and to convert pounds per horsepower-hour to kilograms per kilowatt-hour, multiply by 0.6.

TABLE 20-55 Characteristics of Pelletizing Screw Extruders for Catalysts\*

Screw diameter, in	Drive hp	Typical capacity, lb/h
2.25		60
4	7.5–15	200–600
6	Up to 60	600–1500
8	75–100	Up to 2000

\*Courtesy The Bonnot Co. To convert inches to centimeters, multiply by 2.54; to convert horsepower to kilowatts, multiply by 0.746; and to convert pounds per hour to kilograms per hour, multiply by 0.4535.

NOTE:

1. Typical feeds are high alumina, kaolin carriers, molecular sieves, and gels.
2. Water-cooled worm and barrel, variable-speed drive.
3. Die orifices as small as 1/16 in.
4. Vacuum-deairing option available.

the bed. The aim is to harden the pellets without fusing them together, as is done in the sintering process.

Ceramic bond formation and grain growth by diffusion are the two prominent reactions for bonding at the high temperature (1100 to 1370°C, or 2000 to 2500°F, for iron ore) employed. The minimum temperature required for sintering may be measured by modern **dilatometry** techniques, as well as by differential scanning calorimetry. See Compo et al. [*Powder Tech.*, **51**(1), 87 (1987); *Particle Characterization*, **1**, 171 (1984)] for reviews.

In addition to agglomeration, other useful processes may occur during sintering and heat hardening. For example, carbonates and sulfates may be decomposed, or sulfur may be eliminated. Although the major application is in ore beneficiation, other applications, such as the preparation of lightweight aggregate from fly ash and the formation of clinker from cement raw meal, are also possible. Nonferrous sinter is produced from oxides and sulfides of manganese, zinc, lead, and nickel. An excellent account of the many possible applications is given by Ban et al. [Knepper (ed.), *Agglomeration*, op. cit. p. 511] and Ball et al. [*Agglomeration of Iron Ores* (1973)]. The highest tonnage use at present is in the beneficiation of iron ore.

The machine most commonly used for sintering iron ores is a traveling grate, which is a modification of the Dwight-Lloyd continuous sintering machine formerly used only in the lead and zinc industries. Modern sintering machines may be 4 m (13 ft) wide by 60 m (200 ft) long and have capacities of 7200 Mg/day (8000 tons/day).

The productive capacity of a sintering strand is related directly to the rate at which the burning zone moves downward through the bed. This rate, which is of the order of 2.5 cm/min (1 in/min), is controlled by the air rate through the bed, with the air functioning as the heat-transfer medium.

Heat hardening of green iron-ore pellets is accomplished in a vertical shaft furnace, a traveling-grate machine, or a grate-plus-kiln combination (see Ball et al., op. cit.).

**Drying and Solidification** Granular free-flowing solid products are often an important result of the drying of concentrated slurries and pastes and the cooling of melts. Size enlargement of originally

finely divided solids results. Pressure agglomeration including extrusion, pelleting, and briquetting is used to preform wet material into forms suitable for drying in through-circulation and other types of dryers. Details are given in Sec. 12 in the account of solids-drying equipment.

Rotating-drum-type and belt-type heat-transfer equipment forms granular products directly from fluid pastes and melts without intermediate preforms. These processes are described in Sec. 5 as examples of indirect heat transfer to and from the solid phase. When solidification results from melt freezing, the operation is known as *flaking*. If evaporation occurs, solidification is by drying.

## MODELING AND SIMULATION OF GRANULATION PROCESSES

For granulation processes, granule size distribution is an important if not the most important property. The evolution of the granule size distribution within the process can be followed using population balance modeling techniques. This approach is also used for other size-change processes including crushing and grinding (Sec. 20: "Principles of Size Reduction") and crystallization (Sec. 18). The use of the **population balance (PB)** is outlined briefly below. For more in-depth analysis see Randolph & Larson (*Theory of Particulate Processes, 2d ed.*, Academic Press, 1991), Ennis & Litster (*The Science and Engineering of Granulation Processes*, Chapman-Hall, 1997), and Sastry & Loftus [*Proc. 5th Int. Symp. Agglom.*, IChemE, 623 (1989)].

The key uses of PB modeling of granulation processes are:

- Critical evaluation of data to determine controlling granulation mechanisms
- In design, to predict the mean size and size distribution of product granules
- Sensitivity analysis: to analyze quantitatively the effect of changes to operating conditions and feed variables on product quality
- Circuit simulation, optimization, and process control

The use of PB modeling by practitioners has been limited for two reasons. First, in many cases the kinetic parameters for the models have been difficult to predict and are very sensitive to operating conditions. Second, the PB equations are complex and difficult to solve. However, recent advances in understanding of granulation micromechanics, as well as better numerical solution techniques and faster computers, means that the use of PB models by practitioners should expand.

### THE POPULATION BALANCE

The PB is a statement of continuity for particulate systems. It includes a **kinetic expression** for each mechanism which changes a particle property. Consider a section of a granulator as illustrated in Fig. 20-93. The PB follows the change in the granule size distribution as granules are born, die, grow, and enter or leave the control volume. As discussed in detail previously ("Agglomeration Rate Processes"), the granulation mechanisms which cause these changes are nucleation, layering, coalescence, and attrition (Tables 20-39 and 20-56). The number of particles-per-unit volume of granulator between size volume  $v$  and  $v + dv$  is  $n(v)dv$ , where  $n(v)$  is the **number frequency size distribution** by size volume, having dimensions of number per-unit-granulator and volume per-unit-size volume. For constant granulator volume, the macroscopic PB for the granulator in terms of  $n(v)$  is:

$$\begin{aligned} \frac{\partial n(v,t)}{\partial t} = & \frac{Q_{in}}{V} n_{in}(v) - \frac{Q_{ex}}{V} n_{ex}(v) - \frac{\partial(G^\circ - A^\circ)n(v,t)}{\partial v} \\ & + B_{nuc}(v) + \frac{1}{2N_t} \int_0^v \beta(u,v-u,t)n(u,t)n(v-u,t)du \\ & - \frac{1}{N_t} \int_0^\infty \beta(u,v,t)n(u,t)n(v,t)du \end{aligned} \quad (20-71)$$

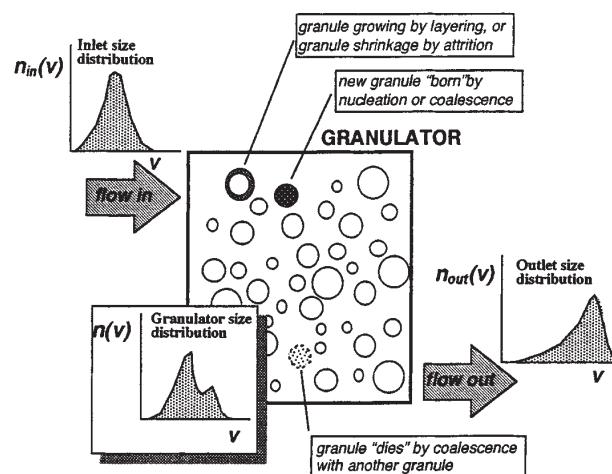
where  $V$  is the volume of the granulator;  $Q_{in}$  and  $Q_{ex}$  are the inlet and

exit flow rates from the granulator;  $G(v)$ ,  $A(v)$ , and  $B_{nuc}(v)$  are the layering, attrition, and nucleation rates, respectively;  $\beta(u,v,t)$  is the coalescence kernel and  $N_t$  is the total number of granules-per-unit volume of granulator. The left-hand side of Eq. 20-71 is the accumulation of particles of a given size volume. The terms on the right-hand side are in turn: the bulk flow into and out of the control volume, the convective flux along the size axis due to layering and attrition, the birth of new particles due to nucleation, and birth and death of granules due to coalescence. Equation 20-71 is written in terms of granule volume  $v$ , but could also be written in terms of granule size  $x$  or could also be expanded to follow changes in other granule properties, e.g., changes in granule density or porosity due to consolidation.

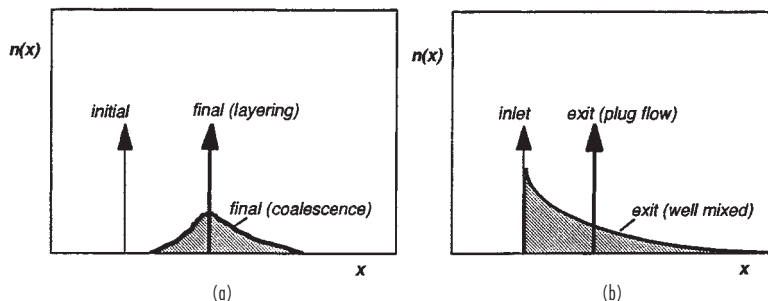
### MODELING INDIVIDUAL GROWTH MECHANISMS

The **granule size distribution (GSD)** is a strong function of the balance between different mechanisms for size change shown in Table 20-53—layering, attrition, nucleation, and coalescence. For example, Fig. 20-94 shows the difference in the GSD for a doubling in mean granule size due to (1) layering only, or (2) coalescence only for batch, plug-flow, and well-mixed granulators. Table 20-56 describes how four key rate mechanisms effect the GSD.

**Nucleation** Nucleation increases both the mass and number of the granules. For the case where new granules are produced by liquid



**FIG. 20-93** Changes to the granule size distribution due to granulation-rate processes as particles move through the granulator. Reprinted from *Granulation and Coating Technologies for High-Value-Added Industries*, Ennis and Litster (1996) with permission of E & G Associates. All rights reserved.



**FIG. 20-94** The effect of growth mechanism and mixing on product granule size distribution for (a) batch growth by layering or coalescence, and (b) layered growth in well-mixed or plug-flow granulators. Reprinted from *Granulation and Coating Technologies for High-Value-Added Industries*, Ennis and Litster (1996) with permission of E & G Associates. All rights reserved.

feed which dries or solidifies, the nucleation rate is given by the new feed droplet size  $n_s$  and the volumetric spray rate  $S$ :

$$B(v)_{nuc} = S n_s(v) \tag{20-72}$$

In processes where new powder feed has a much smaller particle size than the smallest granular product, the feed powder can be considered as a **continuous phase** which can nucleate to form new granules [Sastry & Fuerstenau, *Powder Tech.*, **7**, 97 (1975)]. The size of the nuclei is then related to nucleation mechanism. In the case of nucleation by spray, the size of the nuclei is of the order of the droplet size and proportional to  $\cos\theta$ , where  $\theta$  is binder fluid-particle contact angle (see Fig. 20-67 of "Wetting" section).

**Layering** Layering increases granule size and mass by the progressive coating of new material onto existing granules, but it does not alter the number of granules in the system. As with nucleation, the new feed may be in liquid form (where there is simultaneous drying or cooling) or may be present as a fine powder. Where the feed is a powder, the process is sometimes called **pseudolayering** or **snowballing**. It is often reasonable to assume a linear-growth rate  $G(x)$  which is independent of granule size. For batch and plug-flow granulators, this causes the initial feed distribution to shift forward in time

with the shape of the GSD remaining unaltered and governed by a traveling-wave equation (Table 20-59). As an example, Fig. 20-95 illustrates size-independent growth of limestone pellets by snowballing in a batch drum. Size-independent linear growth rate implies that the volumetric growth rate  $G^o(v)$  is proportional to projected granule surface area, or  $G^o(v) \propto v^{2/3} \propto x^2$ . This assumption is true only if all granules receive the same exposure to new feed. Any form of segregation will invalidate this assumption [Liu and Litster, *Powder Tech.*, **74**, 259 (1993)]. The growth rate  $G^o(v)$  by layering only can be calculated directly from the mass balance:

$$\dot{V}_{feed} = (1 - \epsilon) \int_0^\infty G^o(v)n(v)dv \tag{20-73}$$

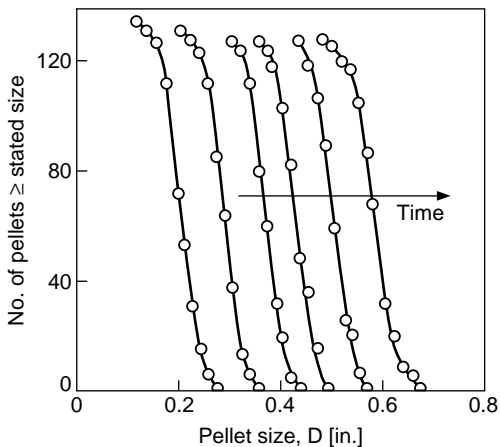
where  $\dot{V}_{feed}$  is the volumetric flow rate of new feed and  $\epsilon$  is the granule porosity.

**Coalescence** Coalescence is the most difficult mechanism to model. It is easiest to write the population balance (Eq. 20-71) in terms of number distribution by volume  $n(v)$  because granule volume is conserved in a coalescence event. The key parameter is the **coalescence kernel** or rate constant  $\beta(u,v)$ . The kernel dictates the overall rate of coalescence, as well as the effect of granule size on coalescence

**TABLE 20-56 Impact of Granulation Mechanisms on Size Distribution**

Mechanism	Changes number of granules?	Changes mass of granules?	Discrete or differential?
	yes	yes	discrete
	no	yes	differential
	yes	no	discrete
	no	yes	differential

Reprinted from *Granulation and Coating Technologies for High-Value-Added Industries*, Ennis and Litster (1996) with permission of E & G Associates. All rights reserved.



**FIG. 20-95** Batch drum growth of limestone pellets by layering with a size-independent linear growth rate [Capes, *Chem. Eng.*, **45**, CE78 (1967).]

rate. The **order** of the kernel has a major effect on the shape and evolution of the granule size distribution. [See Adetayo & Ennis, *AIChE J.* 1997 (In press).] Several empirical kernels have been proposed and used (Table 20-57).

All the kernels are empirical, or semiempirical and must be fitted to plant or laboratory data. The kernel proposed by Adetayo and Ennis is consistent with the granulation regime analysis described above (see section on growth) and is therefore recommended:

$$\beta(u,v) = \begin{cases} k, w < w^{\circ} \\ 0, w > w^{\circ} \end{cases} \quad w = \frac{(uw)^a}{(u+v)^b} \quad (20-74)$$

where  $w^{\circ}$  is the **critical average granule volume** in a collision corresponding to  $St = St^{\circ}$ , and it is related to the critical cutoff diameter defined above (Eq. 20-47). For fine powders in the noninertial regime (See section on growth) where  $St \ll St^{\circ}$ , this kernel collapses to the simple **random** or size-independent kernel  $\beta = k$  for which the mean granule size increases exponentially with time (Eq. 20-51). Where deformation is unimportant, coalescence occurs only in the noninertial regime and stops abruptly when  $St_v = St^{\circ}$ . Based on the granulation regime analysis, the effects of feed characteristics and operating variables on granulation extent has been predicted [Adetayo et al., *Powder Tech.*, **82**, 47–59 (1995)]. (See “Extent of Noninertial Growth” subsection.)

Modeling growth where deformation is significant is more difficult. It can be assumed that a critical cutoff size exists  $w^{\circ}$  which determines which combination of granule sizes are capable of coalescence, based on their inertia. When the harmonic average of sizes of two colliding

granules  $w$  is less than this critical cut-off size  $w^{\circ}$ , coalescence is successful, or

$$w = \frac{(uw)^b}{(u+v)^a} = w^{\circ} = \frac{\pi}{6} \left( \frac{16\mu}{\rho u_0} St^{\circ} \right)^3 \quad (20-75)$$

where  $a$  and  $b$  are model parameters expected to vary with granule deformability, and  $u$  and  $v$  are granule volumes. To be dimensionally consistent,  $2b - a = 1$ .  $w^{\circ}$  and  $w$  involving the parameters  $a$  and  $b$  represent a generalization of the Stokes analysis for non-deforming systems, for which case  $a = b = 1$ . For deformable systems, the kernel is then represented by Eq. 20-74. Figure 20-96 illustrates the evolution of the granule size distribution as predicted by this cutoff-based kernel which accounts for deformability. The cutoff kernel is seen to clearly track the experimental average granule size over the life of the granulation, illustrating that multiple kernels are not necessary to describe the various stages of granule growth, including the initial stage of random noninertial coalescence and the final stage of nonrandom preferential inertial growth by balling or crushing and layering (see Table 20-39).

**Attrition** The wearing away of granule surface material by attrition is the direct opposite of layering. It is an important mechanism when drying occurs simultaneously with granulation and granule velocities are high, e.g., fluidized beds and spouted beds. In a fluid bed [Ennis & Sunshine, *Tribology International*, **26**, 319 (1993)], attrition rate is proportional to excess gas velocity  $(U - U_{mf})$  and approximately inversely proportional to granule-fracture toughness  $K_{fc}$ , or  $A \propto (U - U_{mf})/K_{fc}$ . For spouted beds, most attrition occurs in the spout and the attrition rate may be expressed as:

$$A \propto \frac{A_i U_i^3}{K_c} \quad (20-76)$$

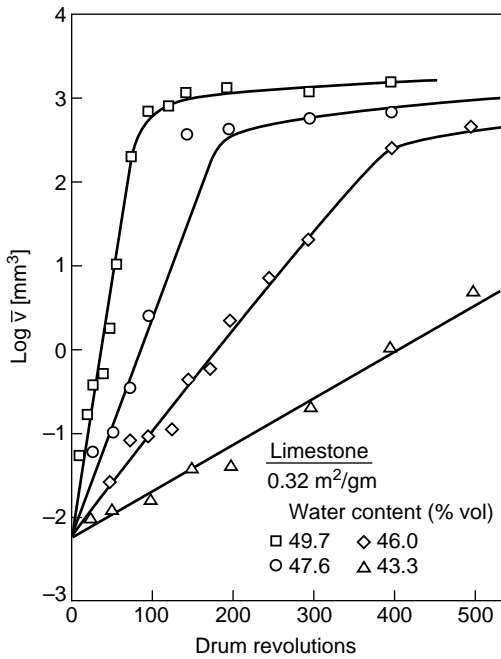
where  $A_i$  and  $U_i$  are the inlet orifice area and gas velocity, respectively. Attrition rate also increases with increasing slurry feed rate [Liu and Litster, *Powder Tech.*, **74**, 259 (1993)]. Granule breakage by fragmentation is also possible, with its rate being described by an **on function** which plays a similar role as the coalescence kernel does for growth. (See “Principles of Size Reduction” and “Breakage” sections for additional details.)

## SOLUTION OF THE POPULATION BALANCE

**Effects of Mixing** As with chemical reactors, the **degree of mixing** within the granulator has an important effect on the final granule size distribution because of its influence on the **residence time distribution**. Fig. 20-94 shows the difference in exit size distribution for a plug-flow and well-mixed granulator for growth by layering only. In general, the exit size distribution is broadened and the extent of growth (for constant rate constants) is diminished for an increased degree of mixing in the granulator. With layering and attrition rates playing the role of generalized velocities, coalescence, and fragmentation rates, the role of reaction rate constants, methodologies of traditional reaction engineering may be employed to design granu-

**TABLE 20-57 Coalescence Kernels for Granulation**

Kernel	Reference and comments
$\beta = \beta_0$	Kapur & Fuerstenau [ <i>I&amp;EC Proc. Des. &amp; Dev.</i> , <b>8</b> (1), 56 (1969)], size-independent kernel.
$\beta = \beta_0 \frac{(u+v)^a}{(uv)^b}$	Kapur [ <i>Chem. Eng. Sci.</i> , <b>27</b> , 1863 (1972)], preferential coalescence of limestone.
$\beta = \beta_0 \frac{(u^{2/3} + v^{2/3})}{1/u + 1/v}$	Sastry [ <i>Int. J. Min. Proc.</i> , <b>2</b> , 187 (1975)], preferential balling of iron ore and limestone.
$\beta(u,v) = \begin{cases} k, & w < w^{\circ} \\ 0, & w > w^{\circ} \end{cases} \quad w = \frac{(uw)^a}{(u+v)^b}$	Adetayo & Ennis [ <i>AIChE J.</i> , (1997) In press], based on granulation regime analysis.



**FIG. 20-96** Batch drum growth of limestone by coalescence. Note granule size increases exponentially with time in the first stage of noninertial growth. Experimental data of Kapur [Adv. Chem. Eng., **10**, 56 (1978)] compared with single deformable granulation kernel (Eqs. 20-74, 20-75). [Adetayo & Ennis, AIChE]. (In press.) Reproduced with permission of the American Institute of Chemical Engineers. Copyright AIChE. All rights reserved.

lation systems or optimize the granule size distribution. [For the related example of crystallization, see Randolph & Larson (*Theory of Particulate Processes*, 2d ed., Academic Press, 1991).] Table 20-58 lists some mixing models that have been used for several types of granulators.

**Analytical Solutions** Solution of the population balance is not trivial. Analytical solutions are available for only a limited number of special cases, of which some of examples of practical importance are summarized in Table 20-59. For other analytical solutions, see general references on population balances given above.

In general, analytical solutions are only available for specific initial or inlet size distributions. However, for batch granulation where the only growth mechanism is coalescence, at long times the size distribution may become **self-preserving**. The size distribution is self-preserving if the normalized size distributions  $\phi = \phi(\eta)$  at long time are independent of mean size  $\bar{v}$ , or

$$\phi = \phi(\eta) \quad \text{only where} \quad \eta = v/\bar{v}$$

$$\bar{v} = \int_0^\infty v \cdot n(v,t) dv \quad (20-77)$$

Analytical solutions for self-preserving growth do exist for some coalescence kernels and such behavior is sometimes seen in practice (Fig. 20-97). Roughly speaking, self-preserving growth implies that the width of the size distribution increases in proportion to mean granule size, i.e., the width is uniquely related to the mean of the distribution.

**Numerical Solutions** For many practical applications, numerical solutions to the population balance are necessary. Several numerical solution techniques have been proposed. It is usual to break the size range into discrete intervals and then solve the resulting series of ordinary differential equations. A geometric discretization reduces the number of size intervals (and equations) that are required. Litster et al. [AIChE J., (1995)] give a general discretized PB for nucleation, growth, and coalescence with a geometric discretization of  $v_j = 2^{1/q}v_{j-1}$  where  $q$  is an integer. Accuracy is increased (at the expense of

**TABLE 20-58** Mixing Models for Continuous Granulators

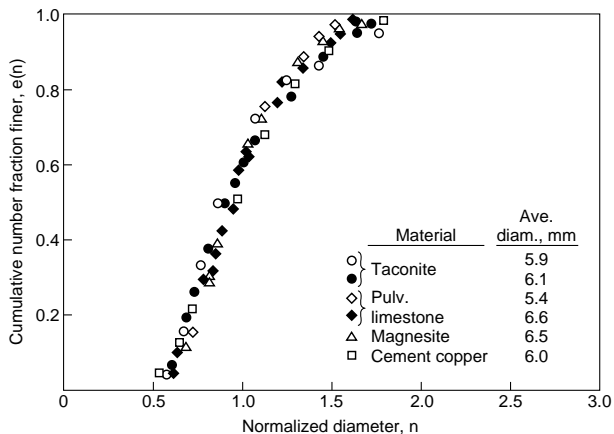
Granulator	Mixing Model	Reference
Fluid bed	Well-mixed	See Sec. 17
Spouted bed	Well-mixed	Liu and Litster, <i>Powder Tech.</i> , <b>74</b> , 259 (1993)
	Two-zone model	Litster, et al. [ <i>Proc. 6th Int. Symp. Agglom., Soc. Powder Tech., Japan</i> , <b>123</b> (1993)].
Drum	Plug-flow	Adetayo et al., <i>Powder Tech.</i> , <b>82</b> , 47-59 (1995)
Disc	Two well-mixed tanks in series with classified exit Well-mixed tank and plug-flow in series with fines bypass	Sastry & Loftus [ <i>Proc. 5th Int. Symp. Agglom., IChemE</i> , 623 (1989)] Ennis, Personal communication (1986)

**TABLE 20-59** Some Analytical Solutions to the Population Balance\*

Mixing state	Mechanisms operating	Initial or inlet size distribution	Final or exit size distribution
Batch	Layering only: $G(x) = \text{constant}$	Any initial size distribution, $n_0(x)$	$n(x) = n_0(x - \Delta x)$ where $\Delta x = Ct$
Continuous & well-mixed	Layering only: $G(x) = \text{constant}$	$n_{in}(x) = N_{in} \delta(x - x_{in})$	$n(x) = \frac{N_0 G}{\tau} \exp\left(-\frac{\tau(x - x_{in})}{G}\right)$
Batch	Coalescence only, size independent:  $\beta(u, v) = \beta_0$	$n_0(v) = N_0 \delta(v - v_0)$	$n(v) = \frac{N_0}{\bar{v}} \exp\left(-\frac{v}{\bar{v}}\right)$  where $\bar{v} = v_0 \exp\left(\frac{\beta_0 t}{6}\right)$
Batch	Coalescence only, size independent:  $\beta(u, v) = \beta_0$	$n_0(v) = \frac{N_0}{v_0} \exp\left(-\frac{v}{v_0}\right)$	$n(v) = \frac{4 N_0}{v_0(N_0 \beta_0 t + 2)^2} \exp\left[\frac{-2t/v_0}{N_0 \beta_0 t + 2}\right]$

\*Randolph and Larson, *Theory of Particulate Processes*, 2d ed., Academic Press, New York (1988); Gelbart and Seinfeld, *J. Computational Physics*, **28**, 357 (1978).





**FIG. 20-97** Self-preserving size distributions for batch coalescence in drum granulation. [Sastry, *Int. J. Min. Proc.*, **2**, 187 (1975).] With kind permission of Elsevier Science -NL, 1055 KV Amsterdam, the Netherlands.

computational time) by increasing the value of  $q$ . Their discretized PB is recommended for general use.

### SIMULATION OF GRANULATION CIRCUITS WITH RECYCLE

When granulation circuits include recycle streams, both steady-state and dynamic responses can be important. Computer simulation packages are now widely used to design and optimize many process flow sheets, e.g., comminution circuits, but simulation of granulation circuits is much less common. Commercial packages do not contain library models for granulators. Some researchers have developed simulations and used these for optimization and control studies [Sastry, *Proc. 3rd Int. Symp. Agglom.* (1981); Adetayo et al., *Computers Chem. Eng.*, **19**, 383 (1995); Zhang et al., *Control of Part. Processes IV* (1995)]. For these simulations, dynamic population-balance models have been used for the granulator. Standard literature models are used for auxiliary equipment such as screens, dryers, and crushers. These simulations are valuable tools for optimization studies and development of control strategies in granulation circuits, and may be employed to investigate the effects of transient upsets in operating variables, particularly moisture level and recycle ratio, on circuit performance.